



UNIVERSITY OF
BIRMINGHAM

**Developing Nucleophilic Nitrenoids for the
Synthesis of Complex Heterocycles**

by

Miguel Garzón Sanz

A thesis submitted to the University of Birmingham for the
degree of DOCTOR OF PHILOSOPHY

School of Chemistry

College of Engineering and Physical Sciences

University of Birmingham

September 2016

UNIVERSITY OF
BIRMINGHAM

University of Birmingham Research Archive

e-theses repository

This unpublished thesis/dissertation is copyright of the author and/or third parties. The intellectual property rights of the author or third parties in respect of this work are as defined by The Copyright Designs and Patents Act 1988 or as modified by any successor legislation.

Any use made of information contained in this thesis/dissertation must be in accordance with that legislation and must be properly acknowledged. Further distribution or reproduction in any format is prohibited without the permission of the copyright holder.

Abstract

The combination of nucleophilic nitrenoids and gold-catalysis has rapidly emerged as a powerful tool in the assembling of different nitrogen-containing motifs. The research presented in this thesis describes the advances in the field and the exploration of pyrimidium *N*-heteroaryl aminides as building blocks in the formation of several fused imidazoheterocycles.

From the initial discovery of this reaction and its application in the synthesis of imidazo[1,2-*a*]pyrimidines, the scope of this convergent gold-catalysed strategy has been adapted to allow the access to fourteen classes of biologically relevant structures. The proposed mechanism and optimisation will be discussed alongside the accommodation of a wide range of useful functionalities difficult to introduce by other methodologies.

Acknowledgements

First and foremost, I would like to thank my supervisor Dr Paul Davies for offering me the opportunity to undertake this research project, for his knowledge and guidance and for teaching me how to always be the best version of myself.

I am very grateful to the University of Birmingham for the funding and to the analytical facilities. In particular, I would like to acknowledge Neil, Cecile, Chi, Peter and Louise for their help.

Thank you Josh, Elli, Andy, Matt, Elsa, Holly, Matt, Michel, Onyeka and Fernando – it has been a pleasure working alongside you as well as besting you at table football. These past years would not have been possible without your help and friendship.

Thanks to François, Tom, Igor and Cindy for being the best housemates anyone could ever hope for. Thanks also to my lunch buddies for the great company.

Thanks to Alex, Sara, Fer, Patri and Javi for your unyielding friendship regardless of the distance. For always being there for me like a second family. Also, thanks to the rest of my friends in Madrid for making every return home unforgettable.

I would like to thank my family, especially my parents for making me the person I am today. Muchas gracias por todo, os quiero.

Last but not least, thank you Graziella, for being my personal cheerleader and a constant source of encouragement and support. Te iubesc.

Table of Contents

Chapter 1	1
1.1 Nitrene transfer processes	2
1.1.1 Gold carbenes	6
1.1.2 Nucleophilic nitrenoids	10
1.2 Intramolecular reactions	12
1.2.1 Azides as nucleophilic nitrenoids	12
1.2.2 Azirines as nucleophilic nitrenoids	16
1.3 Intermolecular reactions	18
1.3.1 Aminides as nucleophilic nitrenoids	18
1.3.2 Isoxazoles and azirines as nucleophilic nitrenoids	19
1.3.3 Azides as nucleophilic nitrenoids	22
1.3.4 Other nucleophilic nitrenoids	25
1.4 Conclusions	27
Chapter 2	29
2.1 Site-specific generation of gold-carbenes	30
2.1.1 Pyridinium aminides in nitrene transfer reactions	32
2.1.2 Pyridinium aminides as <i>N,O</i> -dipole equivalent	36
2.1.3 Pyridinium aminides as <i>N,N</i> -dipole equivalent	37
2.2 Results and Discussion	38
2.2.1 Preparation of pyridinium <i>N</i> -(pyrimidin-2-yl) aminide	38

2.2.2 Synthesis of functionalised ynamides.....	39
2.2.3 Catalyst screening.....	43
2.2.4 Studies into the regiochemistry of 284	46
2.2.5 Reaction Scope	48
2.2.6 Proposed Mechanism.....	52
2.3 Conclusions	57
Chapter 3.....	58
3.1 Fused imidazoheterocycles	59
3.1.1 A common route for the synthesis of fused imidazoheterocycles..	59
3.1.2 Pyridinium <i>N</i> -heteroaryl aminides as building blocks	64
3.2 Results and Discussion.....	66
3.2.1 Synthesis of pyridinium <i>N</i> -diazine/pyridine aminides	66
3.2.2 Synthesis of fused imidazodiazines/pyridines	68
3.2.3 Mechanistic observations.....	71
3.2.4 Post-catalytic functionalisation	74
3.3 Conclusions	75
Chapter 4.....	77
4.1 Fused imidazobenzoheterocycles	78
4.2 Results and discussion	79
4.2.1 Synthesis of π -rich heteroaryl aminides	79
4.2.2 Formation of 5,5-fused scaffolds.....	82

4.2.3 Reactivity towards ynamides	85
4.2.4 Routes for the synthesis of functionalised benzazole aminides	88
4.2.5 Confirmation of the structure of vinyl substituted derivatives.....	94
4.2.6 Reactivity of benzimidazole-based aminides.....	99
4.3 Conclusions	102

Chapter 5.....104

5.1. General information	105
5.2 Precursors for Chapters 2 and 3.....	106
5.2.1 Preparation of ynamides and indolylalkynes	106
5.2.2 Preparation of pyridinium <i>N</i> -(heteroaryl)aminides	119
5.2.3 Preparation of 227	127
5.3 Cycloaddition products for Chapter 2.....	128
5.4 Cycloaddition products for Chapter 3.....	141
5.4 Precursors for Chapter 4.....	152
5.4.1 Preparation of ynamides	152
5.4.2 Preparation of precursors for the formation of aminides	155
5.4.3 Preparation of aminides	166
5.5 Cycloaddition products for Chapter 4.....	172

Appendix 1188

Appendix 1.1 Selected NMR Spectra.....	189
Appendix 1.2 Assignment of the structure for compound 507	198

Appendix 2204

Appendix 2.1 X-Ray crystal structure data..... 205

Appendix 2.1.1 Imidazo[1,2-*c*]pyrimidine 398 205

Appendix 2.1.2 Imidazo[1,2-*a*]pyrimidine 402 215

Appendix 2.1.3 Aminide 436..... 226

Appendix 2.1.4 Aminide 437..... 231

Appendix 2.1.5 Aminide 443..... 236

Bibliography.....244

List of abbreviations

$[\alpha]_D^T$	specific rotation at T (°C)
°C	degree(s) Celsius
1,2-DCB	1,2-dichlorobenzene
1,10-phen	1,10-phenanthroline
Å	angstrom(s)
Ac	acetyl
Au	gold
Alk	alkyl
app.	apparent
Ar	aryl
BINAP	2,2'-bis(diphenylphosphino)-1,1'-binaphthyl
Boc	<i>tert</i> -butoxycarbonyl
Bn	benzyl
Bu	butyl
calcd.	calculated
cm	centimetre(s)
Cy	cyclohexyl
d	doublet
Δ	Heat
δ	chemical shift
dba	dibenzylideneacetone
dppm	1,1-bis(diphenylphosphino)methane
DIPEA	<i>N,N'</i> -diisopropylethylamine

DMAP	4-dimethylaminopyridine
DMEDA	<i>N,N'</i> -dimethylethylenediamine
DMF	dimethylformamide
DMSO	dimethyl sulfoxide
d.r.	diastereomeric ratio
DTBP	tris(2,4-di- <i>tert</i> -butylphenyl) phosphite
EI	electron ionisation
eq.	equivalent(s)
Eq.	equation
ES	electrospray
esp	α , α , α' , α' -tetramethyl-1,3-benzenedipropionic acid
Et	ethyl
EWG	electron-withdrawing group
g	gram(s)
h	hour(s)
Het	heteroaryl
HPLC	high pressure liquid chromatography
HMBC	heteronuclear multiple bond correlation
HRMS	high resolution mass spectrometry
HSQC	heteronuclear single-quantum correlation
h ν	electromagnetic radiation
Hz	Hertz
IPr	1,3-bis(2,6-diisopropylphenyl)imidazol-2-ylidene
^{<i>i</i>} Pr	isopropyl
IR	infrared spectroscopy

<i>J</i>	coupling constant
JohnPhos	2-(di- <i>tert</i> -butylphosphino)biphenyl
K	kelvin
L	litre(s)
LG	leaving group
M	molar
m	multiplet
μL	microlitre(s)
<i>m</i> -	meta
Me	methyl
<i>m</i> CPBA	3-chloroperbenzoic acid
MEG	ethane-1,2-diol
min	minut(s)
mol	mole(s)
mp	melting point
Ms	methanesulfony
MS	mass spectrometry
<i>MS</i>	molecular sieves
m/z	mass/charge
NBS	<i>N</i> -bromosuccinimide
NHC	nucleophilic heterocyclic carbene
NIS	<i>N</i> -iodosuccinimide
NMR	nuclear magnetic resonance
NMP	<i>N</i> -methyl-2-pyrrolidone
nOe	nuclear Overhauser effect

<i>o</i> -	ortho
<i>p</i> -	para
Ph	phenyl
Pic	picolinate
PMB	<i>para</i> -methoxybenzyl
PMP	<i>para</i> -methoxyphenyl
ppm	parts per million
Py	pyridine
q	quartet
quint.	quintet
Ref.	reference(s)
rt	room temperature
s	singlet
t	triplets
T	temperature
^t Bu	<i>tert</i> -butyl
TBAF	tetrabutylammonium fluoride
TCT	2,4,6-trichloro-1,3,5-triazine
Tf	trifluoromethylsulfonyl
TFA	trifluoroacetic acid
THF	tetrahydrofuran
TIPS	triisopropylsilyl
TLC	thin layer chromatography
TMS	trimethylsilyl
TOF	time of flight

Ts	4-toluenesulfonyl
UV	ultraviolet
ν	frequency
XPhos	2-dicyclohexylphosphino-2',4',6'-triisopropylbiphenyl

Chapter 1

Nitrogen-containing heterocycles are prevalent scaffolds in nature, with a fundamental role in living systems and as synthetic frameworks.¹ Particularly, the family of the fused imidazoheterocycles contains many biologically relevant structures,^{1b} as demonstrated by their ubiquity in several commercially available drugs such as Alpidem,^{1c} Divaplon or Zolpidem^{1d} (Figure 1). Thus, C–N bond forming strategies that provide rapid and efficient routes for the assembly of these systems are actively pursued.²

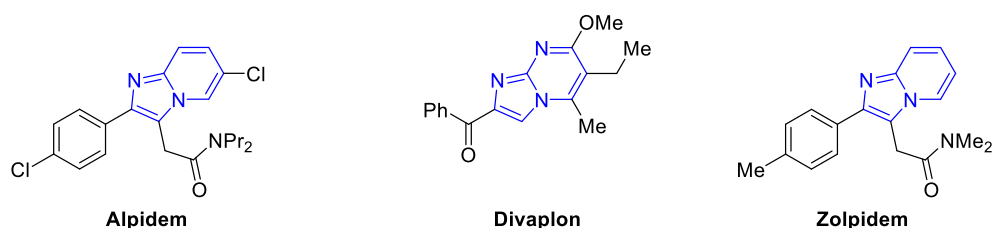


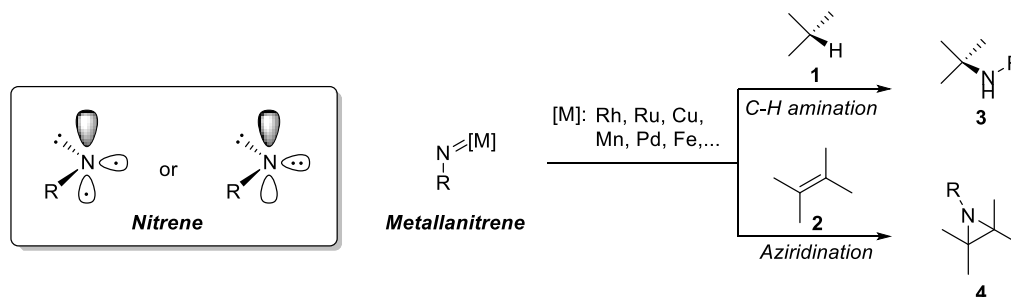
Figure 1: Commercially available drugs based on the fused imidazoheteroaryl scaffold

The present thesis explores the design and development of a novel type of reactivity that has been successfully employed in the synthesis of several of these fused imidazoheteroaryl scaffolds in a modular and convergent fashion. This approach offers a common, simple and practical route to access valuable frameworks.

1.1 Nitrene transfer processes

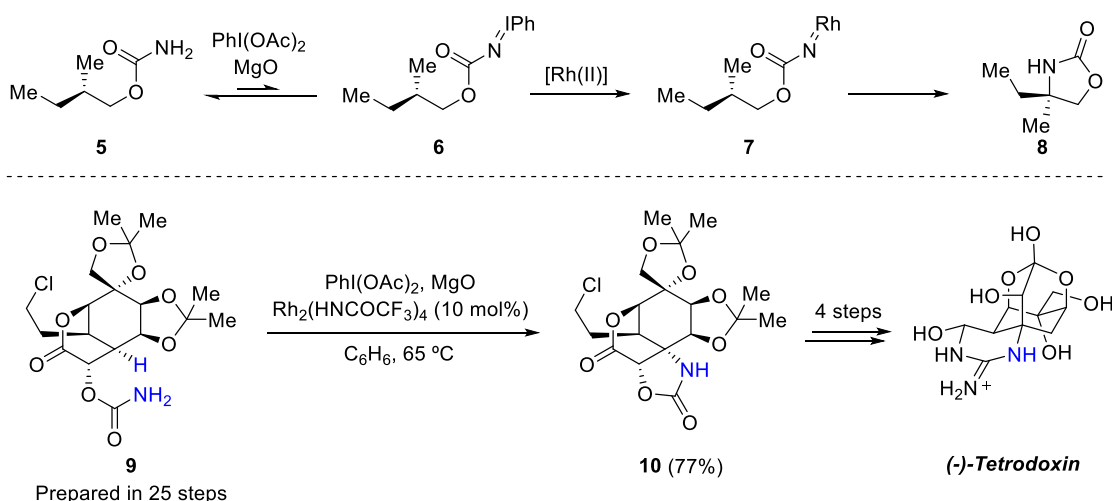
The use of nitrenes as reactants represents one of the most direct approaches to introduce nitrogen into a molecule. These neutral monovalent species with six valence electrons are highly reactive and prone to insert into various types of bond, giving access to aminated products (Scheme 1).³ However, due to their reactive nature they can show poor discrimination and selectivity. Thus, nitrenes are more commonly employed as part of a metal complex. Rhodium, ruthenium or copper, among other metals, often

appear catalysing reactions such as C–H amination and aziridination that have extensively been exploited in the synthesis of nitrogen-containing structures.^{3,4}



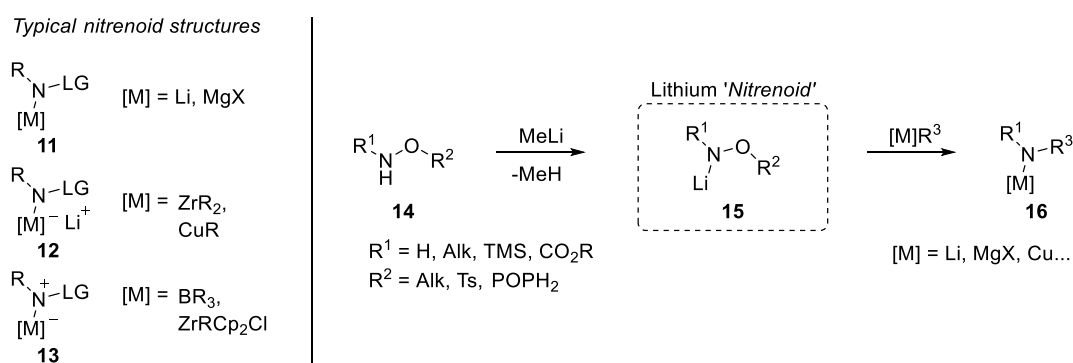
Scheme 1: Nitrene and metallanitrenes for the C–N bond formation

A common route for the generation of these metallanitrenes follows the formation of an iminoiodane precursor **6** obtained by reaction of a carbamate or sulfamate with iodine(III) oxidants such as $\text{PhI}(\text{OAc})_2$ (Scheme 2). The interaction between iminoiodane **6** with a suitable metal species generates complex **7** *in situ* which may undergo several important processes (*e.g.* stereospecific insertion into tertiary C–H bond **8**).⁵ This strategy has seen used in some late stage transformations in the total synthesis of several natural products such as (-)-tetrodotoxin (Scheme 2).⁶



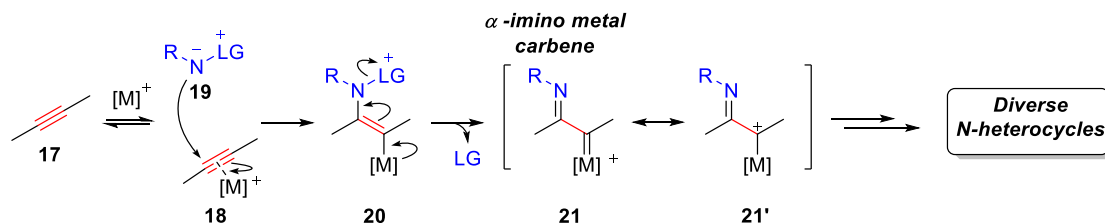
Scheme 2: Generation of metallanitrenes and their application in C–H insertion reactions

As an alternative to the use of metallanitrenes as nitrene transfer agents, other species have been developed that display similar chemical reactivity, known as nitrene equivalents or nitrenoids. Certain controversy exists regarding the actual definition of the term nitrenoid. While Marek and co-workers postulate that only organometallic species carrying both an electrofuge and a nucleofuge (Scheme 3) should receive that denomination **11-13**,⁷ compounds such as iminoiodinane **6**, iminophosphoranes and metallanitrenes are frequently referred to as nitrenoids in literature.⁸ In any case, most of these compounds have in common their application as electrophilic amination reagents. For the purpose of this thesis, nitrenoids are defined as relatively stable compounds able to behave as source of nitrene character over the course of the reaction.



Scheme 3: Nitrenoid structures as defined by Marek and co-workers⁹

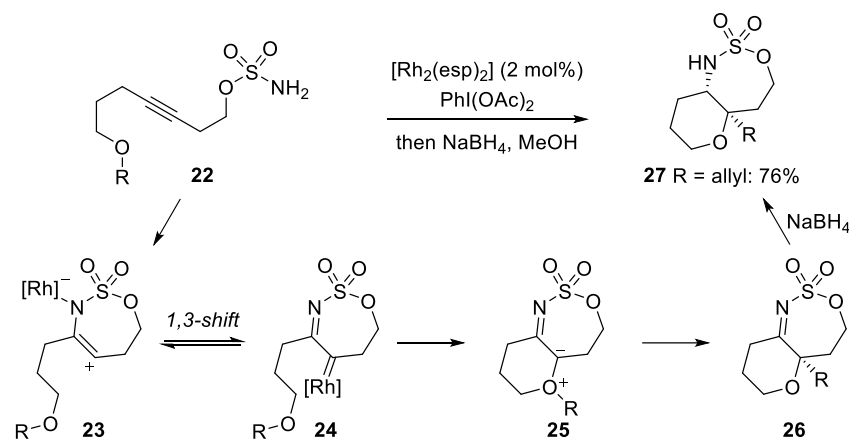
The advent of π -acid catalysis has facilitated the development of novel strategies for the direct formation of C–N bonds.¹⁰ A particularly attractive emerging aspect within the field relies on the generation of α -imino metal carbenes **21** as synthetic intermediates in powerful ring-forming transformations (Scheme 4).



Scheme 4: Reactivity basis for the generation of α -imino metal carbenes through the use of nucleophilic nitrenoids

These species can be accessed by coordination of an alkyne **17** to a π -acidic metal, giving an electrophilic π -system **18** able to interact with a suitable nitrogen-based nucleophile **19**. The resulting vinyl metal carbenoid **20** may evolve to the α -imino metal carbene **21** by elimination of a leaving group on the nitrogen atom (LG). Subsequently, intermediate **21/21'** can be trapped through different pathways (*e.g.* 1,2-migration, cyclopropanation, C–H insertion, 4π -electrocyclisation) to access the desired framework. Overall, the whole sequence can be seen as a nitrene transfer process where compound **19** behaves as a nucleophilic nitrenoid. It must be noticed that these compounds are stable and isolable species and the nitrene character is only invoked on π -activation of the triple bond: by first donating an electron-pair (triggering the development of carbenic character adjacent to the newly formed carbon-nitrogen bond **20**) and then losing a nucleofuge as the intermediate metal carbenoid species evolves.

Interestingly, metallanitrenes intermediates can also lead to related α -imino metal carbenes by reaction with π -systems, although these nitrene equivalents present a contrasting electrophilic behaviour.¹¹ For instance, the sulfamate-derived rhodium nitrene from **22** may intramolecularly cyclise into intermediate **23**, in equilibrium with α -imino rhodium carbene **24** through a 1,3-shift (Scheme 5).^{11b} **24** may then be trapped by the tethered functionality which rearranges into the isolable *N*-(sulfonyl)imine **26**. Alternatively, this imine can be reduced to the more stable amine **27** in good yield.



Scheme 5: Metallanitrenes in the generation of α -imino metal carbenes

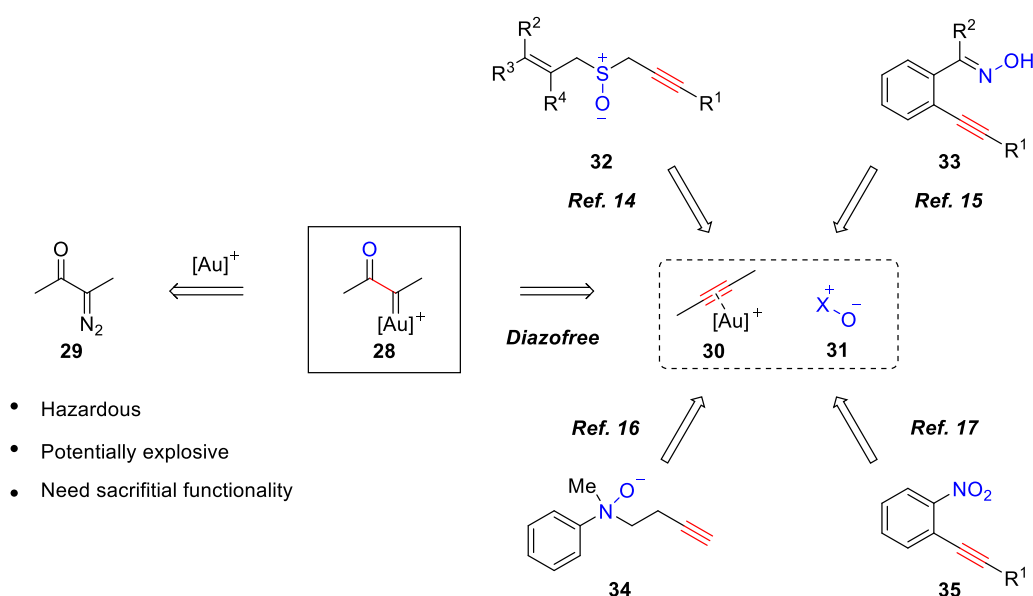
The use of nucleophilic nitrenoids through π -acid catalysis provide a new paradigm in the formation of aza-heterocycles due to their versatility and sought-after features such as mild conditions, simple reaction set-ups and work-ups, good atom economy and generally robust precursors. A review on these areas as contained in the present Chapter was published in: P. W. Davies and M. Garzón, *Asian. J. Org. Chem.* **2015**, 4, 694–708.

1.1.1 Gold carbenes

Over the past decade, the development of transformations involving gold catalysis has seen remarkable growth accounting for the specific carbophilic nature and stability towards air and moisture that these metal complexes provide. The selectivity for π -bonds ensures a superb functional group compatibility which has been exploited in the synthesis of several complex motifs.¹²

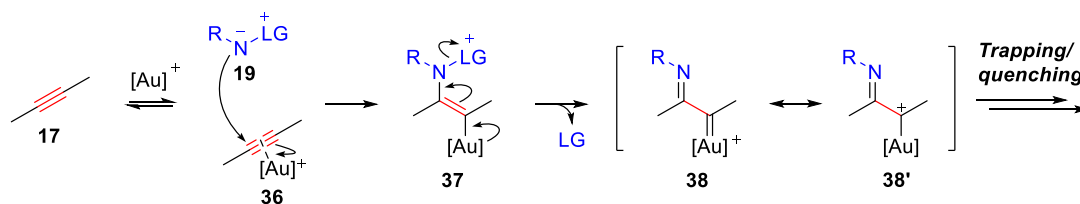
α -Oxo gold carbenes **28** are particularly appealing building blocks due to their selectivity and high reactivity towards different nucleophiles. These versatile intermediates have been largely accessed through the metal-catalysed decomposition of α -diazo carbonyl compounds **29**.¹³ Attending to the hazardous and potentially explosive

character of these precursors, more recent diazo-free alternatives involving the use of alkynes have been gathering notable interest. A number of tethered functional groups, including sulfoxides,¹⁴ oximes/nitrones,¹⁵ amine *N*-oxides,¹⁶ and nitro groups¹⁷ have been employed as oxidants assisting the internal formation of α -oxo gold carbenes.^{12a} The intermolecular generation of gold-carbenes will be discussed in more depth in Chapter 2.



Scheme 6: Common strategies for the synthesis of α -oxo gold carbenes

In contrast with α -oxo gold carbenes **28**, the nitrogen version has received less extensive attention due to the limitations in their synthesis from diazo precursors, which are unstable compounds prone to undergo cyclisation to 1,2,3-triazoles.¹⁸ The recent use of nucleophilic nitrenoids under gold catalysis has provided a powerful tool for the generation of α -imino gold carbenes **38** in the assembly of valuable nitrogen-containing heterocycles (Scheme 7).

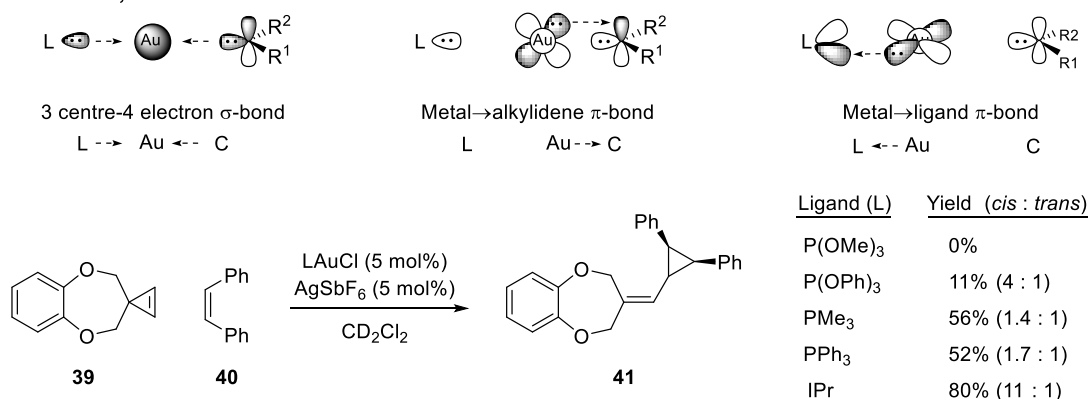


Scheme 7: Nucleophilic nitrenoids in the formation of α -imino gold carbenes through gold catalysis

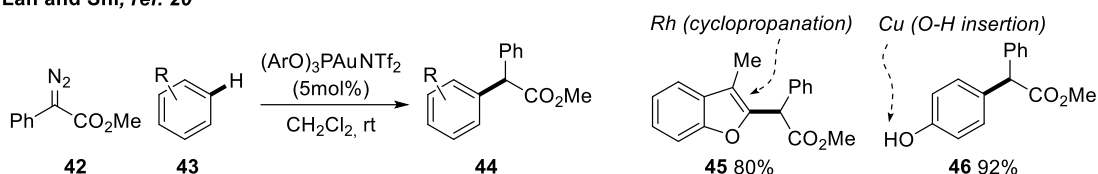
In many transformations described in this chapter gold-carbon double bond **38** and metallated carbocation **38'** have been employed indistinctly to indicate the carbenic reactivity, regardless of the dominant resonance form. The nature and nomenclature for the C–Au bond in various intermediates is a subject of continuing debate.¹⁹ Due to the mixture of π and σ character of these complexes, the actual bonding in the reactive intermediate is going to be greatly influenced in each case by the ligands in the metal and the coordinated organic fragment. Differences in bond distances, orbital participation or charge distribution across related metal-carbon species may have an impact in the resulting reactivity and chemo-/regioselectivity.

Strong σ -donors and weak π -acid ligands (*e.g.* NHCs, electron-rich phosphines) will give more electron density to the gold centre, increasing the gold-to-carbon π -backbonding and resulting in a carbene-like reactivity (Scheme 8 – Top, bonding model proposed by Toste^{19d}). This is exemplified in the work of Toste et al.,^{19d} where a typical carbene behaviour, the stereospecific cyclopropanation of *cis*-stilbene **39**, is progressively encouraged by the σ -donating ability of the ligand (Scheme 8 – Top). By contrast, π -acceptor ligands such as phosphites and electron-poor phosphines reduce the electron density on the gold to be donated into the carbon centre, favouring the carbocation resonance form **38'**.

Toste et al., ref. 19d



Lan and Shi, ref. 20



Scheme 8: Top: Bonding model for gold carbenes and cyclopropanation of *cis*-stilbene; Bottom: Friedel-Craft-type alkylation of arenes induced by electrophilic gold(I) species

This is beautifully represented in the carbophilic addition of α -diazoesters **42** published by Lan and Shi (Scheme 8 – Bottom).²⁰ Here, an electrophilic gold(I) catalyst completely switches the reactivity of a substrate that otherwise presents carbenic character in the presence of rhodium or copper complexes (**45** and **46** respectively).

The recent isolation and inspection of the crystalline structure for complex **47** in the solid state led Fürstner and Seidel to propose an alternative bonding model (Figure 2).^{19b} Based on the long C–Au distance (2.039(5) Å) and shortening of the C–C bonds adjacent to the gold from the aromatic substituent (1.429(7) and 1.444(6) Å), they suggested that there is not significant back-donation from the gold and instead, the carbenic centre is π -stabilised by the organic fragment **47'**. The model is supported by DFT calculations in other gold-complexes.^{19e} However, in complex **47** the structure is stabilised by the presence of strongly-donating groups. As Echavarren and co-workers pointed out: “Predictably, in cases in which the carbene centre cannot obtain sufficient

stabilization from substituents, the back-donation from gold is a source of stabilization, and the gold carbene bonding model is still a pertinent representation.”^{19a}

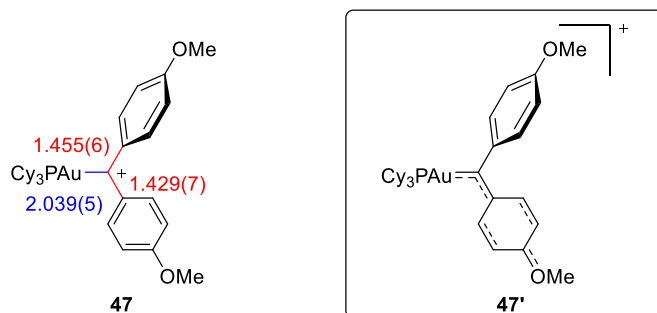
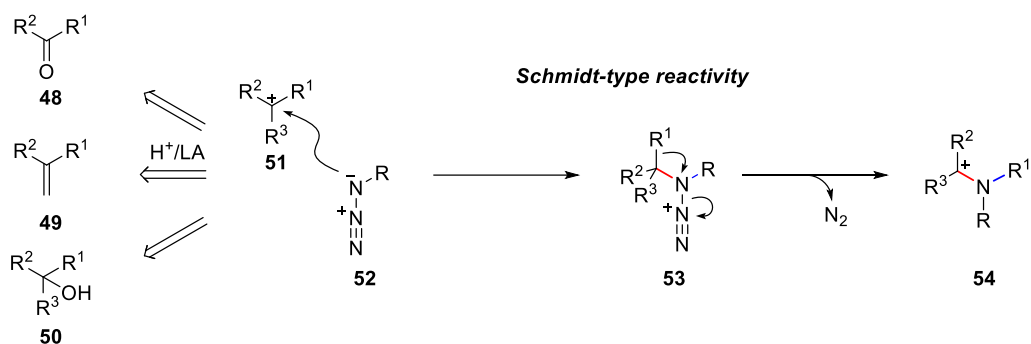


Figure 2: Bond lengths in the solid-state structure for compound **47** and the proposed representation of the bonding. The counterion [NTf₂]⁻ is not shown

Additionally, it should be kept in mind that while α -imino gold carbene **38** is often invoked as the species responsible for the evolution to the final structure (Scheme 7), vinyl gold carbenoid **37** also has electrophilic character. Therefore, reaction at the carbon centre could proceed from either intermediate.

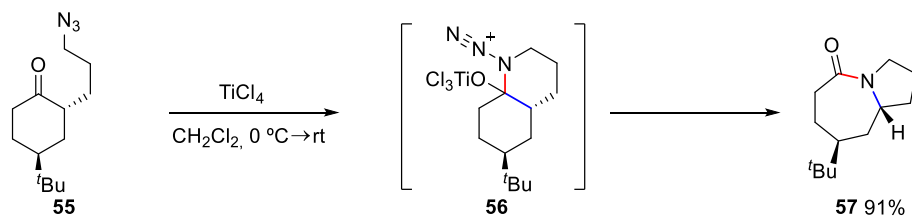
1.1.2 Nucleophilic nitrenoids

The development of synthetic transformations employing nucleophilic nitrenoids can be traced to the Schmidt-type reaction with alkyl azides (Scheme 9),²¹ where a carbocation **51** generated from the Brønsted or Lewis acid activation of a carbonyl, alkene or alcohol **48-50** is attacked by an azide group **52**. The subsequent 1,2-migration onto the nitrogen centre **53** proceeds with elimination of N₂, leading to the formation of two new carbon-nitrogen bonds **54**. The potential of this reaction in nitrogen heterocycle synthesis can be seen in the work done by Aubé^{21e} and Pearson²² (Scheme 10) for the generation of fused scaffolds from the ring expansion of an alkyl azide-substituted cyclic ketone **55** or exocyclic alkene **58** respectively.

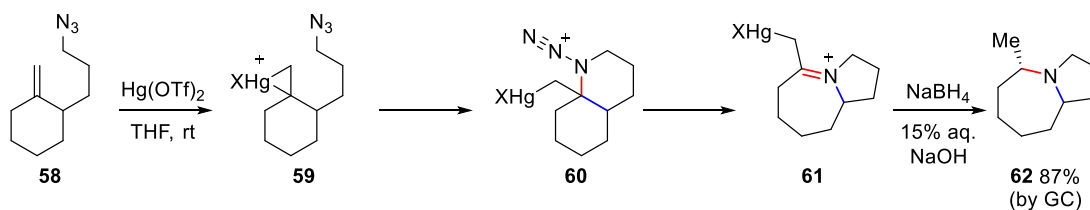


Scheme 9: Reactivity basis of the Schmidt-type reaction

Aubé et al., ref. 21e



Pearson et al., ref. 22



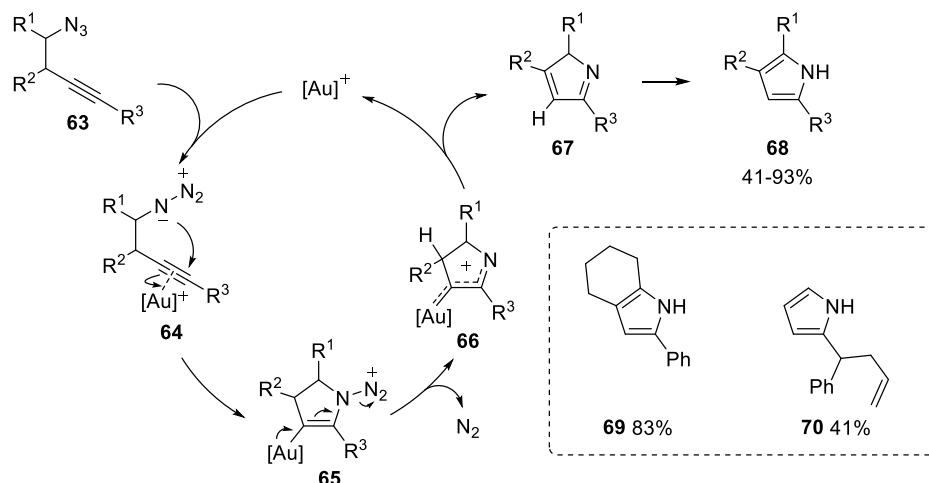
Scheme 10: Schmidt-type reaction in the synthesis of nitrogen-containing heterocycles

Adapting this concept to gold-activated triple bonds allows combining the versatility of alkynes as building block with the excellent functional group compatibility associated with gold catalysis, providing a remarkable tool for the assembly of complex scaffolds.

1.2 Intramolecular reactions

1.2.1 Azides as nucleophilic nitrenoids

The gold-catalysed intramolecular cyclisation of homopropargyl azides **63** under gold catalysis reported by Toste and collaborators (Scheme 11) represents the first example of α -imino gold carbenes generated from the action of a nucleophilic nitrenoid.²³ Analogously to a Schmidt-type process, coordination of the metal to the triple bond **64** triggers the nucleophilic addition of the azide in a *5-endo-dig* fashion, giving vinyl gold carbenoid **65**. This intermediate extrudes N_2 , evolving into a gold carbene **66** that undergoes a 1,2-migration from the adjacent methylene or methine position as the elimination of gold regenerates the catalyst. The resulting *2H*-pyrrole **67** tautomerises to the desired pyrrole **68**.²⁴



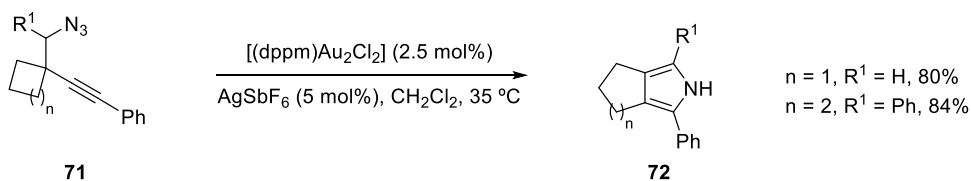
Scheme 11: Synthesis of substituted pyrroles from homopropargyl azides

The reaction tolerated different primary and secondary azides alongside with alkyl- and aryl-substituted alkynes and could be adapted for the synthesis of tetrahydroindoles **69**.

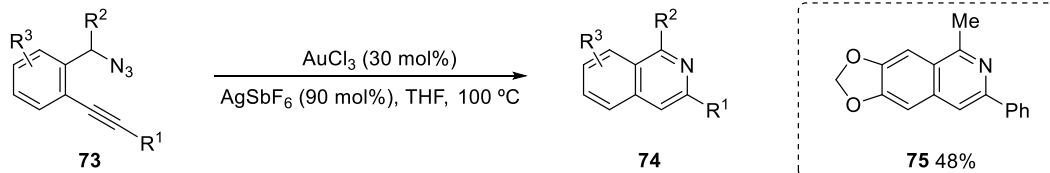
The excellent chemoselectivity discriminated between 1,5-azido-alkyne over a 1,5-enyne, as seen in the formation of compound **70**.

Iterations on this concept using different alkynyl azides have been employed in the synthesis of other useful heterocyclic frameworks (Scheme 12).^{17,23,25}

Toste and co-workers, ref. 23



Yamamoto and co-workers, ref. 25

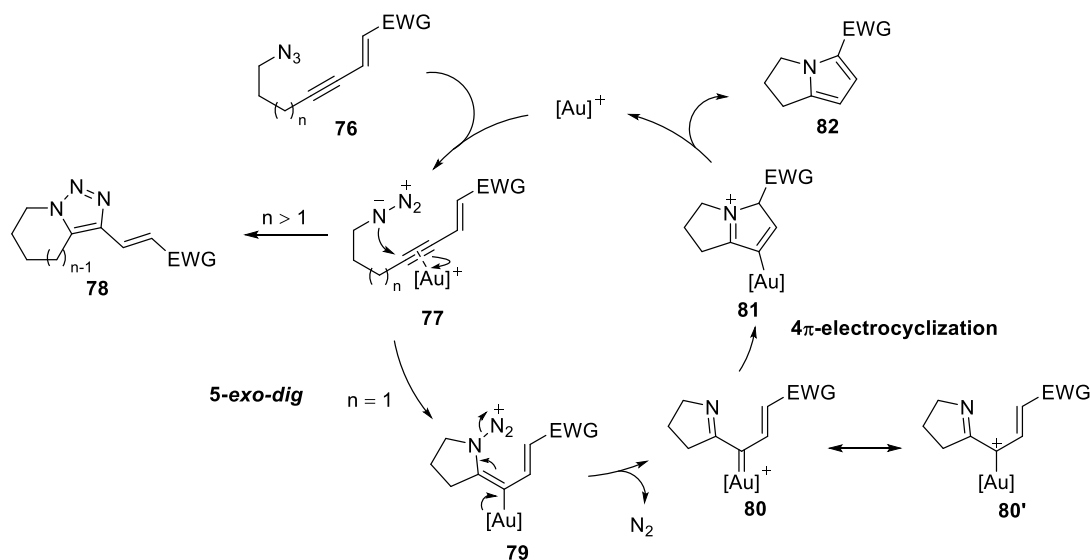


Scheme 12: Top: Tandem cyclisation-ring expansion. Bottom: Synthesis of isoquinoline scaffolds through a 6-*endo-dig* cyclisation of 2-alkynylbenzyl azides

Once the α -imino gold carbenes intermediate is formed, it can evolve following other pathways to the 1,2-migration. Zhang and co-workers took advantage of alkynes conjugated to an electron-deficient alkene **76** (Scheme 13)²⁶ in order to first regioselectively direct the intramolecular attack of an azide group following a desired 5-*exo-dig* cyclisation (**77**→**79**). Secondly, on formation of **80**, the intermediate undergoes a 4π -electrocyclic ring closure to give the bicyclic pyrrole **82**. Alternatively, external nitriles were later employed to capture the reactive species **80** giving analogous fused imidazole systems.²⁷

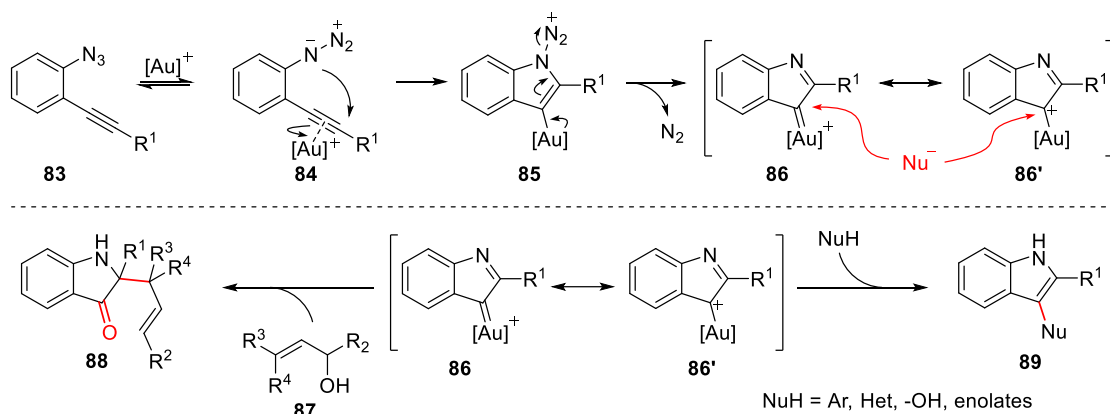
A thermally-induced [3+2]-dipolar cyclisation to the triazole **78** was observed competing with the formation of the α -imino gold carbene **80** on increase of the length of the tethered azide ($n > 1$). The yields of this by-product could be reduced by using

the azidoenyne precursor **76** immediately after purification along with a higher catalyst loading.

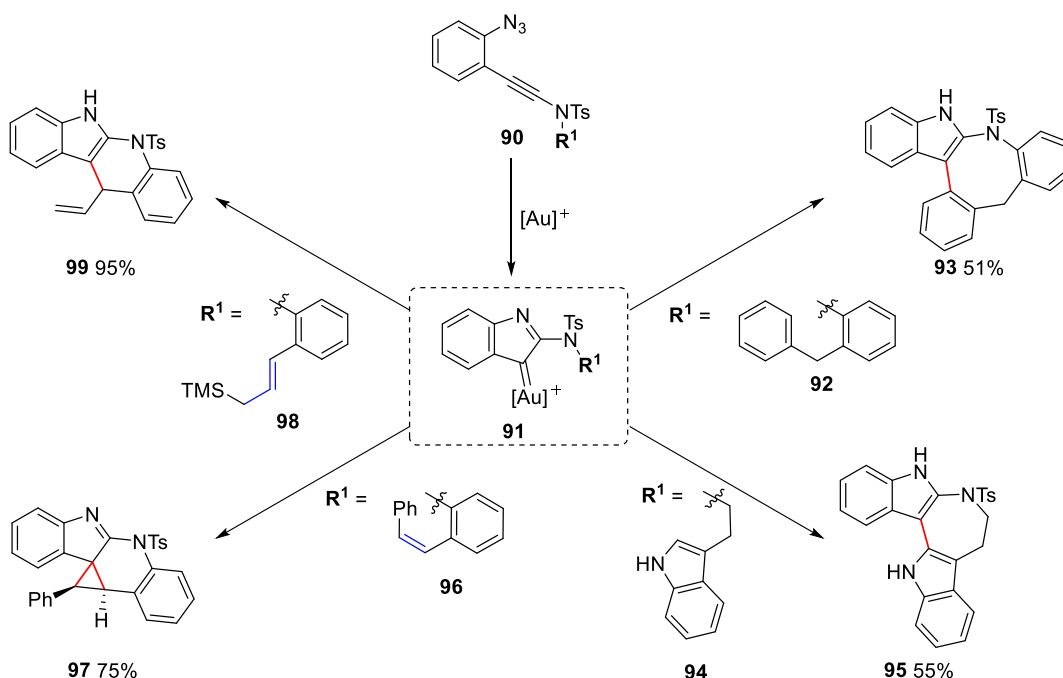


Scheme 13: Tandem cyclisation-ring closure for the synthesis of 2,3-dihydro-1H-pyrrolizines **82**

The groups of Zhang and Gagosz independently reported the reaction of 2-alkynylaryl azides **83** under gold catalysis as means to generate an electrophilic carbenic intermediate **86/86'**, that could be trapped by both internal and external nucleophiles to deliver substituted indole derivatives **89** (Scheme 14).²⁸ This can be seen as an umpolung process, where the typical nucleophilic character at the C3 position of the indole is reversed in **86/86'**. The scope of nucleophiles included several aromatic and heteroaromatic systems as well as alcohols and enolates. Interestingly, trapping of the α -imino gold carbene species **86** with allylic alcohols **87** triggered a Claisen rearrangement to the 2,2-disubstituted indolin-3-one **88**.²⁹

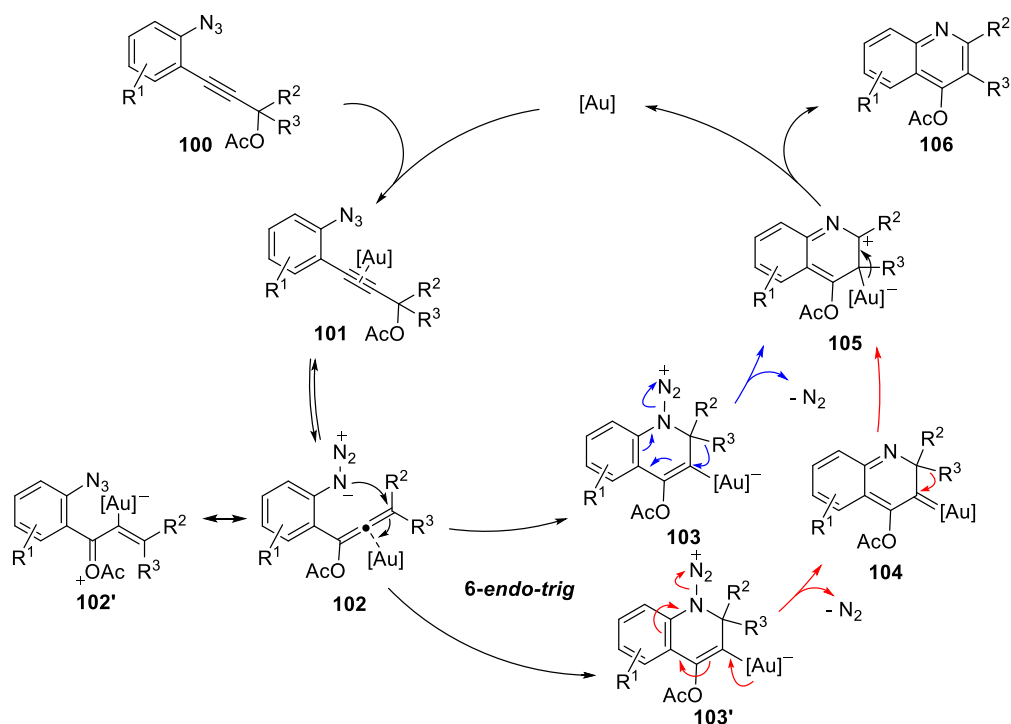


Scheme 14: Synthesis of substituted indoles **89** and indolin-3-ones **88** from 2-alkynylaryl azides **83**



Scheme 15: Gold-catalysed cascade cyclisation of 2-azidoaryl ynamides **90**

A particularly impressive variation of this concept was achieved by modifying the 2-alkynylaryl azides precursor incorporating an ynamide **90** (Scheme 15).³⁰ As a result, a wide range of different *N*-tethered functionality could be employed to capture the incipient α -imino gold carbene (*via* C-H insertion onto aryl- **92** and heteroaryl groups **94** or cyclopropanation **96/98**), providing a simple route for the assembly of several indole-fused polycyclic frameworks.



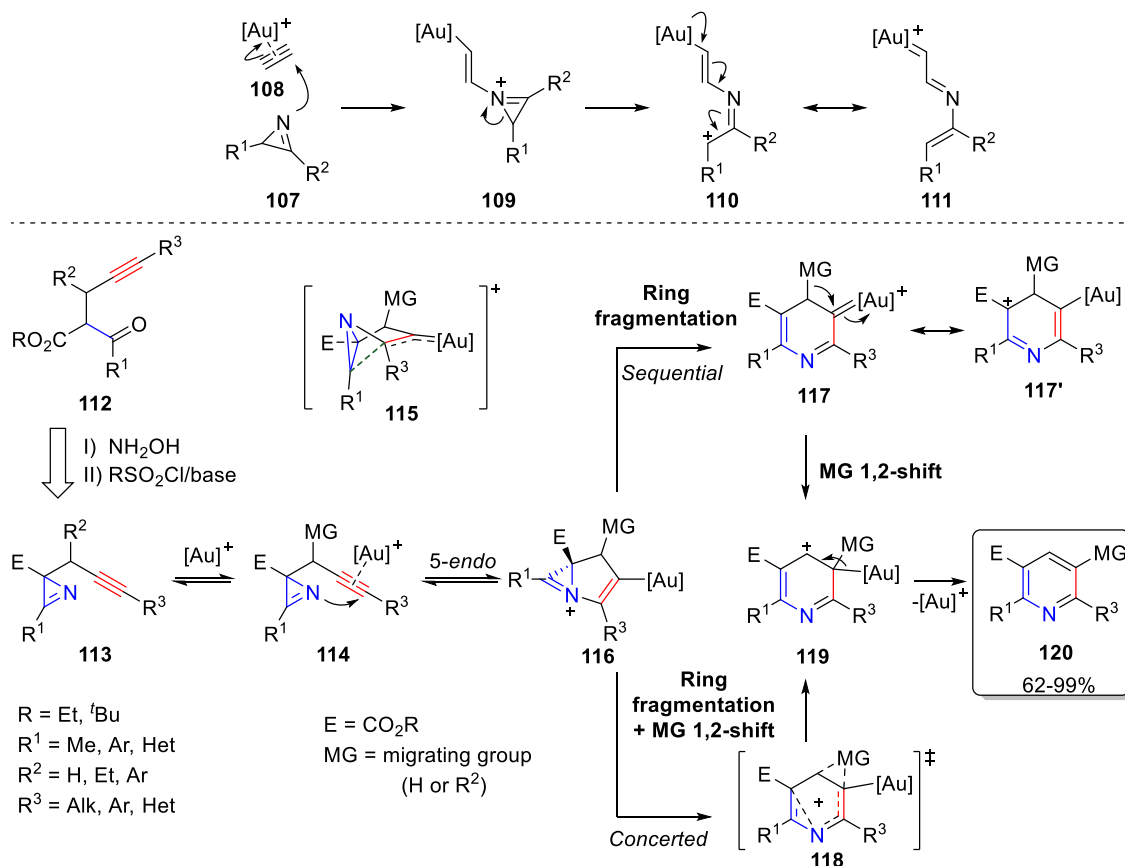
Scheme 16: Gold-catalysed synthesis of substituted quinolines from 2-alkynylaryl azides

Interestingly, by using propargylic carboxylates **100** the reactivity of the gold-activated 2-alkynylaryl azides **101** can be directed away from the α -imino gold carbene and towards a rearranged gold-allenoxo complex **102** that undergoes a *6-endo-trig* cyclisation **103**. The subsequent 1,2-shift from the adjacent substituents can happen either simultaneous (**103**→**105**) or after the extrusion of N_2 (**103'**→**104**→**105**), giving functionalised quinolines **106** on release of the gold species. Precursors with two different propargyl substituents ($R^2 \neq R^3$) afforded mixtures of regioisomers with ratios according to the migratory aptitude of each group ($H > \text{vinyl} > \text{alkyl} > \text{Me}$).

1.2.2 Azirines as nucleophilic nitrenoids

In addition to azides, *2H*-azirines **107** have also been used as nucleophilic nitrenoids in the intramolecular generation of α -imino gold carbene species (Scheme 17).³¹ In this case, after the addition onto the π -acid activated alkyne **108**, the nucleofuge-elimination

step is replaced by the opening of the strained three-membered ring **109**, leading to the familiar vinyl gold intermediate **110**.



Scheme 17: 2*H*-azirines in the gold-catalysed intramolecular synthesis of functionalised pyridines

2-Propargyl-2*H*-azirines **113** were prepared following a two-step procedure from carbonyl **112** through the oxime. On activation by gold **114**, a 5-*endo-dig* cyclisation is triggered giving **116**. It was proposed that the cationic charge in **116** could be stabilised by the overlapping with the vinyl gold π -system (represented in **115**). The intermediate then follows a ring fragmentation and 1,2-migration in either a sequential (**116**→**117/117'**→**119**) or concerted manner (**116**→**118**→**119**) giving polysubstituted pyridines **120** after elimination of gold. The concerted pathway is more supported by the

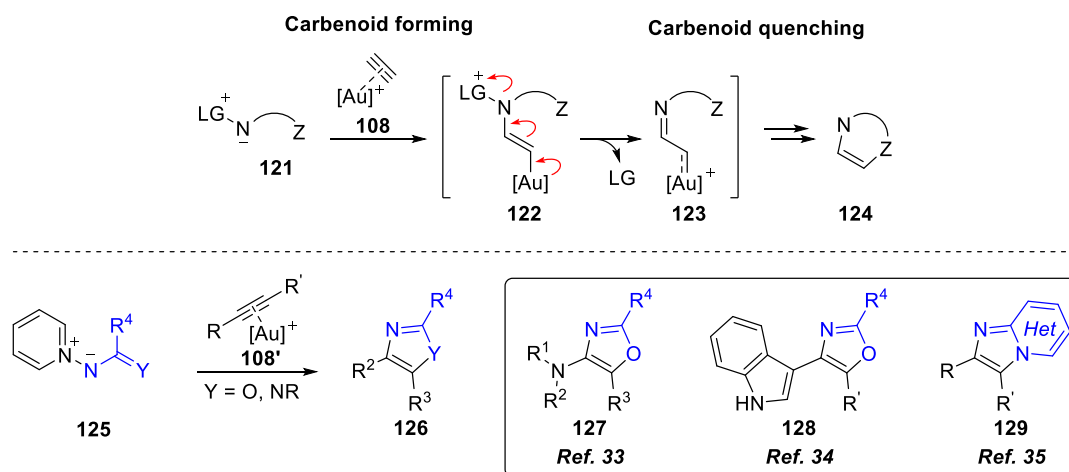
authors as well as by DFT calculations.³² A great number of different substituents were tolerated in azirine scaffold, propargylic position and alkyne.

1.3 Intermolecular reactions

1.3.1 Aminides as nucleophilic nitrenoids

As seen above, previous routes for the generation of α -imino gold carbenes in the synthesis of *N*-heterocycles required a link between the alkyne and the nucleophilic nitrenoid in order to control the cyclisation. Davies and co-workers were the first ones to realise that a suitable functionality (represented by **Z**, Scheme 18) could be incorporated into the nitrene equivalent **121**, trapping the carbenic centre immediately to the formation of intermediate **122/123**.³³ As a result, nitrogen containing cycles **124** can be accessed in a formal cycloaddition process. This convergent approach enables the use of versatile precursors that allow the synthesis of complex nitrogen-containing heterocycles.

For this strategy, pyridinium *N*-acyl^{33,34} and -heteroaryl³⁵ aminides **125** were employed as nucleophilic nitrenoids that on addition to the gold-activated π -system, eliminate a pyridine leaving group to reveal the carbenic character. By its interaction with the tethered heteroatom (**Y** in Scheme 18), polysubstituted oxazole **127-128** and fused imidazole motifs **129** are generated in an efficient and general manner. The process can be seen as a formal [3+2]-dipolar cycloaddition where the aminide behaves as *N,O*- and *N,N*-dipole equivalents. Ynamides and indolylalkynes were employed as π -systems that coordinate to gold, introducing regiocontrol in the addition of the nucleophile due to the predictable reactivity that these compounds provide (Scheme 28 and Scheme 35).

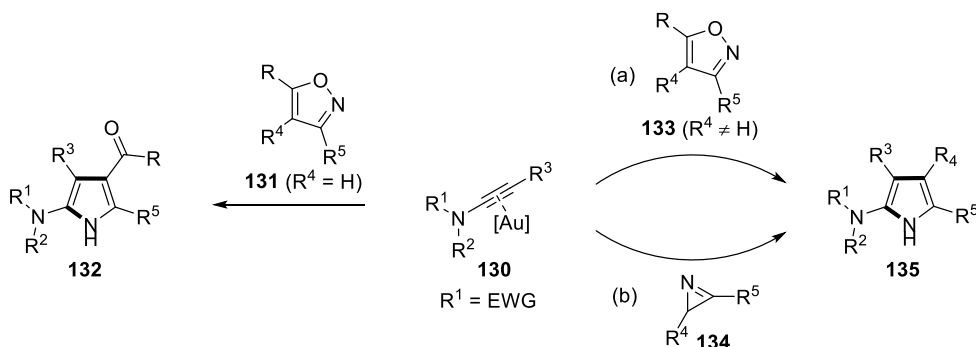


Scheme 18: Aminides as nucleophilic nitrenoids in ring-forming reactions

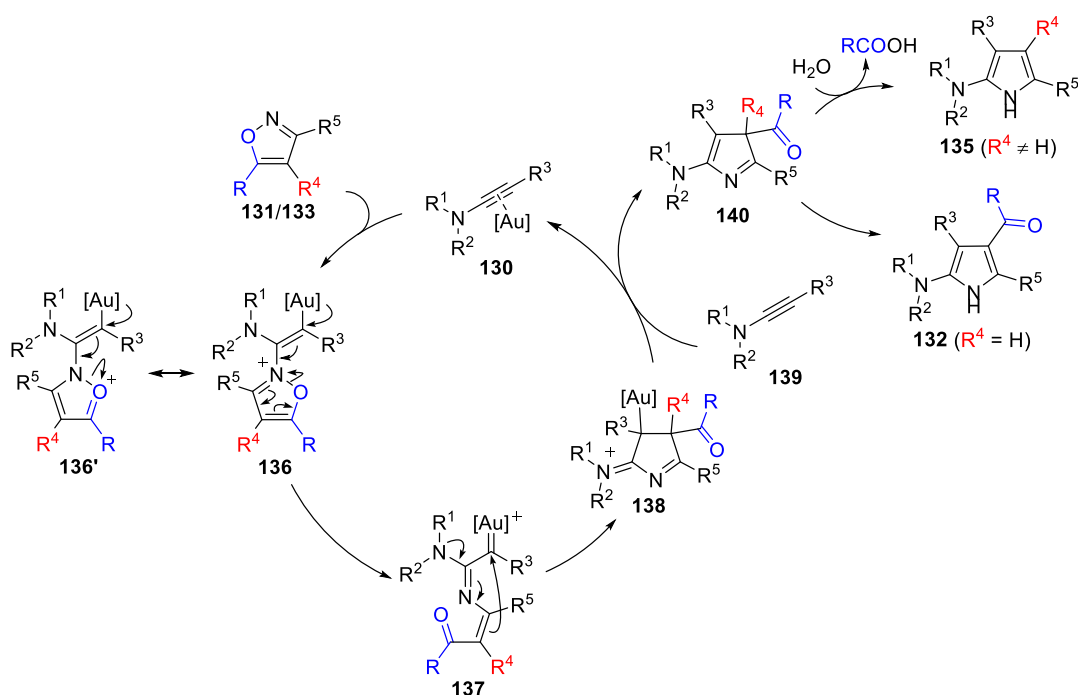
The following intermolecular ring-forming methodologies build upon this idea of envisioning the reaction as a formal dipolar cycloaddition. A more thorough analysis of aminides as nitrene equivalents will be further discussed in Chapter 2 as it is the main topic of the present thesis.

1.3.2 Isoxazoles and azirines as nucleophilic nitrenoids

The following two nucleophilic nitrenoids are combined in the same section due to their similarities in mechanism and resulting products. Both strategies are based on a formal [3+2] dipolar cycloaddition onto a π -activated alkyne **130** where the addition and subsequent ring opening of isoxazoles³⁶ **131/133** or azirines³⁷ **134** lead to polysubstituted pyrrole scaffolds **132/135** through an intermediate α -imino gold carbene (Scheme 19). Ynamides **139** are employed again (*cf.* Scheme 18) as electronically biased triple bond in order to introduce regiocontrol in the intermolecular process.



Scheme 19: Nucleophilic nitrenoids in the intermolecular synthesis of pyrrole derivatives

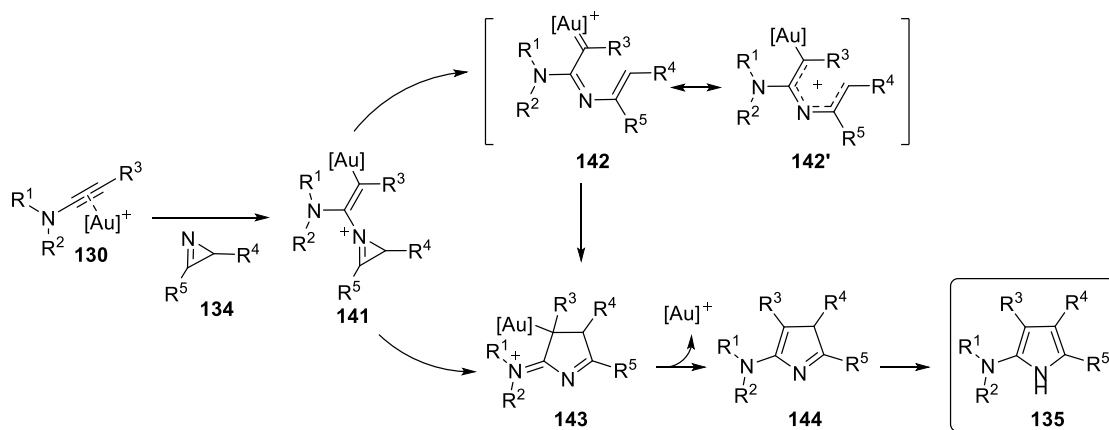


Scheme 20: Proposed mechanism for the isoxazole-based synthesis of 2-aminopyrroles

In the isoxazole system (Scheme 20),³⁶ nucleophilic attack of the heterocycle **131/133** onto the gold-activated ynamide **130** forms the vinyl gold carbenoid species **136**. N–O bond cleavage gives intermediate **137** which cyclises to acylpyrrole **138**. Following deauration to **140**, this system can evolve into two different products depending on the substitution pattern in the isoxazole precursor. The 3,5-disubstituted species **131** ($R^4 = \text{H}$) undergoes a hydride shift affording 4-acylated-2-aminopyrroles **132**. Trisubstituted

isoxazoles **133** ($R^4 \neq H$) are suggested to follow a water-aided deacylation to provide aromatisation **135**.

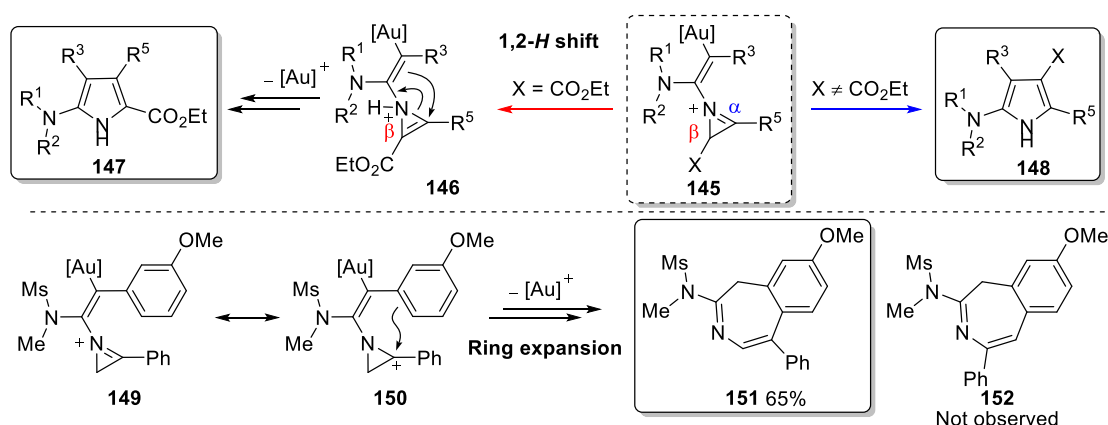
Analogous to the intramolecular version (Scheme 17), the reaction between azirines **134** and gold-activated ynamides **130** are proposed to evolve into the cyclic intermediate **143** (Scheme 21) either by direct addition of the gold-enamide moiety to the azirine *2H*-position (**141**→**143**) or by stepwise, gold-assisted N–C bond cleavage to give a α -imino gold carbene intermediate that undergoes a 4π -electrocyclisation (**141**→**142/142'**→**143**).³⁷



Scheme 21: Proposed mechanism for the *2H*-azirine-based intermolecular synthesis of 2-aminopyrroles

Overall, both nucleophilic nitrenoids can be seen as 1,3-*N,C*-dipole equivalents in a formal cycloaddition process. Substantial structural variations and functionality can be tolerated in each of the constituents, although ynamides with straight-chain aliphatic groups are prone to undergo competitive 1,2-C–H insertion pathways to the α,β -unsaturated amines. This feature will be also characteristic of other intermolecular reactions with nucleophilic nitrenoids discussed in Chapter 2.

Interestingly, Liu and co-workers found that 2-aminopyrrole products **147** afforded by reactions with 2-ester-substituted 2*H*-azirines **145** ($X = \text{CO}_2\text{Et}$) presented a divergent regioselectivity consistent with the cleavage of the azirine $\text{C}_\alpha\text{--N}$ bond (Scheme 22).³⁸ According to the proposed mechanism, the intermediate **145** would undergo a 1,2-hydrogen shift **146** followed by addition and ring opening. The formation of a single regioisomer **147** rules out an intermediate α -imino gold carbene (*i.e.* **142** in Scheme 21) as this requires the cleavage of the $\text{C}_\beta\text{--N}$. This is further supported by the formal [4+3] cyclisation observed when aryl-ynamides bearing electron-donating groups were employed (**149**→**150**), giving 1*H*-benzo[*d*]diazepines **151**.



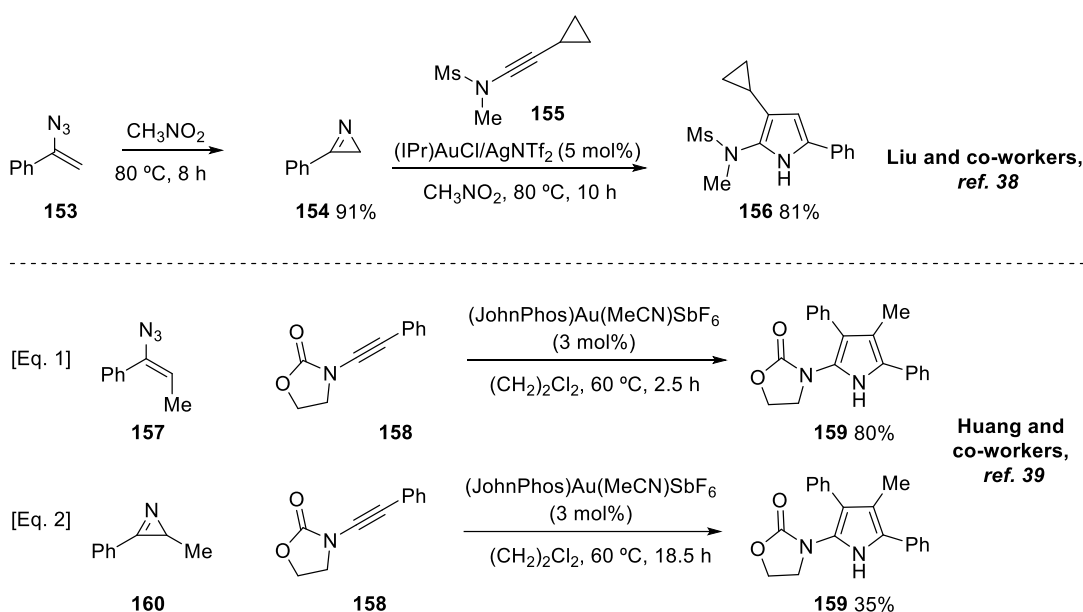
Scheme 22: Diversity in the formal cycloaddition with 2*H*-azirines

1.3.3 Azides as nucleophilic nitrenoids

Following the development of the aforementioned azirine-based strategy for the synthesis of pyrroles, several groups simultaneously envisioned vinyl azides as opened azirines and therefore able to provide a vinyl nitrene/1,3-*N,C*-dipole reactivity in the synthesis of analogous 2-aminopyrroles and 1*H*-benzo[*d*]diazepines.³⁷⁻³⁹ While the precise mechanism is not fully clear yet, Liu and co-workers proved that vinyl azides **153** undergo a thermally-induced cyclisation to the 2*H*-azirines **154** upon heating

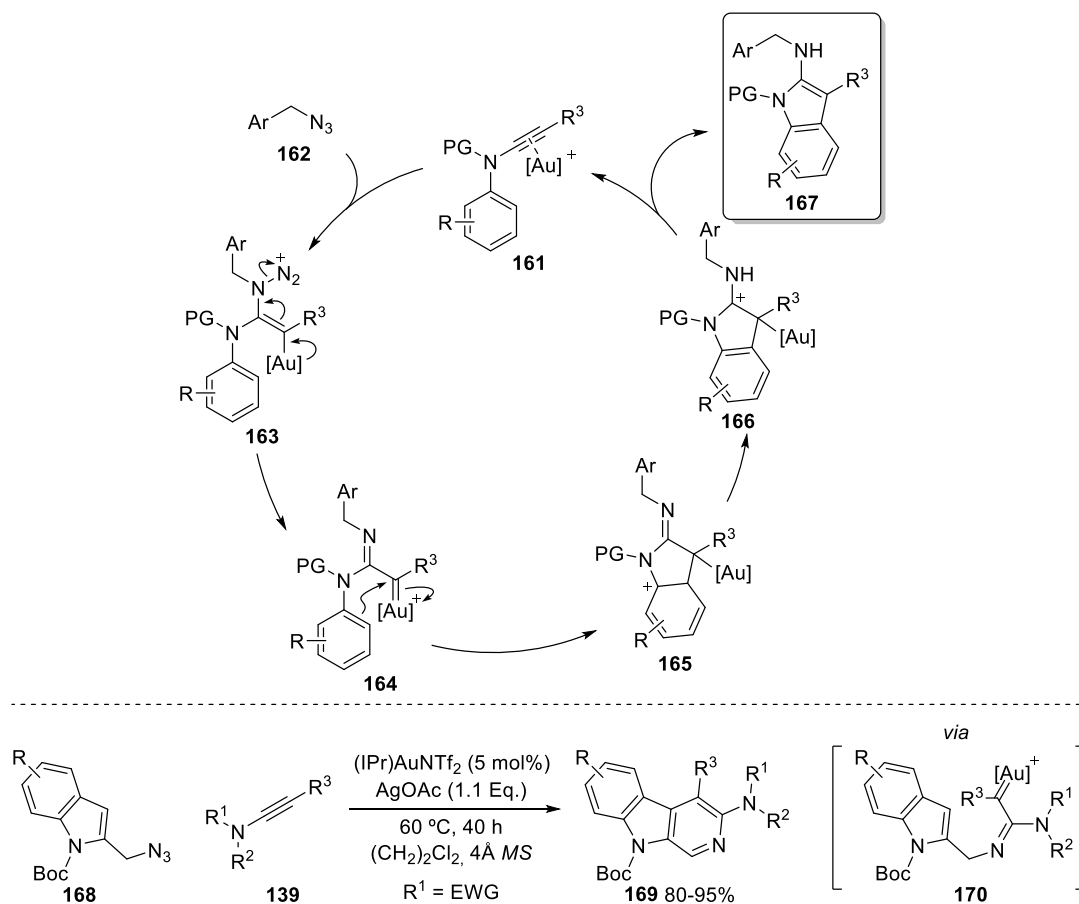
(Scheme 23, Top).^{38,40} Hence, it is possible that the actual reaction intermediate is again the three-membered ring.

It is noteworthy that Huang's conditions applied to 2*H*-azirine **160** (Eq. 2) gave a much lower yield of the resulting 2-aminopyrrole **159** than with vinyl azide **157** (Eq. 1),³⁹ fact that was attributed to the partial poisoning of the gold catalyst by the more nucleophilic aza-heterocycle **160**.



Scheme 23: Vinyl azides in the intermolecular synthesis of pyrroles. Top: Thermally-induced formation of 2*H*-azirines. Bottom: Comparison of the reactivity between **157 and **160****

A more direct use of azides as nitrene transfer reagent in intermolecular reactions was developed by Lu and Ye,⁴¹ by employing benzyl azides **162** in combination with gold-activated ynamides **161** (Scheme 24). Analogously to the work done by Ohno and collaborators using 2-azidoaryl ynamides (Scheme 15),^{30a} the generated α -imino gold carbene intermediate **164** is trapped by the functionality attached to the ynamide (*i.e.* C-H insertion into an aryl group), giving in this case polysubstituted 2-aminoindole derivatives **167**.



Scheme 24: Intermolecular azide-based synthesis of 2-aminoindoles and 3-amino- β -carbolines

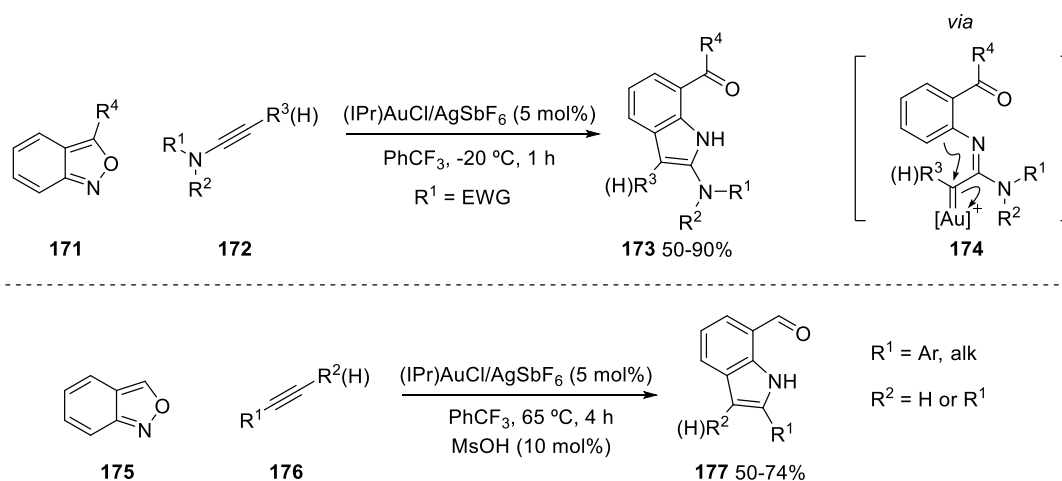
Additionally, the reaction can be adapted to indolyl azides **168**, where the nucleophilic C3 position of this heterocycle captures the gold carbene **170**, leading to 3-amino- β -carbolines **169**. Use of an external oxidant such as AgOAc proved beneficial for this reaction, giving in some cases near quantitative yields of the desired product.

Surprisingly, there are no mentions to the formation of a competitive 1,2,3-triazole product, found in other reactions involving azides and triple bonds (*cf.* Scheme 13).⁴² This could be related with a quick generation of the intermediate **165**, which circumvents the dipolar cycloaddition pathway.

1.3.4 Other nucleophilic nitrenoids

In addition to the previously covered nitrene transfer reagents, two recent methodologies showcase the use of novel nucleophilic nitrenoid types in intermolecular reactions with the added feature that non-heteroatom-polarised gold-activated alkynes (*i.e.* ynamides or 3-indolylalkynes) are required for the control of the regiochemistry.

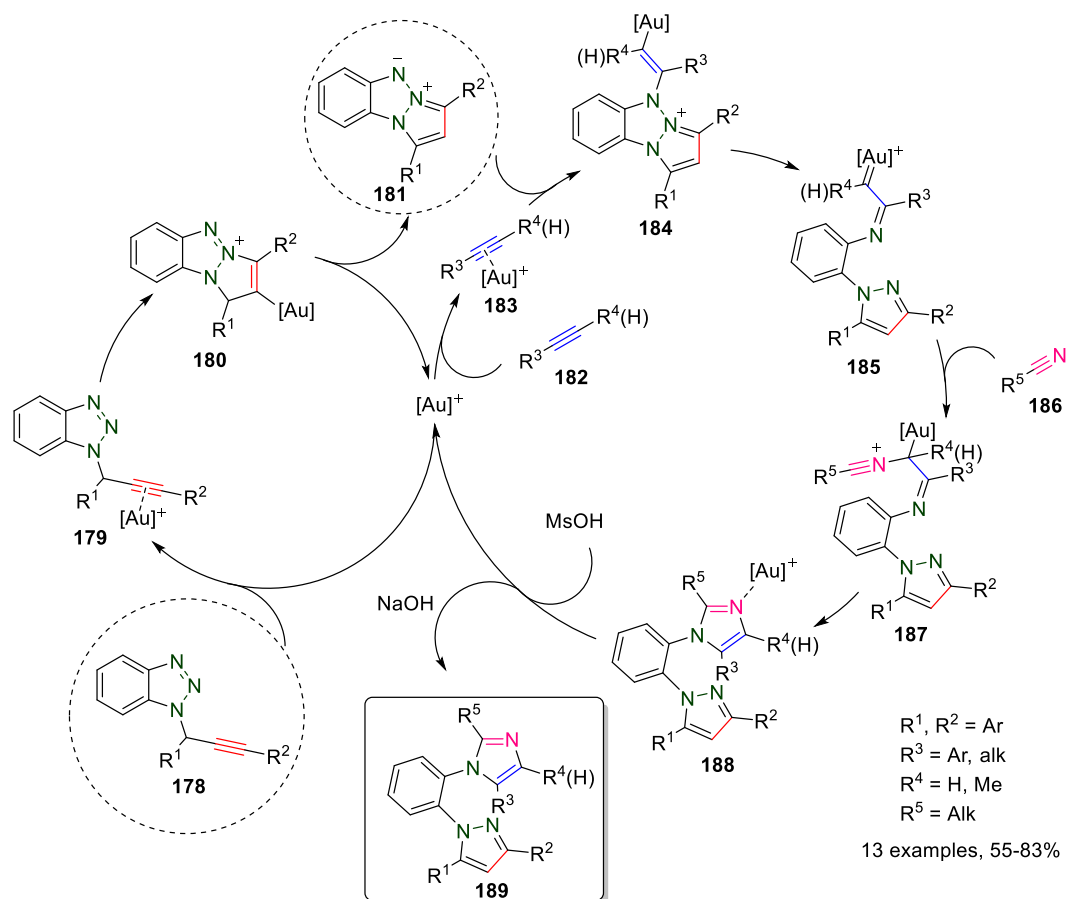
The first one is a variation of the isoxazole-based strategy (Scheme 20)³⁶ where anthranile derivatives **171** (*i.e.* benzo[*c*]isoxazoles) are employed to access the α -imino gold carbene **174** (Scheme 25).⁴³ The electrophilicity of this intermediate triggers an *ortho*-aryl C–H insertion to furnish 7-formyl indoles **173**.



Scheme 25: Anthraniles in the intermolecular synthesis of 7-formyl indoles

Terminal ynamides were mainly employed as π -systems to coordinate the gold catalyst. While aryl-substituted ynamides also underwent smooth conversion to the target product, alkyl-substituted systems afforded unsaturated products consistent with 1,2-C–H insertion. Additionally, terminal/symmetrical alkynes **176** underwent reaction with anthranile **175**, although these less reactive triple bonds required higher temperatures and substoichiometric amounts of MsOH (believed to facilitate the deauration process)

to reach moderate yields. Interestingly, a competing hydride shift pathway was not observed with alkyl-substituted terminal alkynes.



Scheme 26: Proposed mechanism for the gold-catalysed synthesis of 2-imidazolyl-1-pyrazolylbenzene scaffolds

Finally, Ballesteros and collaborators work unveiled azomethine imine-type heterocycles **181**⁴⁴ as nucleophilic nitrenoids in the synthesis of 2-imidazolyl-1-pyrazolylbenzene scaffolds **189** (Scheme 26).⁴⁵ These complex heterocycles are the result of a cascade multicomponent reaction where an *N*-propargyl benzotriazole precursor **178** undergoes an initial gold-catalysed 5-*endo-dig* cyclisation (**179**→**180**) generating an isolable triazapentalene derivative **181**. This compound reacts with a second gold-activated alkyne to give an α -imino gold intermediate after N–N bond scission (**184**→**185**) which is trapped by an external nitrile **186**. Intramolecular ring

closing (**187**→**188**) forms the imidazole part of the molecule which is sequentially treated with MsOH (to aid the protodeauration) and base to afford the desired product **189**.

Overall, this is a highly efficient and atom-economic process where 4 new C–N bonds are created in a single pot.

1.4 Conclusions

In summary, gold carbenes are highly versatile intermediates that provide a quick and efficient route for the synthesis of a wide range of diverse scaffolds. The development of novel nucleophilic nitrenoids through gold catalysis has resulted in the flourishing of many methodologies to access previously elusive α -imino gold carbene reactivity patterns. The evolution of these species through subsequent 1,2-migration, cyclopropanation, C–H insertion or 4π -electrocyclisation pathways allow the assembling of valuable nitrogen-containing heterocycles. These transformations are characterised by a superb functional group compatibility, excellent chemoselectivity and efficiency.

The number of nucleophilic nitrene transfer reagent has undergone a remarkable growth over the last years. The early work in the field has been dominated by intramolecular reactions where azide-substituted substrates were employed to direct the cyclisation towards the synthesis of pyrroles, quinolines and indole derivatives. Analogously, the use of *2H*-azirines has facilitated the formation of polysubstituted pyridines. More recently, these processes have been complemented with intermolecular strategies using pyridinium *N*-aminides, *2H*-azirines, isoxazoles, azomethine imines or vinyl/benzyl

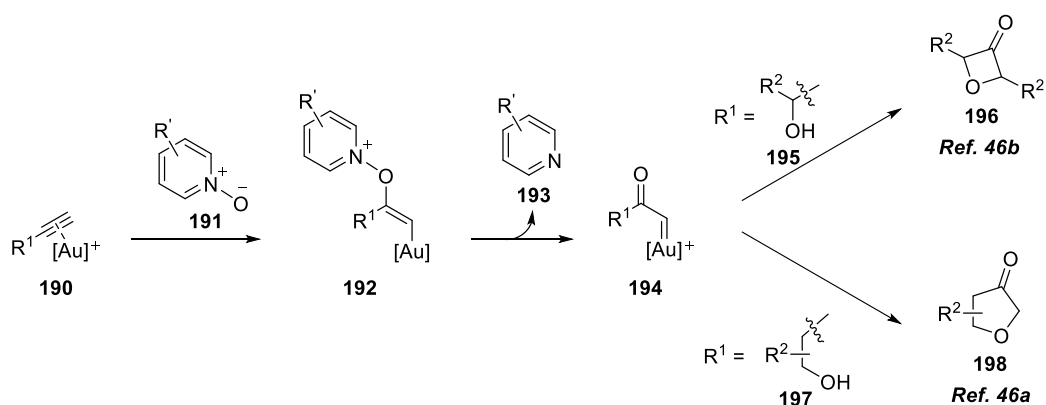
azides in the synthesis of five-membered heteroaromatics. The combination of these nitrene equivalents with π -activated triple bonds can be seen as a formal cycloaddition process, where electronically-biased alkynes are generally exploited to establish regiocontrol in the addition.

The present thesis explores the development and study of one of these families of nucleophilic nitrenoids as well as their application through gold-catalysis in the synthesis of novel *N*-cyclic scaffolds and influence in following methodologies.

Chapter 2

2.1 Site-specific generation of gold-carbenes

Over the previous chapter the use of nitrene transfer reactions onto gold-activated alkynes have been shown as a particularly fertile area for the synthesis of complex aza-heterocycles. Early strategies in this field relied on intramolecular cyclisation modes in order to selectively direct the formation of the versatile α -imino gold carbene intermediate.

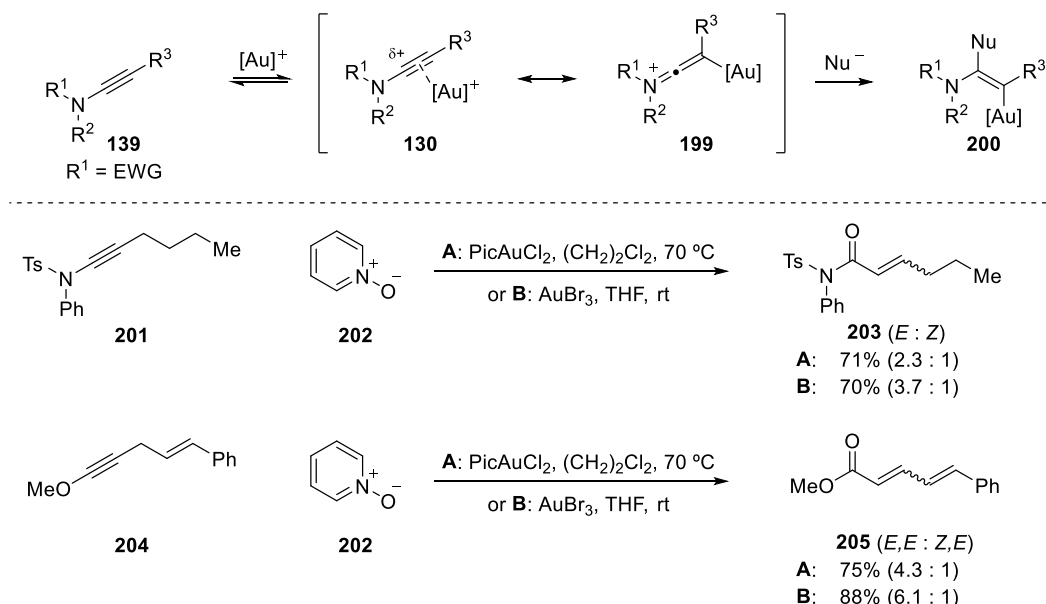


Scheme 27: Gold-activated alkynes in the intermolecular generation of α -oxogold carbenes

The development of intermolecular processes stems from the work done in site-selective generation of α -oxo gold carbene from gold-activated alkynes. Zhang and collaborators first demonstrated that pyridine-*N*-oxides **191** could be used as intermolecular oxidants in the generation of oxetanones **196** and dihydrofuranones **198** from propargyl **195** and homopropargyl alcohols **197** respectively (Scheme 27).⁴⁶ Similarly to the reactivity-basis previously discussed for nucleophilic nitrenoids (Scheme 7), coordination to gold renders the alkyne electrophilic **190**, allowing attack of the oxidant. Subsequent loss of pyridine derivative **193** leads to the reactive α -oxo gold carbene **194** which can be captured by the tethered alcohol giving the desired cycle. By using terminal alkynes the

carbenic centre in **192** was selectively formed on the terminus of the triple bond introducing control over the size of the ring.

In order to establish regiocontrol for the addition of the oxidant onto internal alkynes Davies and co-workers proposed ynamides **139** as suitable substrates for the gold catalysis.⁴⁷ In these compounds, the contribution of the gold keteniminium resonance form **199** to the structure of the metal-activated π -system creates an electronic bias across the triple bond (Scheme 28 – Top). As a result, the attack of the nucleophile is directed selectively to the α -position of the ynamide **200**.



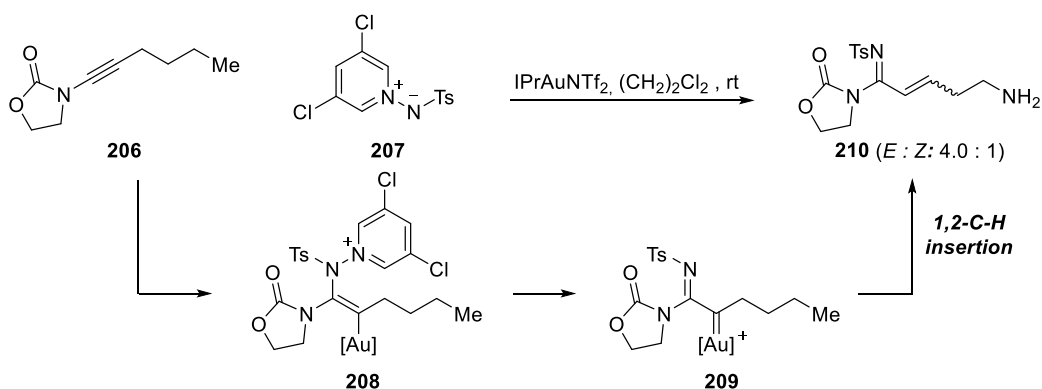
Scheme 28: Top: Gold-activated ynamides in site-selective formation of α -oxo gold carbenes; Bottom: Gold-catalysed synthesis of α,β -unsaturated imines and carboxylic ester

This concept was adapted to the generation of α -oxo gold carbenes by using alkyl-substituted ynamides **201** (Scheme 28 – Bottom). Unlike preceding methodologies, no Brønsted acid was required to obtain productive catalysis and commercially available pyridine-*N*-oxide **202** could be used as external oxidant. Interestingly, on formation the metal carbene undergoes a 1,2-C–H insertion into an adjacent $\text{C}(sp^3)$ position, allowing

the regioselective synthesis of valuable α,β -unsaturated imides **203**. The *E*-isomer was the predominant or sole product formed. The reaction tolerated a wide range of substituents and could be extended to highly reactive ynol ethers **204** in place of ynamides, giving α,β -unsaturated carboxylic ester **205**. A similar reaction was independently reported by Zhang and co-workers where sterically biased all-carbon substituted alkynes were used.^{46c}

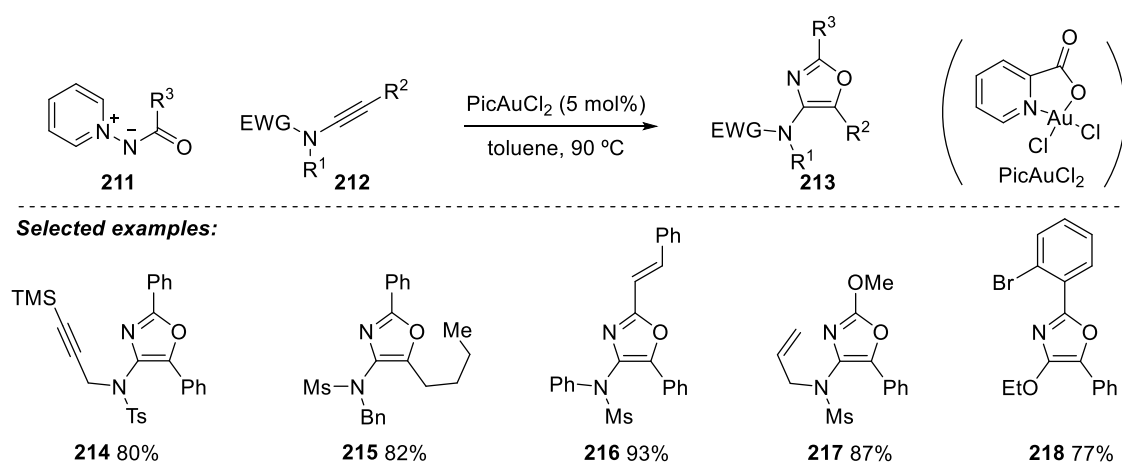
2.1.1 Pyridinium aminides in nitrene transfer reactions

Concurrently in time to the previous transformation (Scheme 28), Li and Zhang published a gold-catalysed ynamide-based methodology for the site-specific generation of α -imino gold carbenes **209**.⁴⁸ These intermediates were obtained by reaction of alkyl-substituted ynamides **206** with *N*-tosyl pyridinium *N*-aminide **207**, undergoing an analogous 1,2-C–H insertion process for the synthesis of α,β -unsaturated amidines **210**. Again, addition of the nucleophile into the gold-activated ynamide is regioselective. This is the first reported example of pyridinium *N*-aminides being used as intermolecular nitrene transfer reagents.⁴⁹



Scheme 29: Gold-activated ynamides in site-selective formation of α -imino gold carbenes

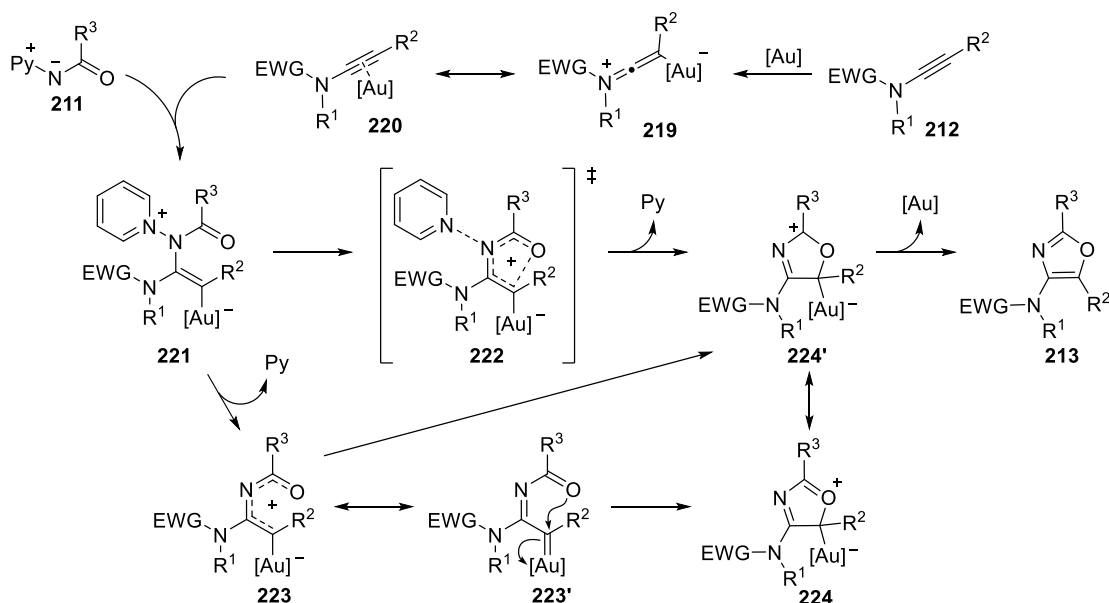
The 1,2-C–H insertion reaction of a putative gold-carbene (*i.e.* **209**→**210** in Scheme 29) is one of several quenching pathways. Concurrently with the above mentioned methodology, Davies and co-workers proposed the formation of α -imino gold carbenes as basis for a formal [3+2]-dipolar cycloaddition strategy, leading to a convergent synthesis of trisubstituted 1,3-oxazoles **213** (Scheme 30).³³ Here, pyridinium *N*-acyl aminides **211** are similarly employed as nitrene transfer reagents for the reaction with gold-activated ynammides. Additionally, after initial attack of the nucleophile **211**, the acyl residue appended to the nucleophilic nitrogen can capture the resulting electrophilic intermediate **221/223** (Scheme 31).



Scheme 30: Gold-catalysed synthesis of trisubstituted oxazoles

The highly reactive ynol ethers can also be used in place of ynammides as electronically biased π -systems that lead to the formation of analogous alkoxyoxazole systems **218**. Superb chemoselectivity and regioselectivity were obtained with the excellent functional group tolerance accounting for a broad substrate scope that includes alkyl, vinyl, alkynyl and different aryl and heteroaryl substituents at the three available positions of the ring (Scheme 30). This strategy has been recently revisited, expanding the substrate scope in every direction while providing a more efficient route for the

synthesis of aminides.^{34b} Additionally, the loading of both catalyst and aminide has been reduced. As a result, not only have more elaborated systems been accessed, but also thio-, *N*-phosphoramidate and *N*-indole-derived ynamides were employed for the first time under gold catalysis.

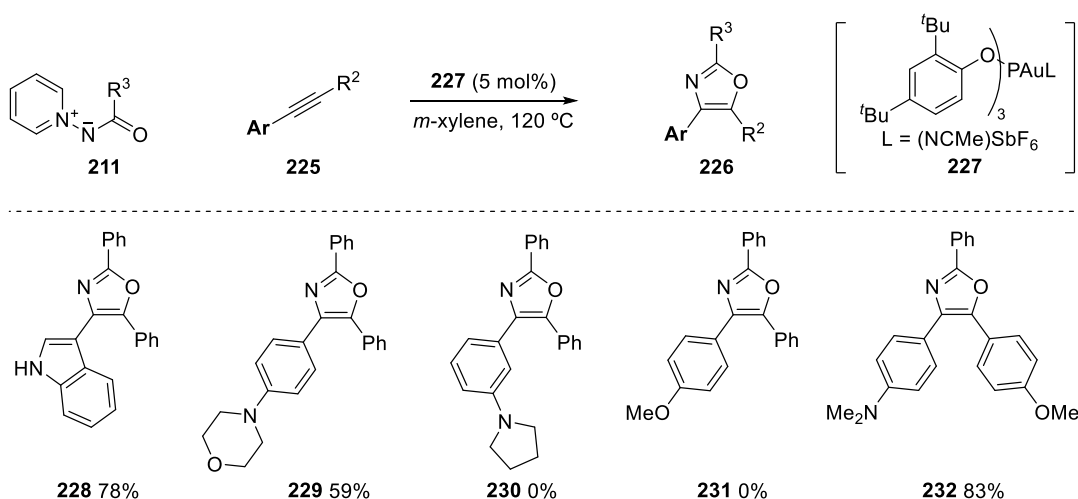


Scheme 31: Proposed mechanism for the gold-catalysed synthesis of trisubstituted oxazoles

The proposed mechanism for this reaction is initiated by the regioselective attack of the aminide **211** onto the gold-activated ynamide **220**, giving the vinyl gold carbenoid **221**. Several routes are suggested for the evolution of this intermediate. Elimination of the nucleofuge in **221** would lead to α -imino gold carbene **223** which could cyclise to **224'** either by interaction of the oxygen lone pair with the electrophilic centre (**223'**→**224**) or undergoing a 4π -electrocyclisation (**223**→**224'**). Considering the tolerance of this strategy towards alkyl groups adjacent to a metal-carbene centre (*e.g.* **215** in Scheme 30), prone to experience competitive 1,2-insertion reactions (*cf.* Scheme 29), the authors indicate that a fast cyclisation must be occurring. Therefore, an alternative pathway is also envisioned where vinyl gold carbenoid **221** undergoes a bis-hetero 4π -

electrocyclisation with concerted scission of the N–N-bond (**221**→**222**→**224'**). The oxazole **213** would be finally obtained after deaurative aromatisation of **224'**.

Chatzopoulou and Davies proved that this reactivity was not limited to heteroatom-substituted triple bonds. Using other π -rich systems such as 3-indolyl- or aniline-based alkynes **225** all-carbon substituted oxazoles **226** were accessed (Scheme 32).^{34a} Similar to ynamides, delocalisation of the more remote nitrogen lone pair across the π -system is crucial for the regioselective cycloaddition of these unsymmetrical alkynes. A reactivity trend was observed in correlation with the ability of the remote heteroatom to donate electron density. Thus, while good yields were obtained from the free indole and aniline systems **228–299**, no reaction occurred with the *m*-aniline or *p*-aniso derivatives **230–231**. Interestingly, a single regioisomer **232** was formed from the reaction with an alkyne bearing two nominal directing groups.



Scheme 32: Gold-catalysed synthesis of all-carbon substituted oxazoles from alkynes bearing a remote nitrogen atom

Higher temperatures, longer reaction times and a re-optimisation of the catalyst to gold(I) phosphite **227** were required in order to achieve productive catalysis. While good yields were obtained by reaction with aryl- and cyclopropyl-substituted

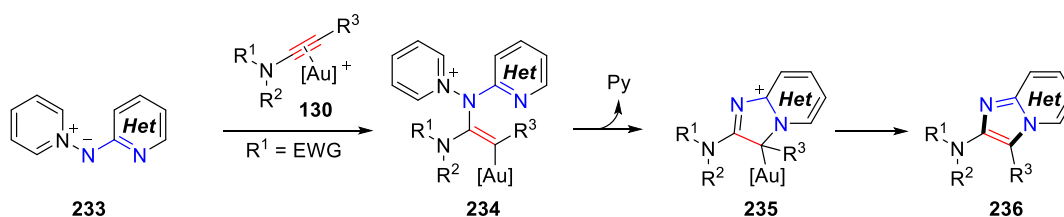
alkynylindoles, complex mixtures of oxazole and 1,2-C–H insertion product were observed when using alkynylindoles bearing alkyl chains. This may be related to the use of more forcing conditions and the different electronic environment around the metal-ynamide complex.

2.1.2 Pyridinium aminides as *N,O*-dipole equivalent

Conceptually, this transformation can be viewed as formal a [3+2]-dipolar cycloadditions where *N*-acyl aminides **211** are used as *N*-nucleophilic *N,O*-dipole equivalents. [3+2]-Dipolar cycloadditions reactions are usually accompanied by a series of desirable characteristics such as efficiency, simplicity, wide scope, selectivity and atom economy; as exemplified by the iconic metal-catalysed synthesis of 1,2,3-triazoles.⁵⁰ Here, azides are employed as general 1,3-*N,N* dipoles that in combination with activated alkynes offer a straightforward way to connect building blocks containing different functionalities. However, adapting this concept to the assembling of other azole systems has been limited by the reachability of the required dipole equivalents. An alkyne-based [3+2]-dipolar cycloaddition for the synthesis of oxazole rings requires the *in situ* generation of electrophilic acyl nitrenes, induced by either thermal or photochemical decomposition of acyl azides.^{3,51} Acyl nitrenes are highly reactive and prone to undergo other rearrangement and insertion pathways, which in practice make them unsuitable for the cyclisation. A modified methodology has recently been published where copper-stabilised acyl nitrenes lead to the formation of disubstituted oxazoles.⁵² In stark contrast, *N*-acyl aminides are bench-stable solids, easy to functionalise and handle making them attractive substrates in these cyclisations.^{34b}

2.1.3 Pyridinium aminides as *N,N*-dipole equivalent

At the start of this PhD the goal was to adapt the aminide-based formal [3+2]-dipolar cycloaddition strategy to the synthesis of unexplored imidazole based scaffolds. To this end pyridinium *N*-(heteroaryl) aminides **233** were selected as prospective 1,3-*N,N*-dipole equivalents that in combination with a gold-activated alkyne could trigger a cycloaddition process (Scheme 33). Similarly to the oxazole-forming methodology (Scheme 31) it was initially suggested that these aminides could behave as both nucleophilic nitrenoids and reactant to quench the resulting organogold intermediate **234** (either from a vinyl gold carbenoid or a gold carbene) in the assembly of fused imidazoheterocycles **236**. Ynamides were again chosen as alkyne derivative in order to induce regioselectivity in the addition of the nucleophile.



Scheme 33: Proposed reactivity basis for the gold-catalysed synthesis of fused imidazoheterocycles

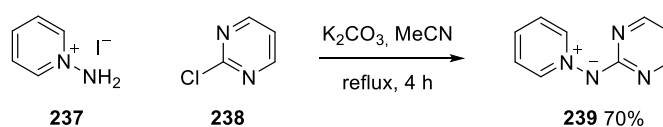
A number of challenges were, nevertheless, anticipated when considering this transformation. First, the reactivity of the endocyclic nitrogen in **233** is known to be reduced by an intramolecular hydrogen bonding with the α -proton of the pyridine.⁵³ This could lead to an incomplete catalytic processes where intermediate **234** is unable to cyclise to the desired heterocycle. Secondly, the several basic nitrogen atoms present in starting materials, products and possible by-products could act as coordination sites for the metal, reducing the effective concentration of active species. Despite these possible pitfalls, a successful outcome would potentially provide a practical, simple and

convergent method for the regioselective synthesis of novel substituted fused imidazoles. Part of the work that will be presented in chapters 2 and 3 has been previously published in: M. Garzón and P. W. Davies, *Org. Lett.* **2014**, 16, 4850–4853.

2.2 Results and Discussion

2.2.1 Preparation of pyridinium *N*-(pyrimidin-2-yl) aminide **239**

For the initial study of the proposed reactivity, pyridinium *N*-(pyrimidin-2-yl) aminide **239** was selected as a suitable precursor (Scheme 34). This aminide is a bench-stable crystalline solid, soluble in several common organic solvents and readily accessible. Additionally, the characteristic resonances of the pyrimidine ring in starting material and products can be easily tracked in the ^1H -NMR spectra of reaction mixtures, simplifying analysis during the screening process.

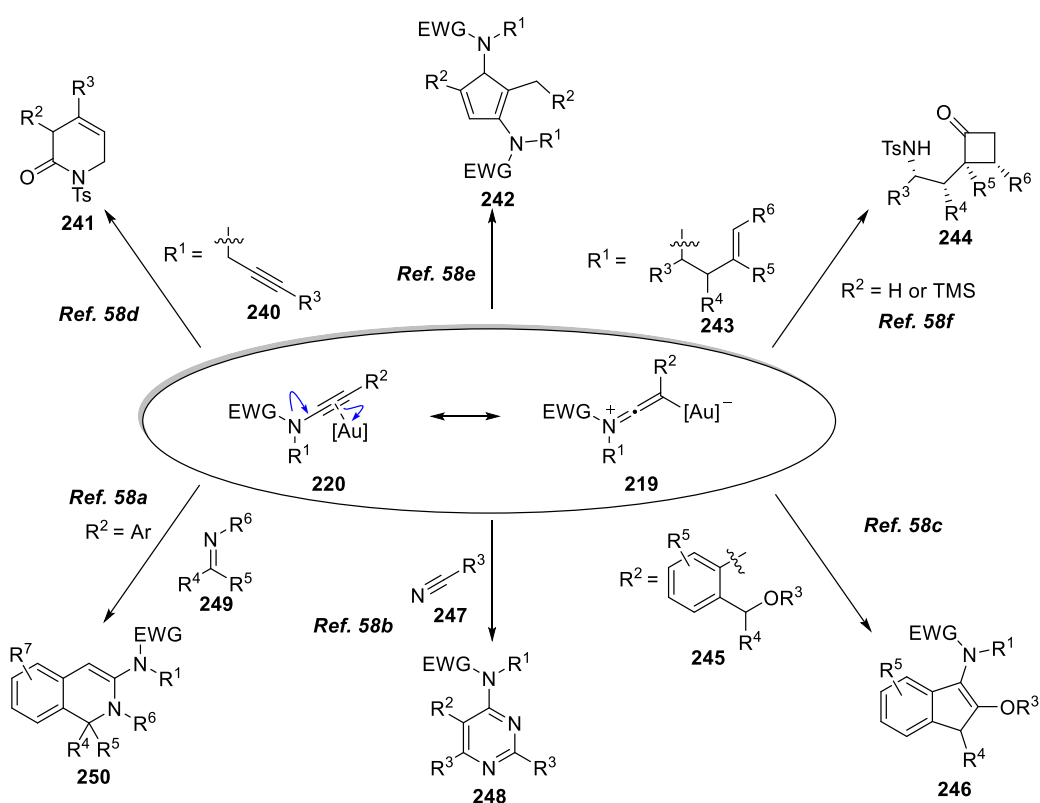


Scheme 34: Synthesis of aminide **239**

Following the reported method by Builla and co-workers,⁵⁴ commercially available *N*-aminopyridinium iodide **237** was used in combination with 2-chloropyrimidine **238** to obtain the desired ylide **239** (Scheme 34). Whilst the reported procedure specified a work-up consisting of a filtration through celite followed by flash chromatography in silica gel and recrystallization in ethanol, it was noticed that some impurities persisted after the purification. Concerned of the effect that such contaminant could introduce in the subsequent catalysis, the procedure was slightly modified. Once the reaction reached completion it was allowed to reach room temperature. The solvent was removed under

reduced pressure and the residue redissolved in dichloromethane as unlike acetonitrile, this is not miscible with water. By washing the mixture several times with NaOH [2.5 M] most of the impurities were removed which suggests that they originate from incomplete deprotonation of the exocyclic nitrogen. A final chromatography stage ensured the purity of the product.

2.2.2 Synthesis of functionalised ynamides



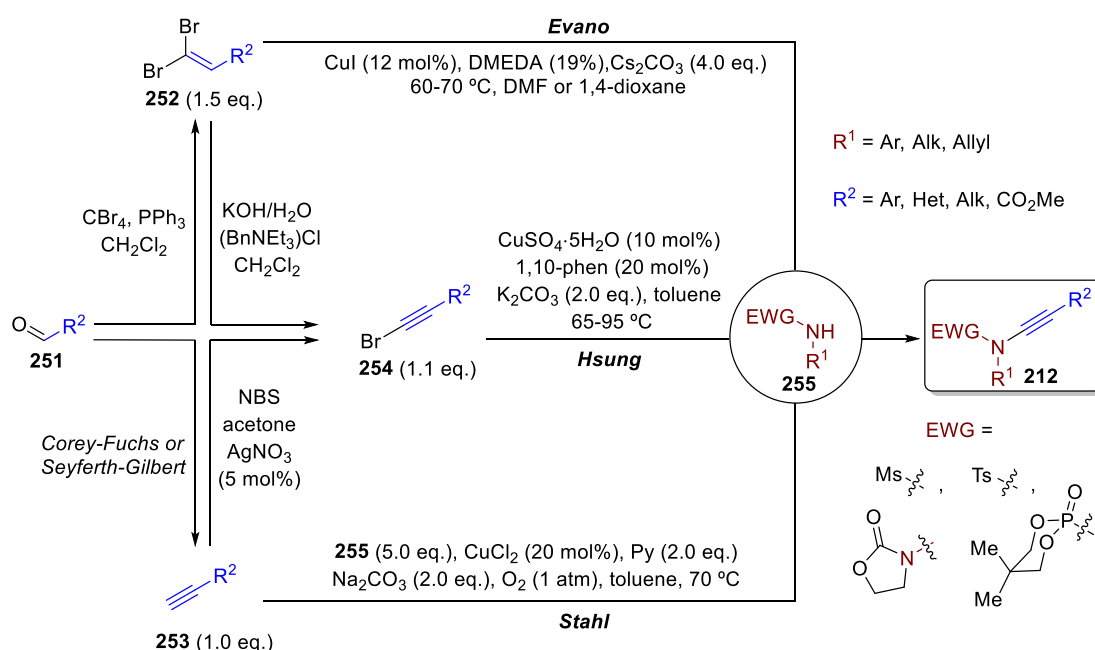
Scheme 35: Regioselectivity in the gold-catalysed transformation of ynamides

The development of ynamides as common building blocks in organic chemistry has blossomed over the last decade. The increased use of these systems results from their high versatility but also, by the design of more efficient and general methods for their preparation.⁵⁵ These compounds have seen extended use in ring-forming reactions,^{30b,56} including the total synthesis of some natural products,⁵⁷ and more recently in gold-

catalysed intermolecular transformations, due to the predictable reactivity of their π -system (Scheme 35).⁵⁸

Almost all the ynamides used in the following investigation were obtained using the copper-catalysed amidative cross-coupling methods reported by Evano,⁵⁹ Stahl,⁶⁰ and Hsung (Scheme 36).⁶¹ These reactions are characterised by mild conditions, high yields and excellent functional group tolerance. Furthermore, the versatility and readily interconversion between the precursors of each procedure allow generating great structural variation from simple starting materials.

Numerous aldehydes **251** can be converted through the Ramirez olefination,⁶² into the dibromoalkenes **252** required for the Evano method (Scheme 36 – Top). The main limitation is the use of a high excess of base and the low yields obtained with aniline-based sulfonamides.

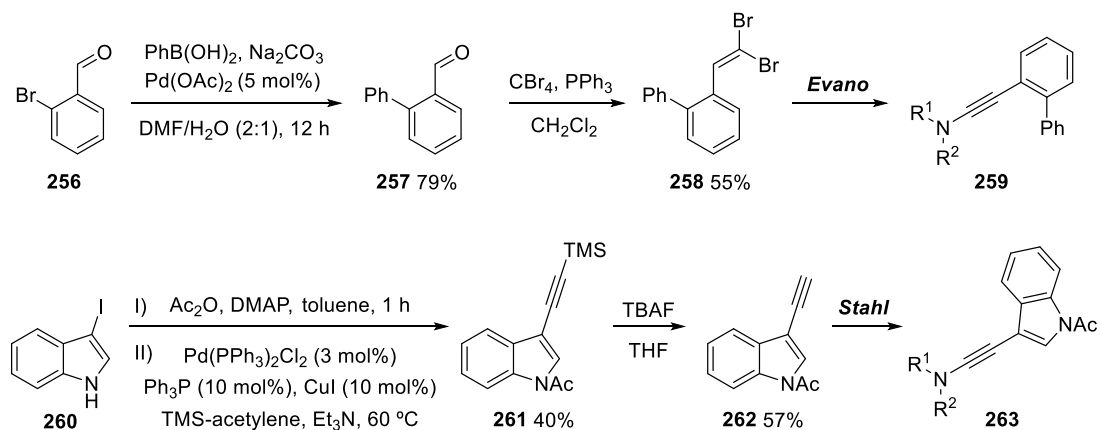


Scheme 36: Synthesis of ynamides through copper-catalysed cross coupling

Alternatively, Stahl's procedure (Scheme 36 – Bottom) employs terminal alkynes **253** under copper-catalysed oxidative cross-coupling conditions to tether the sulfonamide moiety. This offers a more direct methodology as many alkynes are commercially available, although again, sophisticated substrates may be synthesised from aldehyde precursors using either Corey-Fuchs⁶³ or Seyferth-Gilbert⁶⁴ protocols. In order to reduce the formation of homocoupling side products, large excess of sulfonamide and slow addition of the alkyne (generally added using a syringe pump over 4 hours) are required. While it is a more involved procedure, the excess of sulfonamide can be recovered and the previously problematic protected anilines are well tolerated.

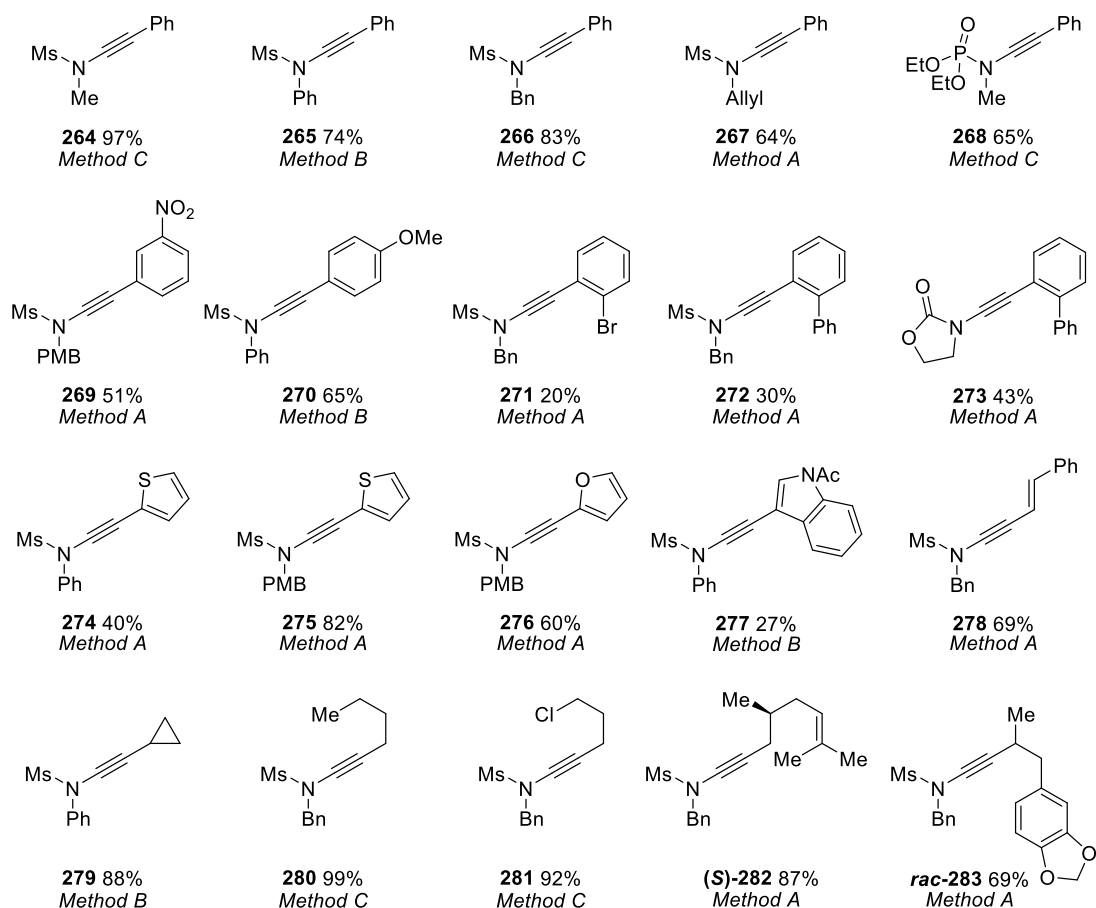
Finally, both terminal alkynes **253**⁶⁵ and dibromoalkenes **252**⁶⁶ can be readily converted into the bromoalkynes **254** used in the ynamide forming reaction reported by Hsung (Scheme 36 – Middle). These substrates are less stable than the intermediates employed in the other two methodologies and they usually cannot be stored for long periods of time. The again low reactivity against protected anilines is balanced by an otherwise greater tolerance to substitution that even allows the formation of *N*-phosphoryl⁶⁷ and 3-indolyl⁶⁸ ynamides (Scheme 38 – **268** and **277** respectively).

All the sulfonamides were prepared according to literature procedures,⁶⁹ by protection of the corresponding amine with mesyl chloride. Biphenyl systems **259** and 3-indolyl ynamide **263** were accessed through palladium-catalysed cross-coupling Suzuki and Sonogashira strategies (Scheme 37).⁷⁰



Scheme 37: Synthesis of precursors for ynamides

Overall, a wide range of ynamides covering different structural and electronic variations were obtained by combination of the three methods (Scheme 38).



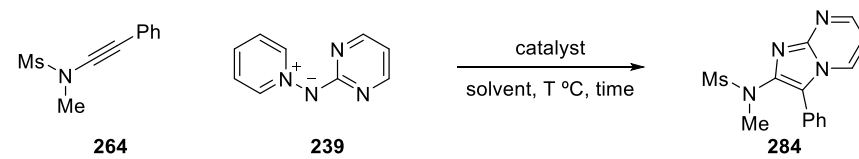
Scheme 38: Ynamides synthesised through copper-catalysed strategies. Method A: Evans; Method B: Stahl; Method C: Hsung

2.2.3 Catalyst screening

A reaction survey was initiated using a near equimolar mixture of *N,N*-methylmesy-substituted ynamide **264** (1.0 eq.) and aminide **239** (1.2 eq.) under inert conditions, where several solvents, temperatures, reaction times, concentrations and catalysts were screened. All the reactions were followed by TLC until completion or no further progress was detected. The optimal conditions for the oxazole-forming reaction (Scheme 30)³³ were tested initially: Gold(III) precatalyst dichloro(2-pyridinecarboxylate)gold (PicAuCl₂)⁷¹ in toluene at 90 °C (Table 1- Entry 1). Remarkably, despite the multiple basic nitrogen atoms present in the reaction media, productive catalysis was observed with 66% yield after 40 hours of reaction. Formation of the desired imidazo[1,2-*a*]pyrimidine **284** was confirmed by ¹H-NMR spectroscopy (Figure 3 – Top spectrum). However, on attempted isolation of the fused bicycle by flash chromatography a small impurity co-eluted (Figure 3 – Bottom spectra). Based on the presence of similar resonances for aromatic and aliphatic protons this impurity was proposed to be an isomer of the desired product. Analysis of the mixture by HPLC-MS allowed the detection of the impurity and confirmed it to be an isomer of **284** although the separation between compounds was never enough to use preparative HPLC for their isolation. Further attempts to isolate and characterise this isomeric impurity using other eluents and recrystallization techniques were not successful.

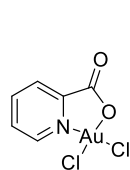
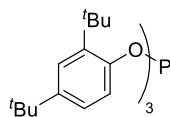
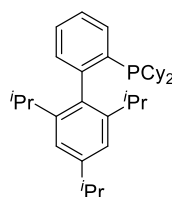
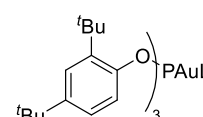
The sluggish behaviour of the reaction in toluene was partially attributed to the low solubility of the aminide **239**. These ylides are fairly polar due to the compensation of charges in the structure. As a result, the ynamide **264** degraded after the prolonged heating reducing the available concentration to form the imidazopyrimidine.

Table 1: Survey of the conditions for the reaction between aminide **239** and ynamide **264**^a



264 **239** **284**

Entry	Catalyst	Solvent (°C)	Time (h)	Rec 264 (%) ^b	284 (%) ^b
1	PicAuCl ₂	toluene (90)	40	7	66 (4)
2	PicAuCl ₂	1,2-DCB (90)	18	-	73 (12)
3	PicAuCl ₂	1,4-dioxane (90)	5	-	73 (11)
4 ^c	DTBPAuCl +AgSbF ₆	1,4-dioxane (90)	24	-	86
5 ^c	(C₆F₅)₃PAuCl +AgSbF ₆	1,4-dioxane (90)	24	-	76
6 ^c	Ph₃PAuCl +AgSbF ₆	1,4-dioxane (90)	24	30	65
7 ^c	XPhosAuCl +AgSbF ₆	1,4-dioxane (90)	24	67	8
8	AgSbF ₆	1,4-dioxane (90)	24	95	-
9	227	1,4-dioxane (90)	24	-	88
10	227	1,4-dioxane (70)	48	7	64
11	227	1,4-dioxane (50)	48	65	29
12 ^d	227	1,4-dioxane (90)	22	40	58
13 ^e	227	1,4-dioxane (90)	24	-	90
14	-	1,4-dioxane (90)	24	98	-
15	TFA	1,4-dioxane (90)	24	95	-

PicAuCl₂**DTBP****XPhos**L = (NCMe)SbF₆
227

^a Reaction conditions: Catalyst (5 mol%), **264** (0.10 mmol), **239** (0.12 mmol) heated at the given temperature in the named solvent (0.10 M with respect to **264** unless otherwise specified). ^b Yields calculated by ¹H-NMR spectroscopy against a known quantity of internal standard (1,2,4,5-tetramethylbenzene). Yields in parenthesis relate to a co-eluting isomer. ^c Catalyst formed *in situ* by combination of AgSbF₆ (5 mol%) and corresponding gold(I) chloride precursor (5 mol%). ^d 0.05 M reaction concentration. ^e 0.20 M reaction concentration.

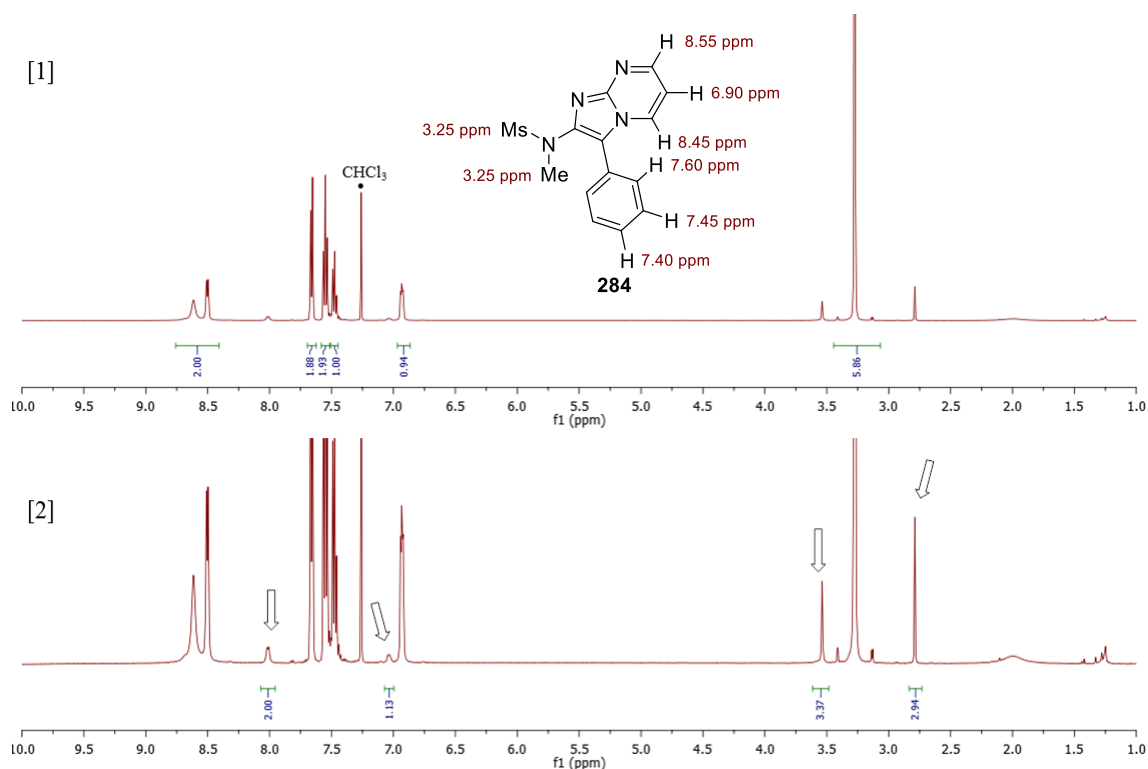


Figure 3: ^1H -NMR spectra of **284** isolated from the reaction described in Table 1, entry 3. [1] Identification of **284**; [2] Spectrum highlighting the signals of the co-eluting impurity

Therefore, the more polar, high boiling point solvents 1,2-dichlorobenzene (DCB) and 1,4-dioxane were subsequently screened (Entries 2 and 3 respectively). An improved reactivity was seen but, unfortunately, this was accompanied by an increase in the formation of the impurity.

Seeking to improve the selectivity of the reaction, electrophilic gold(I) catalyst **DTBPAuSbF₆** was generated *in situ* by combination of the corresponding gold chloride with **AgSbF₆** (Table 1 – Entry 4). Interestingly, the total conversion was maintained but no by-product was observed in this case, accounting for a higher yield of desired product. Other gold(I) species (Entries 5–7) also led to cleaner outcomes, though the conversion was dramatically reduced as the electron-donating ability of the ligand

increased. Both observations will be discussed later in the proposed mechanism (Scheme 44).

Although no reactivity was accessed using exclusively AgSbF_6 as catalytic system (Entry 8), different groups have been reporting the non-innocent role played by the silver salts in some *so-called* gold catalysed reactions.⁷² Echavarren and collaborators recently detected and isolated a chloride-bridged dinuclear gold(I) complex generated when mixing gold(I) precatalyst and silver salt in absence of substrate.⁷³ These complexes had deleterious effect in the catalysis, thus requiring a careful sequence of reagent addition to avoid their formation.

In order to avoid similar complications, the preformed system **227** was instead used which also bypassed the need to weigh and introduce hygroscopic AgSbF_6 into the reaction. As seen in Scheme 32, **227** has already been successfully used in other gold-catalysed nitrene transfer reactions, and gratifyingly, a minor increase in the yield was produced here compared to the related complex DTBPAuSbF_6 (Entry 9 vs Entry 4).

Diluting concentration or decreasing temperature had a detrimental effect in the system, with progressively lower yields and slower reactions (Entries 10–13). Finally, control reactions showed that no reaction was observed in the absence of gold or when a Brønsted acid was employed in its place (Entries 14–15).

2.2.4 Studies into the regiochemistry of **284**

The assignment of the structure of **284** was confirmed by nOe experiments. Irradiation of the aromatic signal at 7.60 ppm (corresponding to H^A ; Figure 4 – b) showed a nuclear Overhauser effect in the adjacent methyl groups of the sulfonamide and also in the

proximal pyrimidinic H^3 . The correlation H^4-H^3 indicates that the phenyl fragment is in 3-position of the core heterocycles, proving an attack of the aminide to the α -position of the ynamide (Scheme 39). This is further evidenced by the lack of correlation between the methyl groups of the sulfonamide fragment and H^3 (irradiation at 3.35 ppm, Figure 4—c).

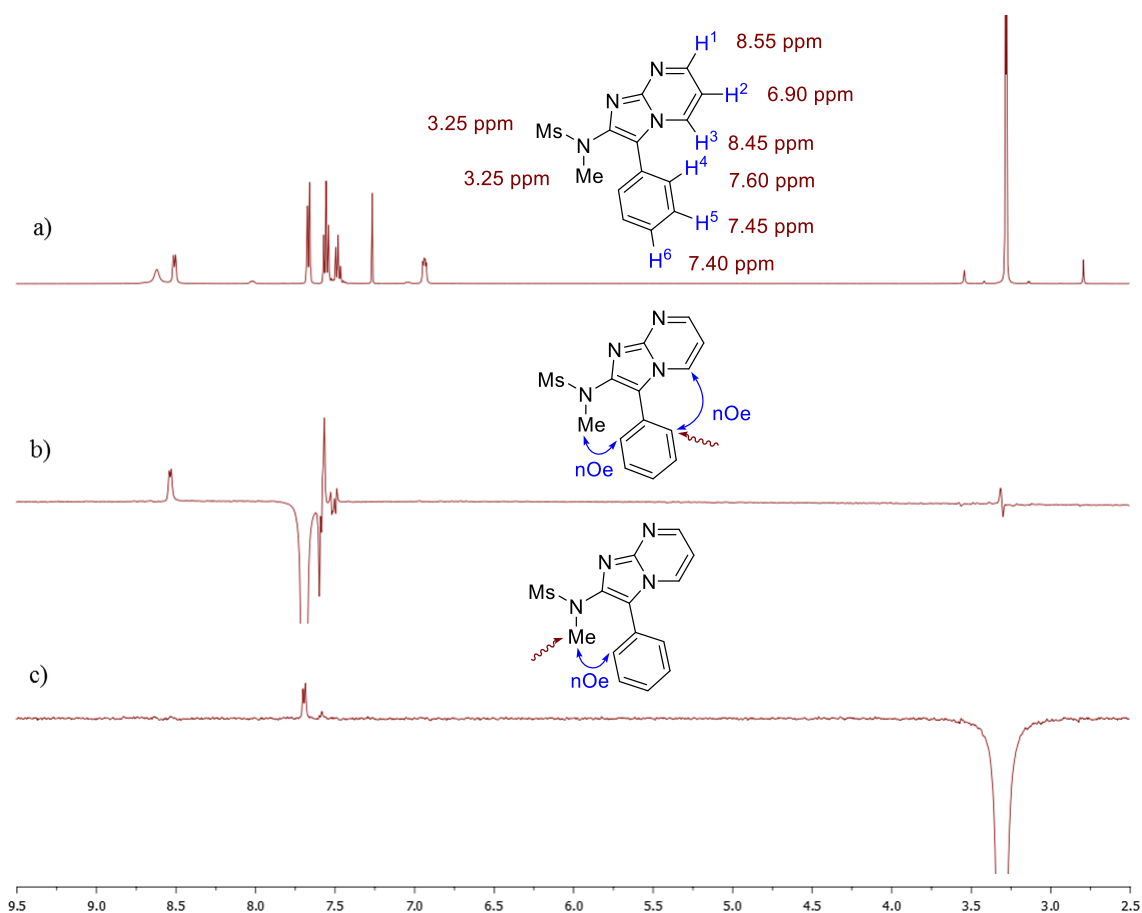
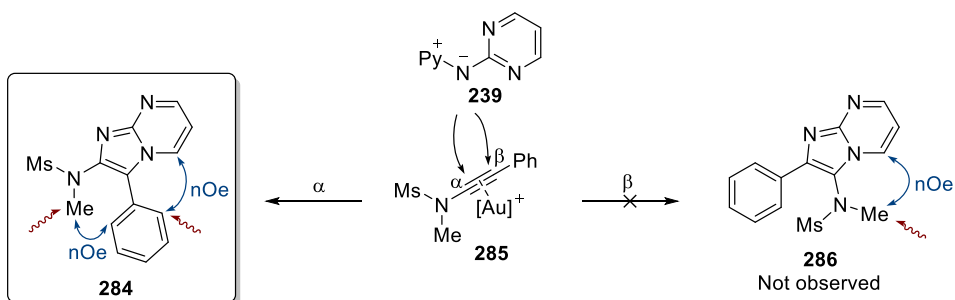
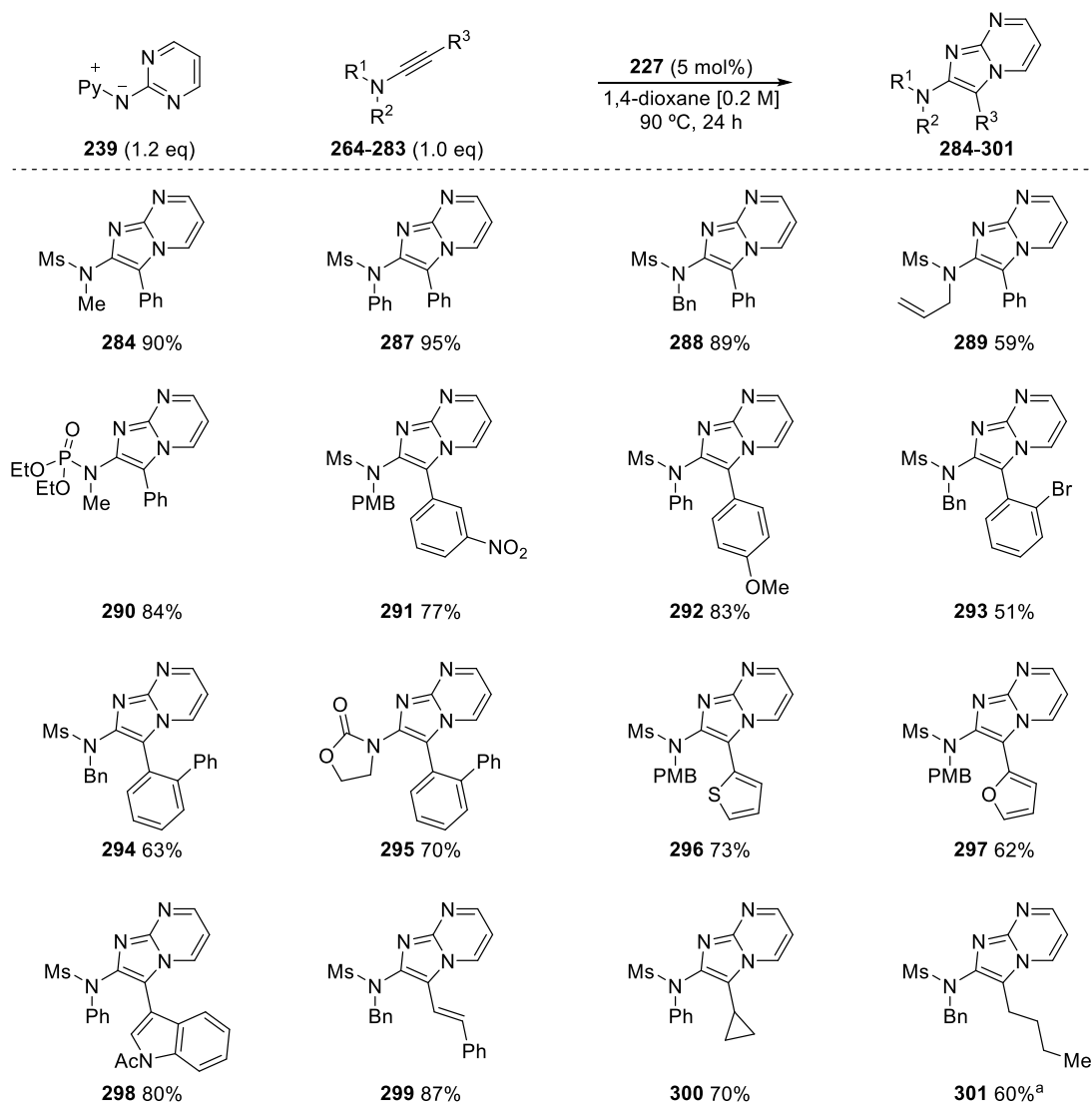


Figure 4: nOe Difference experiments for 284. a) ^1H -NMR spectrum of 284; b) Irradiation at 7.60 ppm; c) Irradiation at 3.25 ppm



Scheme 39: Confirmation of the regioselectivity of the reactivity to form **284** through nOe experiments

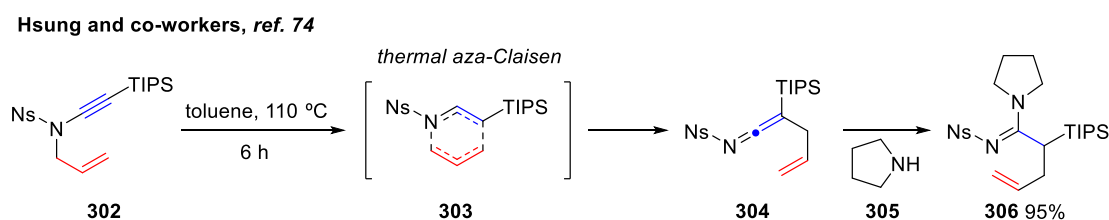
2.2.5 Reaction Scope



Scheme 40: Scope of the reaction between aminide **239** and different ynamides. ^a Complex mixture

At this point, the scope of the imidazopyrimidine-forming methodology was explored by testing a range of different ynamides **264-283** alongside aminide **239** (Scheme 40) using the best conditions found during the screening (Table 1, Entry 12). The reactions were heated until either total consumption of the ynamide or no further progress was detected by TLC (usually 24 h).

High yields were obtained across a variety of *N*-substituted ynamides, allowing the introduction of *N*-methyl **284**, *N*-phenyl **287**, *N*-benzyl **288** and even *N*-phosphoryl groups **290**. Despite the potential of *N*-allyl ynamides **302** to undergo aza-Claisen rearrangements at high temperatures (Scheme 41),⁷⁴ 2-aminoimidazopyrimidine **289** was obtained in good yield.



Scheme 41: Thermal aza-claisen reaction of *N*-allyl ynamides

Substitution at C3 tolerated different aryl groups **291-295**, including the bulky *o*-bromo benzene ring **293**. This is remarkable as arene fragments have been employed in other nitrene transfer reactions to trap α -imino gold carbene intermediates through C–H insertion pathways (*cf.* Scheme 15, Scheme 24 and Scheme 25). Fortunately, no competing products were detected even with strong electron-rich systems such as *p*-methoxy **292** and *o*-phenyl-substituted rings **294-295**. Similarly, imidazopyrimidines bearing π -rich heteroaromatic groups such as thiophene **296**, furan **297** and *N*-acetylindole **298** were obtained in excellent yields.

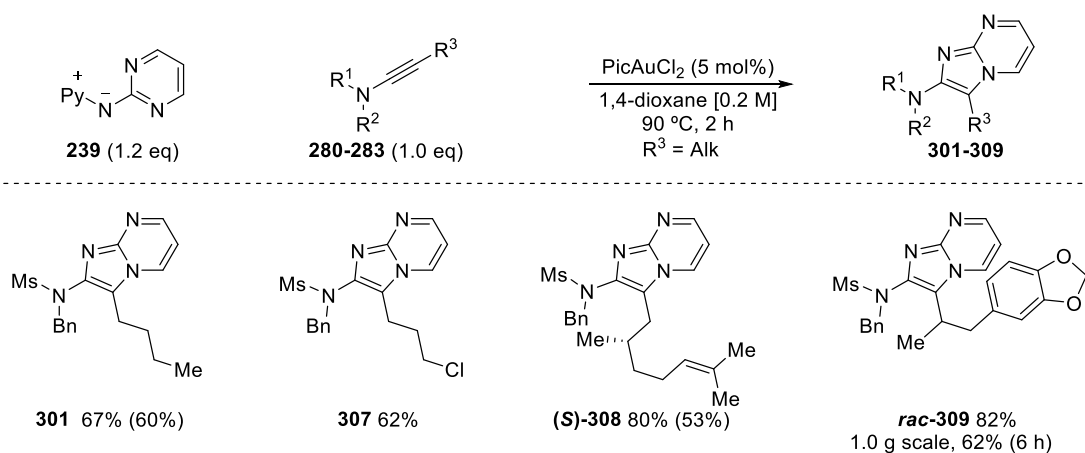
Conjugated ene-ynamide **278** which can potentially undergo cyclopropanation routes into metal-carbenes (*e.g.* Scheme 15) also gave smooth conversions to the desired vinyl heterocycle **299**.

Good yield of the cyclopropyl substituted product **300** was similarly obtained. Compared with this system, other alkyl-substituted ynamides proved to be more problematic substrates, giving sluggish reactions, partial degradation of the precursor and complex mixtures that hampered separation and overall reduced the formation of the desired product **301**. This was consistent with competing C–H insertion pathways previously described in other gold-catalysed nitrene transfer reactions onto alkylynamides (Scheme 28).^{33,34,48}

Returning to the reaction survey (Table 1), gold(III) precatalyst PicAuCl₂ was observed to give faster cycloadditions than the gold(I) complexes under the same conditions (Entry 3 *vs* Entry 9). Expecting to similarly accelerate the reaction with alkylynamide **280**, PicAuCl₂ was tested. This resulted in not only an improved rate but also better conversions and cleaner outcomes that allowed the isolation and characterisation of the sought after heterocycle (Scheme 42). It was proposed that the C–H insertion into the alkyl chain is a slower process than the cycloaddition to the fused heterocycle. Therefore, the shorter reaction times reduced the formation of side products and degradation of the ynamide. Interestingly, no traces of the impurity previously encountered during the screening with PicAuCl₂ were detected in this case.

Analogously, other more elaborate alkyl-substituted ynamides **281–283** were introduced on the bicyclic scaffold, as demonstrated by the formation of alkyl chloride derivative **307** and terpene-based citronellal and helional derivatives **308–309**.

A larger scale synthesis of **309** (0.99 g) was performed using a reduced catalyst loading (2 mol%, 22.1 mg). Probably due to the lower concentration of active catalytic species this reaction was slower than the one performed with 5 mol% of PicAuCl_2 and after 6 hours part of the starting material remained unconsumed. However the reaction was allowed to reach room temperature and purified to prevent the formation of insertion products and degradation of the ynamide, giving **309** in a 62% yield.



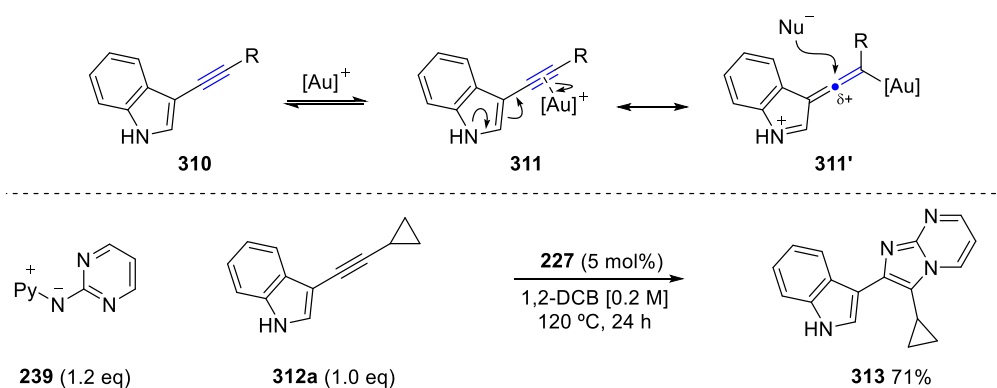
Scheme 42: Synthesis of alkyl-substituted imidazo[1,2-*a*]pyrimidines. Yields in parenthesis related to those achieved using **227** as catalytic system

Finally, the strategy was expanded to the use of alkynylindole **310** as an electron-rich π -system (Scheme 43). These compounds have been employed before as an alternative to ynamides in the gold-catalysed synthesis of oxazoles. The addition of the nucleophile is similarly determined by the conjugation of the nitrogen lone pair into the gold-activated triple bond **311/311'**.^{34a}

A good yield of the desired bis-heteroaryl scaffold **313** was obtained after 24 h of reaction at 120 °C in 1,2-DCB (used instead of 1,4-dioxane to reach the desired temperature). Also considering the indole-based structure **298** (Scheme 40), these two combined examples showcase the flexibility of the transformation and how it can be

finely tuned to regioselectively introduce biologically relevant frameworks into different positions of the scaffolds.

The higher reaction temperature required to achieve productive catalysis when using indolylalkynes instead of ynamides was also required in the oxazole-forming reaction (Scheme 32). This could be related with a lower contribution of the remote heteroatom lone pair into the alkyne due to its additional conjugation into the π -system of the aromatic ring. As a result, the electron density of the alkyne would be reduced. Considering that these aminide-based nitrene transfer reactions employ π -rich triple bonds, the variation in the electronic environment of the coordinated gold would be affecting the catalysis.



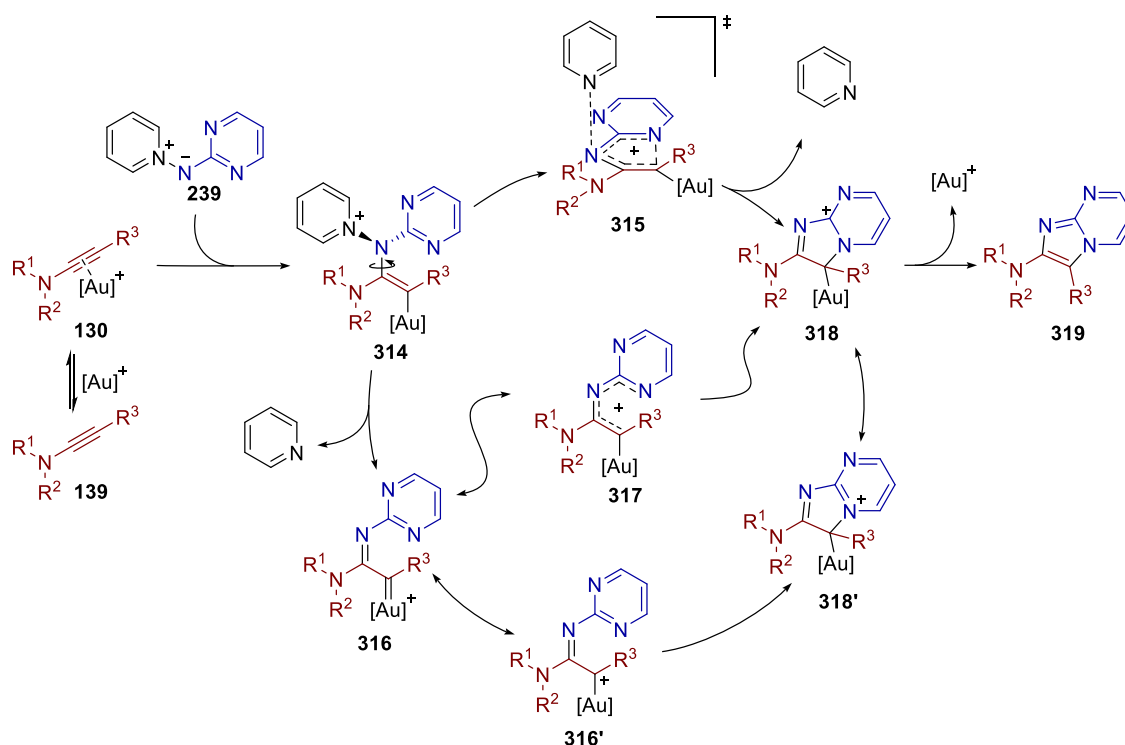
Scheme 43: Use of electron-rich internal alkynes in the synthesis of biaryl linked products

2.2.6 Proposed Mechanism

The successful isolation of imidazo[1,2-*a*]pyrimidines unveils pyridinium *N*-(pyrimidin-2-yl) aminide **239** as a 1,3-*N,N*-dipole equivalent. By analogy with the oxazole reaction (Scheme 31), the suggested mechanism involves the nucleophilic addition of aminide **239** to the α -position of the gold activated ynamide **130**. As discussed before, the

selectivity in the attack arises from the electronic difference across the π -system seen in the gold keteniminium resonance form **219**.

It is proposed that aminide **239** approaches perpendicular to the plane of the ynamide in order to reduce steric hindrance, resulting in vinyl gold carbenoid **314**. Reconfiguration of the aminide exocyclic nitrogen in **314** aligns the pyridine perpendicular to the π -system as the pyrimidine fragment is brought into the plane of the aurated carbon centre (**314**→**315**). The scission of the N–N bond would occur simultaneous with formation of the new N–C bond as a positive charge develops across the π -system in a bis-hetero 4π -electrocyclisation (**315**→**318**). A subsequent deauration step delivers the imidazo[1,2-*a*]pyrimidine scaffold (**318**→**319**) as the aromaticity is regenerated.



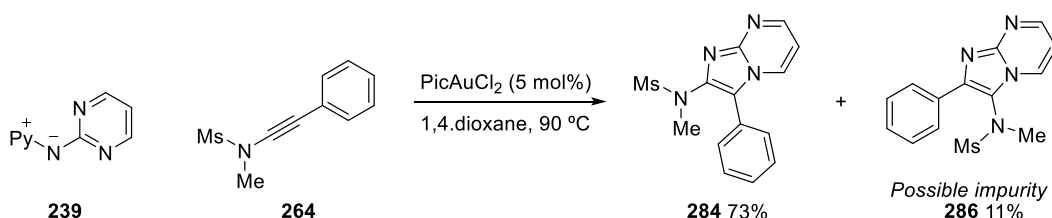
Scheme 44: Proposed mechanism for the formation of imidazo[1,2-*a*]pyrimidines **319**

A more stepwise pathway can also be envisioned where the vinyl gold carbenoid **314** evolves into an α -imino gold carbene **316** by extrusion of the pyridine leaving group

prior to the cyclisation. This electrophilic intermediate can be intramolecularly captured by the pyrimidinic nitrogen lone pair leading to **318'**. Alternatively, a 4π -electrocyclisation might also be triggered after liberation of the nucleofuge (**316**→**317**→**318**).

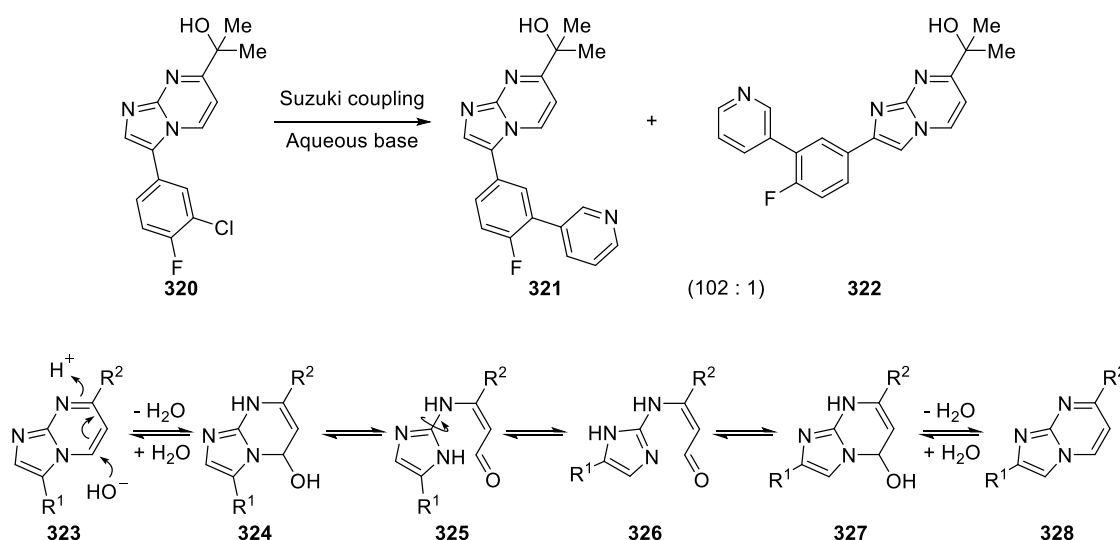
The interaction of the pyrimidine group with the metallated carbon centre (**316**→**318**) requires the adoption of a *cis* configuration in the newly formed C–N double bond in **316**. This process might be slowed by the steric clash with the substituents in R^3 giving time for the reactive gold carbene to undergo alternative evolution pathways such as C–H insertions in adjacent $C(sp^3)$. However, the preferential formation of cycloaddition products in the reaction with alkyl-substituted ynamides (Scheme 42) indicates a fast cyclisation probably through the more concerted pathway (**314**→**315**→**318**). Additionally, attending to the nature of the metal species, the reaction rate was improved with electrophilic gold(I) and gold(III) complexes (Table 1). Therefore, formation of gold carbene **316** as the nucleofuge is eliminated by contribution of gold-to-carbon π -donation in **314** would be a disfavoured process with these catalytic species.

Returning to the impurity observed in the reaction screening with the gold(III) precatalyst $PicAuCl_2$ (Table 1 – Entries 1-3), it was initially proposed to be isomer **286** (Scheme 45).



Scheme 45: Proposed structure for the isomeric impurity **286**

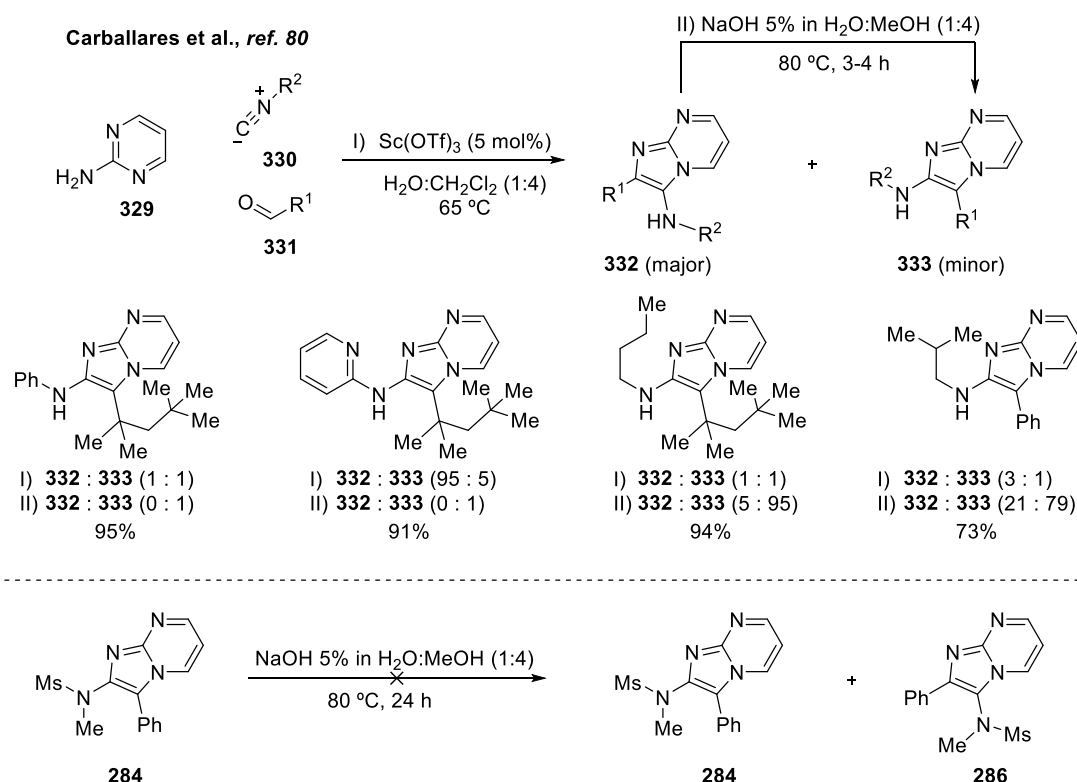
Interestingly, imidazo[1,2-*a*]pyrimidines are known to undergo Dimroth rearrangements where, under acid/basic conditions endocyclic and exocyclic nitrogen atoms switch places (Scheme 46).⁷⁶ Formation of mixture of isomers through this reaction has had in some cases a deleterious impact in development of synthetic processes. An example of this can be seen in the synthesis of compound **321**, designed as GABA_A $\alpha_{2,3}$ -selective allosteric modulator, where the last step was hampered by the formation of isomeric impurity **322**.⁷⁷ Even after an extended screening of conditions a 102:1 mixture of isomers was finally obtained, although a subsequent recrystallization step afforded the pure compound **321** in 96% yield.



Scheme 46: Isomeric mixture of imidazopyrimidines obtained during the synthesis of GABA_A $\alpha_{2/3}$ -selective agonist **321** and the proposed mechanism through a Dimroth rearrangement⁷⁷

This rearrangement, nonetheless, can be advantageously exploited in the synthesis of the valuable but elusive 2-aminoimidazo[1,2-*a*]pyrimidine scaffold.^{78,79} Carballares and collaborators developed a reaction where 3-substituted isomer **332** was selectively converted into the 2-substituted **333** under basic conditions (Scheme 47 – Top).⁸⁰ The strategy could be coupled with an isocyanide-based multicomponent synthesis of imidazopyrimidines,⁸¹ usually limited by the formation of isomeric mixtures. Although

the process tolerates diverse aryl and alkyl substituents, the conversion into the desired 2-substituted isomer **333** is substrate dependant and the use of basic conditions excludes the introduction of more sensitive functionality. The selectivity of this process was briefly attributed to a combination of steric and electronic differences between **332** and **333** due to the presence of the amino group.



Scheme 47: Top: synthesis of 2-aminoimidazopyrimidines through a multicomponent reaction/rearrangement sequence.⁸⁰ Bottom: attempted rearrangement reaction

In an attempt to identify the co-eluting impurity as the 3-amino substituted isomer **286**, 2-aminoimidazopyrimidine **284** was subjected to the reported rearrangement conditions (Scheme 47 – Bottom). However, **284** resulted inert and no reaction was observed even after prolonged heating. It must be noted that this impurity was not observed in the reaction with other aryl- or alkyl-substituted ynamides and this result could have just been a misleading one-off with the selected model. As it will be discussed in the

following chapter, both PicAuCl_2 and **227** can be generally used to catalyse the reaction with different aminides.

2.3 Conclusions

Pyridinium *N*-(pyrimidin-2-yl) aminide **239** has been revealed as suitable nitrene transfer reagent in the synthesis of novel imidazo[1,2-*a*]pyrimidines **319**. This ylide behaves as 1,3-*N,N*-dipole equivalent in the first example of an alkyne-based [3+2]-dipolar cycloaddition reaction for the regioselective assembly of substituted imidazole scaffolds. The procedure is practical and simple, requiring only the combination of stable and readily-accessible precursors without the need of additives or arduous work-ups, and where the only waste product is pyridine. As a result, generally good to excellent yield are obtained, allowing the introduction of challenging and/or otherwise unexplored functionality. This strategy can be adapted for the preparation of imidazo[1,2-*a*]pyrimidines at gram scale.

In the cases where alternative 1,2-C–H insertion pathways were possible (alkyl-substituted ynamides) the more reactive gold(III) precatalyst PicAuCl_2 proved to be more effective. Additionally, it has been shown that the reaction is not restricted to ynamides as other electron-rich alkynes can be used instead.

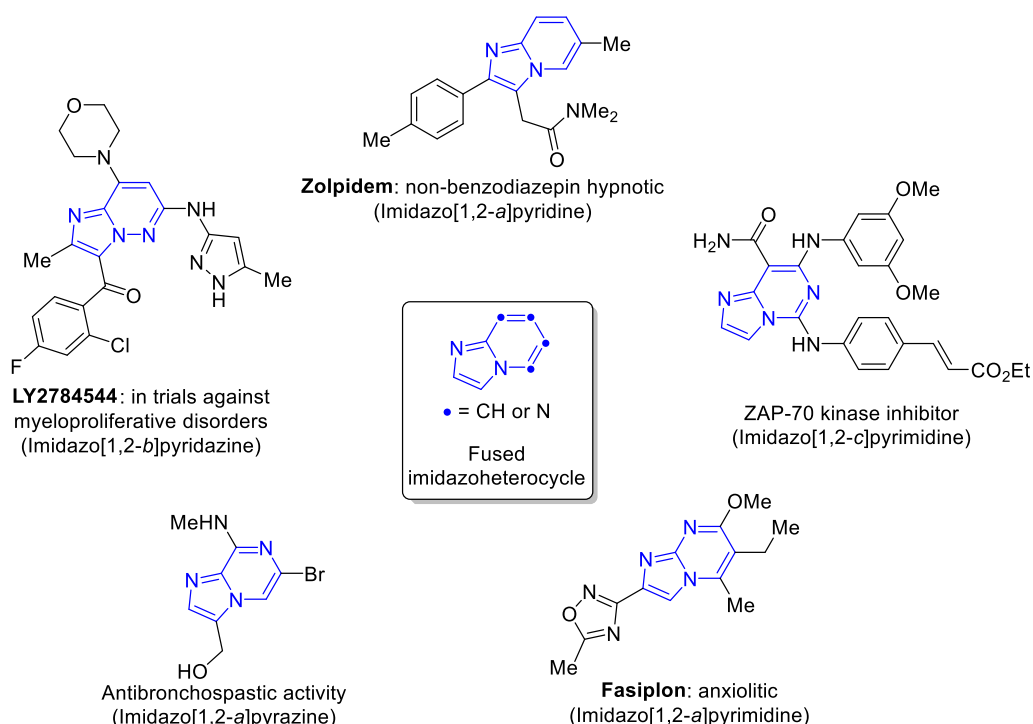
This strategy sets the basis for a nitrene transfer methodology that will be expanded in chapters 3 and 4 with the design of new fused frameworks.

Chapter 3

3.1 Fused imidazoheterocycles

3.1.1 A common route for the synthesis of fused imidazoheterocycles

In the previous chapter, the reaction between pyridinium *N*-(2-pyrimidin-yl) aminide **239** and a gold-activated π -rich alkyne was introduced as a novel and reliable route for the assembling of imidazo[1,2-*a*]pyrimidines. The chemistry presented in Scheme 46 already offered a glimpse of the applicability of these scaffolds. Imidazopyrimidines and the imidazo-fused diazines/pyridine analogues family are an important class of compounds.



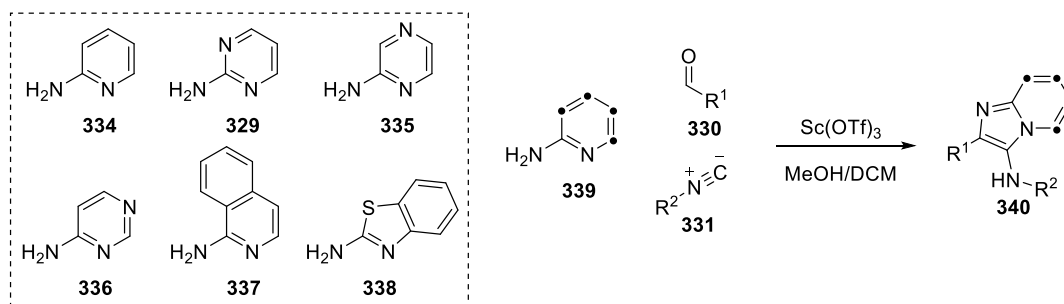
Scheme 48: Examples of fused imidazoheterocycles and their biological activity

For instance, they display an agonist effect against the γ -aminobutyric acid receptor (GABA_A receptor) which is similar to benzodiazepines, and are used as inhibitors of the central nervous system. Therefore, these frameworks are promising lead candidates in

the discovery of novel drugs and are recurrent pharmacophores in many molecules with potent biological activity such as anticancer,⁸² antiviral,⁸³ antimicrobial, antibacterial,⁸⁴ anti-inflammatory⁸⁵ and/or anxiolytic,⁸⁶ among others. Several of them have progressed to market such as Fasiplon⁸⁶ and Zolpidem, based on imidazo[1,2-*a*]pyrimidine and imidazo[1,2-*a*]pyridine systems respectively (Scheme 48).

Owing to their attractive therapeutic features as well as their luminescent properties as organic materials,⁸⁷ many strategies have been developed over the years for the synthesis of these imidazo-fused heterocycles. In particular, assembly of the core structure through an aminodiazine/2-aminopyridine precursor tends to be the predominant approach. Classical routes are based on substitution or condensation reactions with preformed electrophiles such as α -halocarbonyl and 1,3-dicarbonyl moieties,⁸⁸ however these methodologies are often compromised by narrow substrate scope and the use of lachrymatory and/or difficult to access starting materials.

Some of these restrictions can be partially circumvented in the three-component acid-mediated condensation between 2-aminopyridine **334**, aldehydes **330** and isocyanides **331**, also known as Groebke-Blackburn reaction (Scheme 49).⁸⁹ The procedure can be readily adapted to cover other imidazoazines **339** such as –pyrimidine **329/336**, –pyrazines **335**, –isoquinoline **337** and –benzothiazole **338**, and is one of the most widespread strategies for the synthesis of these imidazo-fused scaffolds. Due to the high reactivity of the precursors, the compatibility between substrates restricts the possibilities of diversification, limiting the scope of tolerated functionality and, as seen in Scheme 47, in occasion leading to mixtures of regioisomers.

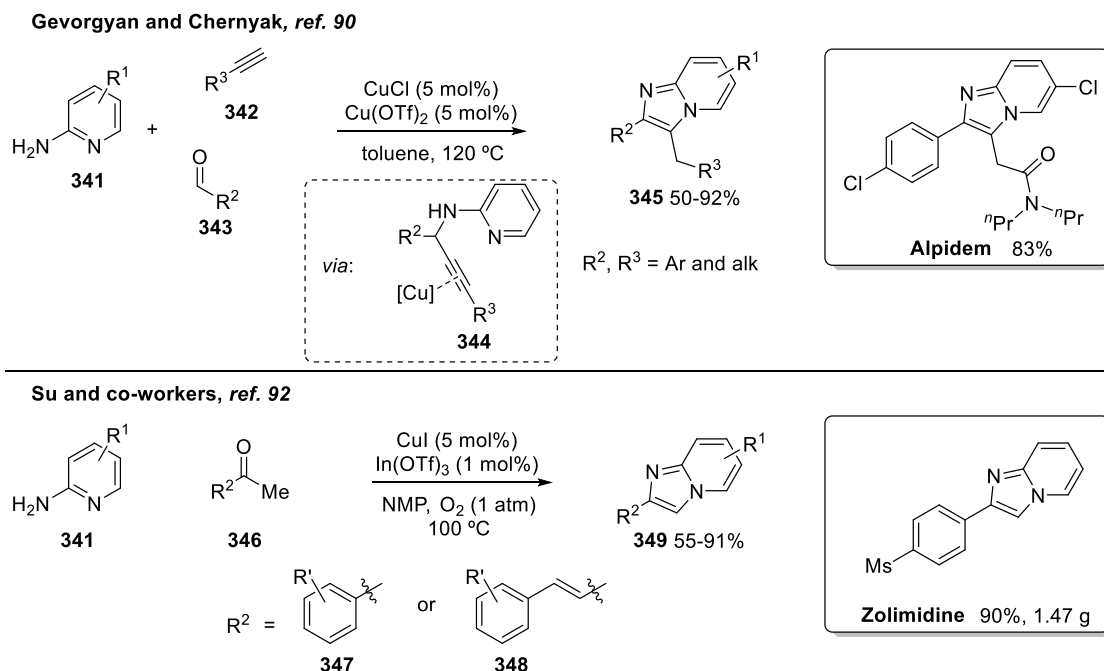


Scheme 49: Groebke-Blackburn reaction

Transition-metal-catalysed reactions offer elegant alternatives to the aforementioned methods, due to simpler starting materials and better atom economy. This is reflected in Scheme 50 where two independent copper-catalysed methods are employed for the one-pot synthesis of commercially available drugs based on imidazo[1,2-*a*]pyridine scaffolds (Alpidem and Zolimidine). The first example is a three-component coupling reaction where formation of intermediate metal-activated propargylic amine **344** precedes a 5-*exo-dig* cyclisation to form the fused system **345** (Scheme 51 – Top).⁹⁰ An analogous silver-catalysed intramolecular version of this process was later published by Chioua *et al.*⁹¹

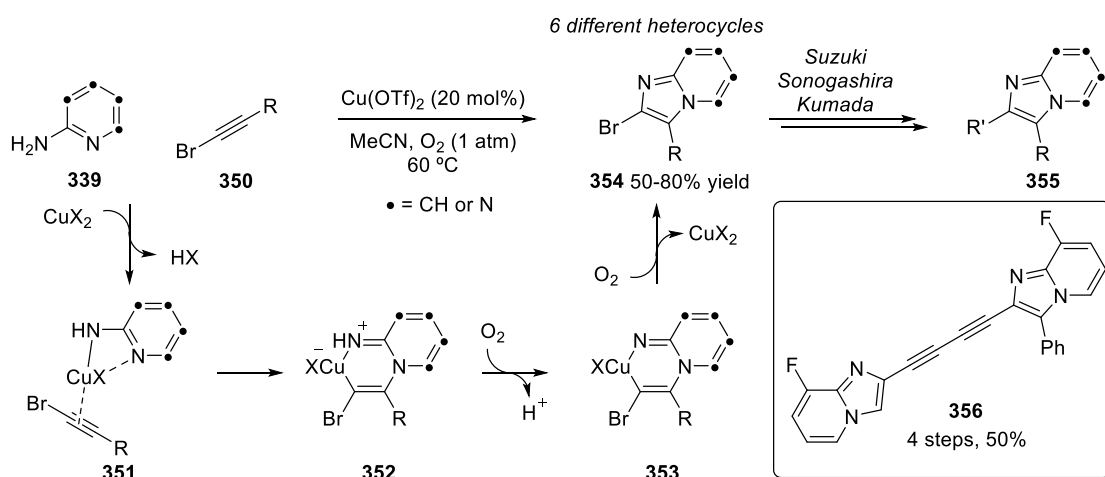
The second example is a copper-mediated cyclisation of aryl- and vinylketones **346**.⁹² In this case, substoichiometric amounts of iodide are oxidised to iodine, *in situ* generating an α -iodoketone that reacts with 2-aminopyridine **341** giving the fused scaffold.^{87c}

Preliminary results indicated that both reactions can incorporate other substituted aminoazines, although the harsh conditions reduce the tolerated substitution.



Scheme 50: Copper-catalysed reactions in the synthesis of imidazo[1,2-*a*]pyridine-based drugs

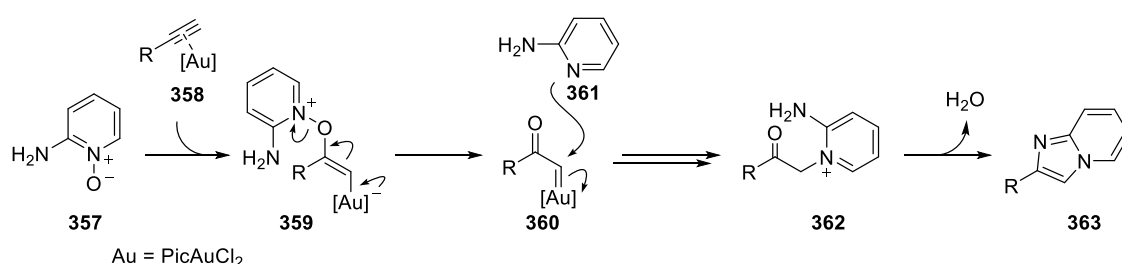
The copper-catalysed oxidative cyclisation of 2-aminoazoles **339** with haloalkynes **350** developed by Gao et al. is one of the most general routes for the synthesis of several *N*-bridgehead heterocycles **354** (Scheme 51).⁹³



Scheme 51: Synthesis of fused imidazoheterocycles through copper-catalysed oxidative cyclisation of haloalkynes

Moreover, the narrow substitution scope associated with the instability of haloalkynes **350** is partially compensated by the possibility of introducing additional functionality *via* subsequent cross-coupling reactions, giving complex structures such as **356**.

A few months prior to the publication of the work described in this thesis,³⁵ Toste and co-workers reported a gold-catalysed synthesis of imidazo[1,2-*a*]pyridines **363** (Scheme 52).⁹⁴ In this reaction, the combination of 2-aminopyridine *N*-oxide **357** and a metal-activated triple bond **358** generates a vinyl gold intermediate **359**. This evolves into the gold carbene **360** by cleavage of the aminopyridine group **361** that subsequently attacks the carbenic centre. Intermediate **362**, identified in the reaction mixture by LC-MS, can be formed by either reaction of a gold carbenoid with the newly formed aminopyridine **361** or from direct rearrangement of the vinyl gold precursor **359**. Final condensation of the resulting aminoketone **362** yields the fused scaffold **363**. The procedure was compatible with a wide range of different terminal alkynes, but failed with internal triple bonds. Additionally, the substrate scope was limited to pyridine derivatives due to the challenges in the formation of *N*-oxides from other azines.



Scheme 52: Proposed mechanism for the gold-catalysed synthesis of imidazo[1,2-*a*]pyridines through α -oxo gold carbenoids

Overall, most of the current strategies for the formation of imidazo-fused heterocyclic frameworks have underlying mechanistic similarities and/or have precursors in common. Consequently, the resulting compounds present closely related substitution

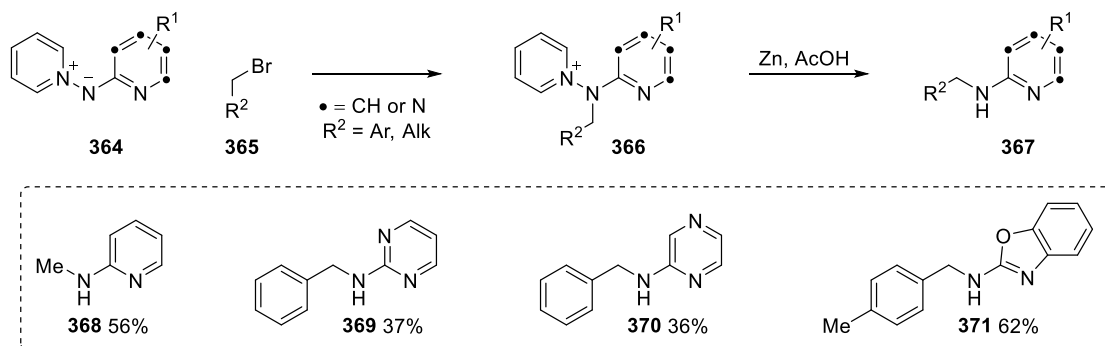
patterns, especially around the imidazole core. This lack of variation in the assembly of a structurally diverse family of heterocycles highlights the need for complementary and more flexible methodologies.

At this point of the research project it was considered that the newly developed reaction for the synthesis of imidazo[1,2-*a*]pyrimidines (Scheme 40) could potentially be expanded towards other diazine/pyridine-based aminide systems, providing a common and general route for the assembly of different fused imidazoheterocycles.

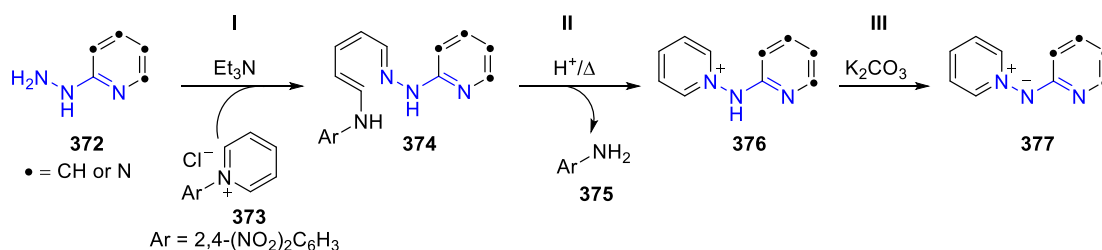
3.1.2 Pyridinium *N*-heteroaryl aminides as building blocks

N-Acyl aminides **211** were presented in chapter 2 as valuable precursors for the synthesis of oxazoles (Scheme 30).^{34,75} Not only can they be employed as 1,3-*N,O* dipole but also they have been widely explored in other important transformations such as stereoselective reductions,⁹⁵ intramolecular cyclisation with tethered enolates or thiocyanates,⁹⁶ or as 1,3-*N,C* dipole equivalent in [3+2] dipolar cycloadditions⁹⁷.

In stark contrast, *N*-heteroaryl aminides **364** have attracted less interest. Virtually all the research available for these systems is encompassed by the work done by Alvarez-Builla and collaborators.^{53,98} These aminides have been mainly used as masked 2-aminoazines for the selective alkylation of the exocyclic nitrogen in **364** (Scheme 53).⁹⁹ Attempts into a wider application as building blocks through condensation reactions¹⁰⁰ and intramolecular radical arylations¹⁰¹ were less successful due to the reduced substrate scope.

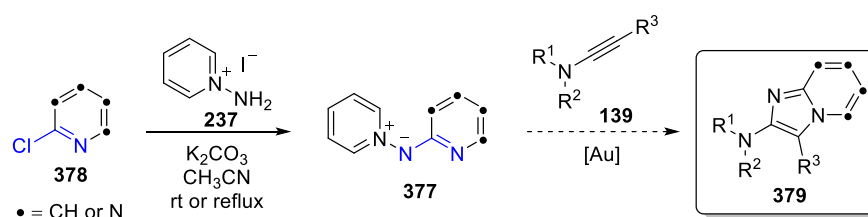
Scheme 53: Pyridinium *N*-heteroaryl aminides as masked 2-aminoazines

Traditionally, these aminides were prepared following an ANRORC-type process (Addition of the Nucleophile, Ring Opening, Ring Closing) by combination of the corresponding 2-heteroaryl hydrazine **372** with 2,4-dinitrophenyl pyridinium chloride **373** to form hydrazone **374**, which under acid catalysis and posterior base treatment delivers the desired compound (Scheme 54).^{53,102} The length and inefficiency of the sequence may account for the marginal use of these substrates.

Scheme 54: Classical route for the synthesis of pyridinium *N*-heteroaryl aminides

A more direct and attractive route was recently developed by Alvarez-Builla,^{54,103} where commercially available *N*-aminopyridinium iodide **237** was employed as precursor for a nucleophilic aromatic substitution reaction (S_NAr) on π -deficient haloheterocycles **378** (used in the chapter 2 for the synthesis of pyridinium *N*-(2-pyrimidin-yl) aminide **239**, Scheme 34).

This methodology greatly expands the scope of tolerated systems to cover a broad range of heterocyclic motifs that could ideally be used as candidates for the gold-catalysed formal [3+2]-dipolar cycloaddition (Scheme 55). It was, nonetheless, anticipated that electronic variations across the different heterocycles might substantially affect the feasibility of the reaction.



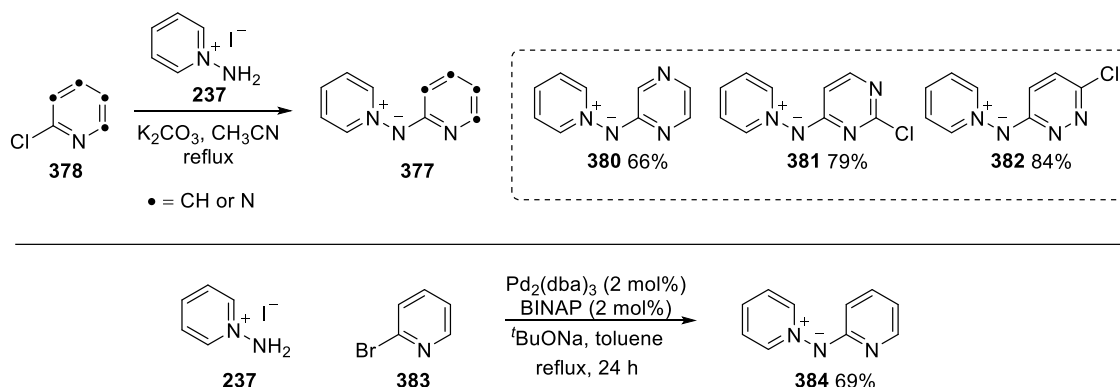
Scheme 55: Proposed expanded route for the gold-catalysed synthesis of imidazoheterocycles

3.2 Results and Discussion

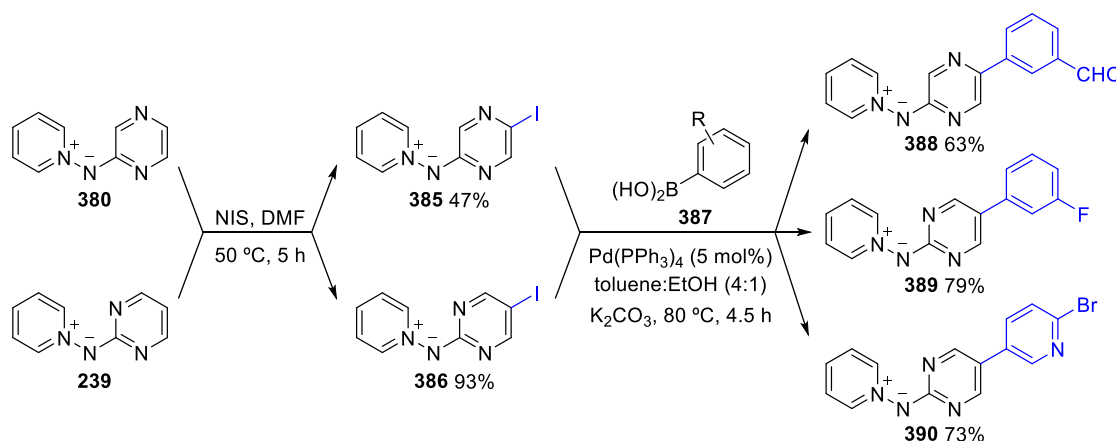
3.2.1 Synthesis of pyridinium *N*-diazine/pyridine aminides

Following the optimisation and synthesis of imidazo[1,2-*a*]pyrimidines discussed in chapter 2, several aminides were prepared using Alvarez-Builla's procedure (Scheme 56).^{54,103} Using the corresponding 2-chloroheterocycle **378**, all the remaining structural combinations of diazine ring **380-383** were obtained in good yields. While these compounds had already been reported in the original paper, the described work-up requires the use large amounts of ethanol as eluent for both the flash chromatography and subsequent recrystallisation. This was replaced with a base treatment followed by purification using a mixture of 5% of methanol in either ethyl acetate or dichloromethane, which greatly reduced the amount of solvent and time employed.

The more π -rich pyridine ring **384** was unreactive under S_NAr conditions and had to be synthesised through an alternative aminopalladation reaction (Scheme 56 - Bottom).¹⁰³

Scheme 56: Synthesis of pyridinium heteroaryl *N*-aminides

Additionally, most of these aminides could be treated with *N*-iodosuccinimide to selectively halogenate the diazine ring (Scheme 57).^{98b} Iodo-pyrazines/pyrimidine derivatives **385** and **386** were synthesised and subsequently modified through Suzuki-Miyaura cross-coupling reactions using various boronic acids **387**.¹⁰⁴ Following this relatively simple sequence, three novel and more complex aminides **388-390** were quickly formed in good yields.



Scheme 57: Halogenation/Suzuki-Miyaura cross-coupling sequence for the synthesis of complex aminides

All these compounds were colourful crystalline solids, from green to orange depending of the heterocycle attached (Figure 5). Their high stability must be highlighted, as they

could be stored on the bench for a period of more than two years with no signs of degradation.

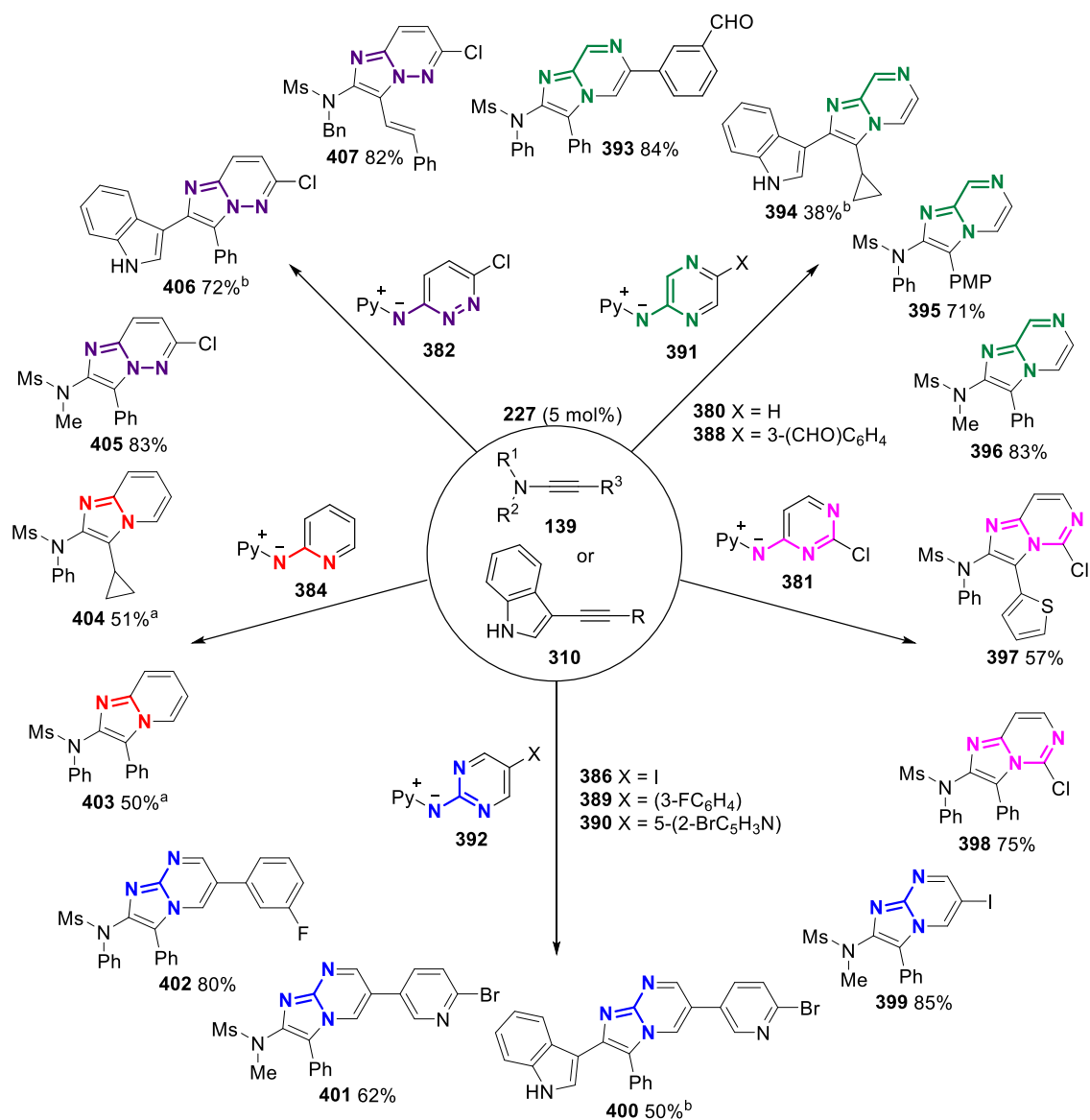


Figure 5: Picture of some of the aminides synthesised during this investigation

3.2.2 Synthesis of fused imidazodiazines/pyridines

Using the conditions developed in chapter 2 for the synthesis of imidazo-fused scaffolds the new library of aminides was explored under gold-catalysis: ynamide **380-390** (1.0 eq.), aminide **139** (1.2 eq.) and gold(I) phosphite complex **227** (5 mol%) in 1,4-dioxane at 90 °C for 22-24 h (Scheme 58).

Remarkably, regardless of the combination of diazine and ynamide used, all the systems successfully underwent the desired cyclisation pathway, affording novel imidazo[1,2-*a*]pyrazine **393-396**, imidazo[1,2-*c*]pyrimidine **397-398** and imidazo[1,2-*b*]pyridazines structures **405-407**.



Scheme 58: Reaction scope for heteroaryl aminides 380-390. ^a Reaction run for 48 h. ^b Reaction run in 1,2-DCB at 125 °C

In most of the cases, the yields were good and comparable to the imidazo[1,2-*a*]pyrimidine analogues obtained from the same ynamides (Scheme 40), showing an comparable reactivity profile across the different members of the family. Similarly, excellent chemoselectivity was observed for pyrazine and pyrimidine aminides bearing potentially labile functional groups as halogen atoms **386**, aldehydes **388** and 2-bromopyridines **390**.

In addition to ynamides, 3-indolylalkynes **310** also afforded the desired bis-heterocyclic structures **394**, **400** and **406**, although again use of more forcing conditions was required (1,2-DCB at 120 °C).

Crystals of compounds **402** and **398** were grown and analysed through single crystal X-ray diffraction technique (Figure 6), confirming what was already inferred from the nOe experiments carried out in chapter 2 (Scheme 39): the addition to the ynamide regioselectively gives 2-amino-substituted imidazoheterocycles **379**.

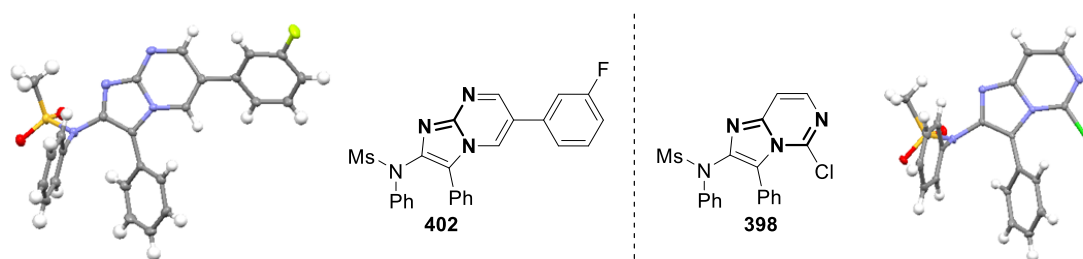
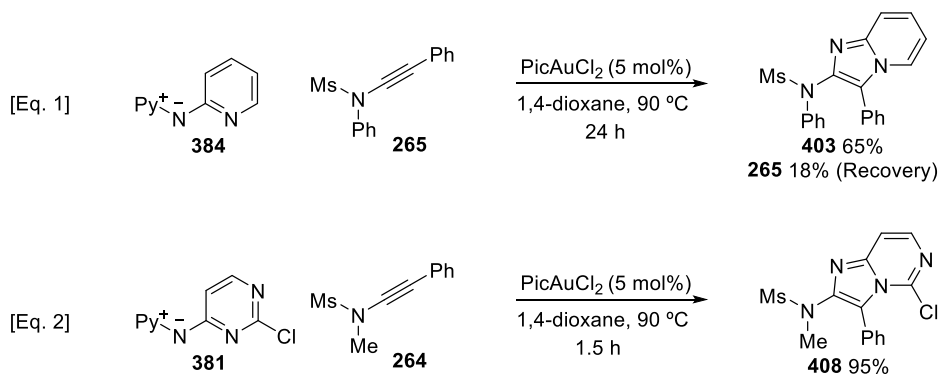


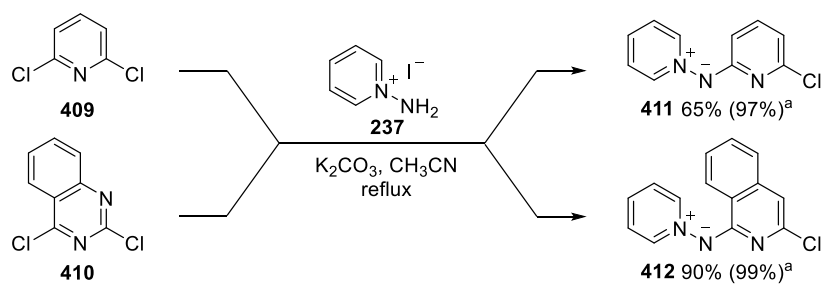
Figure 6: Single crystal X-ray diffraction analysis for compounds **398** and **402**. Data was obtained and solved by Dr Louise Male. Ellipsoids drawn at 50% probability

Contrasting with the diazine systems, pyridine aminide **384** was less reactive, giving more sluggish reactions and large recoveries of unreacted ynamide (around 40% for both **403** and **404** after 48 hours of reaction). Use of gold precatalyst PicAuCl_2 in the synthesis of imidazo[1,2-*a*]pyridine **403** resulted in an improvement of the reaction rate and efficiency (Scheme 59 – Eq. 1), although with less clean outcomes. Likewise, this higher reactivity of the gold(III) species was observed for the diazine systems, giving imidazo[1,2-*c*]pyrimidine **408** in 95% yield in less than two hours (Eq. 2) and with no traces of the unidentified impurity seen during the reaction survey done in Chapter 2.

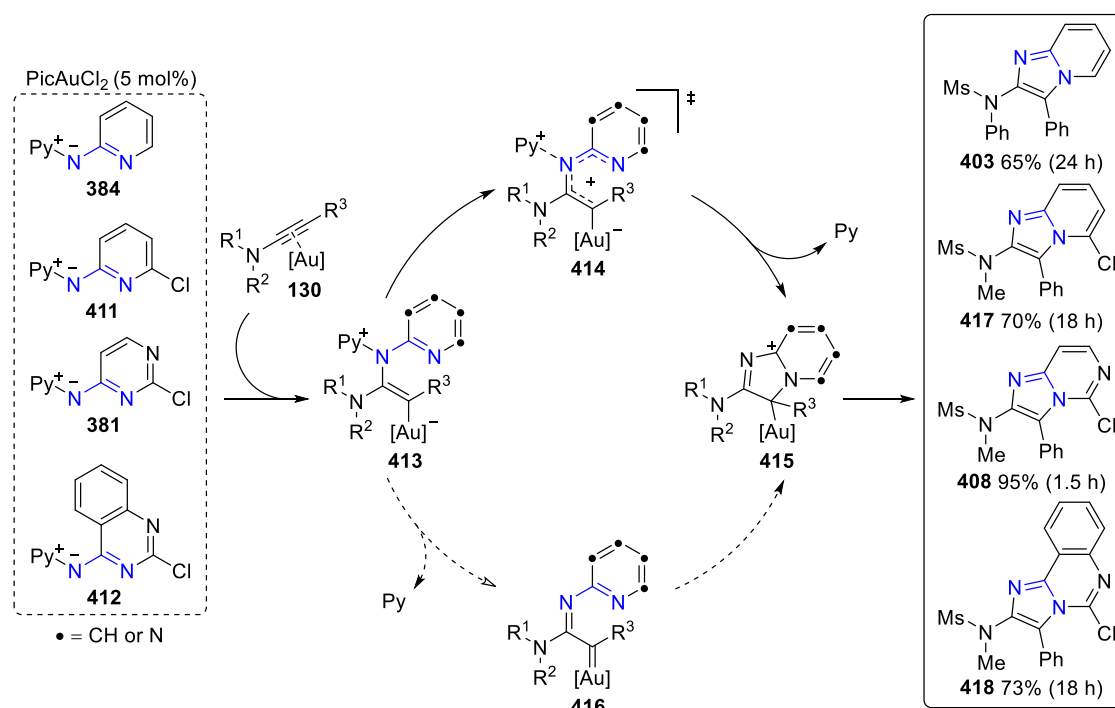
Scheme 59: Synthesis of fused imidazoheterocycles using PicAuCl₂ precatalyst

3.2.3 Mechanistic observations

To gain more insight into the mechanism of the gold-catalysis of Scheme 58, aminides **411** and **412** were synthesised (Scheme 60). Interestingly, 2,6-dichloropyridine **409** was electrophilic enough to undergo a S_NAr reaction with *N*-aminopyridinium iodide **237**, readily giving pyridinium *N*-(6-chloropyridin-2-yl) aminide **411**. This reactivity contrasts with that from monohalogenated pyridines which required an alternative strategy for the synthesis of the corresponding ylide **384** (Scheme 56). The reaction with **409** was further improved when the acetonitrile was replaced with methanol at room temperature, probably due to the better solubility of both *N*-aminopyridinium iodide **237** and potassium carbonate in this solvent. Similar effect was observed with 2,4-dichloroquinazoline **410**, giving aminide **412** in 99% yield after two hours.

Scheme 60: Synthesis of aminides **411** and **412**. ^a Reaction performed in MeOH at rt

Comparison of the results obtained using structurally related aminides **381**, **384**, **411** and **412** in the gold catalysis (Scheme 61) outlined a reactivity trend based on the electronics of the attached heterocycle. Moving from pyridine aminide **384** to the 6-chloro substituted system **411** resulted in a slight increase of the reaction rate and yield of the corresponding imidazo[1,2-*a*]pyridine **417**. Chloropyrimidine derivative **381** led to a more dramatic increase of reactivity as the reaction reached completion in a couple of hours and in almost quantitative yield.

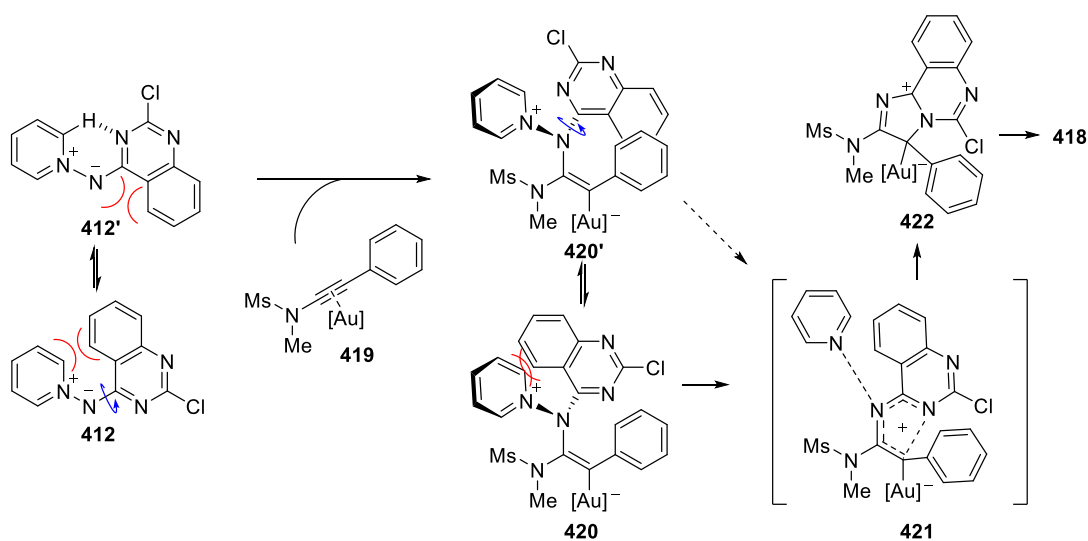


Scheme 61: Comparison of reactivity between structurally related aminides.

According to the proposed mechanism (simplified in Scheme 61), the cyclisation step to the fused system **415** could occur from either vinyl gold carbenoid **413** or from α -imino gold carbene **416** after elimination of pyridine. As discussed in chapter 2, the selectivity of the reaction and the improvement in the reactivity observed with electrophilic gold(I) and gold(III) species suggest that direct cyclisation from vinyl gold carbenoid intermediate **413** was the most likely pathway (**413**→**414**→**415**).

Based on the contrasting reactivity between pyridine **384** and pyrimidine aminides **381** it was hypothesised that cyclisation to the fused imidazo-scaffold (**414**→**415**) was the rate-determining step of the reaction. Therefore, disruption of the aromaticity in the pyridine ring would be a less favourable step giving less efficient processes than diazines.¹⁰⁵

While it was expected that quinazoline **412** would follow this trend due to the lesser aromaticity resulting from the extended conjugation, both reaction rate and product yield were lower than with the pyrimidine derivative **381**. A possible explanation is that the steric clash between the bulky quinazoline ring and the pyridinium fragment forces aminide **412** to adopt a more favourable conformation **412'** which is also stabilised by the hydrogen bonding between the two rings (Scheme 62).



Scheme 62: Proposed mechanism for the formation of imidazoquinazoline 418

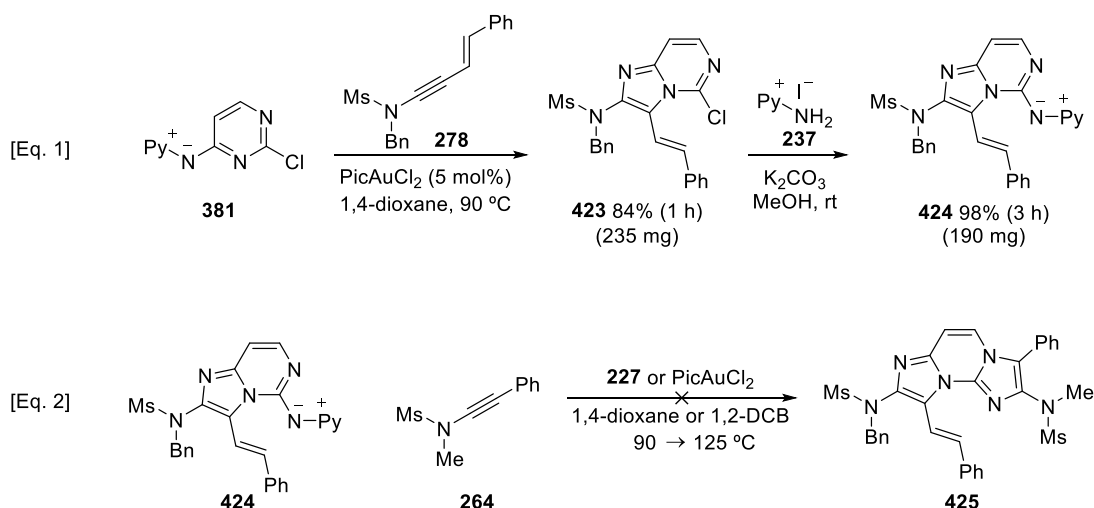
The orthogonal approach of aminide **412'** to the plane of the gold-activated triple bond to give vinyl gold carbenoid **420'** would be sterically hindered by the fused benzene ring, slowing the addition. In order for the 4π -electrocyclisation to take place (**421**→**422**), the exocyclic nitrogen in **420** reconfigures aligning the quinazoline system

in the plane with the metallated carbon centre (**420**→**421**). This requires vinyl gold carbenoid **420'** to adopt conformation **420** which is again (*cf.* **412**) sterically hindered. As a result, the formation of the fused imidazoquinazoline **421** would be considerably slowed down. Nonetheless, imidazo[1,2-*c*]quinazoline **418** could be incorporated to the library of heterocycles available through this transformation.

Since completing this research,³⁵ Zhang and Geng have reported some density functional theory calculations (DFT) of the reaction between pyridinium *N*-(2-pyriminyl) aminide **239** and ynamide **264** that also pointed to the ring-forming stage as the turnover-limiting step. For this analysis they employed trimethylphosphite [(CH₃O)₃P] as computational simpler model of the ligand in the gold(I) complex. The calculated energy profiles indicated that formation of the 5-membered ring (**414**→**415**) was indeed strongly endothermic, controlling the rate of the reaction.

3.2.4 Post-catalytic functionalisation

At this stage of the investigation, several novel halosubstituted imidazoheterocycles had been synthesised as result of the reaction survey (*e.g.* **397-402** in Scheme 58). Examples in the literature show how similar systems can be readily functionalised through metal-catalysed cross-coupling procedures.^{93,106} However, for the purposes of this research a different avenue was pursued. 2,4-Chloropyrimidine was identified as possible candidate to be subjected to an iterative aminide-imidazole ring formation sequence (Scheme 63). Using the corresponding aminide **381**, imidazo[1,2-*c*]pyrimidine **423** was synthesis in larger scale (235 mg, 0.64 mmol). After its isolation, the compound was treated with *N*-aminopyridinium iodide **237** under basic conditions. Gratifyingly, this system rapidly formed aminide **424** in excellent yield (Eq. 1).



Scheme 63: Post-catalytic functionalisation of imidazo[1,2-*c*]pyrimidine **423**

In an attempt to prepare fused tricycle **425** (Eq. 2), aminide **424** was combined with a second ynamide **264**. Different conditions were screened including higher catalyst loading (10 mol%) of either **227** or PicAuCl₂ and more forcing condition using the higher boiling point solvent 1,2-DCB. No reaction was detected in any of the cases, recovering large amounts of starting materials. It was proposed that the basic nitrogen of the imidazole core in **424** could be stabilising a gold-aminide complex, sequestering the catalytic species away from the ynamide **264** and preventing the cyclisation.

Nevertheless, these preliminary results indicate alternative routes for the further diversification of the catalysis products, giving an easy access to complex and varied structures.

3.3 Conclusions

The gold-catalysed reaction between π -rich alkynes and pyridinium *N*-heteroaryl aminides was significantly expanded to cover the synthesis of six types of therapeutically relevant scaffolds: imidazo[1,2-*a*]pyrimidine, imidazo[1,2-*c*]pyrimidine,

imidazo[1,2-*b*]pyridazine, imidazo[1,2-*a*]pyrazines, imidazo[1,2-*a*]pyridine and imidazo[1,2-*c*]quinazoline.

This versatile reaction presents excellent functional group compatibility and chemoselectivity, tolerating the introduction of potentially labile electrophilic substituents that can be used in post-catalysis transformations.

The cyclisation step was identified as possible turnover-limiting step in the mechanism, due to the correlation observed between the aromaticity of the heterocycle in the aminide and the outcome of the reaction.

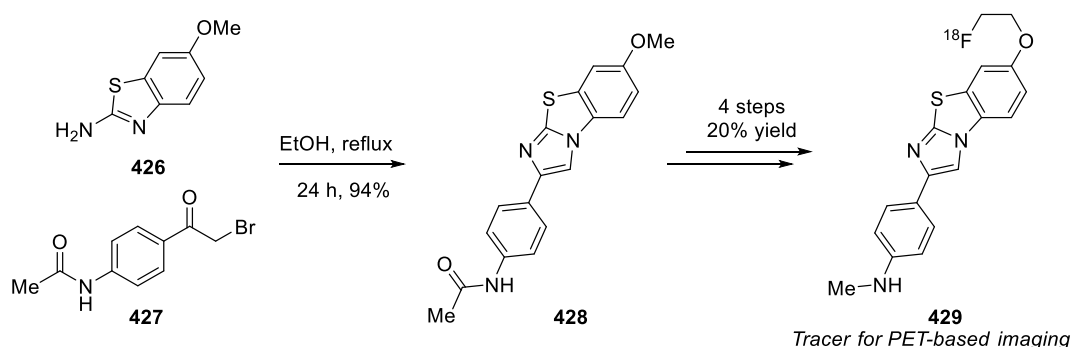
Additionally, it is expected that the revealed potential of pyridinium *N*-heteroaryl aminides as flexible and stable building blocks collaborates to increase the relevance of these underused substrates in synthetic chemistry.

Chapter 4

4.1 Fused imidazobenzoheterocycles

Imidazo-fused heterocycles have been previously introduced as rich and diverse family of scaffolds actively pursued due to their varied biological activity. Structures featuring a 5,5-fused system are, however, less ubiquitous as therapeutic agents or organic materials. With the increase in skeletal complexity, the number of synthetic routes available becomes scarcer.

The condensation between 2-aminoazoles and α -haloketones represents the most extended strategy despite the limitations in terms of availability and compatibility of the substrates (Scheme 64). Consequently, from the different combinations of 5,5-fused imidazoheterocycles, only the imidazo[2,1-*b*]benzothiazole motif has received more widespread use, being present in some candidates for antitumor¹⁰⁷ and antibacterial¹⁰⁸ or labelled with ^{18}F **429** for their use in PET (positron emission tomography)-based imaging in the study of Alzheimer's disease.¹⁰⁹



Scheme 64: Synthesis of an imidazobenzothiazole-base candidate for high-contrast PET imaging in the study of Alzheimer's disease

Heteroaryl aminides have been identified and investigated as versatile building blocks in the assembling of valuable imidazodiazines/pyridines in the previous two chapters. In spite of their individual differences, all the aminides employed so far were based on π -

deficient heterocycles, which facilitated the formation of the ylide *via* simple and general substitution reactions (Scheme 56). As a result, the catalysis products obtained presented a common 5,6-fused scaffold. Seeking to explore the boundaries of the developed nitrenoid approach, 5,5-fused imidazole systems were selected as next goal through the use of complementary π -rich heterocycles. However, considering the obstacles previously encountered due to the electronic differences between diazines and pyridine, the incorporation of five-membered rings in the gold-catalysis was expected to be accompanied by challenges in the preparation of both precursors and products.

4.2 Results and discussion

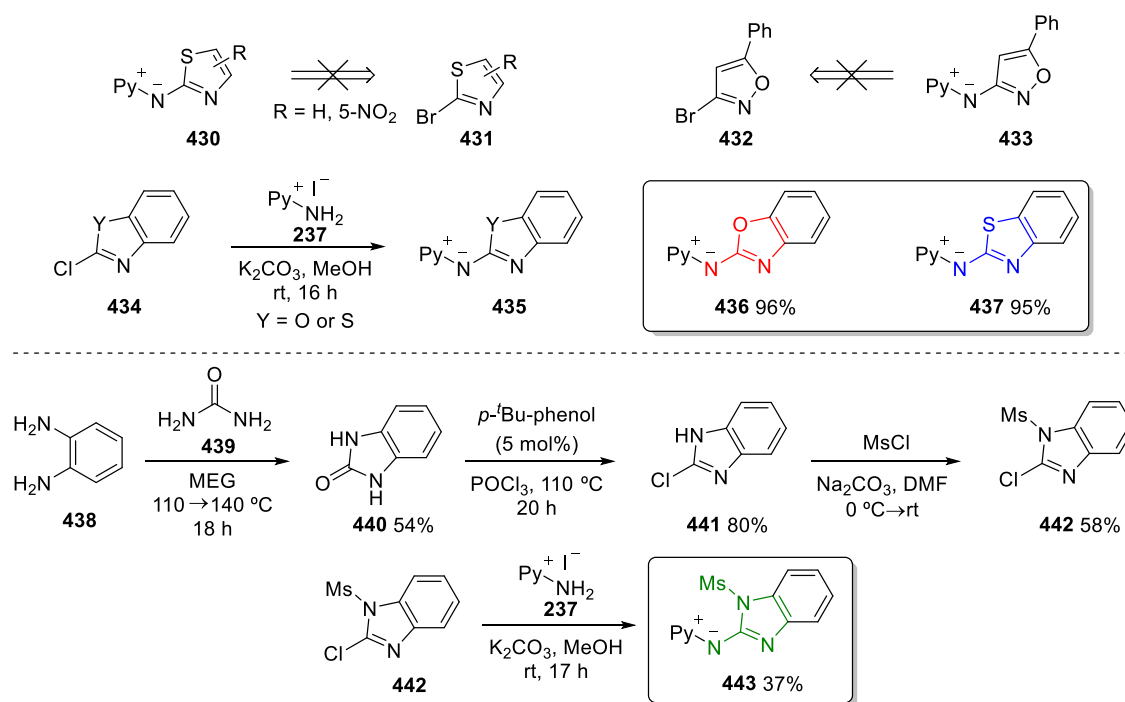
4.2.1 Synthesis of π -rich heteroaryl aminides

In order to make a library of π -rich heteroaryl aminides, several halosubstituted azole derivatives were tested (Scheme 65). Thiazole **430** and isoxazole **432** systems were quickly discarded as feasible precursors due to the high electron density of the ring that hampered the conversion to the desired product either *via* S_NAr or aminopalladation routes.

In contrast, commercially available 2-chlorobenzoxa/thiazoles **434** were suitable substrates that efficiently reacted with *N*-aminopyridinium iodide **237** to give the corresponding aminides **436** and **437** in excellent yields. Based on these promising results, benzimidazole derivative **443** was also selected as an attractive motif for the future gold-catalysis.

For its synthesis, *o*-phenyldiamine **438** was transformed into the cyclic urea **440** and subsequently converted to 2-chlorobenzimidazole **441** by treatment with phosphoryl

chloride (Scheme 65 – Bottom). Following the protection with mesyl chloride, aminide **443** was isolated in a workable 37% yield. Attempts into forming the aminide derivative from the Boc- or benzoyl-protected benzimidazole were unreactive even under more forcing conditions, leading to degradation of the materials.



Scheme 65: Synthesis of azole-based aminides

Similarly to the diazine-based systems, the pyridinium *N*-(benzazole) aminides were bench-stable, bright yellow solids. Crystals of the three compounds were analysed through X-ray (data was obtained and solved by Dr Louise Male. Ellipsoids drawn at 50% probability. Hydrogen atoms omitted. Figure 7–8). There was little difference in the key bond lengths or angles across the series. In the three structures the pyridinium ring was almost coplanar with the fused azole system, with a smaller deviation in the benzoxazole derivative **436**. Analogously to the data reported in the literature for other diazine-based aminides,⁵³ in solid state there seem to be an intramolecular hydrogen

bonding between the endocyclic nitrogen (N1) and the hydrogen atoms in 2-position of the pyridine ring.

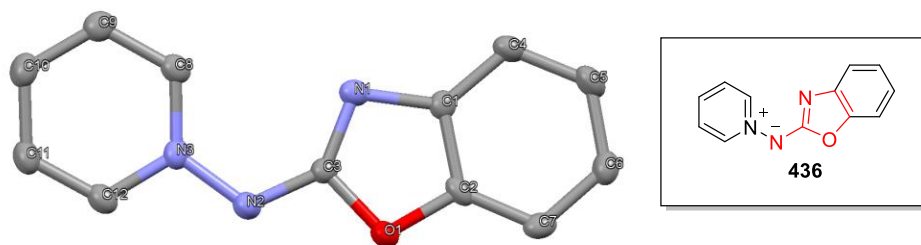


Figure 7: X-Ray structure of 436. N2–N3: 1.37(8) Å, N2–C3: 1.34(1) Å, C3–N1: 1.31(8) Å, N2–C3–N1: 135.8°, N3–N2–C3–N1: -4.1°

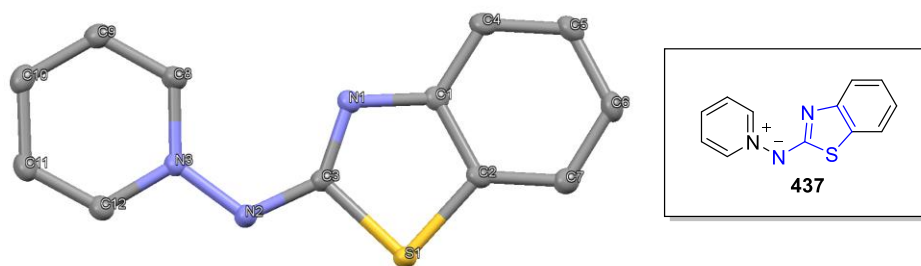


Figure 8: X-Ray structure of 437. N2–N3: 1.38(4) Å, N2–C3: 1.34(1) Å, C3–N1: 1.31(5) Å, N2–C3–N1: 133.8°, N3–N2–C3–N1: 0.5°

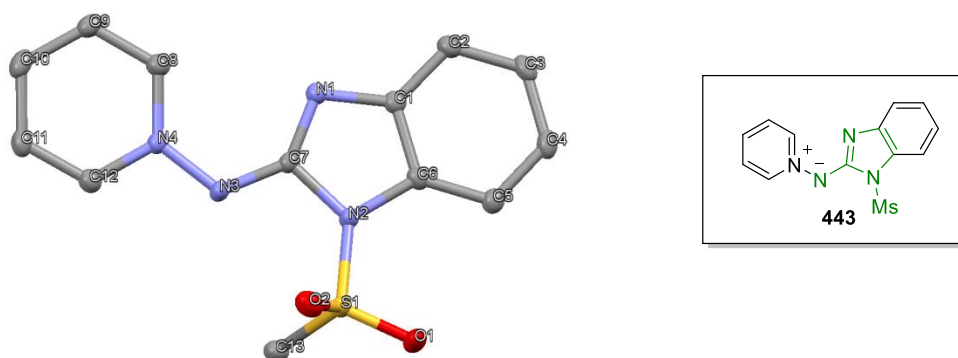
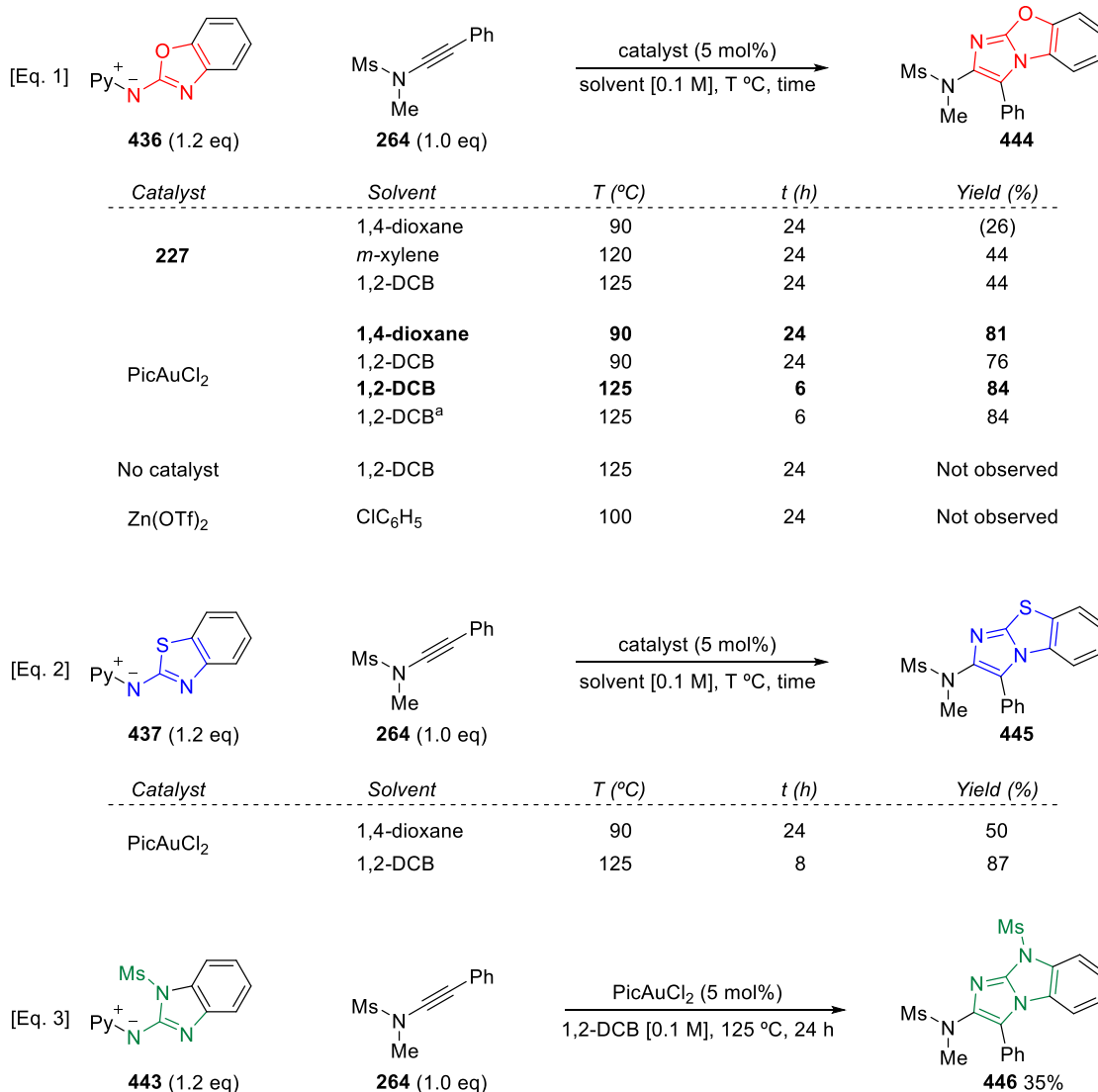


Figure 9: X-Ray structure of 443. N3–N4: 1.37(5) Å, N3–C7: 1.33(7) Å, C7–N1: 1.32(0) Å, N2–C3–N1: 134.5°, N3–N2–C3–N1: 1.1°

4.2.2 Formation of 5,5-fused scaffolds

The use of these π -rich aminides under gold-catalysis was investigated. In a preliminary test, benzoxazole-substituted system **436** was combined with ynamide **264** and gold(I) complex **227** following the original conditions developed in Chapter 2 for the synthesis of imidazo-fused heterocycles (Scheme 66 – Eq. 1). After 24 hours of reaction imidazo[2,1-*b*]benzoxazole **444** had been formed, although most of the starting material remained unreacted. Use of more forcing conditions in either *m*-xylene^{34a} or 1,2-DCB aided in the conversion to the fused system. Due to the higher boiling point of these solvents, after reaction completion the mixtures were directly purified through flash chromatography and therefore, all the given yields are from the isolated product.

In light of previous results where gold(III) precatalyst PicAuCl₂ enhanced the rate of cyclisation to the five-membered ring, this complex was subsequently introduced in the present screening. Gratifyingly, the yield of isolated product was almost duplicated over the same period of time at 90 °C in 1,4-dioxane. Reaction in 1,2-DCB gave slightly lower amounts of products at the same temperature but on increase to 125 °C, imidazo[2,1-*b*]benzoxazole **444** was isolated in a higher 84% yield after only 6 hours. It is worth noticing that the reaction afforded the same yield when no precautions were taken to exclude air or moisture (opened flask and non-dried solvent). As expected, no reactivity was observed in absence of catalyst or when zinc triflate (recently unveiled as surrogate of gold in some transformations)¹¹⁰ was employed.



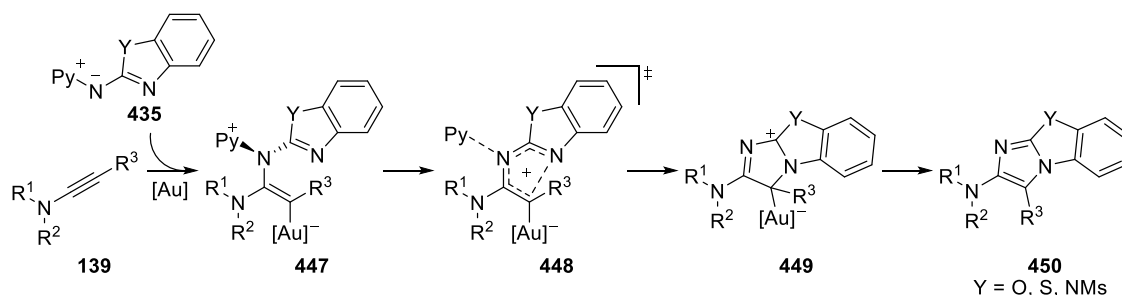
Scheme 66: Survey for the reaction with π -rich heteroaryl aminides. Yields given as isolated product after chromatography. ^a Reaction performed in an opened-flask with non-dried solvent

Analogously, imidazo[2,1-*a*]benzothiazole derivative **445** was isolated in excellent yield after 8 hours at 125 °C using PicAuCl₂ complex (Scheme 66 – Eq. 2). A considerable drop in the yield was observed when the reaction was performed in 1,4-dioxane at 90 °C. Hence, 1,2-DCB at 125 °C were selected as general conditions for the formation of the 5,5-fused systems.

While protected benzimidazole derivative **443** also underwent a formal [3+2]-dipolar cyclisation to deliver the desired imidazo[1,2-*a*]benzimidazole **446**, it was found to be

substantially less reactive than the other annulated aminides giving large recoveries of unreacted ynamide (Eq. 3). Only the more forcing conditions yielded some product, in spite of the longer reaction times.

A plausible explanation for the lower reactivity of the benzimidazole derivative **443** could be assigned to a higher aromaticity of this system when compared with the benzoxazole **436** and benzothiazole aminides **437**. Attending to the proposed mechanism (Scheme 67), a bis-heteroatom 4π -electrocyclisation from vinyl gold carbenoid intermediate **447** seems the most likely pathway considering the better result obtained with electrophilic gold species. As seen in chapter 3, the ring-forming stage (**448**→**449**) was indicated to be the turnover-limiting step of the reaction and therefore, a less favourable loss of aromaticity in the conjugated heterocycle would reduce the reactivity of the aminide.



Scheme 67: Proposed mechanism for the gold-catalysed synthesis of fused imidazobenzoheterocycles

Combining the crystallographic data and HOMA (Harmonic Oscillator Model of Aromaticity) index for benzazole heterocyclic motifs, Karolak-Wojciechowka and collaborators determined that the aromaticity for the parent series follows the order: benzoxazole < benzothiazole < benzoimidazole.¹¹¹ While the study does not take into account the *N*-protecting group in the benzoimidazole (*i.e.* the authors acknowledge that

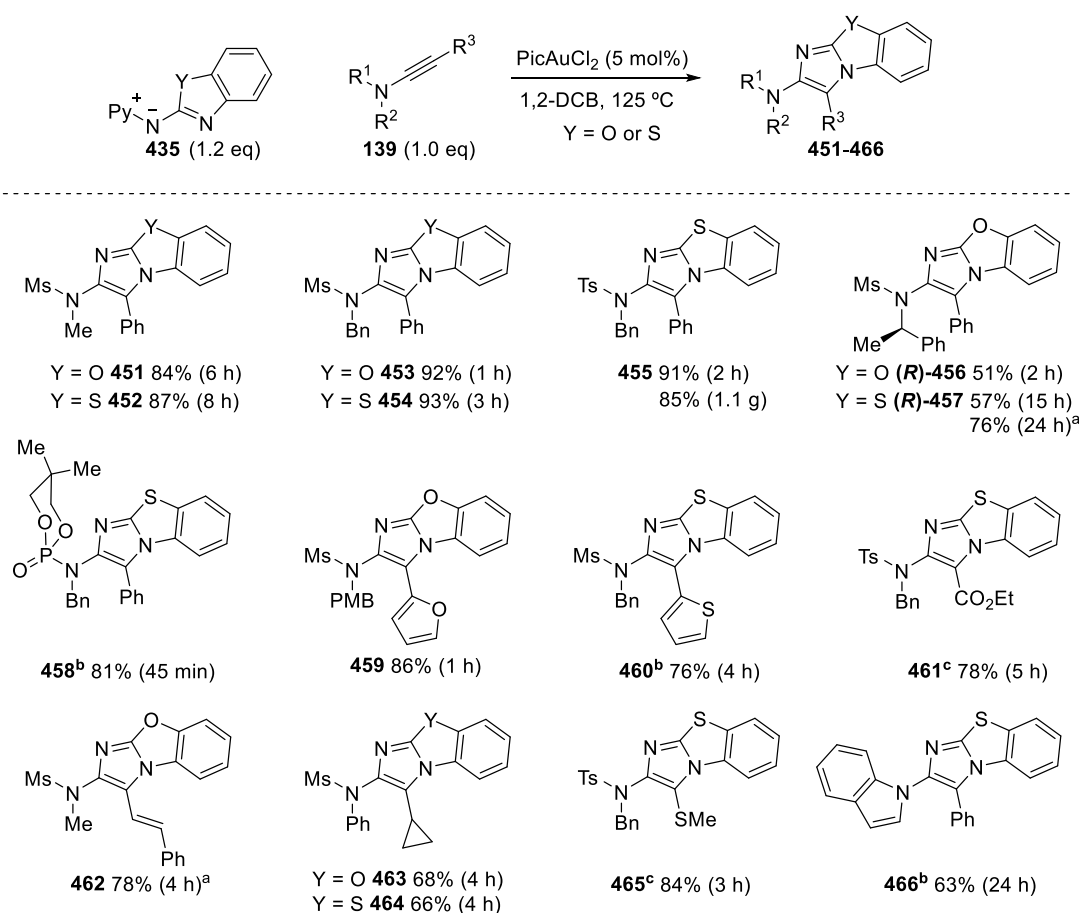
the effect of the *N*-substituent in the electronegativity of the heteroatom can significantly change the parameters), this trend would be consistent with the experimental observations for the current reaction.

The reactivity profile observed for these aminides could also be derived from the more π -rich character of benzazole rings in comparison with diazine/pyridine-substituted systems. A higher nucleophilicity of the endocyclic nitrogen might lead to stronger intramolecular hydrogen bonding with the α -protons of the pyridine group (as reported by Alvarez-Builla and collaborators).⁹⁹ To some extent, this could lock an unreactive conformation where exocyclic and endocyclic nitrogen atoms point in opposite directions of the plane (as seen in the crystal structures in Figure 7-3). Use of more forcing conditions (1,2-DCB at 125 °C) would reduce this interaction aiding in the cyclisation step. Alternatively, the more π -rich character of the aminide/product might be favouring its coordination to the gold complex, reducing the effective concentration of catalytic species.

4.2.3 Reactivity towards ynamides

Once benzazole-based aminides were established as valid nucleophilic nitrenoids in the formal [3+2]-dipolar cycloaddition, the more reactive benzoxazole **436** and benzothiazole derivatives **437** were reacted with different gold-activated ynamides. Scheme 68 presents some of the examples synthesised to test the scope of the methodology. This table of substrates was prepared in collaboration with Elsa Martínez Arce (E.M.A.) and Dr. Raju Jannapureddy (R.J.), both members of the Davies Group (compounds obtained by them are indicated in the Scheme).

Both aminides had a similar behaviour and gave comparable good yields when combined with the same ynamide, although the reactions with benzothiazole derivative **437** were generally slower. Mesityl, tosyl and phosphoryl protected ynamides were well tolerated and in most of the cases the reaction reached completion after a few hours **451-458**. While these conditions allowed the installation of stereogenic centres adjacent to the tricyclic scaffold (**456** and **457**), the ynamide precursor was quickly degraded at 125 °C. Switching to 1,4-dioxane 90 °C improved the yield at expenses of longer reaction times.



Scheme 68: Synthesis of fused imidazobenzoxazoles/thiazoles from different ynamides. ^a Reaction performed in 1,4-dioxane at 90 °C. ^b Example prepared by *E.M.A.* ^c Example prepared by *R.J.*

The synthesis of imidazo[2,1-*b*]benzothiazole **455** was also performed at larger scale giving 1.1 grams of the fused heterocycle. The 1,2-dichlorobenzene employed for this scaled-up reaction (25 mL) was removed through distillation under reduced pressure before purification of the residue through flash chromatography, affording the desired compound. After full characterisation, **455** was redissolved in CHCl_3 , transferred to a 10 mL flask and loosely capped with a Teflon stopper to allow a slow evaporation of the solvent. After one month, **455** had crystallised into a white needle-like solid shown in Figure 10.

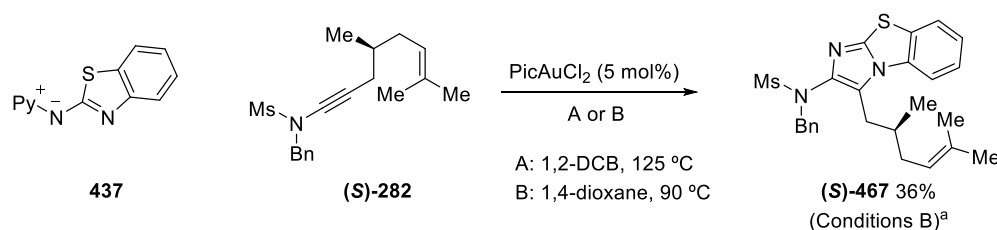


Figure 10: Crystals of imidazo[2,1-*b*]benzothiazole **455** grown after the gram scale reaction

Generally good yields were obtained independently of the electronic differences between ynamides, allowing even the introduction of versatile carboxylic ester **461** and heteroaromatics such as furan **459** and thiophene **460** at C-3. Highly reactive enynamides were also tolerated, although at 125 °C the ynamide quickly degraded affording **462** in 35% yield. By switching the conditions to 1,4-dioxane at 90 °C the yield was highly improved to 78% after 4 hours. Interestingly, on formation **462** crashed out in the solution and once the reaction mixture reached room temperature was readily purified by filtration and washing with cold diethyl ether. 2-Amino-3-thioether

derivative **465** was obtained as a single regioisomer despite the presence of a second nominal directing group in the ynamide.^{34b} Similarly, *N*-indole derivative **466** was obtained in good yield although at slower rate.

In contrast, alkyl-substituted ynamides gave complex reaction mixtures difficult to separate using either set of conditions (Scheme 69). These mixtures would be again (*cf.* Scheme 42) consistent with 1,2-*C,H* insertion pathways that drastically reduced the formation of the desired product, with the exception of cyclopropyl-ynamide **279** which successfully underwent the cyclisation to give the corresponding fused heterocycles **463** and **464**.

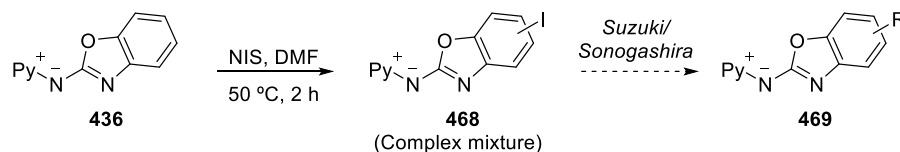


Scheme 69: Reaction of aminide **437 with alkyl-substituted ynamide. Complex mixtures obtained. ^a Yield calculated by ¹H-NMR against a known quantity of internal standard**

4.2.4 Routes for the synthesis of functionalised benzazole aminides

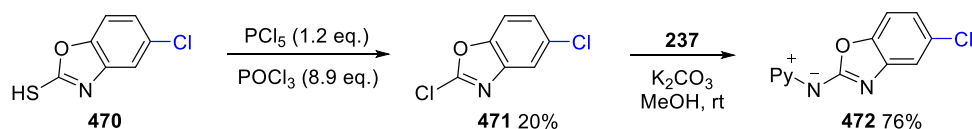
The introduction of more varied functionality in the catalysis product was subsequently pursued. In an attempt to prepare iodine-substituted aminides for a posterior functionalization step using cross coupling reactions (following the synthetic procedure in Scheme 57), aminide **436** was treated with *N*-iodosuccinimide in DMF (Scheme 70). These conditions led to an inseparable mixture of unreacted material and regioisomers from the halogenation in different positions of the fused benzene ring. Similar selectivity challenges were encountered by other members of the group when trying to

functionalise the 2-chlorobenzoxa/thiazole precursor prior to the formation of the aminide.



Scheme 70: Failed sequence for the functionalization of benzazole aminides

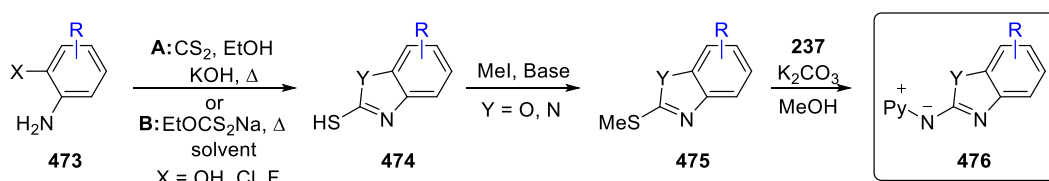
Thus, it was decided to assemble 2-halobenzazole rings bearing a preinstalled substituent. Following a literature procedure,¹¹² 2,5-dichlorobenzoxazole **470** was synthesised by chlorination of 2-mercapto derivative **471** using a mixture of POCl_3 and PCl_5 (Scheme 71). While aminide **472** was subsequently obtained in good yield by reaction of **471** with *N*-aminopyridinium iodide **237**, the low efficiency and hazards of the chlorination step (use of toxic, harmful and corrosive reagents) were highly undesirable.



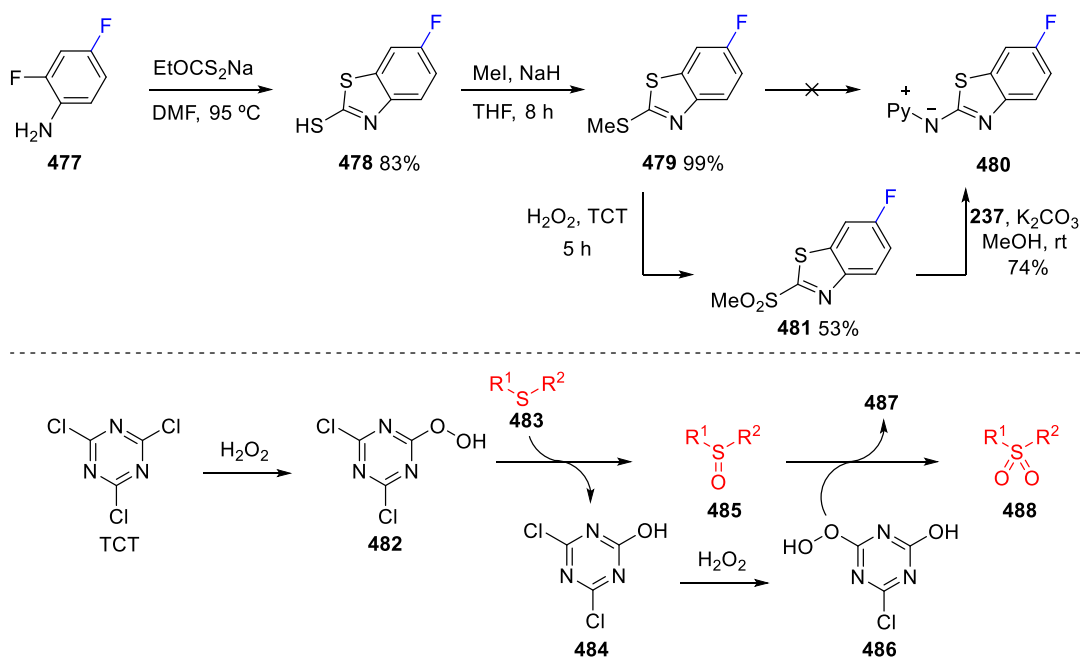
Scheme 71: Synthesis of chloro-substituted aminide 472

Therefore, 2-methylthio benzazoles **475** were selected as synthetic equivalents of 2-halobenzazole **434** in the formation of heteroaryl aminide (Scheme 72). Both benzoxazole and benzothiazole thioether derivatives **475** were readily accessed from commercially available substituted *o*-halo or *o*-hydroxy aromatic amines **473** following a general and straightforward sequence:¹¹³ heating in either carbon disulfide and base in ethanol (method A) or sodium ethyl xanthate (method B) formed the annulated thiol **474** which precipitated in the solution after allowing it to cool down to room temperature.

These compounds were successfully treated with methyl iodide to form the corresponding thioether derivative **475** which in most of the cases rapidly underwent aminide formation. Using this synthetic protocol other members of the group were able to prepare several aminides bearing halogen atoms (F, Cl and Br) and nitro groups attached to 4-,5- and 7-positions of the fused benzene ring in good yields.



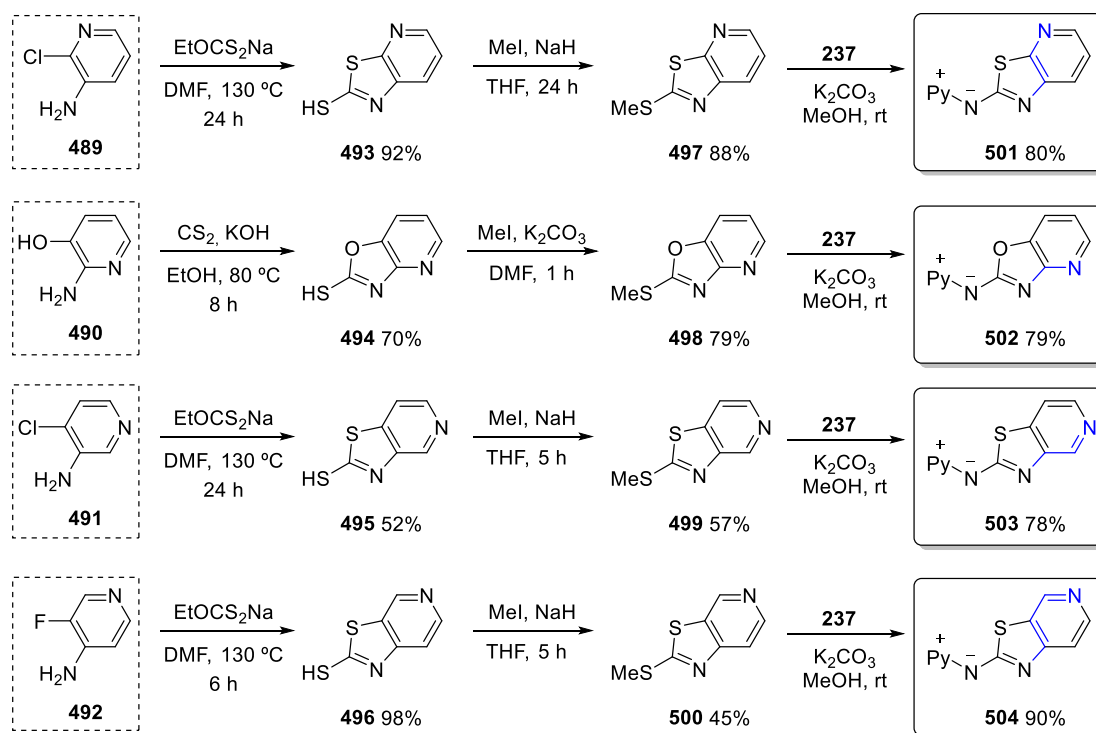
Scheme 72: Strategy for the preparation of functionalised *N*-(heteroaryl) aminides from thioether derivatives.



Scheme 73: Top: Synthesis of fluoro-substituted aminide **480; Bottom: Mechanism for the TCT-promoted oxidation of sulfides to sulfones**

Interestingly, 6-fluoro-substituted thioether **479** resulted insufficiently reactive in the substitution step and the compound degraded before formation of the corresponding aminide **480** was detected (Scheme 73 – Top). In order to enhance its electrophilicity,

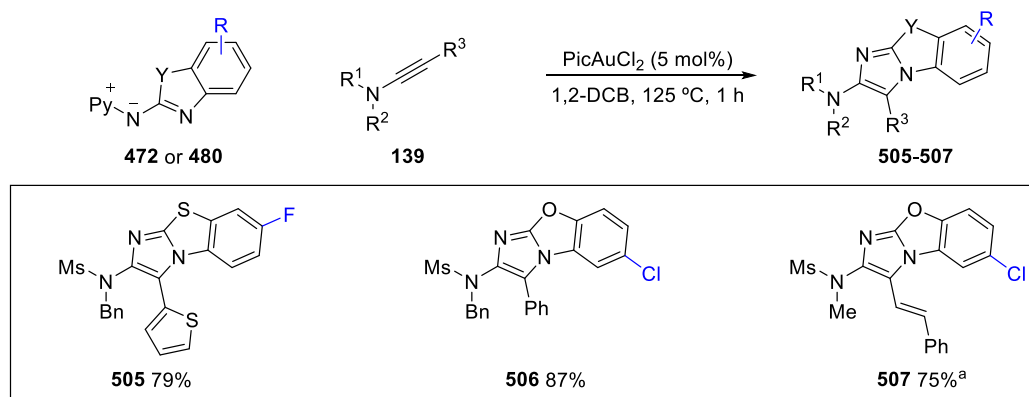
479 was oxidised to sulfone **481** by reaction with H_2O_2 . **481** smoothly reacted with *N*-aminopyridinium iodide **237** in a subsequent step to give the desired aminide **480**. Cyanuric chloride (2,4,6-trichloro[1,3,5]triazine, TCT) is proposed to promote the oxidation of **479** by forming an electrophilic peroxide intermediate **484** that is attacked by sulfide **483** (Scheme 73 – Bottom).¹¹⁴ The resulting sulfoxide **485** can be reoxidised with intermediate **486** from the addition of a second molecule of H_2O_2 , giving sulfone **488**.



Scheme 74: Synthesis of fused aza-analogues

The synthetic protocol in Scheme 72 was also applied to hydroxyl- and halo-substituted aminopyridines **489-492** giving the corresponding thioethers **497-500** (Scheme 74). These sulfides smoothly reacted with *N*-aminopyridinium iodide **237** affording novel fused aza-analogues **501-504** in good yields. Similarly to previous aminides, these compounds were bright yellow crystalline solids.

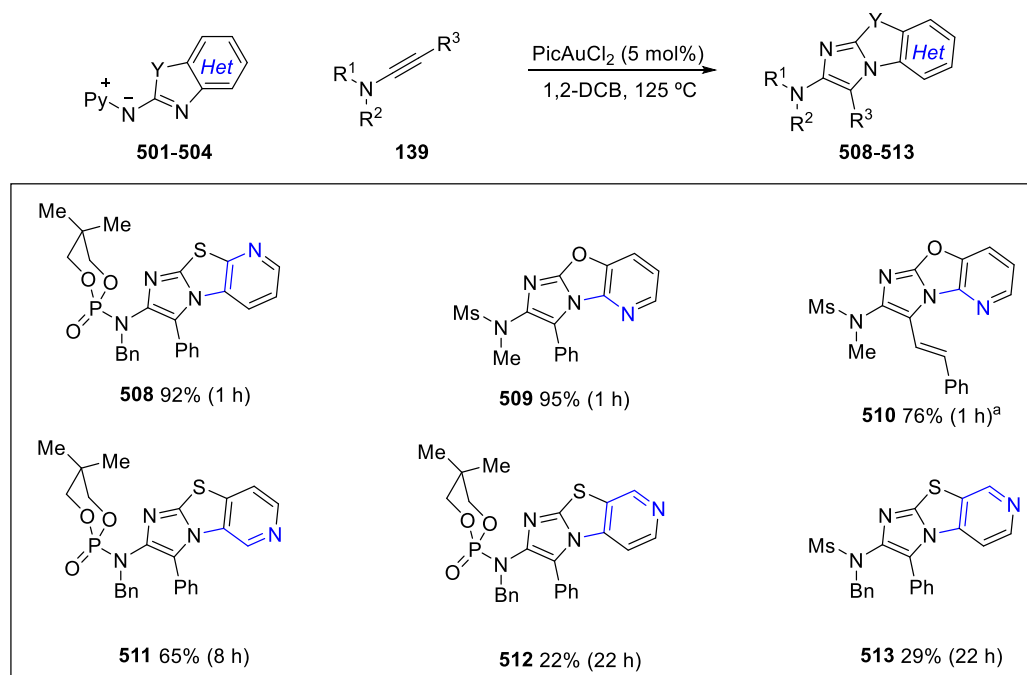
All these structures were tested in combination with various aminides under the standard conditions (1,2-DCB at 125 °C), revealing a similar behaviour to aminides **436** and **437** (Scheme 75). Both 5-chloro **472** and 6-fluoro-substituted derivatives **480** rapidly underwent formation of the desired fused heterocycles **505-507**.



Scheme 75: Use of halo-substituted aminides in the synthesis of fused imidazobenzoxa/thiazoles.^a
Reaction performed in 1,4-dioxane at 90 °C

Considering the challenges previously encountered in the reaction with enynamides (**462** in Scheme 68), 1,4-dioxane at 90 °C was directly employed in the synthesis of **507** which was rapidly formed in 75% yield after 1 hour.

Likewise, pyridine-fused aminides **501-504** led to novel tri-hetero-fused scaffolds **508-513** (Scheme 76), although in this case the profile of the reaction was significantly affected by the position of the nitrogen in the six-membered ring. The 4- and 7- aza-analogues **502** and **501** quickly afforded excellent yields of the corresponding heterocycles **508-510**. In contrast, the reaction with 5- analogue **503** reached completion only after eight hours **511**, and 6-aza derivative **504** was even less reactive, giving relatively low yields of **512** and **513** after prolonged heating independently of the ynamide used.

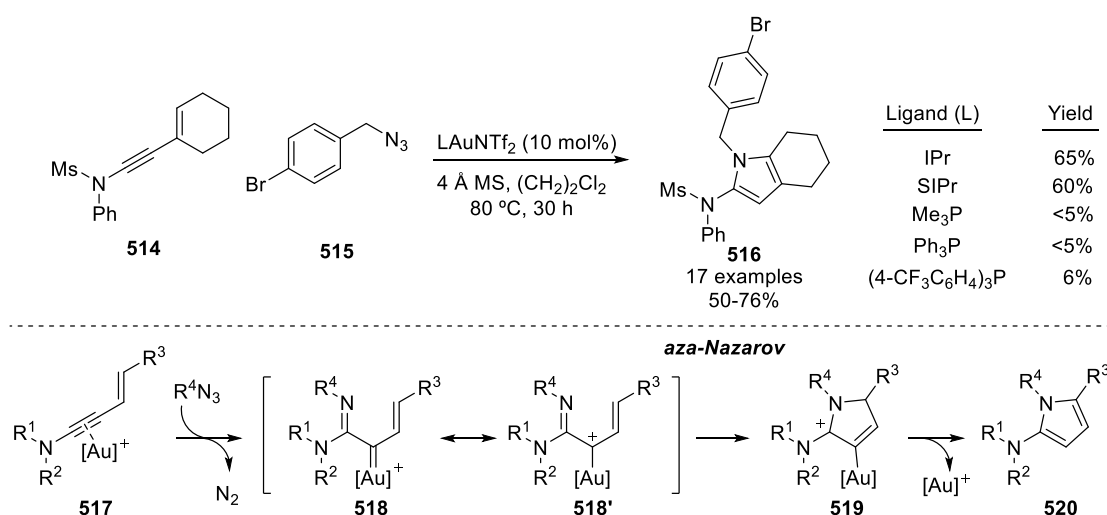


Scheme 76: Use of aza-analogues in the synthesis of fused imidazobenzoxa/thiazoles: ^a Reaction performed in 1,4-dioxane at 90 °C

The reason for this trend could originate from the coordination of the metal with the nitrogen atoms of the fused pyridine ring in these aminides, reducing the concentration of active catalyst to interact with the ynamide. Nitrogen atoms in 4- and 6-position would be more basic due to the conjugative effect of the exocyclic nitrogen in the aminide system. However, inductive and steric effects in 4 and 7-position could be destabilising the N–Au complex. As a result, aminides **501** and **502** were very reactive while the reaction with **504** did not progress further after few minutes. A nitrogen atom in 5-position would be less basic than in 6- giving a less stabilised metal complex. Nevertheless, **503** is more sterically accessible to the metal than **501** and **502** which could explain the sluggish reaction obtained with aminide **503**.

4.2.5 Confirmation of the structure of vinyl substituted derivatives

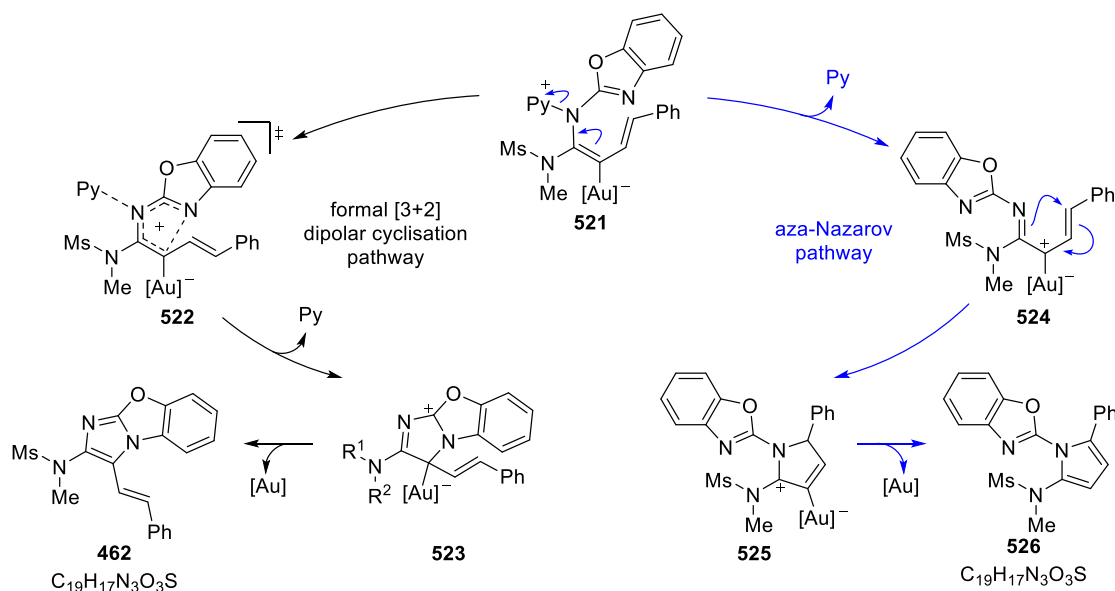
As discussed in Scheme 67, the formation of fused imidazoheterocycle **450** is proposed to follow a formal [3+2]-dipolar cycloaddition process analogous to the described for the reaction with diazine-based aminides. On gold-activation of the ynamide, the aminide **435** regioselectively attacks on the π -system giving vinyl gold carbenoid **447**. This intermediate would undergo a bis-heteroaryl 4π -electrocyclisation simultaneous to the elimination of the pyridine leaving group to form **449**. A final deaurative aromatisation step affords the desired fused heterocycle **450**. With the exception of ynamides bearing an alkyl chain that afforded complex mixtures (Scheme 69), all the systems tested were highly reactive and selectively gave the fused benzoheterocycle. Particularly, enynamides were similarly found to be suitable substrates for the cycloaddition process although milder conditions (1,4-dioxane at 90 °C) were required in those cases in order to afford good yields of the corresponding products **462**, **507** and **510**.



Scheme 77: Synthesis of 2-aminopyrroles through gold-catalysed aza-Nazarov cyclisation of enynamides and azides

Interestingly, Shu et al. have recently reported a gold-catalysed azide-based intermolecular nitrene transfer reaction onto enynamides **514** (Scheme 77).¹¹⁵ Under their reported conditions enynamides undergo an alternative aza-Nazarov pathway to furnish valuable 2-aminopyrrole derivatives **516**. Similarly to the reaction with aminides, the mechanism would be initiated with the attack of the nucleophilic nitrenoid into the gold-activated triple bond **517**. Subsequent extrusion of N₂ leads to the α -imino gold carbene **518/518'**. This species undergoes a 4 π -electrocyclisation giving intermediate **519** which after protodemetalation affords pyrrole **520**.

At this point of the studies detailed in this thesis, it was considered that the reaction between aminides (either diazine/pyridine- or benzazole-based) and enynamides could potentially be giving the corresponding aza-Nazarov product **520** in place of the desired fused imidazoheterocycle as both compounds are isomers (*e.g.* as indicated in Scheme 78 using aminide **436**).



Scheme 78: Potential alternative pathway from the reaction with enynamides

Direct analysis of **462** could not be used to unambiguously confirm the structure of the isolated compound, although resonances for the pyrrole fragment were not seen in the expected range (Figure 11). The aromatic region of the spectrum was too complex due to overlapping of the signals which diffculted the identification of individual resonances (Appendix 1.1 – p.194).

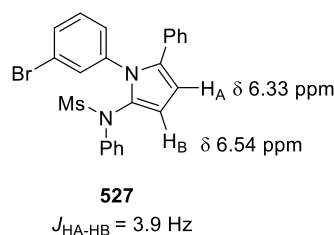


Figure 11: Reported values for the ^1H -NMR shifts of the characteristic pyrrole protons in aza-Nazarov product **527¹¹⁵**

A better resolved spectrum was obtained for chloro-substituted analogue **507**. Attending to the coupling constants every peak could be matched to the corresponding proton in the scaffold (Figure 12; Full assignment in Appendix 1.2 – p.198). More importantly, the olefinic signals were identified through the large J value ($^3J_{\text{trans}} = 16.6 \text{ Hz}$) confirming the formation of the imidazo[2,1-*b*]benzoxazole system **507**.

2D-NMR spectroscopy experiments (HSQC and HMBC pulse sequences) allowed the carbocyclic skeleton of **507** to be fully assigned. Comparison of the ^{13}C -spectra for compounds **462**, **507** and **510** (Figure 13) showed a correlation between the peaks across the three molecules.

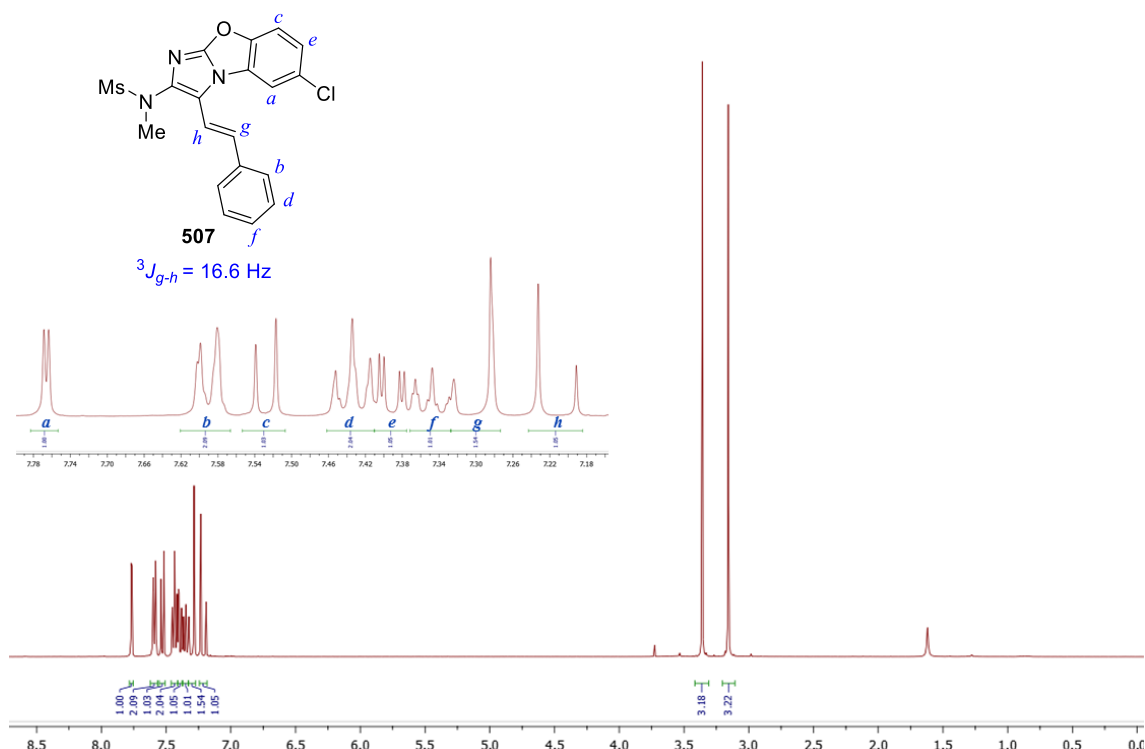


Figure 12: $^1\text{H-NMR}$ spectrum of compound **507** and assignment of the resonances

Despite the structural modifications in the core scaffold, the signals for the styryl fragment remained mostly unchanged. For instance, the olefinic peaks *e* and *o* consistently appeared around 131.0 and 113.0 ppm respectively. The correlation is maintained even in aza-derivative **510**, where the presence of an extra nitrogen atom greatly affects the shifting of the surrounding carbons *b* and *f*. These values contrast with those reported for pyrrole derivatives (Scheme 77),¹¹⁵ where both resonances for the characteristic carbon atoms in 3- and 4-position of the five-membered ring consistently appear at approximately 108.0 ppm. Therefore, it was concluded that in the three cases, the desired imidazobenzoxazole system was the product of the catalysis.

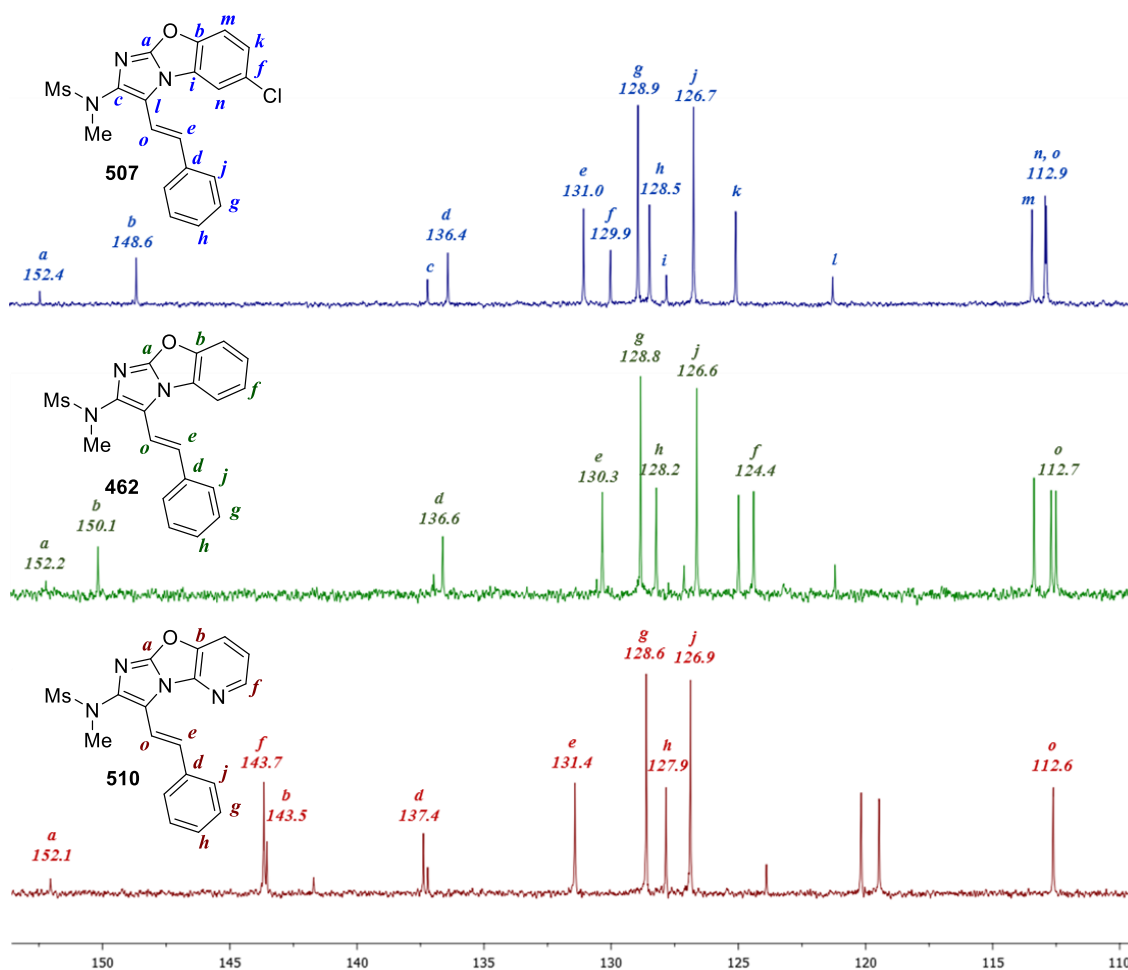


Figure 13: Expansion comparing ^{13}C -NMR spectra of compounds 462, 507 and 510

Additionally, analysis of the ^1H -NMR spectrum of styryl-substituted imidazo[1,2-*a*]pyrimidine **299** obtained through the same methodology (Scheme 40) similarly displays resonances typical for olefinic protons with *trans*-configuration ($^3J_{\text{trans}} = 16.7$ Hz) (Figure 14).

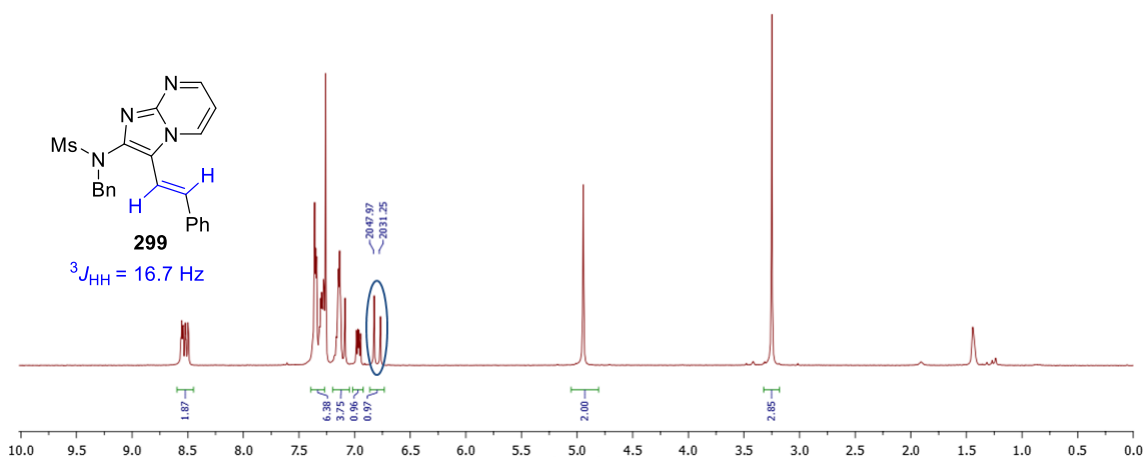


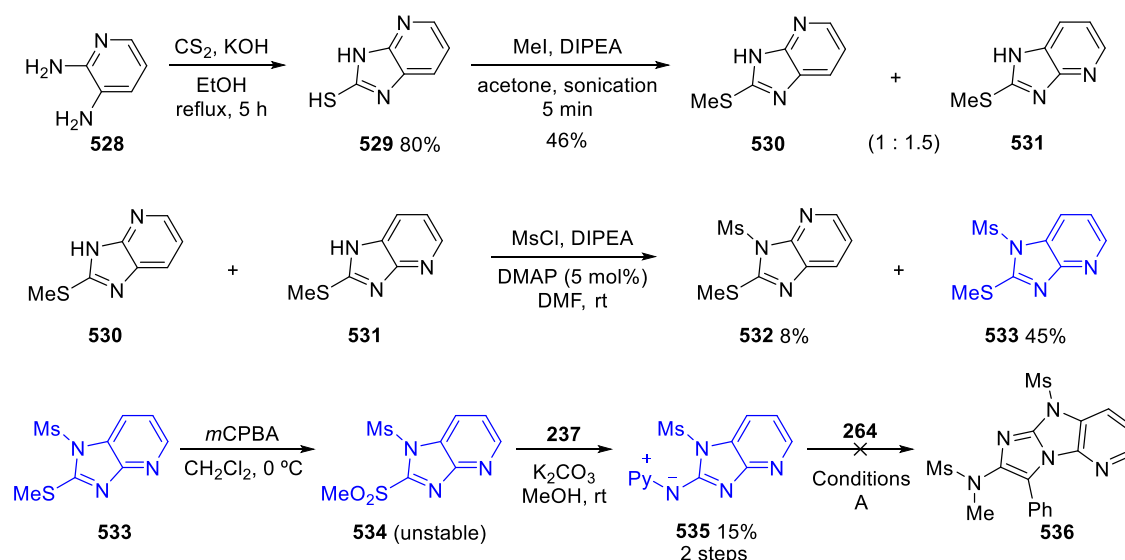
Figure 14: ^1H -NMR spectrum of imidazo[1,2-*a*]pyrimidine **299**

Returning to the aza-Nazarov cyclisation (Scheme 77), Shu *et al.* proposed a mechanism involving the cyclisation from gold carbene intermediate **518**, formed after the elimination of N_2 . Workable yields of product **516** were only obtained by employing σ -donating ligand on the gold(I) complex (IPr and SIPr) (Scheme 77). This trend directly opposes to the studies detailed in this thesis, where electrophilic gold(I) phosphide **227** and gold(III) precatalyst PicAuCl_2 were found to be the most suitable complexes for catalysing the formal [3+2]-dipolar cycloaddition process. Thus, the cyclisation step is believed to precede from the vinyl gold carbenoid intermediate **447** with near-synchronous elimination of the nucleofuge (Scheme 67).

4.2.6 Reactivity of benzimidazole-based aminides

Based on the good results obtained with aza-derivatives **501** and **502** (Scheme 76), it was proposed that an analogous pyridine-fused imidazole aminide might reduce the π -density on the five-membered ring and therefore, be more reactive than the parent benzimidazole **443** (Scheme 66).

For its synthesis (Scheme 79), 2,3-diaminopyridine **528** was treated with carbon disulfide to form the thiol derivative **529**. Sulfide formation lead to an inseparable mixture of tautomers **530** and **531** (1:1.5 ratio) that was directly taken into the next step. Protection with mesyl chloride gave preferentially **533**, although in this case the mixture of isomers could be separated through flash chromatography. Sulfide **533** resulted unreactive under aminide-forming conditions and had to be oxidised to the sulfone **534** by treatment with *m*CPBA. **534** Was unstable and decomposed during the purification. Thus, the substitution with *N*-aminopyridinium iodide **237** was immediately performed once the oxidation was completed.



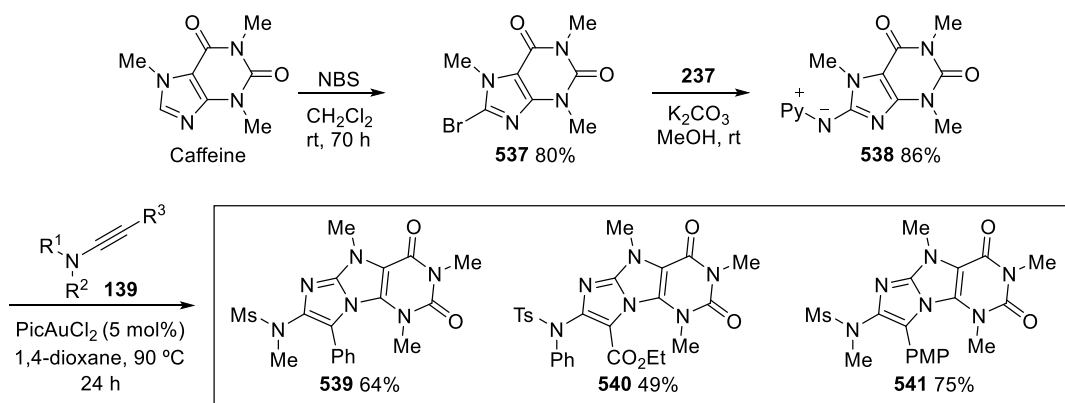
Scheme 79: Synthesis and reactivity of aza-analogue 535. Conditions A: PicAuCl₂ (5 mol%+ additional 5 mol% after 20 h) in 1,2-DCB at 125 °C for 24 h

Aminide **535** was isolated as a pure bench-stable solid, although in low yield after the two consecutive reactions. Unfortunately, no reactivity was achieved when it was treated with ynamide **264** under the standard conditions (1,2-DCB at 125 °C). After 24 hours no progress was detected and most of the starting material remained unreacted in spite of the addition of an extra 5 mol% of catalyst.

This may be again attributed to the formation of an aminide-metal complex, sequestering gold away from ynamide. The stabilisation of this complex may be related with a higher basicity of the pyridine nitrogen atom due to the more π -rich character of the imidazole system.

Considering the apparent inefficiency in the reaction with benzimidazole-based aminides, caffeine derivate **538** was selected as potentially attractive substrate (Scheme 80). It was expected that the presence of an electron-withdrawing 1,3-dimethyluracil group in **538** would reduce the π -density of the xanthine system. Thus, the stabilisation of an unproductive aminide-metal complex would be less favoured or even restricted by the *N*-methyl groups, giving an improved reactivity in comparison with aminides **443** and **536**.

To test this hypothesis, 8-caffeine **537** was selected as precursor in the synthesis of aminide **538**. Reported conditions for the selective bromination at C-8 gave inconsistent low yields of **537**.¹¹⁶ The reaction was repeated using both freshly recrystallised and aged NBS, the latter giving an improved outcome probably derived from the presence of highly reactive molecular bromine in it. **537** Smoothly underwent substitution with **237** to form aminide **538** as a bright orange solid (Scheme 80). This aminide successfully reacted with different electron rich/poor ynamides to form the desired cyclisation adducts **539-541** in good yields. Milder conditions (1,4-dioxane at 90 °C) were however required as **538** degraded on prolonged heating at 125 °C. This structures appear to be the first synthesised examples of functionalised fused imidazo[1,2-*e*]purine derivatives.

Scheme 80: Synthesis and reactivity of caffeine-based aminide **538**

4.3 Conclusions

The formal [3+2]-dipolar cycloaddition reaction between pyridinium *N*-heteroaryl aminides and ynamides has been adapted to cover a wider group of aza-heterocycles. Novel polysubstituted imidazo[2,1-*b*]benzothiazoles and imidazo[2,1-*b*]benzoxazoles scaffolds have been synthesised through the use of π -rich aminides. These systems required more forcing conditions to enhance the formation of the 5,5,6-fused framework, probably in order to reduce the unproductive metal-aminide interaction.

An alternative route for the synthesis of more complex π -rich *N*-heteroaryl aminides has been developed, employing sulfide-substituted heterocycles as direct precursors. This method allows the formation of halo- and nitro-functionalised ylides as well as novel fused pyridineoxazole/thiazole derivatives that have been successfully applied in the gold catalysis.

The strategy tolerates the introduction of orthogonal functionality that may be selectively exploited for further manipulation and diversification. Additionally, the

synthesis of imidazo[2,1-*b*]benzothiazole **455** could be performed at gram-scale with no detriment in the yield.

Aminides based on the benzimidazole system resulted less reactive, leading to incomplete reactions. This trend may be associated with the more π -rich character of the heterocycles, favouring the stabilisation of a metal-aminide complex. Nevertheless, workable yields of imidazo[1,2-*a*]benzoimidazole **446** could be isolated. In comparison, reaction with caffeine system **538** proved to be a more efficient process, probably due to the lower π -density of the xanthine ring that allowed the preparation of unprecedented substituted imidazo[1,2-*e*]purine derivatives.

Considering all the structures obtained in the present investigation, future work to further develop this synthetic strategy could focus on several areas. Altering the nature of the aminide would lead to different and otherwise difficult to access fused imidazole scaffold. Alternatively, considering the recent advent of azides in the intermolecular formation of α -imino gold carbene intermediates (*e.g.* Scheme 23, Scheme 24 and Scheme 77), it would be interesting to prepare aza-heteroaryl azides analogous to the aminides detailed in this thesis and compare the outcome of the gold catalysis.

The research presented in this thesis describes the development of a new type of reactivity that has been successfully adapted for the synthesis of fourteen classes of novel structures in a modular and convergent fashion. The compounds synthesised across this investigation are based on biologically relevant frameworks. Thus, they have been requested and submitted to industrial partners to be tested against several disease targets.

Chapter 5

5.1. General information

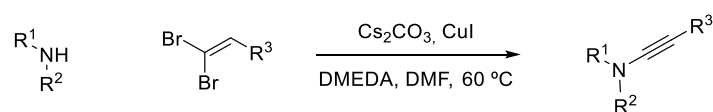
Commercially available chemicals/reagents were purchased from major suppliers (Aldrich, Fisher, Acros, Alfa Aesar, Fluorochem or VWR) and used without further purification unless otherwise stated. For all reactions carried out under inert atmosphere, solvents were purified using a PureSolv-MD solvent purification system and transferred under nitrogen except for DMF, 1,4-dioxane and 1,2-dichlorobenzene which were dried over activated 4 Å molecular sieves. For reactions above room temperature pre-heated paraffin oil baths or Asynt DrySyn heating blocks on stirrer hotplates were employed with temperature control *via* external probe. The following cooling baths were used: -10–0 °C (ice/NaCl) and -78 °C (dry ice/acetone). Reactions were monitored by thin layer chromatography using Merck silica gel 60 F254 (aluminium support) TLC plates which were developed using standard visualizing agents: UV fluorescence (254 nm), potassium permanganate/ Δ or vanillin/ Δ . Flash column chromatography was performed using Merk Geduran Si 60 (40-63 μ m) silica gel as the stationary phase. Melting points were measured in open capillaries using Stuart Scientific melting point apparatus and are uncorrected. Specific rotations were determined using a PolAAr 2001 instrument and are given as follows: $[\alpha]_D^T$ (in deg dm⁻¹cm³g⁻¹), c (in g/100 mL), solvent used. All ¹H NMR and ¹³C NMR spectroscopic experiments were recorded using Bruker AVIII400 (¹H = 400 MHz, ¹³C = 101 MHz) or AVIII300 (¹H = 300 MHz, ¹³C = 75 MHz) spectrometers at 300 K, in commercial, TMS free, deuterated solvents. ¹³C NMR spectra were recorded using either the UDEFT or the PENDANT pulse sequences from the Bruker standard pulse program library. 2D COSY, HSQC and HMBC spectra were recorded in order to assist with NMR assignment when necessary. Spectra were processed using MestReNova software. Chemical shifts (δ) are given in ppm and

coupling constants (J) are quoted in Hz to one decimal place. The spectra were calibrated using the solvent peaks relative to the TMS scale (CDCl_3 : $\delta_{\text{C}} \equiv 77.16$ ppm; residual CHCl_3 in CDCl_3 : $\delta_{\text{H}} \equiv 7.26$ ppm; DMSO-d_6 : $\delta_{\text{C}} \equiv 39.52$ ppm; residual DMSO in DMSO-d_6 : $\delta_{\text{H}} \equiv 2.50$ ppm). Spectral data for ^1H NMR spectroscopy is reported as follows: Chemical shift (multiplicity, coupling constant, number of protons); and for ^{13}C NMR spectroscopy: Chemical shift (multiplicity and coupling constant if needed, assignment). The following abbreviations were used for multiplicity in ^1H NMR: s (singlet), d (doublet), t (triplet), q (quadruplet), dd (doublet of doublets), td (triplet of doublets), quin (quintuplet), br. (broad), m (multiplet), app. (apparent). Infra-red spectra were recorded neat on a Perkin-Elmer Spectrum 100 FTIR spectrometer. Wavelengths (ν) are reported in cm^{-1} . HRMS (EI or ES): Waters LCT, Time of Flight. HRMS was obtained using leucine enkephalin as lock-mass.

5.2 Precursors for Chapters 2 and 3

5.2.1 Preparation of ynamides and indolylalkynes

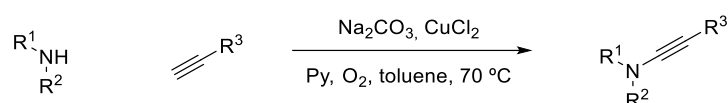
General Procedure 1 (GP1)



Following the method reported by Evano and co-workers,⁵⁹ a 10-25 mL flask was charged with sulfonamide (1.0 eq.), 1,1-dibromo-1-alkene (1.5 eq.), Cs_2CO_3 (4.0 eq.) and CuI (12 mol%). The flask was fitted with a rubber septum, evacuated under high vacuum and backfilled with argon (this operation was repeated three times). Dry DMF [0.5 M relative to the amount of sulfonamide] and N,N' -dimethylethylenediamine (19

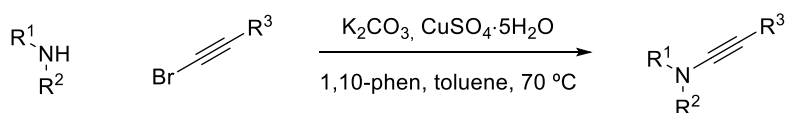
mol%) were then added and the mixture was stirred at 60 °C until complete consumption of the starting sulfonamide was observed by TLC. The reaction was diluted with water, extracted with diethyl ether and the combined organic layers were washed with brine, dried over MgSO_4 , filtered and concentrated. The crude residue was purified by flash chromatography over silica gel.

General Procedure 2 (GP2)



Following the method reported by Stahl and co-workers,⁶⁰ CuCl_2 (20 mol%), sulfonamide (5.0 eq.) and Na_2CO_3 (2.0 eq.) were added to a 500 mL three-necked round-bottomed flask. The flask was purged with oxygen for 15 min and a solution of pyridine (2.0 eq.) in dry toluene [0.2 M relative to the amount of alkyne] was added. A balloon filled with oxygen was connected to the flask and the stirred mixture was heated at 70 °C. After 15 min, a solution of alkyne (1.0 eq.) in dry toluene (0.2 M) was added by syringe pump over 4 h. The mixture was stirred at 70 °C for another 4 h and allowed to cool to rt. The reaction mixture was filtered through a plug of silica gel, washed with ethyl acetate and concentrated. The crude residue was purified by flash chromatography over silica gel.

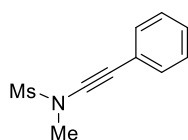
General Procedure 3 (GP3)



Following the method reported by Hsung and co-workers,¹¹⁷ $\text{CuSO}_4\cdot 5\text{H}_2\text{O}$ (10 mol%), 1,10-phenanthroline (20 mol%), K_2CO_3 (2.0 eq.) and the corresponding sulfonamide

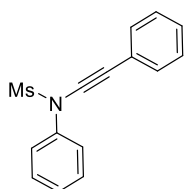
(1.0 eq.) were added to a round-bottomed flask and flushed with argon for 15 min. Bromoalkyne (1.3 eq.) and dry toluene [1 mL/mmol of sulfonamide] were then added and the reaction mixture was allowed to react at 70 °C until complete consumption of the starting sulfonamide was observed by TLC. The reaction mixture was filtered over a plug of silica gel, washed with ethyl acetate and concentrated. The crude residue was purified by flash chromatography over silica gel.

***N*-Methyl-*N*-(phenylethynyl)methanesulfonamide (264)**



Following **GP1** using *N*-methylmethanesulfonamide (0.82 g, 7.4 mmol) and (2,2-dibromovinyl)benzene (1.63 g, 9.0 mmol). After purification by flash chromatography [hexane:ethyl acetate (7:3)] ynamide **264** was obtained as a pale yellow solid (1.51 g, 97% yield). ¹H NMR (300 MHz, CDCl₃) δ 7.46–7.37 (m, 2H), 7.36–7.27 (m, 3H), 3.30 (s, 3H), 3.13 (s, 3H); ¹³C NMR (101 MHz, CDCl₃) δ 131.7 (2×CH), 128.5 (2×CH), 128.2 (CH), 122.5 (C), 83.2 (C), 69.6 (C), 39.3 (CH₃), 36.9 (CH₃); IR ν_{max}/cm⁻¹ 2241, 1347, 1320, 1155, 1107, 957, 763. Analytical data matches that reported in the literature.¹¹⁸

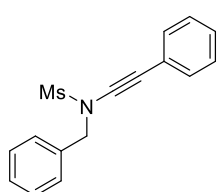
***N*-Phenyl-*N*-(phenylethynyl)methanesulfonamide (265)**



Following **GP2** using *N*-phenylmethanesulfonamide (1.29 g, 7.5 mmol) and phenylacetylene (0.18 mL, 1.5 mmol). After purification by flash chromatography [hexane:ethyl acetate (7:3)] ynamide **265** was obtained as a pale yellow solid (300.3 mg, 74% yield). ¹H NMR (300 MHz, CDCl₃) δ 7.64–7.55 (m, 2H), 7.51–7.28 (m, 8H), 3.17 (s, 3H); ¹³C NMR (101 MHz, CDCl₃) 138.7 (C), 131.6 (2×CH), 129.5 (2×CH), 128.3 (CH), 128.3 (2×CH), 128.2 (CH), 125.6 (2×CH),

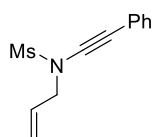
122.3 (C), 82.0 (C), 71.0 (C), 36.8 (CH₃); IR $\nu_{\text{max}}/\text{cm}^{-1}$ 3078, 3009, 2928, 2243, 1588, 1482, 1365, 1156, 962. Analytical data matches that reported in the literature.⁷⁵

***N*-Benzyl-*N*-(phenylethynyl)methanesulfonamide (266)**

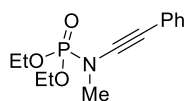


Following **GP1** using *N*-benzylmethanesulfonamide (0.36 g, 2.0 mmol) and (2,2-dibromovinyl)benzene (0.54 g, 3.1 mmol). After purification by flash chromatography [hexane:ethyl acetate (4:1)] ynamide **266** was obtained as a pale yellow solid (473.5 mg, 83% yield). ¹H NMR (300 MHz, CDCl₃) δ 7.60–7.15 (m, 10H), 4.68 (s, 2H), 2.90 (s, 3H); ¹³C NMR (101 MHz, CDCl₃) δ 134.5 (C), 131.3 (2 \times CH), 129.0 (2 \times CH), 128.8 (2 \times CH), 128.7 (C), 128.3 (2 \times CH), 128.0 (CH), 122.4 (CH), 82.0 (C), 71.6 (C), 55.9 (CH₂), 38.9 (CH₃); IR $\nu_{\text{max}}/\text{cm}^{-1}$ 3056, 3036, 2926, 2235, 1498, 1457, 1349, 1156. Analytical data matches that reported in the literature.⁷⁵

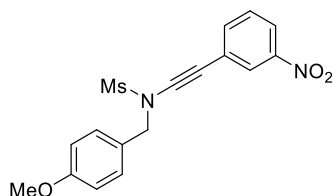
***N*-Allyl-*N*-(phenylethynyl)methanesulfonamide (267)**



Following **GP1** using *N*-allylmethanesulfonamide (180.1 mg, 1.3 mmol) and (2,2-dibromovinyl)benzene (525.0 mg, 2.0 mmol). After purification by flash chromatography [hexane:ethyl acetate (9:1)] ynamide **267** was isolated as a pale yellow solid (202.3 mg, 64%); ¹H NMR (300 MHz, CDCl₃) δ 7.48–7.35 (m, 2H), 7.34–7.26 (m, 3H), 6.00 (ddt, J = 16.6, 10.1, 6.4 Hz, 1H), 5.44 (app. dq, J = 16.6, 1.3 Hz, 1H), 5.38 (app. dq, J = 10.1, 1.3 Hz, 1H), 4.17 (app. dt, J = 6.4, 1.3 Hz, 2H), 3.14 (s, 3H); ¹³C NMR (101 MHz, CDCl₃) δ 131.6 (CH), 131.0 (CH), 128.4 (2 \times CH), 128.2 (2 \times CH), 122.6 (C), 120.7 (CH₂), 81.7 (C), 71.3 (C), 54.5 (CH₂), 39.1 (CH₃); IR $\nu_{\text{max}}/\text{cm}^{-1}$ 3032, 2933, 2238, 1441, 1348, 1158, 1106, 1025. Analytical data matches that reported in the literature.⁷⁵

Diethyl methyl(phenylethynyl)phosphoramidate (268)

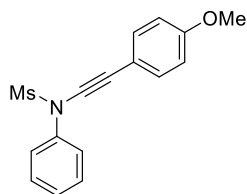
Following **GP3** using diethyl methylphosphoramidate (0.84 g, 5.0 mmol) and (bromoethynyl)benzene (1.08 g, 6.0 mmol). After purification by flash chromatography [hexane:ethyl acetate (1:4)] ynamide **268** was isolated as a pale yellow solid (0.87 g, 65%); ^1H NMR (300 MHz, CDCl_3) δ 7.39–7.32 (m, 2H), 7.32–7.23 (m, 3H), 4.29–4.15 (m, 4H), 3.17 (d, $J = 7.9$ Hz, 3H), 1.41 (td, $J = 7.1$, 1.0 Hz, 6H); ^{13}C NMR (101 MHz, CDCl_3) δ 131.1 (2 \times CH), 128.3 (2 \times CH), 127.1 (CH), 123.9 (C), 87.3 (d, $J_{\text{C-P}} = 4.4$ Hz, C), 64.0 (d, $J_{\text{C-P}} = 5.6$ Hz, 2 \times CH₂), 63.8 (d, $J_{\text{C-P}} = 5.1$ Hz, C), 39.0 (d, $J_{\text{C-P}} = 5.7$ Hz, CH₃), 16.2 (d, $J_{\text{C-P}} = 6.8$ Hz, 2 \times CH₃); IR $\nu_{\text{max}}/\text{cm}^{-1}$ 2983, 2236, 1442, 1350, 1269, 1115, 991, 795. Analytical data matches that reported in the literature.^{34b}

***N*-(4-Methoxybenzyl)-*N*-((3-nitrophenyl)ethynyl)methanesulfonamide (269)**

Following **GP1** using *N*-(4-methoxyphenyl)-methanesulfonamide (0.43 mg, 2.0 mmol) and 1,1-dibromo-2-(3-nitrophenyl)ethene (0.86 mg, 2.8 mmol). After purification by flash chromatography [hexane:ethyl acetate (4:1)] ynamide **269** was isolated as a white solid (366.8 mg, 51%); mp: 90–92 °C; ^1H NMR (300 MHz, CDCl_3) δ 8.17 (app. t, $J = 1.7$ Hz, 1H), 8.16–8.11 (m, 1H), 7.65 (app. dt, $J = 8.0$, 1.7 Hz, 1H), 7.49 (app. t, $J = 8.0$ Hz, 1H), 7.43 (d, $J = 8.7$ Hz, 2H), 6.97 (d, $J = 8.7$ Hz, 2H), 4.71 (s, 2H), 3.86 (s, 3H), 2.98 (s, 3H); ^{13}C NMR (101 MHz, CDCl_3) δ 160.2 (C), 148.1 (CH), 136.6 (C), 130.5 (2 \times CH), 129.3 (CH), 126.1 (CH), 125.7 (CH), 124.6 (C), 122.4 (C), 114.3 (2 \times CH), 84.7 (C), 70.1 (C), 55.6 (CH₂), 55.3 (CH₃), 39.5 (CH₃); IR $\nu_{\text{max}}/\text{cm}^{-1}$

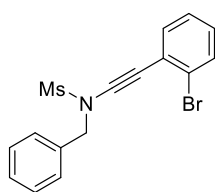
3106, 3008, 2929, 2230, 1514, 1349, 1158, 965, 757; HR-MS (ES-TOF): m/z : calcd. for $C_{17}H_{17}N_2O_5S$: 361.0858 found 361.0853 $[M+H]^+$

***N*-((4-Methoxyphenyl)ethynyl)-*N*-phenylmethanesulfonamide (270)**



Following **GP2** using *N*-phenylmethanesulfonamide (1.85 g, 10.9 mmol) and 1-ethynyl-4-methoxybenzene (0.24 g, 1.8 mmol). After purification by flash chromatography [hexane:ethyl acetate (17:1)] ynamide **270** was isolated as a white solid (346.9 mg, 65%); mp: 92–94 °C; 1H NMR (300 MHz, $CDCl_3$) δ 7.58 (d, $J = 7.9$ Hz, 2H), 7.50–7.31 (m, 5H), 6.85 (d, $J = 7.9$ Hz, 2H), 3.82 (s, 3H), 3.16 (s, 3H); ^{13}C NMR (101 MHz, $CDCl_3$) δ 159.8 (C), 138.9 (C), 133.6 (2 \times CH), 129.5 (2 \times CH), 128.2 (CH), 125.6 (2 \times CH), 114.1 (C), 114.0 (2 \times CH), 80.6 (C), 70.7 (C), 55.3 (CH_3), 36.7 (CH_3); IR ν_{max}/cm^{-1} 3155, 3028, 2933, 2257, 1496, 1287, 1161, 963, 752; HR-MS (ES-TOF): m/z : calcd. for $C_{16}H_{15}NO_3NaS$: 324.0670 found 324.0678 $[M+Na]^+$.

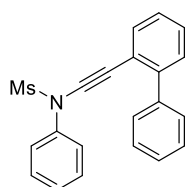
***N*-Benzyl-*N*-((2-bromophenyl)ethynyl)methanesulfonamide (271)**



Following **GP1** using *N*-benzylmethanesulfonamide (326 mg, 1.80 mmol) and 1,1-dibromo-2-(2-bromophenyl)ethene (0.90 g, 2.7 mmol). After purification by flash chromatography [hexane:ethyl acetate (4:1)] ynamide **271** was isolated as an orange solid (130.3 mg, 20%); mp: 90–92 °C; 1H NMR (300 MHz, $CDCl_3$) δ 7.59–7.52 (m, 3H), 7.45–7.34 (m, 4H), 7.22 (dd, $J = 7.7, 1.2$ Hz, 1H), 7.13 (app. td, $J = 7.7, 1.7$ Hz, 1H), 4.75 (s, 2H), 2.96 (s, 3H); ^{13}C NMR (101 MHz, $CDCl_3$) δ 134.4 (C), 132.7 (CH), 132.3 (CH), 129.1 (2 \times CH), 128.9 (CH), 128.9 (2 \times CH), 128.8 (CH), 127.0 (CH), 125.0 (C), 124.8 (C), 86.5 (C), 70.9 (C),

56.0 (CH₂), 39.3 (CH₃); IR $\nu_{\text{max}}/\text{cm}^{-1}$ 3059, 3029, 2235, 1411, 1347, 1155, 1050, 962; HR-MS (ES-TOF): m/z : calcd. for C₁₆H₁₅NO₂S⁷⁹Br: 364.0007 found 364.0000 [M+H]⁺.

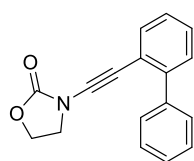
N-([1,1'-Biphenyl]-2-ylethynyl)-N-phenylmethanesulfonamide (272)



Following **GP1** using *N*-phenylmethanesulfonamide (182.2 mg, 1.1 mmol) and 1,1-dibromo-2-(2-biphenyl)ethene (450.0 mg, 1.4 mmol).

After purification by flash chromatography [hexane:ethyl acetate (4:1)] ynamide **272** was isolated as a white solid (114.4 mg, 30%); mp: 96–98 °C; ¹H NMR (300 MHz, CDCl₃) δ 7.61–7.52 (m, 3H), 7.47–7.27 (m, 11H), 2.81 (s, 3H); ¹³C NMR (101 MHz, CDCl₃) δ 143.9 (C), 140.9 (C), 138.6 (C), 132.7 (CH), 129.3 (CH), 129.3 (2×CH), 129.3 (2×CH), 128.3 (CH), 128.1 (2×CH), 128.1 (CH), 127.4 (CH), 127.2 (CH), 125.5 (2×CH), 120.9 (C), 84.5 (C), 70.9 (C), 36.4 (CH₃); IR $\nu_{\text{max}}/\text{cm}^{-1}$ 3077, 3021, 3004, 2953, 2236, 1589, 1360, 1166, 957, 756; HR-MS (ES-TOF): m/z : calcd. for C₂₁H₁₇NO₂NaS: 370.0878 found 370.0874 [M+Na]⁺.

3-([1,1'-Biphenyl]-2-ylethynyl)oxazolidin-2-one (273)

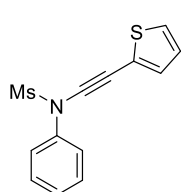


Following **GP1** using oxazolidin-2-one (0.13 g, 1.5 mmol) and 1,1-dibromo-2-(2-biphenyl)ethene (0.76 g, 2.3 mmol). After purification by flash chromatography [hexane:ethyl acetate (4:1)] ynamide **273** was

isolated as a white solid (170.1 mg, 43%); mp: 94–96 °C; ¹H-NMR (300 MHz, CDCl₃) δ 7.64–7.52 (m, 3H), 7.48–7.26 (m, 6H), 4.41 (app. t, J = 7.8 Hz, 2H), 3.80 (app. t, J = 7.8 Hz, 2H); ¹³C-NMR (101 MHz, CDCl₃) δ 155.6 (C), 143.5 (C), 140.5 (C), 132.5 (CH), 129.4 (CH), 129.3 (2×CH), 128.3 (CH), 128.0 (2×CH), 127.5 (CH), 127.1 (CH), 120.6 (C), 81.8 (C), 71.2 (C), 63.0 (CH₂), 46.6 (CH₂); IR $\nu_{\text{max}}/\text{cm}^{-1}$ 3066, 2983, 2252,

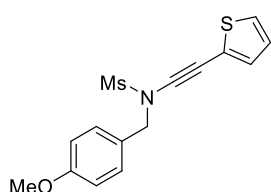
1762, 1477, 1197, 1164, 1029, 949, 745; HR-MS (ES-TOF): m/z : calcd. for $C_{17}H_{14}NO_2$: 264.1025 found 264.1031 $[M+H]^+$.

***N*-(Phenyl)-*N*-(thiophen-2-ylethynyl)methanesulfonamide (274)**



Following **GP1** using *N*-phenylmethanesulfonamide (0.29 g, 1.7 mmol) and 1,1-dibromo-2-thiophenylethene (0.69 g, 2.6 mmol). After purification by flash chromatography [hexane:ethyl acetate (4:1)] ynamide **274** was isolated as a white solid (188.9 mg, 40%); mp: 66–68 °C; 1H NMR (300 MHz, $CDCl_3$) δ 7.62–7.55 (m, 2H), 7.51–7.43 (m, 2H), 7.43–7.36 (m, 1H), 7.33 (dd, J = 5.2, 1.1 Hz, 1H), 7.30 (dd, J = 3.7, 1.1 Hz, 1H), 7.01 (dd, J = 5.2, 3.7 Hz, 1H), 3.20 (s, 3H); ^{13}C NMR (101 MHz, $CDCl_3$) δ 138.6 (CH), 133.5 (C), 129.6 (2 \times CH), 128.5 (CH), 128.2 (CH), 127.1 (CH), 125.6 (2 \times CH), 122.2 (C), 85.4 (C), 64.4 (C), 37.2 (CH₃); IR ν_{max}/cm^{-1} 3102, 3026, 2933, 2233, 1490, 1367, 1166, 960, 777; HR-MS (ES-TOF): m/z : calcd. for $C_{13}H_{12}NO_2S_2$: 278.0214 found 278.0221 $[M+H]^+$.

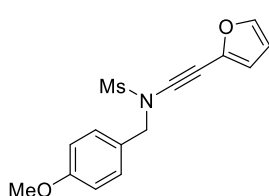
***N*-(4-Methoxybenzyl)-*N*-(thiophen-2-ylethynyl)methanesulfonamide (275)**



Following **GP1** using *N*-(4-methoxyphenyl)-methanesulfonamide (0.43 g, 2.0 mmol) and 1,1-dibromo-2-thiophenylethene (0.78 g, 2.9 mmol). After purification by flash chromatography [hexane:ethyl acetate (4:1)] ynamide **275** was isolated as a white solid (529.1 mg, 82%); mp: 64–66 °C; 1H NMR (300 MHz, $CDCl_3$) δ 7.43 (d, J = 8.7 Hz, 2H), 7.30 (dd, J = 5.2, 1.1 Hz, 1H), 7.22 (dd, J = 3.6, 1.1 Hz, 1H), 7.00 (dd, J = 5.2, 3.6 Hz, 1H), 6.95 (d, J = 8.7 Hz, 2H), 4.68 (s, 2H), 3.85 (s, 3H), 2.92 (s, 3H); ^{13}C NMR (101 MHz, $CDCl_3$) δ 160.0 (C), 133.2 (C), 130.5 (2 \times CH), 128.0 (CH), 127.0 (CH), 126.5 (CH), 122.5 (C), 114.2 (2 \times CH), 85.6 (C), 64.9 (C), 55.8 (CH₃), 55.3 (CH₂), 39.3

(CH₃); IR $\nu_{\text{max}}/\text{cm}^{-1}$ 3106, 3007, 2964, 2229, 1514, 1348, 1159, 965, 758; HR-MS (ES-TOF): m/z : calcd. for C₁₅H₁₅NO₃NaS₂: 344.0391 found 344.0392 [M+Na]⁺.

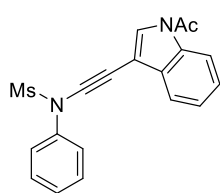
***N*-(4-Methoxybenzyl)-*N*-(furan-2-ylethynyl)methanesulfonamide (276)**



Following **GP1** using *N*-(4-methoxyphenyl)-methanesulfonamide (0.43 g, 2.0 mmol) and 1,1-dibromo-2-furanylene (0.71 g, 2.8 mmol). After purification by flash chromatography

[hexane:ethyl acetate (4:1)] ynamide **276** was isolated as a white solid (371.1 mg, 60%); mp: 54–56 °C; ¹H NMR (300 MHz, CDCl₃) δ 7.45–7.39 (m, 3H), 6.94 (d, J = 8.7 Hz, 2H), 6.65 (dd, J = 3.4, 0.7 Hz, 1H), 6.42 (dd, J = 3.4, 1.9 Hz, 1H), 4.69 (s, 2H), 3.85 (s, 3H), 2.92 (s, 3H); ¹³C NMR (101 MHz, CDCl₃) δ 160.0 (C), 144.2 (C), 136.5 (C), 130.5 (2×CH), 126.5 (CH), 117.5 (CH), 114.2 (2×CH), 111.1 (CH), 86.3 (C), 62.4 (C), 55.8 (CH₃), 55.3 (CH₂), 39.4 (CH₃); IR $\nu_{\text{max}}/\text{cm}^{-1}$ 3147, 3015, 2932, 2226, 1512, 1348, 1154, 948, 764; HR-MS (ES-TOF): m/z : calcd. for C₁₅H₁₅NO₄NaS: 328.0619 found 328.0610 [M+Na]⁺.

***N*-((1-Acetyl-1*H*-indol-3-yl)ethynyl)-*N*-phenylmethanesulfonamide (277)**

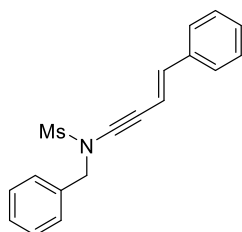


Following **GP2** using *N*-phenylmethanesulfonamide (1.03 g, 6.0 mmol) and 1-(3-ethynyl-1*H*-indol-1-yl)ethen-1-one (0.18 mg, 1.0 mmol). After purification by flash chromatography [toluene:ethyl

acetate (95:5)] ynamide **277** was isolated as a white solid (96.3 mg, 27%); mp: 142–144 °C; ¹H NMR (300 MHz, CDCl₃) δ 8.42 (d, J = 8.0 Hz, 1H), 7.73–7.57 (m, 4H), 7.54–7.30 (m, 5H), 3.21 (s, 3H), 2.64 (s, 3H); ¹³C NMR (101 MHz, CDCl₃) δ 168.3 (C), 138.8 (C), 135.1 (C), 130.7 (C), 129.8 (2×CH), 128.6 (CH), 128.5 (CH), 126.3 (CH), 125.7 (2×CH), 124.4 (CH), 120.0 (CH), 116.8 (CH), 104.3 (C), 85.8 (C), 62.8 (C), 37.2

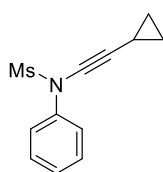
(CH₃), 24.0 (CH₃); IR $\nu_{\max}/\text{cm}^{-1}$ 3155, 3028, 2933, 1716, 1491, 1348, 1283, 1052, 996, 818, 742; HR-MS (ES-TOF): m/z : calcd. for C₁₉H₁₆N₂O₃NaS: 375.0779 found 375.0782 [M+Na]⁺.

(*E*)-*N*-Benzyl-*N*-(4-phenylbut-3-en-1-yn-1-yl)methanesulfonamide (278)



Following **GP1** using *N*-benzylmethanesulfonamide (0.32 g, 1.7 mmol) and (*E*)-(4,4-dibromobuta-1,3-dien-1-yl)benzene (0.72 mg, 2.6 mmol). After purification by flash chromatography [hexane:ethyl acetate (7:3)] ynamide **278** was isolated as a white solid (367.2 mg, 69%); mp: 84–86 °C; ¹H NMR (300 MHz, CDCl₃) δ 7.57–7.22 (m, 10 H), 6.84 (d, J = 16.2 Hz, 1H), 6.24 (d, J = 16.2 Hz, 1H), 4.68 (s, 2H), 2.92 (s, 3H); ¹³C NMR (101 MHz, CDCl₃) δ 140.0 (CH), 136.3 (C), 134.5 (C), 128.9 (2×CH), 128.9 (2×CH), 128.8 (CH), 128.7 (2×CH), 128.5 (CH), 126.1 (2×CH), 107.2 (CH), 83.9 (C), 71.2 (C), 55.9 (CH₂), 39.1 (CH₃); IR $\nu_{\max}/\text{cm}^{-1}$ 3059, 3026, 2929, 2221, 1494, 1351, 1161, 946, 746; HR-MS (ES-TOF): m/z : calcd. for C₁₈H₁₇NO₂NaS: 334.0878 found 334.0883 [M+Na]⁺.

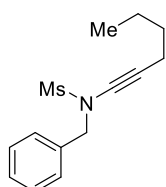
***N*-(Cyclopropylethynyl)-*N*-phenylmethanesulfonamide (279)**



Following **GP2** using *N*-phenylmethanesulfonamide (1.26 g, 7.4 mmol) and cyclopropylacetylene (120.0 μ L, 1.5 mmol). After purification by flash chromatography [hexane:ethyl acetate (9:1)] ynamide **279** was isolated as a white solid (303.7 mg, 88%); mp: 62–64 °C; ¹H NMR (300 MHz, CDCl₃) δ 7.51–7.45 (m, 2H), 7.44–7.36 (m, 2H), 7.35–7.29 (m, 1H), 3.07 (s, 3H), 1.38 (tt, J = 8.0, 4.9 Hz, 1H), 0.87–0.70 (m, 4H); ¹³C NMR (101 MHz, CDCl₃) δ 139.3 (C), 129.5 (2×CH), 128.1 (CH), 125.6 (2×CH), 75.3 (C), 68.8 (C), 36.5 (CH₃), 9.0 (2×CH₂), -0.6;

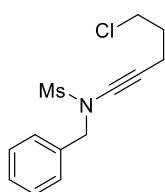
IR $\nu_{\max}/\text{cm}^{-1}$ 3157, 3014, 2933, 2220, 1715, 1490, 1348, 1283, 1157, 965, 779; HR-MS (ES-TOF): m/z : calcd. for $\text{C}_{12}\text{H}_{14}\text{NO}_2\text{S}$: 236.0745 found 236.0746 $[\text{M}+\text{H}]^+$.

***N*-Benzyl-*N*-(hex-1-yn-1-yl)methanesulfonamide (280)**

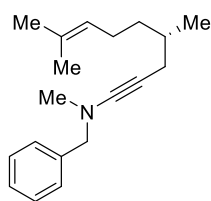


Following **GP3** using *N*-benzylmethanesulfonamide (0.43 g, 2.4 mmol) and (bromoethynyl)benzene (0.47 g, 3.1 mmol). After purification by flash chromatography [hexane:ethyl acetate (9:1)] ynamide **280** was obtained as a colourless oil (628.8 mg, 99% yield). ^1H NMR (300 MHz, CDCl_3) δ 7.48–7.33 (m, 5H), 4.57 (s, 2H), 2.86 (s, 3H), 2.26 (t, $J = 6.9$ Hz, 2H), 1.52–1.25 (m, 4H), 0.88 (t, $J = 7.2$ Hz, 3H); ^{13}C NMR (101 MHz, CDCl_3) δ 134.8 (C), 128.9 (2 \times CH), 128.6 (2 \times CH), 128.5 (CH), 72.9 (C), 71.4 (C), 55.6 (CH_2), 38.2 (CH_3), 30.9 (CH_2), 21.8 (CH_2), 18.1 (CH_2), 13.5 (CH_3); IR $\nu_{\max}/\text{cm}^{-1}$ 2957, 2932, 2254, 1684, 1456, 1351, 1159, 1026. Analytical data matches that reported in the literature.⁷⁵

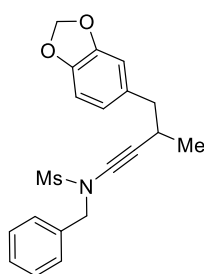
***N*-Benzyl-*N*-(5-chloropent-1-yn-1-yl)methanesulfonamide (281)**



Following **GP3** using *N*-benzylmethanesulfonamide (0.38 g, 2.0 mmol) and 1-bromo-5-chloropent-1-yne (0.45 mg, 2.5 mmol). After purification by flash chromatography [hexane:ethyl acetate (4:1)] ynamide **281** was isolated as a colourless oil (534.0 mg, 92%); ^1H NMR (300 MHz, CDCl_3) δ 7.49–7.32 (m, 5H), 4.58 (s, 2H), 3.51 (t, $J = 6.6$ Hz, 2H), 2.89 (s, 3H), 2.47 (t, $J = 6.6$ Hz, 2H), 1.89 (app. quin, $J = 6.6$ Hz, 2H); ^{13}C NMR (101 MHz, CDCl_3) δ 134.6 (C), 128.9 (2 \times CH), 128.8 (2 \times CH), 128.7 (CH), 73.9 (C), 69.5 (C), 55.5 (CH_2), 43.5 (CH_2), 38.4 (CH_3), 31.3 (CH_2), 15.9 (CH_2); IR $\nu_{\max}/\text{cm}^{-1}$ 3104, 3046, 2927, 2255, 1484, 1348, 1217, 1154, 960, 754; HR-MS (ES-TOF): m/z : calcd. for $\text{C}_{13}\text{H}_{17}\text{ClNO}_2\text{S}$: 286.0679, found: 286.0678 $[\text{M}+\text{H}]^+$.

(S)-(+)-N-Benzyl-N-(4,8-dimethylnon-7-en-1-yn-1-yl)methanesulfonamide (282)

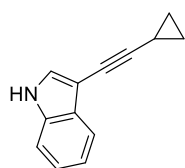
Following **GP1** using *N*-benzylmethanesulfonamide (0.26 g, 1.4 mmol) and (*S*)-1,1-dibromo-3,7-dimethylocta-1,6-diene (0.63 g, 2.1 mmol). After purification by flash chromatography [hexane:ethyl acetate (85:5)] ynamide **282** was isolated as a colourless oil (412.4 mg, 87%); $[\alpha]_D^{24} = 10.7$ (c 1.31, CHCl_3); ^1H NMR (300 MHz, CDCl_3) δ 7.52–7.34 (m, 5H), 5.08 (t, $J = 8.5$ Hz, 1H), 4.60 (s, 2H), 2.88 (s, 3H), 2.25 (dd, $J = 16.6, 5.6$ Hz, 1H), 2.17 (dd, $J = 16.6, 6.6$ Hz, 1H), 2.05–1.89 (m, 2H), 1.70 (s, 3H), 1.67–1.54 (m, 4H), 1.45–1.29 (m, 1H), 1.28–1.11 (m, 1H), 0.92 (d, $J = 6.7$ Hz, 3H); ^{13}C NMR (101 MHz, CDCl_3) δ 134.8 (C), 131.4 (C), 128.9 (2 \times CH), 128.7 (2 \times CH), 128.5 (CH), 124.4 (CH), 73.8 (C), 70.1 (C), 55.6 (CH_2), 38.3 (CH_3), 36.0 (CH_2), 32.3 (CH), 25.7 (CH_3), 25.7 (CH_2), 25.5 (CH_2), 19.4 (CH_3), 17.7 (CH_3); IR $\nu_{\text{max}}/\text{cm}^{-1}$ 2967, 2925, 2255, 1682, 1493, 1351, 1325, 1151, 967, 761; HR-MS (ES-TOF): m/z : calcd. for $\text{C}_{19}\text{H}_{28}\text{NO}_2\text{S}$: 334.1841, found: 334.1831 $[\text{M}+\text{H}]^+$.

***N*-(4-(Benzo[*d*][1,3]dioxol-5-yl)-3-methylbut-1-yn-1-yl)-N-benzylmethanesulfonamide (283)**

Following **GP1** using *N*-benzylmethanesulfonamide (0.23 g, 1.3 mmol) and 5-(4,4-dibromo-2-methylbut-3-en-1-yl)benzo[*d*][1,3]-dioxole (0.64, 1.9 mmol). After purification by flash chromatography [hexane:ethyl acetate (4:1)] ynamide **283** was isolated as a colourless oil (370.6 mg, 69%); ^1H NMR (300 MHz, CDCl_3) δ 7.43–7.31 (m, 5H), 6.71 (d, $J = 7.9$ Hz, 1H), 6.69 (d, $J = 1.5$ Hz, 1H), 6.61 (dd, $J = 7.9, 1.5$ Hz, 1H), 5.94–5.91 (m, 2H), 4.64–4.46 (m, 2H), 2.84–2.69 (m, 4H), 2.66–2.60 (m, 2H), 1.18 (d, $J = 6.7$ Hz, 3H); ^{13}C

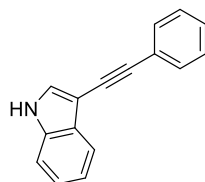
NMR (101 MHz, CDCl_3) δ 147.4 (C), 146.0 (C), 134.7 (C), 133.4 (C), 129.0 (2 \times CH), 128.7 (2 \times CH), 128.6 (CH), 122.2 (CH), 109.7 (CH), 107.9 (CH), 100.8 (CH_2), 74.9 (C), 74.4 (C), 55.6 (CH_2), 42.8 (CH_2), 38.2 (CH_3), 28.1 (CH), 20.8 (CH_3); IR $\nu_{\text{max}}/\text{cm}^{-1}$ 3026, 2970, 2930, 2250, 1488, 1351, 1245, 1158, 1036, 793; HR-MS (ES-TOF): m/z : calcd. for $\text{C}_{20}\text{H}_{22}\text{NO}_4\text{S}$: 372.1270, found: 372.1274 $[\text{M}+\text{H}]^+$.

3-(Cyclopropylethynyl)-1H-indole (312a)



Following the literature procedure,^{34a} using 3-iodoindole (0.49 mg, 2.0 mmol) and cyclopropyl acetylene (0.50 mL, 5.9 mmol). After purification by flash chromatography [hexane:toluene (9:1)] alkynylindole **312a** was isolated as a dark brown solid (289.5 mg, 80%); ^1H NMR (300 MHz, CDCl_3) δ 8.09 (br., 1H), 7.73 (dd, $J = 7.6, 1.3$ Hz, 1H), 7.40–7.36 (m, 1H), 7.35 (d, $J = 2.6$ Hz, 1H), 7.26–7.24 (m, 1H), 7.22 (dd, $J = 8.2, 1.5$ Hz, 1H), 1.58–1.50 (m, 1H), 0.92–0.80 (m, 4H); ^{13}C NMR (101 MHz, CDCl_3) δ 135.3 (C), 129.0 (C), 127.4 (CH), 123.0 (CH), 120.6 (CH), 120.1 (CH), 111.3 (CH), 99.5 (C), 94.8 (C), 68.6 (C), 8.8 (2 \times CH_2), 0.5 (CH); IR $\nu_{\text{max}}/\text{cm}^{-1}$ 23380, 1607, 1485, 1432, 1174, 930, 830, 736. Analytical data matches that reported in the literature.^{34a}

3-(Phenylethynyl)-1H-indole (312b)

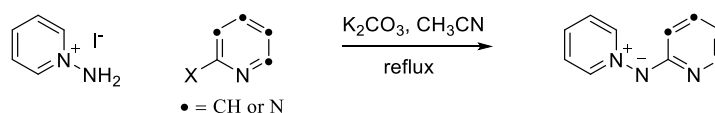


Following the literature procedure,^{34a} using 3-iodoindole (1.21 g, 5.0 mmol) and phenyl acetylene (0.71 mL, 6.0 mmol). After purification by flash chromatography [hexane:toluene (9:1)] alkynylindole **312b** was isolated as a brown solid (759.4 mg, 70%); ^1H NMR (300 MHz, $\text{DMSO}-d_6$) δ 11.58 (br., 1H), 7.78 (d, $J = 2.7$ Hz, 1H), 7.67 (d, $J = 7.6$ Hz, 1H), 7.57–7.51 (m, 2H), 7.47–7.30 (m, 4H), 7.24–7.01 (m, 2H); ^{13}C NMR (101 MHz, $\text{DMSO}-d_6$) δ 135.5 (C), 130.8

(2×CH), 129.7 (CH), 128.5 (2×CH), 128.1 (C), 127.7 (C), 123.9 (CH), 122.4 (CH), 120.1 (CH), 119.0 (CH), 112.2 (CH), 96.1 (C), 90.6 (C), 84.4 (C); IR $\nu_{\text{max}}/\text{cm}^{-1}$ 3386, 2214, 1484, 1421, 1456, 1333, 1236, 1100, 819. Analytical data matches that reported in the literature.^{34a}

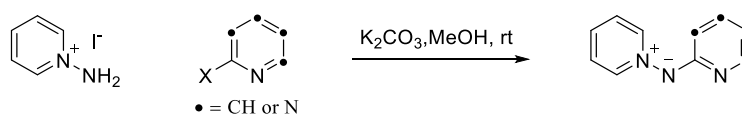
5.2.2 Preparation of pyridinium *N*-(heteroaryl)aminides

General Procedure 4 (GP4)



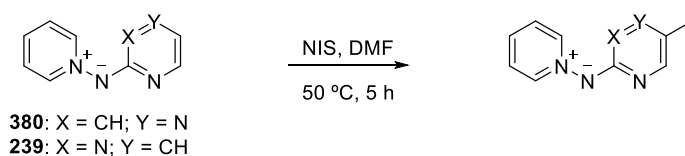
Following the method reported by Alvarez-Builla and co-workers,¹⁰³ potassium carbonate (2.8 eq.) was added to a solution of *N*-aminopyridinium iodide (1.0 eq.) in acetonitrile [0.2 M relative to the amount of *N*-aminopyridinium iodide] and the reaction mixture was stirred for 45 min. at rt to give a purple solution. The corresponding haloheterocycle (1.04 eq.) was added to the reaction mixture and heated under reflux for the indicated amount of time. After this time the solvent was evaporated under reduced pressure and the residue redissolved in CH_2Cl_2 and washed with NaOH (2.5 M). The combined organic layers were dried with MgSO_4 , filtered off and the solvent removed under reduced pressure, purifying the resulting compound by flash chromatography over silica gel using the indicated eluent.

General Procedure 5 (GP5)



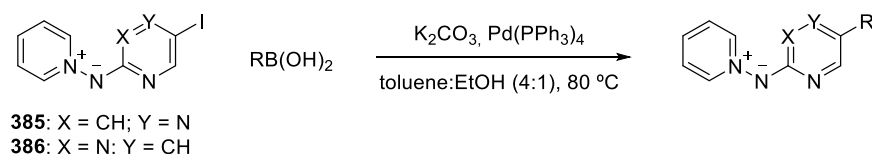
Following and adaptation of **GP4** where the solvent was replaced for methanol and the mixture was stirred at rt for the indicated amount of time.

General Procedure 6 (GP6)



Following the method reported by Alvarez-Builla and co-workers,¹¹⁹ *N*-iodosuccinimide (1.1 eq.) was added to a stirred solution of the corresponding aminide (1.0 eq.) in DMF [0.2 M relative to the amount of aminide]. The reaction mixture was stirred at 50 °C for 5 h. Once the starting material was consumed (detected by TLC), the mixture was extracted with CH₂Cl₂ and washed with brine. The combined organic layers were dried with MgSO₄, filtered off and the solvent removed under reduced pressure, purifying the resulting compound by flash chromatography over silica gel using the indicated eluent.

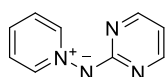
General Procedure 7 (GP7)



Following the method reported by Alvarez-Builla and co-workers,¹⁰⁴ aminide (1.0 eq.), the corresponding boronic acid (1.5 eq.) and K₂CO₃ (10.0 eq.) were combined in a toluene/ethanol mixture [4:1, 15 mL/mmol of aminide]. Pd(PPh₃)₄ (5 mol%) was added

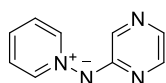
and the mixture was stirred under argon at 80 °C for 4.5 h. Once the starting material was consumed (detected by TLC), the solution was filtered and concentrated under reduced pressure. The crude residue was purified by flash chromatography over silica gel using the indicated eluent.

***N*-(Pyrimidin-2-yl)pyridinium aminide (239)**



Following **GP4** using *N*-aminopyridinium iodide (0.40 g, 1.8 mmol), 2-chloropyrimidine (0.21 g, 1.9 mmol) and potassium carbonate (0.70 g, 5.0 mmol) for 4 h. After purification by flash chromatography [CH₂Cl₂:MeOH (98:2)] aminide **239** was isolated as a bright yellow solid (217.4 mg, 70%); mp: 152–154 °C (lit.⁵³ 150-152 °C); ¹H NMR (300 MHz, CDCl₃) δ 8.71 (dd, *J* = 6.9, 1.3 Hz, 2H), 8.20 (tt, *J* = 7.8, 1.3 Hz, 1H), 8.11 (d, *J* = 4.8 Hz, 2H), 7.91 (dd, *J* = 7.8, 6.9 Hz, 2H), 6.38 (t, *J* = 4.8 Hz, 1H); ¹³C NMR (101 MHz, CDCl₃) δ 169.4 (C), 159.2 (2×CH), 145.8 (2×CH), 139.9 (CH), 128.8 (2×CH), 109.0 (CH). Analytical data matches that reported in the literature.¹⁰³

***N*-(Pyrazin-2-yl)pyridinium aminide (380)**

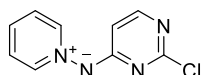


Following **GP4** using *N*-aminopyridinium iodide (0.40 g, 1.8 mmol), 2-chloropyrazine (0.21 g, 1.9 mmol) and potassium carbonate (0.70 g, 5.0 mmol) for 4 h. After purification by flash chromatography [CH₂Cl₂:MeOH (9:1)] aminide **380** was isolated as a bright yellow solid (203.9 mg, 66%); mp: 159–161 °C (lit.⁵³ 157-159 °C); ¹H NMR (300 MHz, CDCl₃) δ 8.82 (dd, *J* = 7.0, 1.2 Hz, 2H), 8.21 (t, *J* = 7.8 Hz, 1H), 7.93 (dd, *J* = 7.8, 7.0 Hz, 2H), 7.86 (d, *J* = 1.5 Hz, 1H), 7.61 (dd, *J* = 3.1, 1.5 Hz, 1H), 7.45 (d, *J* = 3.1 Hz, 1H); ¹³C NMR (101 MHz, CDCl₃) δ 162.0 (C),

145.3 (2×CH), 141.9 (CH), 140.0 (CH), 136.8 (CH), 129.5 (CH), 128.9 (2×CH).

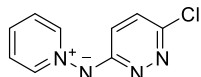
Analytical data matches that reported in the literature.¹⁰³

***N*-(2-Chloropyrimidin-4-yl)pyridinium aminide (381)**

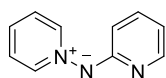


Following **GP4** using *N*-aminopyridinium iodide (0.40 g, 1.8 mmol), 2,4-dichloropyrimidine (0.21 g, 1.9 mmol) and potassium carbonate (0.70 g, 5.0 mmol) for 15 h. After purification by flash chromatography [AcOEt:MeOH (4:1)] aminide **381** was isolated as a bright yellow solid (333.0 mg, 79%); mp: 130–132 °C (lit.¹⁰³ 134–136 °C); ¹H NMR (300 MHz, CDCl₃) δ 8.65 (dd, *J* = 6.9, 1.4 Hz, 2H), 8.27 (t, *J* = 7.6 Hz, 1H), 7.94 (dd, *J* = 7.6, 6.9 Hz, 2H), 7.65 (d, *J* = 6.2 Hz, 1H), 6.25 (d, *J* = 6.2 Hz, 1H); ¹³C NMR (101 MHz, CDCl₃) δ 168.9 (C), 160.8 (C), 153.8 (CH), 145.5 (2×CH), 141.2 (CH), 128.6 (2×CH), 105.8 (CH). Analytical data matches that reported in the literature.¹⁰³

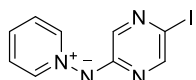
***N*-(6-Chloropyridazin-3-yl)pyridinium aminide (382)**



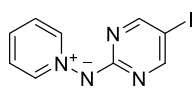
Following **GP4** using *N*-aminopyridinium iodide (0.40 g, 1.8 mmol), and 3,6-dichloropyridazine (0.21 g, 1.9 mmol) and potassium carbonate (0.70 g, 5.0 mmol) for 15 h. After purification by flash chromatography [AcOEt:MeOH (3:2)] aminide **382** was isolated as a bright yellow solid (310.8 mg, 84%); mp: 154–156 °C (lit.¹⁰³ 154–155 °C); ¹H NMR (300 MHz, CDCl₃) δ 8.79 (dd, *J* = 6.9, 1.3 Hz, 2H), 8.22 (t, *J* = 7.8 Hz, 1H), 7.93 (dd, *J* = 7.8, 6.9 Hz, 2H), 7.18 (d, *J* = 9.4 Hz, 1H), 6.83 (d, *J* = 9.4 Hz, 1H); ¹³C NMR (101 MHz, CDCl₃) δ 164.9 (C), 145.5 (2×CH), 144.8 (C), 140.3 (CH), 129.9 (CH), 128.9 (2×CH), 122.3 (CH). Analytical data matches that reported in the literature.¹⁰³

***N*-(Pyridin-2-yl)pyridinium aminide (384)**

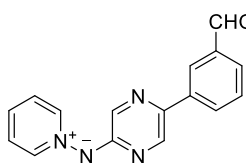
Following the method reported by Alvarez-Builla,¹⁰³ a flame-dried flask was charged with *N*-aminopyridinium iodide (125.2 mg, 0.56 mmol), 2-bromopyridine (37.0 μ L, 0.37 mmol), sodium *tert*-butoxide (220.5 mg, 2.25 mmol) and BINAP (10.1 mg, 0.02 mmol). The mixture was flushed with argon for 10 min. Dry toluene [0.04 M relative to the amount of bromopyridine] and tris(dibenzylidenacetone)-palladium(0) (15.6 mg, 0.02 mmol) were added and the mixture heated under reflux for 24 h. After purification by flash chromatography [CH_2Cl_2 :MeOH (95:5)] aminide **384** was isolated as a bright yellow solid (43.5 mg, 69%); mp: 117–119 $^{\circ}\text{C}$ (lit.⁵³ 115–116 $^{\circ}\text{C}$); ^1H NMR (300 MHz, CDCl_3) δ 9.07 (dd, J = 5.6, 2.8 Hz, 2H), 7.90 (dd, J = 5.1, 1.2 Hz, 1H), 7.42–7.36 (m, 4H), 6.60 (d, J = 8.5 Hz, 1H), 6.54–6.41 (m, 1H); ^{13}C NMR (101 MHz, CDCl_3) δ 163.0 (C), 145.9 (CH), 139.1 (2 \times CH), 136.8 (CH), 129.4 (CH), 125.5 (2 \times CH), 113.5 (CH), 112.4 (CH). Analytical data matches that reported in the literature.⁵³

***N*-(5-Iodopyrazin-2-yl)pyridinium aminide (385)**

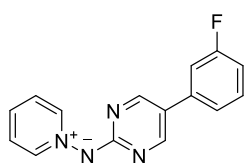
Following **GP6** using aminide **380** (242.3 mg, 1.4 mmol) and NIS (346.7 mg, 1.5 mmol) for 4 h. After purification by flash chromatography [CH_2Cl_2 :MeOH (9:1)] aminide **380** was isolated as an orange solid (299.0 mg, 47%); mp: 133–135 $^{\circ}\text{C}$ (lit.¹¹⁹ 132–134 $^{\circ}\text{C}$); ^1H NMR (300 MHz, CDCl_3) δ 9.03–8.96 (m, 2H), 7.89 (d, J = 1.4 Hz, 1H), 7.88 (d, J = 1.4 Hz, 1H), 7.78–7.68 (m, 1H), 7.59 (app. t, J = 7.0 Hz, 2H); ^{13}C NMR (101 MHz, CDCl_3) δ 149.8 (C), 147.0 (2 \times CH), 141.4 (CH), 139.2 (CH), 134.5 (CH), 126.3 (2 \times CH), 123.7 (C). Analytical data matches that reported in the literature.¹¹⁹

N-(5-Iodopyrimidin-2-yl)pyridinium aminide (**386**)

Following **GP6** using aminide **239** (200.5 mg, 1.2 mmol) and NIS (286.2 mg, 1.3 mmol) for 4 h. After purification by flash chromatography [CH_2Cl_2 :MeOH (9:1)] aminide **386** was isolated as a yellow solid (323.3 mg, 93%); ^1H NMR (300 MHz, CDCl_3) δ 8.80 (d, $J = 5.6$ Hz, 2H), 8.25 (s, 2H), 7.80 (t, $J = 7.3$ Hz, 1H), 7.71–7.53 (m, 2H); ^{13}C NMR (101 MHz, CDCl_3) δ 165.5 (C), 162.4 (2 \times CH), 142.4 (2 \times CH), 134.6 (CH), 126.1 (2 \times CH), 72.6 (C); HRMS (ES-TOF): m/z : calcd. for $\text{C}_9\text{H}_7\text{N}_4^{127}\text{I}$: 298.9794, found: 298.9784 $[\text{M}]^+$. Analytical data matches that reported in the literature.¹¹⁹

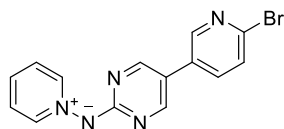
N-(5-(3-Formylphenyl)pyrazin-2-yl)pyridinium aminide (**388**)

Following **GP7** using (3-formylphenyl)boronic acid (143.1 mg, 0.9 mmol) and aminide **385** (189.8 mg, 0.6 mmol). After purification by flash chromatography [ethyl acetate:methanol (4:1)] aminide **388** was isolated as a bright yellow solid (135.2 mg, 63% at ~90% purity estimated by ^1H NMR); mp: 126–128 °C; ^1H NMR (300 MHz, CDCl_3) δ 10.10 (s, 1H), 9.14 (d, $J = 5.9$ Hz, 2H), 8.38 (s, 1H), 8.28 (d, $J = 1.2$ Hz, 1H), 8.19 (d, $J = 1.2$ Hz, 1H), 8.16 (d, $J = 7.8$ Hz, 1H), 7.82 (d, $J = 7.8$ Hz, 1H), 7.73 (app. t, $J = 7.8$ Hz, 1H), 7.66–7.56 (m, 3H); ^{13}C NMR (101 MHz, CDCl_3) δ 192.6 (CH), 157.6 (C), 140.9 (C), 140.8 (CH), 138.9 (C), 137.9 (CH), 137.8 (CH), 136.9 (2 \times CH), 133.3 (C), 130.6 (CH), 129.4 (CH), 127.8 (CH), 126.5 (CH), 126.2 (2 \times CH); IR $\nu_{\text{max}}/\text{cm}^{-1}$ 3118, 3062, 3923, 1690, 1467, 1395, 1145, 997, 750; HRMS (ES-TOF): m/z : calcd. for $\text{C}_{16}\text{H}_{13}\text{N}_4\text{O}$: 277.1089, found: 277.1092 $[\text{M}+\text{H}]^+$.

N-(5-(3-Fluorophenyl)pyrimidin-2-yl)pyridinium aminide (**389**)

Following **GP7** using (3-fluorophenyl)boronic acid (167.8 mg, 1.2 mmol) and aminide **386** (239.0 mg, 0.8 mmol). After purification by flash chromatography [ethyl acetate:methanol (7:3)] aminide

389 was isolated as a bright orange solid (137.5 mg, 79% at ~90% purity estimated by ^1H NMR); mp: 152–154 °C; ^1H NMR (300 MHz, CDCl_3) δ 8.88 (d, J = 6.8 Hz, 2H), 8.45 (s, 2H), 7.76 (t, J = 6.8 Hz, 1H), 7.60 (app. t, J = 6.8 Hz, 2H), 7.40–7.29 (m, 1H), 7.22 (d, J = 8.5 Hz, 1H), 7.14 (d, $J_{\text{H-F}}$ = 9.1 Hz, 1H), 6.95 (app. t, J = 8.5 Hz, 1H); ^{13}C NMR (101 MHz, CDCl_3) δ 165.8 (d, $J_{\text{C-F}}$ = 245.8 Hz, CF), 162.1 (C), 156.1 (2 \times CH), 142.3 (2 \times CH), 138.7 (d, $J_{\text{C-F}}$ = 8.0 Hz, C), 134.3 (CH), 130.4 (d, $J_{\text{C-F}}$ = 8.5 Hz, CH), 126.1 (2 \times CH), 120.7 (CH), 120.4 (C), 113.3 (d, $J_{\text{C-F}}$ = 20.2 Hz, CH), 111.9 (d, $J_{\text{C-F}}$ = 22.0 Hz, CH); IR $\nu_{\text{max}}/\text{cm}^{-1}$ 3109, 3040, 3023, 1582, 1420, 1273, 1160, 864, 767; HRMS (ES-TOF): m/z : calcd. for $\text{C}_{15}\text{H}_{12}\text{N}_4\text{F}$: 267.1047, found: 267.1045 $[\text{M}+\text{H}]^+$.

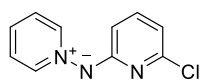
N-(5-(2-Bromopyridin-5-yl)pyrimidin-2-yl)pyridinium aminide (**390**)

Following **GP7** using (6-bromopyridin-3-yl)boronic acid (242.4 mg, 1.2 mmol) and aminide **386** (239.6 mg, 0.8 mmol). After

purification by flash chromatography [ethyl acetate:methanol (7:3)] aminide **390** was isolated as a bright yellow solid (191.1 mg, 73% at ~90% purity estimated by ^1H NMR); mp: 221–222 °C; ^1H NMR (300 MHz, CDCl_3) δ 8.82 (d, J = 6.9 Hz, 2H), 8.46 (d, J = 2.5 Hz, 1H), 8.40 (s, 2H), 7.83 (t, J = 7.6 Hz, 1H), 7.68–7.57 (m, 3H), 7.48 (d, J = 8.3 Hz, 1H); ^{13}C NMR (101 MHz, CDCl_3) δ 167.3 (C), 155.9 (CH), 146.5 (CH), 142.7 (2 \times CH), 139.7 (C), 135.0 (CH), 134.8 (CH), 131.7 (C), 128.1 (2 \times CH), 126.2 (2 \times CH),

116.8 (C); IR $\nu_{\text{max}}/\text{cm}^{-1}$ 3130, 3014, 1572, 1498, 1352, 1183, 1074, 957, 1052, 864, 795; HRMS (ES-TOF): m/z : calcd. for $\text{C}_{14}\text{H}_{11}\text{N}_5^{79}\text{Br}$: 328.0197, found: 328.0198 $[\text{M}+\text{H}]^+$.

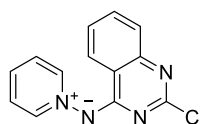
***N*-(6-Chloropyridin-2-yl)pyridinium aminide (411)**



Following **GP4** using *N*-aminopyridinium iodide (221.3 mg, 1.0 mmol), 2,6-dichloropyridine (152.4 mg, 1.1 mmol) and potassium carbonate (386.6 mg, 2.1 mmol) for 6 h. After purification by flash chromatography [CH_2Cl_2 :MeOH (8:2)] aminide **411** was isolated as a brown solid (130.7 mg, 65%); ^1H NMR (300 MHz, CDCl_3) δ 9.07–9.00 (m, 2H), 7.64–7.56 (m, 1H), 7.55–7.47 (m, 2H), 7.32 (dd, $J = 8.3, 7.3$ Hz, 1H), 6.50 (dd, $J = 8.3, 0.6$ Hz, 1H), 6.46 (dd, $J = 7.3, 0.6$ Hz, 1H); ^{13}C NMR (101 MHz, CDCl_3) δ 151.0 (C), 147.8 (C), 140.2 (CH), 138.8 (2 \times CH), 131.9 (CH), 125.8 (2 \times CH), 110.8 (CH), 110.6 (CH); HRMS (ES-TOF): m/z : calcd. for $\text{C}_{10}\text{H}_9\text{N}_3\text{Cl}$: 206.0485, found: 206.0483 $[\text{M}+\text{H}]^+$. Data matches that reported in the literature.⁵⁴

This transformation was also performed following **GP5**, using *N*-aminopyridinium iodide (221.9 mg, 1.0 mmol), 2,6-dichloropyridine (152.5 mg, 1.1 mmol) and potassium carbonate (388.0 mg, 2.1 mmol) for 24 h to give aminide **411** (199.4 mg, 97%).

***N*-(2-Chloroquinazolin-4-yl)pyridinium aminide (412)**

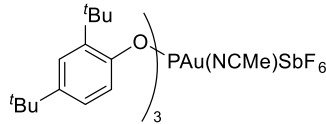


Following **GP4** using *N*-aminopyridinium iodide (322.4 mg, 1.5 mmol), 2,4-dichloroquinazoline (300.3 mg, 0.5 mmol) and potassium carbonate (563.8 mg, 4.1 mmol) for 24 h. After purification by flash chromatography [CH_2Cl_2 :MeOH (95:5)] aminide **412** was isolated as a bright yellow solid (347.0 mg, 90%); mp: 205–207 °C; ^1H NMR (300 MHz, CDCl_3) δ 8.75 (dd, $J = 6.9, 1.2$ Hz, 2H),

8.18 (dd, $J = 7.6, 1.5$ Hz, 1H), 8.00 (t, $J = 7.7$ Hz, 1H), 7.80–7.71 (m, 2H), 7.66–7.54 (m, 2H), 7.34 (ddd, $J = 8.2, 6.1, 1.5$ Hz, 1H); ^{13}C NMR (101 MHz, CDCl_3) δ ^{13}C NMR (101 MHz, CDCl_3) δ 164.7 (C), 158.0 (C), 151.0 (C), 143.5 (2 \times CH), 137.8 (CH), 132.4 (CH), 126.6 (2 \times CH), 126.1 (CH), 125.1 (CH), 124.0 (CH), 116.1 (C); IR $\nu_{\text{max}}/\text{cm}^{-1}$ 3096, 3012, 1569, 1481, 1430, 1352, 1261, 1150, 943; HRMS (ES-TOF): m/z : calcd. for $\text{C}_{13}\text{H}_{10}\text{N}_4\text{Cl}$: 257.0594, found: 257.0600 $[\text{M}+\text{H}]^+$.

This transformation was also performed following **GP5**, using *N*-aminopyridinium iodide (320.6 mg, 1.5 mmol), 2,6-dichloropyridine (152.4 mg, 1.1 mmol) and potassium carbonate (388.9 mg, 2.1 mmol) for 3 h to give aminide **412** (369.8 mg, 99%).

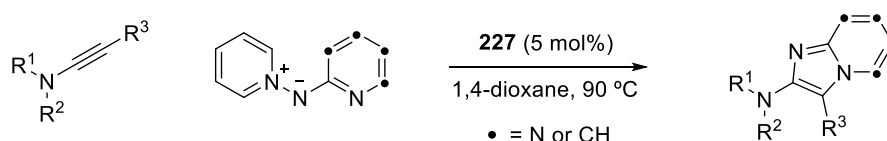
5.2.3 Preparation of **227**

Following a reported procedure,^{34a} a double-neck, round-bottom flask covered with aluminium foil was charged with  $\text{PAu}(\text{NCMe})\text{SbF}_6$ bottom flask covered with aluminium foil was charged with AgSbF_6 (61.0 mg, 0.18 mmol) dissolved in MeCN (10 mL). Chloro[tris(2,4-di-tert-butylphenyl)phosphite]gold (130.2 mg, 0.15 mmol) was added at room temperature to the reaction mixture forming a white suspension. The reaction mixture was stirred at room temperature overnight. The solvent was removed under reduced pressure and the white solid residue was redissolved in CH_2Cl_2 (15 mL). After filtration through a plug of silica, evaporation of the solvent and drying on the high vacuum line for at least 3 hours, the gold complex **227** was afforded as a white powder (126.6 mg, 80%); ^1H NMR (300 MHz, CDCl_3) δ 7.50–7.46 (m, 3H), 7.37 (dd, $J = 8.5, 1.5$ Hz, 3H), 7.25 (d, $J = 8.5$ Hz, 3H), 2.50 (s, 3H), 1.46 (s, 27H), 1.32 (s, 27H); ^{13}C NMR (101 MHz, CDCl_3) δ ^{13}C NMR (101 MHz, CDCl_3) δ 149.2 (3 \times C), 147.1 (3 \times C), 139.1 (3 \times C), 125.9 (3 \times CH), 124.7 (3 \times CH), 119.2 (3 \times CH), 35.3 (3 \times C), 34.7 (3 \times C), 31.4 (9 \times CH₃), 30.5 (9 \times CH₃), 2.9

(CH₃); *One resonance for a quaternary carbon was not visible*; IR $\nu_{\text{max}}/\text{cm}^{-1}$ 3096, 3012, 1569, 1481, 1430, 1352, 1261, 1150, 943; Analytical data matches that reported in the literature.^{34a}

5.3 Cycloaddition products for Chapter 2

General Procedure 8 (GP8)



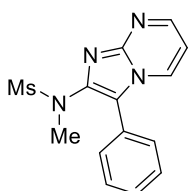
A heat gun-dried reaction tube was charged with the corresponding heterocyclic aminide (1.2 eq.), **227** (5 mol%) and solid ynamide (1.0 eq.) under an argon atmosphere before 1,4-dioxane [0.2 M relative to the amount of ynamide] was added. In cases when the ynamide was an oil it was prepared as a solution in 1,4-dioxane [0.2 M] and added to the aminide and catalyst. The mixture was stirred at 90 °C until the reaction was either complete or appeared to be proceeding no further (24 h unless otherwise specified). Heating was removed and the reaction mixture allowed to cool down to rt before being filtered through a pad of silica gel (~1 cm) and washing with chloroform. The filtrate was concentrated under reduced pressure and the residue was purified by flash chromatography.

General Procedure 9 (GP9)

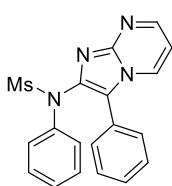
Following the same procedure as **GP8** but using dichloro(2-pyridincarboxylato)gold(III) (PicAuCl₂) (5 mol%) as catalyst.

General Procedure 10 (GP10)

Following the same procedure as **GP8** but using 1,2-DCB [0.2 M] as solvent and stirring at 120 °C until reaction was either complete or appeared to be proceeding no further. Heating was removed and the reaction mixture allowed to cool down to rt. The reaction mixture was directly placed onto a column of silica gel for purification by flash chromatography.

Imidazo[1,2-a]pyrimidine 284

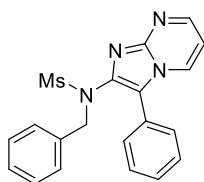
Following **GP8** using ynamide **264** (41.8 mg, 0.20 mmol) and aminide **239** (41.4 mg, 0.24 mmol). After purification by flash chromatography [hexane:ethyl acetate (3:7)] compound **284** was isolated as a white solid (53.2 mg, 88%); mp. 185–186 °C; ^1H NMR (300 MHz, CDCl_3) δ 8.55 (dd, $J = 4.1$, 2.0 Hz, 1H), 8.45 (dd, $J = 6.9$, 2.0 Hz, 1H), 7.62–7.58 (m, 2H), 7.48–7.41 (m, 2H), 7.42–7.36 (m, 1H), 6.90 (dd, $J = 6.9$, 4.1 Hz, 1H), 3.25 (s, 3H), 3.25 (s, 3H); ^{13}C NMR (101 MHz, CDCl_3) δ 150.6 (CH), 145.4 (C), 142.2 (C), 131.5 (CH), 129.4 (2 \times CH), 129.3 (2 \times CH), 129.2 (CH), 126.1 (C), 119.7 (C), 109.6 (CH), 38.9 (CH_3), 37.1 (CH_3); IR $\nu_{\text{max}}/\text{cm}^{-1}$ 3086, 3012, 2984, 2853, 1624, 1502, 1379, 1237, 1145, 970, 766; HRMS (ES-TOF): m/z : calcd. for $\text{C}_{14}\text{H}_{15}\text{N}_4\text{O}_2\text{S}$: 303.0916, found: 303.0912 $[\text{M}+\text{H}]^+$.

Imidazo[1,2-a]pyrimidine 287

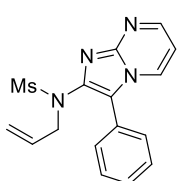
Following **GP8** using ynamide **265** (54.6 mg, 0.20 mmol) and aminide **239** (41.5 mg, 0.24 mmol). After purification by flash chromatography [hexane:ethyl acetate (3:7)] imidazopyrimidine **287** was isolated as a white solid (69.4 mg, 95%); mp. 225–226 °C; ^1H NMR (300 MHz, CDCl_3) δ 8.60 (dd, J

= 4.2 Hz, J = 2.0 Hz, 1H), 8.44 (dd, J = 6.9, 2.0 Hz, 1H), 7.58–7.40 (m, 7H), 7.30–7.18 (m, 3H), 6.91 (dd, J = 6.9, 4.2 Hz, 1H), 3.44 (s, 3H); ^{13}C NMR (101 MHz, CDCl_3) δ 150.5 (CH), 145.2 (C), 141.6 (C), 140.4 (C), 131.4 (CH), 129.3 (CH), 129.2 (2 \times CH), 129.2 (2 \times CH), 129.1 (2 \times CH), 127.9 (2 \times CH), 127.8 (CH), 125.8 (C), 120.2 (C), 109.6 (CH), 38.9 (CH_3); IR $\nu_{\text{max}}/\text{cm}^{-1}$ 3100, 3057, 3008, 2931, 1605, 1484, 1384, 1152, 963, 746; HRMS (ES-TOF): m/z : calcd. for $\text{C}_{19}\text{H}_{17}\text{N}_4\text{O}_2\text{S}$: 365.1072, found: 365.1081 $[\text{M}+\text{H}]^+$.

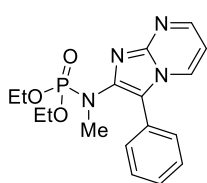
Imidazo[1,2-a]pyrimidine 288



Following **GP8** using ynamide **266** (57.0 mg, 0.20 mmol) and aminide **239** (41.4 mg, 0.24 mmol). After purification by flash chromatography [hexane:ethyl acetate (3:7)] compound **288** was isolated as a white solid (68.3 mg, 89%); mp. 152–153 °C; ^1H NMR (300 MHz, CDCl_3) δ 8.57 (dd, J = 4.1, 2.0 Hz, 1H), 8.27 (dd, J = 6.9, 2.0 Hz, 1H), 7.43–7.32 (m, 3H), 7.23–7.16 (m, 2H), 7.12–7.04 (m, 1H), 6.98–6.90 (m, 4H), 6.84 (dd, J = 6.9, 4.1 Hz, 1H), 4.79 (s, 2H), 3.33 (s, 3H); ^{13}C NMR (101 MHz, CDCl_3) δ 150.5 (CH), 145.4 (C), 140.0 (C), 134.9 (C), 131.5 (CH), 129.5 (2 \times CH), 129.1 (2 \times CH), 129.1 (CH), 129.0 (2 \times CH), 128.0 (2 \times CH), 127.6 (CH), 125.8 (C), 121.9 (C), 109.4 (CH), 55.3 (CH_2), 38.4 (CH_3); IR $\nu_{\text{max}}/\text{cm}^{-1}$ 3097, 3062, 3028, 3001, 2925, 1624, 1504, 1388, 1334, 1154, 971; HRMS (ES-TOF): m/z : calcd. for $\text{C}_{20}\text{H}_{19}\text{N}_4\text{O}_2\text{S}$: 379.1229, found: 379.1224 $[\text{M}+\text{H}]^+$.

Imidazo[1,2-a]pyrimidine 289

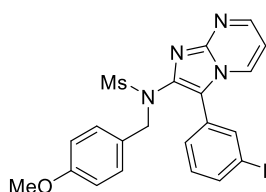
Following **GP8** using ynamide **267** (47.4 mg, 0.20 mmol) and aminide **239** (41.4 mg, 0.24 mmol). After purification by flash chromatography [hexane:ethyl acetate (3:7)] compound **289** was isolated as a white solid (37.9 mg, 59%); mp. 142–143 °C; ^1H NMR (300 MHz, CDCl_3) δ 8.59 (dd, $J = 4.1, 2.0$ Hz, 1H), 8.44 (dd, $J = 6.9, 2.0$ Hz, 1H), 7.67–7.62 (m, 2H), 7.57–7.51 (m, 2H), 7.50–7.44 (m, 1H), 6.91 (dd, $J = 6.9, 4.1$ Hz, 1H), 5.63 (ddt, $J = 16.8, 10.1, 6.6$ Hz, 1H), 5.03 (app. dq, $J = 16.8, 1.3$ Hz, 1H), 4.95 (app. dq, $J = 10.1, 1.3$ Hz, 1H), 4.22 (app. dt, $J = 6.6, 1.3$ Hz, 2H), 3.31 (s, 3H); ^{13}C NMR (101 MHz, CDCl_3) δ 150.5 (CH), 145.3 (C), 140.4 (C), 132.2 (CH), 131.1 (CH), 129.5 (2 \times CH), 129.3 (2 \times CH), 129.3 (CH), 126.1 (C), 121.1 (C), 119.3 (CH_2), 109.5 (CH), 54.3 (CH_2), 39.0 (CH_3); IR $\nu_{\text{max}}/\text{cm}^{-1}$ 3025, 3010, 2924, 2854, 1625, 1505, 1382, 1152, 972, 766; HRMS (ES-TOF): m/z : calcd. for $\text{C}_{16}\text{H}_{17}\text{N}_4\text{O}_2\text{S}$: 329.1079, found: 329.1072 $[\text{M}+\text{H}]^+$.

Imidazo[1,2-a]pyrimidine 290

Following **GP8** using ynamide **268** (54.0 mg, 0.20 mmol) and aminide **239** (41.4 mg, 0.24 mmol). After purification by flash chromatography [ethyl acetate:MeOH (4:1)] compound **290** was isolated as a white solid (60.8 mg, 84%); mp. 167–169 °C; ^1H NMR (400 MHz, CDCl_3) δ 8.51 (dd, $J = 4.1, 1.8$ Hz, 1H), 8.33 (dd, $J = 6.8, 1.8$ Hz, 1H), 7.59 (d, $J = 8.1$ Hz, 2H), 7.52 (app. t, $J = 7.6$ Hz, 2H), 7.44 (t, $J = 7.3$ Hz, 1H), 6.82 (dd, $J = 6.8, 4.1$ Hz, 1H), 3.99 (app. quin, $J = 7.2$ Hz, 4H), 3.13 (d, $J = 8.8$ Hz, 3H), 1.23 (t, $J = 7.1$ Hz, 6H); ^{13}C NMR (101 MHz, CDCl_3) δ 149.3 (CH), 145.3 (C), 145.20 (d, $J_{\text{C-P}} = 5.3$ Hz, C), 130.7 (CH), 130.0 (2 \times CH), 129.1 (2 \times CH), 128.9 (CH), 127.6 (C), 116.7 (d, $J_{\text{C-P}} = 4.8$ Hz, C),

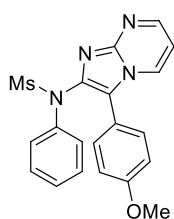
108.9 (CH), 62.6 (d, $J_{C-P} = 4.8$ Hz, $2\times\text{CH}_2$), 37.3 (d, $J_{C-P} = 3.5$ Hz, CH_3), 16.10 (d, $J_{C-P} = 7.2$ Hz, $2\times\text{CH}_3$); IR $\nu_{\text{max}}/\text{cm}^{-1}$ 3029, 2982, 2924, 1620, 1555, 1447, 1342, 1150, 1026; HRMS (ES-TOF): m/z : calcd. for $\text{C}_{17}\text{H}_{21}\text{N}_4\text{O}_3\text{PNa}$: 383.1249, found: 383.1248 $[\text{M}+\text{Na}]^+$.

Imidazo[1,2-a]pyrimidine 291



Following **GP8** using ynamide **269** (72.5 mg, 0.20 mmol) and aminide **239** (41.4 mg, 0.24 mmol). After purification by flash chromatography [hexane:ethyl acetate (1:9)] compound **291** was isolated as a white solid (68.8 mg, 77%); mp. 86–88 °C; ^1H NMR (300 MHz, CDCl_3) δ 8.66 (dd, $J = 4.1, 2.0$ Hz, 1H), 8.25 (dd, $J = 6.9, 2.0$ Hz, 1H), 8.23–8.20 (m, 1H), 7.86 (app. dt, $J = 7.9, 1.9$ Hz, 1H), 7.66 (app. t, $J = 1.9$ Hz, 1H), 7.61 (app. t, $J = 7.9$ Hz, 1H), 6.97 (dd, $J = 6.9, 4.1$ Hz, 1H), 6.84–6.78 (m, 2H), 6.48–6.40 (m, 2H), 4.70 (s, 2H), 3.65 (s, 3H), 3.36 (s, 3H); ^{13}C NMR (101 MHz, CDCl_3) δ 159.3 (C), 151.3 (CH), 148.1 (C), 145.9 (C), 140.7 (C), 136.4 (CH), 131.2 (CH), 130.6 ($2\times\text{CH}$), 130.3 (CH), 127.6 (C), 126.4 (C), 123.6 (CH), 123.0 (CH), 119.9 (C), 113.2 ($2\times\text{CH}$), 110.0 (CH), 55.0 (CH_3), 54.8 (CH_2), 38.4 (CH_3); IR $\nu_{\text{max}}/\text{cm}^{-1}$ 3096, 3078, 2969, 1613, 1524, 1333, 1243, 1149, 808, 760; HRMS (ES-TOF): m/z : calcd. for $\text{C}_{21}\text{H}_{20}\text{N}_5\text{O}_5\text{S}$: 454.1182 found: 454.1185 $[\text{M}+\text{H}]^+$.

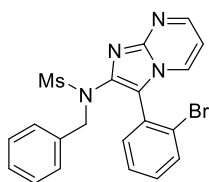
Imidazo[1,2-a]pyrimidine 292



Following **GP8** using ynamide **270** (58.2 mg, 0.20 mmol) and aminide **239** (41.4 mg, 0.24 mmol). After purification by flash chromatography [hexane:ethyl acetate (3:7)] compound **292** was isolated as a white solid

(65.2 mg, 83%); mp. 212–214 °C; ^1H NMR (300 MHz, CDCl_3) δ 8.59 (dd, $J = 4.1, 2.0$ Hz, 1H), 8.40 (dd, $J = 6.9, 2.0$ Hz, 1H), 7.57–7.50 (m, 2H), 7.48 (d, $J = 8.8$ Hz, 2H), 7.31–7.18 (m, 3H), 7.04 (d, $J = 8.8$ Hz, 2H), 6.89 (dd, $J = 6.9, 4.1$ Hz, 1H), 3.87 (s, 3H), 3.44 (s, 3H); ^{13}C NMR (101 MHz, CDCl_3) δ 160.3 (C), 150.3 (CH), 145.1 (C), 141.3 (C), 140.5 (C), 131.4 (CH), 130.8 (2 \times CH), 129.1 (2 \times CH), 128.0 (2 \times CH), 127.8 (CH), 120.3 (C), 117.9 (C), 114.7 (2 \times CH), 109.5 (CH), 55.4 (CH_3), 38.9 (CH_3); IR $\nu_{\text{max}}/\text{cm}^{-1}$ 3023, 3007, 2957, 2927, 2851, 1618, 1577, 1503, 1486, 1389, 1347, 1298, 1245, 1147, 1021, 965, 841, 753; HRMS (ES-TOF): m/z : calcd. for $\text{C}_{20}\text{H}_{19}\text{N}_4\text{O}_3\text{S}$: 395.1172, found: 395.1178 $[\text{M}+\text{H}]^+$.

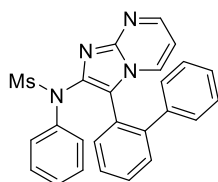
Imidazo[1,2-a]pyrimidine 293



Following **GP8** using ynamide **271** (72.8 mg, 0.20 mmol) and aminide **239** (41.7 mg, 0.24 mmol). After purification by flash chromatography [hexane:ethyl acetate (3:7)] compound **293** was isolated as a white solid (47.3 mg, 51%); mp. 158–160 °C; ^1H NMR (300 MHz, CDCl_3) δ 8.63 (dd, $J = 4.1, 2.0$ Hz, 1H), 7.89 (dd, $J = 6.8, 2.0$ Hz, 1H), 7.52 (dd, $J = 7.9, 1.1$ Hz, 1H), 7.47 (dd, $J = 7.6, 1.7$ Hz, 1H), 7.39 (app. td, $J = 7.6, 1.1$ Hz, 1H), 7.31 (app. td, $J = 7.9, 1.7$ Hz, 1H), 7.18–7.15 (m, 1H), 7.09–7.03 (m, 4H), 6.90 (dd, $J = 6.8, 4.1$ Hz, 1H), 4.91 (d, $J = 13.7$ Hz, 1H), 4.68 (d, $J = 13.7$ Hz, 1H), 3.32 (s, 3H); ^{13}C NMR (101 MHz, CDCl_3) δ 150.7 (CH), 145.5 (C), 141.1 (C), 135.1 (C), 135.0 (CH), 133.1 (CH), 132.8 (CH), 131.2 (CH), 128.8 (2 \times CH), 128.3 (2 \times CH), 127.8 (CH), 127.8 (CH), 126.9 (C), 124.9 (C), 120.6 (C), 109.0 (CH), 55.3 (CH_2), 38.7 (CH_3); IR $\nu_{\text{max}}/\text{cm}^{-1}$ 3027, 3001, 2924, 2854, 1623, 1562, 1495, 1454, 1390, 1361, 1325, 1230, 1147, 1026, 968, 814,

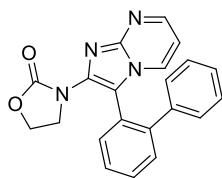
755; HRMS (ES-TOF): m/z : calcd. for $C_{20}H_{18}^{79}BrN_4O_2S$: 457.0334 found: 457.0336 $[M+H]^+$.

Imidazo[1,2-a]pyrimidine 294



Following **GP8** using ynamide **272** (67.4 mg, 0.20 mmol) and aminide **239** (41.3 mg, 0.24 mmol). After purification by flash chromatography [hexane:ethyl acetate (3:7)] compound **294** was isolated as a white solid (56.1 mg, 63%); mp. 64–65 °C; 1H NMR (300 MHz, $CDCl_3$) δ 8.38 (dd, J = 4.1, 2.0 Hz, 1H), 7.66 (dd, J = 7.4, 1.2 Hz, 1H), 7.60–7.44 (m, 6H), 7.36–7.24 (m, 3H), 7.00 (app. t, J = 7.4 Hz, 1H), 6.93 (app. t, J = 7.7 Hz, 2H), 6.72 (d, J = 7.1 Hz, 2H), 6.45 (dd, J = 6.9, 4.1 Hz, 1H), 3.51 (s, 3H); ^{13}C NMR (101 MHz, $CDCl_3$) δ 150.1 (CH), 144.8 (C), 142.3 (C), 141.6 (C), 140.3 (C), 139.8 (C), 133.5 (CH), 131.4 (CH), 130.3 (2 \times CH), 129.2 (2 \times CH), 128.5 (2 \times CH), 128.3 (2 \times CH), 128.1 (CH), 128.0 (CH), 127.6 (2 \times CH), 127.4 (CH), 123.7 (C), 120.2 (C), 108.5 (CH), 39.2 (CH_3); IR ν_{max}/cm^{-1} 3066, 3023, 1620, 1491, 1427, 1379, 1345, 1154, 967, 741; HRMS (ES-TOF): m/z : calcd. for $C_{25}H_{21}N_4O_2S$: 441.1387, found: 441.1372 $[M+H]^+$.

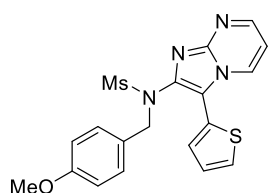
Imidazo[1,2-a]pyrimidine 295



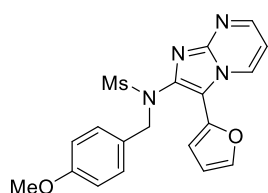
Following **GP8** using ynamide **273** (52.7 mg, 0.20 mmol) and aminide **239** (41.8 mg, 0.24 mmol). After purification by flash chromatography [hexane:ethyl acetate (1:9)] and recrystallisation [chloroform-hexane] compound **295** was isolated as a white solid (49.6 mg, 70%); mp. 206–207 °C; 1H NMR (300 MHz, $CDCl_3$) δ 8.48 (dd, J = 4.2, 2.0 Hz, 1H), 8.20 (dd, J = 6.9, 2.0 Hz, 1H), 7.62–7.42 (m, 4H), 7.21–7.16 (m, 3H), 7.15–7.09 (m, 2H), 6.76 (dd, J = 6.9, 4.2 Hz, 1H), 4.43–4.29 (m, 1H), 4.25–4.03 (m, 2H), 3.36–3.14 (m, 1H); ^{13}C NMR

(101 MHz, CDCl_3) δ 154.5 (C), 149.4 (CH), 145.4 (C), 142.0 (C), 140.9 (C), 139.5 (C), 130.7 (CH), 130.7 (CH), 130.4 (CH), 129.8 (CH), 128.3 (2 \times CH), 128.2 (2 \times CH), 128.1 (CH), 127.3 (CH), 125.9 (C), 113.4 (C), 108.8 (CH), 62.7 (CH_2), 45.2 (CH_2); IR $\nu_{\text{max}}/\text{cm}^{-1}$ 3090, 2992, 2914, 1757, 1681, 1568, 1439, 1419, 1203, 1156, 1068, 1026, 787, 741; HRMS (ES-TOF): m/z : calcd. for $\text{C}_{21}\text{H}_{17}\text{N}_4\text{O}_2$: 357.1352, found: 357.1355 $[\text{M}+\text{H}]^+$.

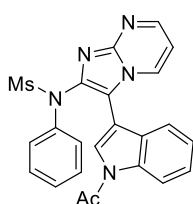
Imidazo[1,2-a]pyrimidine 296



Following **GP8** using ynamide **275** (62.4 mg, 0.19 mmol) and aminide **239** (40.2 mg, 0.23 mmol). After purification by flash chromatography [hexane:ethyl acetate (3:7)] compound **296** was isolated as a yellow solid (58.4 mg, 73%); mp. 187–189 °C; ^1H NMR (300 MHz, CDCl_3) δ 8.55 (dd, $J = 4.1, 2.0$ Hz, 1H), 8.49 (dd, $J = 6.9, 2.0$ Hz, 1H), 7.46 (dd, $J = 5.1, 1.1$ Hz, 1H), 7.20 (dd, $J = 3.5, 1.1$ Hz, 1H), 7.11 (dd, $J = 5.1, 3.5$ Hz, 1H), 7.00 (d, $J = 8.7$ Hz, 2H), 6.92 (dd, $J = 6.9, 4.1$ Hz, 1H), 6.58 (d, $J = 8.7$ Hz, 2H), 4.77 (s, 2H), 3.69 (s, 3H), 3.27 (s, 3H); ^{13}C NMR (101 MHz, CDCl_3) δ 159.1 (C), 150.7 (CH), 145.6 (C), 141.0 (C), 131.9 (CH), 130.3 (2 \times CH), 129.4 (CH), 127.9 (CH), 127.6 (CH), 126.9 (C), 125.7 (C), 116.1 (C), 113.5 (2 \times CH), 109.7 (CH), 55.2 (CH_3), 54.6 (CH_2), 38.3 (CH_3); IR $\nu_{\text{max}}/\text{cm}^{-1}$ 3116, 3071, 3013, 2955, 1611, 1509, 1244, 1152, 842, 799; HRMS (ES-TOF): m/z calcd. for $\text{C}_{19}\text{H}_{19}\text{N}_4\text{O}_3\text{S}_2$: 415.1049 found: 415.1054 $[\text{M}+\text{H}]^+$.

Imidazo[1,2-a]pyrimidine 297

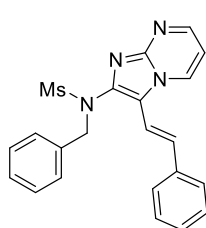
Following **GP8** using ynamide **276** (61.7 mg, 0.20 mmol) and aminide **239** (41.4 mg, 0.24 mmol). After purification by flash chromatography [hexane:ethyl acetate (3:7)] compound **297** was isolated as a yellow solid (49.7 mg, 62%); mp. 210–212 °C; ^1H NMR (300 MHz, CDCl_3) δ 8.88 (dd, $J = 7.0, 2.0$ Hz, 1H), 8.58 (dd, $J = 4.1, 2.0$ Hz, 1H), 7.48 (d, $J = 1.8$ Hz, 1H), 7.11 (d, $J = 8.7$ Hz, 2H), 6.97 (d, $J = 3.5$ Hz, 1H), 6.94 (dd, $J = 7.0, 4.1$ Hz, 1H), 6.62 (d, $J = 8.7$ Hz, 2H), 6.51 (dd, $J = 3.5, 1.8$ Hz, 1H), 4.86 (s, 2H), 3.69 (s, 3H), 3.23 (s, 3H); ^{13}C NMR (101 MHz, CDCl_3) δ 159.1 (C), 150.7 (CH), 145.2 (C), 142.2 (CH), 141.8 (C), 139.9 (C), 133.7 (CH), 130.3 (2 \times CH), 126.9 (C), 123.6 (C), 113.5 (2 \times CH), 111.9 (CH), 111.3 (CH), 109.7 (CH), 55.2 (CH_3), 54.6 (CH_2), 38.1 (CH_3); IR $\nu_{\text{max}}/\text{cm}^{-1}$ 3101, 3072, 2932, 2228, 1622, 1505, 1338, 1156, 963, 761; HRMS (ES-TOF): m/z : calcd. for $\text{C}_{19}\text{H}_{18}\text{N}_4\text{O}_4\text{SNa}$: 421.0956 found: 421.0959 $[\text{M}+\text{Na}]^+$.

Imidazo[1,2-a]pyrimidine 298

Following **GP8** using ynamide **277** (70.5 mg, 0.20 mmol) and aminide **239** (41.3 mg, 0.24 mmol). After purification by flash chromatography [hexane:ethyl acetate (3:7)] compound **298** was isolated as a white solid (71.1 mg, 80%); mp. 228–230 °C; ^1H NMR (300 MHz, CDCl_3) δ 8.67 (dd, $J = 4.0, 2.0$ Hz, 1H), 8.57 (d, $J = 8.4$ Hz, 1H), 8.24 (dd, $J = 6.9, 2.0$ Hz, 1H), 7.86 (s, 1H), 7.59–7.54 (m, 2H), 7.43 (app. t, $J = 7.8$ Hz, 1H), 7.59–7.54 (m, 4H), 7.09 (d, $J = 7.8$ Hz, 1H), 6.94 (dd, $J = 6.9, 4.0$ Hz, 1H), 3.43 (s, 3H), 2.70 (s, 3H); ^{13}C NMR (101 MHz, CDCl_3) δ 168.7 (C), 150.7 (CH), 145.8 (C), 142.6 (C), 140.6 (C), 135.8 (C), 132.7 (CH), 129.2 (2 \times CH), 127.9 (2 \times CH), 127.9 (CH), 127.6 (CH), 126.0 (CH), 124.3 (CH), 119.7 (CH),

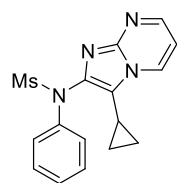
117.4 (CH), 113.7 (C), 109.5 (CH), 107.0 (C), 38.9 (CH₃), 24.0 (CH₃); *One resonance for a quaternary carbon was not visible.* IR $\nu_{\text{max}}/\text{cm}^{-1}$ 3103, 3063, 3019, 2931, 1702, 1626, 1493, 1373, 1225, 805, 763; HRMS (ES-TOF): m/z : calcd. for C₂₃H₂₀N₅O₃S: 446.1284 found: 446.1287 [M+H]⁺.

Imidazo[1,2-a]pyrimidine 299



Following **GP8** using ynamide **278** (62.2 mg, 0.20 mmol) and aminide **239** (41.3 mg, 0.24 mmol). After purification by flash chromatography [hexane:ethyl acetate (2:8)] compound **299** was isolated as a pale yellow solid (73.1 mg, 90%); mp. 258–260 °C; ¹H NMR (300 MHz, CDCl₃) δ 8.55 (dd, J = 4.1, 1.9 Hz, 1H), 8.51 (dd, J = 6.9, 1.9 Hz, 1H), 7.42–7.32 (m, 4H), 7.32–7.23 (m, 4H), 7.19–7.15 (m, 2H), 7.10 (d, J = 16.7 Hz, 1H), 6.97 (dd, J = 6.9, 4.1 Hz, 1H), 6.80 (d, J = 16.7 Hz, 1H), 4.95 (s, 2H), 3.24 (s, 3H); ¹³C NMR (101 MHz, CDCl₃) δ 150.2 (CH), 145.6 (C), 141.0 (C), 136.6 (C), 135.3 (C), 132.0 (CH), 131.5 (CH), 129.2 (2×CH), 128.7 (2×CH), 128.3 (CH), 128.3 (2×CH), 128.0 (2×CH), 126.5 (2×CH), 126.5 (2×CH), 119.8 (C), 55.2 (CH₂), 38.0 (CH₃); IR $\nu_{\text{max}}/\text{cm}^{-1}$ 3136, 3063, 3003, 2922, 2851, 1618, 1495, 1452, 1395, 1242, 1154, 960; HRMS (ES-TOF): m/z : calcd. for C₂₂H₂₁N₄O₂S: 405.1385 found: 405.1390 [M+H]⁺.

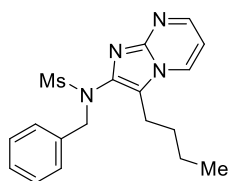
Imidazo[1,2-a]pyrimidine 300



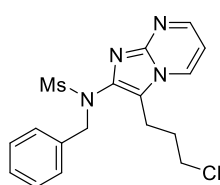
Following **GP8** using ynamide **279** (47.3 mg, 0.20 mmol) and aminide **239** (41.4 mg, 0.24 mmol). After purification by flash chromatography [hexane:ethyl acetate (3:7)] compound **300** was isolated as a white solid (48.0 mg, 70%); mp. 182–183 °C; ¹H NMR (300 MHz, CDCl₃) δ 8.58 (dd, J = 4.1, 2.0 Hz, 1H), 8.48 (dd, J = 6.8, 2.0 Hz, 1H), 7.73 (dd, J = 8.3, 1.1 Hz, 2H), 7.40–7.32 (m,

2H), 7.31–7.24 (m, 1H), 6.95 (dd, $J = 6.8, 4.1$ Hz, 1H), 3.39 (s, 3H), 1.62 (tt, $J = 8.1, 5.2$ Hz, 1H), 1.12–1.02 (m, 2H), 0.95–0.87 (m, 2H); ^{13}C NMR (101 MHz, CDCl_3) δ 149.8 (CH), 144.6 (C), 142.5 (C), 140.6 (C), 131.5 (CH), 129.2 (2 \times CH), 128.0 (2 \times CH), 127.7 (CH), 119.9 (C), 109.1 (CH), 38.8 (CH_3), 5.1 (2 \times CH_2), 2.3 (CH); IR $\nu_{\text{max}}/\text{cm}^{-1}$ 3092, 3035, 2932, 2854, 1619, 1501, 1845, 1412, 1347, 1316, 1211, 1151, 960, 756; HRMS (ES-TOF): m/z : calcd. for $\text{C}_{16}\text{H}_{17}\text{N}_4\text{O}_2\text{S}$: 329.1072, found: 329.1075 $[\text{M}+\text{H}]^+$.

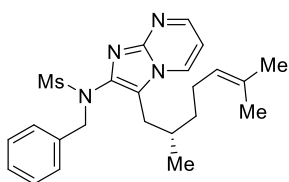
Imidazo[1,2-*a*]pyrimidine 301



Following **GP9** using ynamide **280** (64.5 mg, 0.20 mmol) and aminide **239** (41.4 mg, 0.24 mmol). After purification by flash chromatography [hexane:ethyl acetate (3:7)] compound **301** was isolated as a yellow solid (47.9 mg, 67%); mp. 140–142°C; ^1H NMR (300 MHz, CDCl_3) δ 8.52 (dd, $J = 4.1, 2.0$ Hz, 1H), 8.11 (dd, $J = 6.9, 2.0$ Hz, 1H), 7.34–7.25 (m, 2H), 7.24–7.16 (m, 3H), 6.87 (dd, $J = 6.9, 4.1$ Hz, 1H), 4.92 (s, 2H), 3.17 (s, 3H), 2.64 (t, $J = 8.0$ Hz, 2H), 1.11 (app. quin, $J = 8.0$ Hz, 2H), 1.02–0.88 (m, 2H), 0.77 (t, $J = 7.1$ Hz, 3H); ^{13}C NMR (101 MHz, CDCl_3) δ 149.4 (CH), 145.2 (C), 139.1 (C), 136.0 (C), 131.3 (CH), 129.4 (2 \times CH), 128.3 (2 \times CH), 127.9 (CH), 122.6 (C), 108.8 (CH), 54.7 (CH_2), 37.4 (CH_3), 28.7 (CH_2), 22.7 (CH_2), 21.8 (CH_2), 13.7 (CH_3); IR $\nu_{\text{max}}/\text{cm}^{-1}$ 3103, 3034, 2930, 1526, 1338, 1296, 1157, 959, 820, 744; HRMS (ES-TOF): m/z : calcd. for $\text{C}_{18}\text{H}_{23}\text{N}_4\text{O}_2\text{S}$: 359.1542 found: 359.1542 $[\text{M}+\text{H}]^+$.

Imidazo[1,2-a]pyrimidine 307

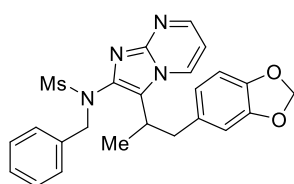
Following **GP9** using ynamide **281** (59.1 mg, 0.21 mmol) and aminide **239** (43.3 mg, 0.25 mmol). After purification by flash chromatography [hexane:ethyl acetate (3:7)] compound **307** was isolated as a yellow solid (49.3 mg, 62%); mp. 134–138 °C; ¹H NMR (300 MHz, CDCl₃) δ 8.55 (dd, *J* = 4.1, 2.0 Hz, 1H), 8.23 (dd, *J* = 6.9, 2.0 Hz, 1H), 7.33–7.17 (m, 5H), 6.91 (dd, *J* = 6.9, 4.1 Hz, 1H), 4.91 (s, 2H), 3.25–3.12 (m, 5H), 2.81 (t, *J* = 7.6 Hz, 2H), 1.60–1.45 (m, 2H); ¹³C NMR (101 MHz, CDCl₃) δ 149.8 (CH), 145.3 (C), 139.7 (C), 135.9 (C), 131.3 (CH), 129.5 (2×CH), 128.5 (2×CH), 128.1 (CH), 120.7 (C), 109.1 (CH), 54.6 (CH₂), 44.4 (CH₂), 37.4 (CH₃), 29.5 (CH₂), 18.9 (CH₂); IR ν_{max} /cm⁻¹ 3106, 2955, 2930, 2865, 1620, 1502, 1342, 1157, 1053, 731; HRMS (ES-TOF): *m/z*: calcd. for C₁₇H₂₀ClN₄O₂S: 379.0995 found: 379.0993 [M+H]⁺.

(S)-(-)-Imidazo[1,2-a]pyrimidine 308

Following **GP9** using ynamide **282** (67.7 mg, 0.20 mmol) and aminide **239** (41.6 mg, 0.24 mmol). After purification by flash chromatography [hexane:ethyl acetate (3:7)] compound **308** was isolated as a yellow oil (67.8 mg, 80%); $[\alpha]_D^{24} = -25.8$ (c 1.24, CHCl₃); ¹H-NMR (300 MHz, CDCl₃) δ 8.59–8.52 (m, 1H), 8.17 (dd, *J* = 6.9, 1.9 Hz, 1H), 7.39–7.30 (m, 2H), 7.25–7.19 (m, 3H), 6.89 (dd, *J* = 6.9, 4.1 Hz, 1H), 5.02–4.91 (m, 3H), 3.13 (s, 3H), 2.73 (dd, *J* = 15.3, 6.1, 1H), 2.48 (dd, *J* = 15.3, 6.1, 1H), 1.97–1.84 (m, 1H), 1.84–1.72 (m, 1H), 1.68 (s, 3H), 1.58 (s, 3H), 1.47–1.29 (m, 2H), 1.08–0.93 (m, 1H), 0.38 (d, *J* = 6.6, 3H); ¹³C NMR (101 MHz, CDCl₃) δ 149.3 (CH), 145.1 (C), 140.2 (C), 135.8 (C), 131.5 (C), 131.4 (CH), 129.8 (2×CH), 128.4 (2×CH), 128.0 (CH), 124.4 (CH), 121.5

(C), 108.8 (CH), 54.7 (CH₂), 37.2 (CH₃), 36.8 (CH₂), 31.5 (CH), 29.2 (CH₂), 25.7 (CH₃), 25.4 (CH₂), 19.1 (CH₃), 17.7 (CH₃); IR $\nu_{\text{max}}/\text{cm}^{-1}$ 2960, 2924, 2854, 1620, 1562, 1500, 1335, 1152, 1026, 697; HRMS (ES-TOF): m/z : calcd. for C₂₃H₃₁N₄O₂S: 427.2168 found: 427.2179 [M+H]⁺.

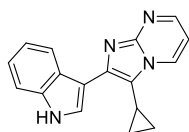
rac*-Imidazo[1,2-*a*]pyrimidine **309*



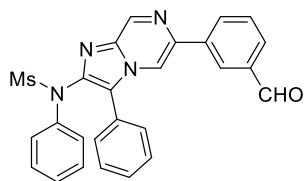
Following **GP8** using ynamide **282** (75.7 mg, 0.20 mmol) and aminide **239** (41.2 mg, 0.24 mmol). After purification by flash chromatography [hexane:ethyl acetate (3:7)] compound **309**

was isolated as a white solid (74.2 mg, 81%); mp. 194–196 °C; ¹H NMR (300 MHz, CDCl₃) δ 8.51 (dd, J = 4.1, 1.9 Hz, 1H), 7.92 (dd, J = 7.0, 1.9 Hz, 1H), 7.38–7.15 (m, 5H), 6.75 (dd, J = 7.0, 4.1 Hz, 1H), 6.70–6.62 (m, 1H), 6.49–6.39 (m, 2H), 5.90 (s, 2H), 5.04–4.83 (m, 2H), 3.42–3.27 (m, 1H), 3.22 (s, 3H), 2.58–2.46 (m, 2H), 0.98 (d, J = 7.3 Hz, 3H); ¹³C NMR (101 MHz, CDCl₃) δ 149.5 (CH), 147.7 (C), 146.2 (C), 145.1 (C), 138.6 (C), 135.6 (C), 133.1 (C), 132.3 (CH), 129.7 (2×CH), 128.5 (2×CH), 128.1 (CH), 125.6 (C), 122.1 (CH), 109.5 (CH), 108.5 (CH), 108.2 (CH), 100.8 (CH₂), 55.0 (CH₂), 39.7 (CH₂), 37.5 (CH₃), 31.4 (CH), 15.2 (CH₃); IR $\nu_{\text{max}}/\text{cm}^{-1}$ 2983, 2924, 2855, 1623, 1559, 1502, 1491, 1328, 1248, 1150, 1037, 969, 762; HRMS (ES-TOF): m/z : calcd. for C₂₄H₂₅N₄O₄S: 465.1591 found: 465.1597 [M+H]⁺.

This transformation was also performed on larger scale using ynamide **282** (1.12 g, 2.93 mmol), PicAuCl₂ (22.1 mg, 2 mol%) and aminide **239** (608.8 mg, 3.52 mmol), affording **309** (991.8 mg, 61%) after 6 h.

Imidazo[1,2-a]pyrimidine 313

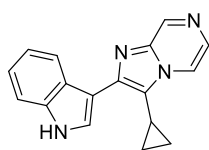
Following **G10** using alkynylindole **312a** (36.1 mg, 0.20 mmol) and aminide **239** (41.3 mg, 0.24 mmol). After purification by flash chromatography [hexane:ethyl acetate (3:7)] compound **313** was isolated as a yellow solid (38.7 mg, 71%); mp. 258–260 °C; ^1H NMR (300 MHz, DMSO- D_6) δ 11.22 (br., 1H), 8.63 (dd, $J = 6.7, 1.9$ Hz, 1H), 8.29–8.17 (m, 2H), 7.65 (d, $J = 2.6$ Hz, 1H), 7.21 (d, $J = 7.5$ Hz, 1H), 6.98–6.80 (m, 3H), 1.95–1.82 (m, 1H), 1.05–0.90 (m, 2H), 0.38–0.21 (m, 2H); ^{13}C NMR (101 MHz, DMSO D_6) δ 148.4 (CH), 147.1 (C), 141.8 (C), 136.5 (C), 132.3 (CH), 126.7 (C), 126.0 (CH), 122.2 (CH), 122.0 (CH), 119.8 (CH), 117.4 (C), 111.9 (CH), 109.3 (C), 108.5 (CH), 7.9 ($2\times\text{CH}_2$), 4.0 (CH); IR $\nu_{\text{max}}/\text{cm}^{-1}$ 3147, 3106, 2919, 2851, 1610, 1580, 1491, 1344, 1227, 765; HRMS (ES-TOF): m/z : calcd. for $\text{C}_{17}\text{H}_{15}\text{N}_4$: 275.1297 found: 275.1300 $[\text{M}+\text{H}]^+$.

5.4 Cycloaddition products for Chapter 3*Imidazo[1,2-a]pyrazine 393*

Following **GP8** using ynamide **265** (54.4 mg, 0.20 mmol) and aminide **388** (67.2 mg, 0.24 mmol). After purification by flash chromatography [hexane:ethyl acetate (7:3)] compound **393** was isolated as a white solid (79.2 mg, 84%); mp. 200–202 °C; ^1H NMR (400 MHz, CDCl_3) δ 10.10 (s, 1H), 9.26 (d, $J = 1.4$ Hz, 1H), 8.46 (d, $J = 1.4$ Hz, 1H), 8.38 (app. t, $J = 1.6$ Hz, 1H), 8.18 (app. dt, $J = 7.6, 1.6$ Hz, 1H), 7.93 (app. dt, $J = 7.6, 1.6$ Hz, 1H), 7.65 (app. t, $J = 7.6$ Hz, 1H), 7.61–7.50 (m, 5H), 7.48–7.42 (m, 2H), 7.33–7.22 (m, 3H), 3.45 (s, 3H); ^{13}C NMR (101 MHz, CDCl_3) δ 192.0 (CH), 143.4 (CH), 142.9 (C), 140.1

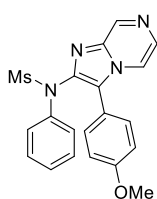
(C), 139.4 (C), 137.3 (C), 137.0 (C), 136.5 (C), 132.2 (CH), 130.1 (CH), 129.9 (CH), 129.8 (CH), 129.5 (2×CH), 129.4 (2×CH), 129.2 (2×CH), 128.0 (CH), 127.9 (2×CH), 127.3 (CH), 125.5 (C), 123.4 (C), 113.0 (CH), 39.1 (CH₃); IR $\nu_{\max}/\text{cm}^{-1}$ 3020, 2936, 1699, 1482, 1380, 1345, 1154, 965, 750; HRMS (ES-TOF): m/z : calcd. for C₂₆H₂₁N₄O₃S: 469.1334, found: 469.1336 [M+H]⁺.

Imidazo[1,2-a]pyrazine 394



Following **GP10** using alkynylindole **312a** (36.0 mg, 0.20 mmol) and aminide **380** (41.5 mg, 0.24 mmol). After purification by flash chromatography [hexane:ethyl acetate (3:7)] compound **394** was isolated as a yellow solid (20.4 mg, 38%); mp. 224–226 °C; ¹H NMR (300 MHz, CDCl₃) δ 9.09 (d, J = 1.1 Hz, 1H), 8.62 (br, 1H), 8.47–8.40 (m, 1H), 8.21 (dd, J = 4.5, 2.0 Hz, 1H), 7.92 (d, J = 4.5 Hz, 1H), 7.73 (d, J = 2.0 Hz, 1H), 7.49–7.38 (m, 1H), 7.34–7.19 (m, 2H), 2.06–1.96 (m, 1H), 1.22–1.11 (m, 2H), 0.68–0.58 (m, 2H); ¹³C NMR (101 MHz, CDCl₃) δ 142.7 (C), 142.5 (CH), 139.8 (C), 136.1 (C), 129.1 (CH), 126.5 (C), 124.8 (CH), 122.6 (CH), 121.7 (CH), 121.0 (C), 120.7 (CH), 116.5 (CH), 111.1 (CH), 110.2 (C), 7.2 (2×CH₂), 3.8 (CH); IR $\nu_{\max}/\text{cm}^{-1}$ 3150, 3120, 2931, 2863, 1618, 1576, 1492, 1380, 1117, 760; HRMS (ES-TOF): m/z : calcd. for C₁₇H₁₅N₄: 275.1297 found: 275.1293 [M+H]⁺.

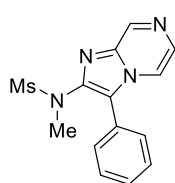
Imidazo[1,2-a]pyrazine 395



Following **GP8** using ynamide **270** (48.2 mg, 0.20 mmol) and aminide **380** (41.4 mg, 0.24 mmol). After purification by flash chromatography [hexane:ethyl acetate (7:3)] compound **395** was isolated as a white solid (55.6 mg, 71%); mp. 206–208 °C; ¹H NMR (300 MHz, CDCl₃) δ 9.13 (s, 1H), 8.03 (d, J

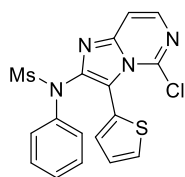
= 4.7 Hz, 1H), 7.90 (d, J = 4.7 Hz, 1H), 7.50–7.41 (m, 4H), 7.33–7.23 (m, 3H), 7.08–7.00 (m, 2H), 3.89 (s, 3H), 3.42 (s, 3H); ^{13}C NMR (101 MHz, CDCl_3) δ 160.6 (C), 143.6 (C), 142.2 (C), 140.1 (CH), 137.0 (C), 130.7 (2 \times CH), 129.8 (CH), 129.2 (2 \times CH), 127.9 (CH), 127.8 (2 \times CH), 122.9 (CH), 117.5 (C), 116.7 (C), 114.8 (2 \times CH), 55.4 (CH₃), 39.1 (CH₃); IR $\nu_{\text{max}}/\text{cm}^{-1}$ 3021, 2925, 2842, 1608, 1498, 1483, 1349, 1159, 969, 759; HRMS (ES-TOF): m/z : calcd. for $\text{C}_{20}\text{H}_{19}\text{N}_4\text{O}_3\text{S}$: 395.1178, found: 395.1184 $[\text{M}+\text{H}]^+$.

Imidazo[1,2-*a*]pyrazine 396



Following **GP8** using ynamide **264** (42.5 mg, 0.20 mmol) and aminide **380** (41.5 mg, 0.24 mmol). After purification by flash chromatography [hexane:ethyl acetate (1:9)] compound **396** was isolated as a white solid (50.4 mg, 83%); mp. 128–130 °C; ^1H NMR (300 MHz, CDCl_3) δ 9.06 (d, J = 1.4 Hz, 1H), 8.11 (dd, J = 4.7, 1.4 Hz, 1H), 7.91 (d, J = 4.7 Hz, 1H), 7.66 (d, J = 7.8 Hz, 2H), 7.60–7.46 (m, 3H), 3.25 (s, 3H), 3.25 (s, 3H); ^{13}C NMR (101 MHz, CDCl_3) δ 144.0 (CH), 142.7 (C), 137.4 (C), 130.4 (CH), 129.7 (CH), 129.5 (2 \times CH), 129.1 (2 \times CH), 125.9 (C), 122.1 (C), 116.6 (CH), 38.8 (CH₃), 37.3 (CH₃); IR $\nu_{\text{max}}/\text{cm}^{-1}$ 3060, 3030, 2928, 1620, 1489, 1472, 1380, 1154, 967, 742; HRMS (ES-TOF): m/z : calcd. for $\text{C}_{14}\text{H}_{15}\text{N}_4\text{O}_2\text{S}$: 303.0916, found: 303.0920 $[\text{M}+\text{H}]^+$.

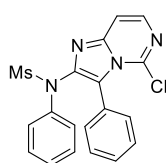
Imidazo[1,2-*c*]pyrimidine 397



Following **GP8** using ynamide **274** (55.4 mg, 0.20 mmol) and aminide **381** (49.6 mg, 0.24 mmol). After purification by flash chromatography [hexane:ethyl acetate (8:2)] compound **397** was isolated as a white solid (46.9 mg, 58%); mp. 148–150 °C; ^1H NMR (300 MHz, CDCl_3) δ 7.91 (d, J = 6.3

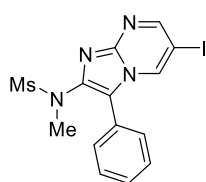
Hz, 1H), 7.57–7.53 (m, 2H), 7.29–7.26 (m, 5H), 7.11–7.07 (m, 2H), 3.34 (s, 3H); ^{13}C NMR (101 MHz, CDCl_3) δ 145.5 (C), 145.0 (C), 140.2 (C), 139.8 (C), 139.5 (CH), 137.6 (C), 133.9 (CH), 129.8 (CH), 129.1 (2 \times CH), 128.2 (2 \times CH), 128.1 (CH), 126.6 (CH), 126.3 (C), 111.7 (CH), 39.5 (CH_3); IR $\nu_{\text{max}}/\text{cm}^{-1}$ 3088, 3015, 2927, 1616, 1473, 1426, 1345, 1154, 966, 762; HRMS (ES-TOF): m/z : calcd. for $\text{C}_{17}\text{H}_{14}\text{ClN}_4\text{O}_2\text{S}_2$: 405.0247 found: 405.0240 $[\text{M}+\text{H}]^+$.

Imidazo[1,2-*c*]pyrimidine 398



Following **GP8** using ynamide **265** (54.4 mg, 0.20 mmol) and aminide **381** (50.2 mg, 0.24 mmol). After purification by flash chromatography [hexane:ethyl acetate (3:7)] compound **398** was isolated as a white solid (60.3 mg, 75%); mp. 104–106 °C; ^1H NMR (300 MHz, CDCl_3) δ 7.87 (d, J = 6.3 Hz, 1H), 7.54 (d, J = 6.3 Hz, 1H), 7.49–7.41 (m, 1H), 7.40–7.32 (m, 2H), 7.29–7.15 (m, 7H), 3.31 (s, 3H); ^{13}C NMR (101 MHz, CDCl_3) δ 144.1 (C), 143.4 (C), 140.0 (C), 138.9 (CH), 137.4 (C), 132.2 (2 \times CH), 129.4 (CH), 129.1 (2 \times CH), 128.0 (2 \times CH), 127.9 (CH), 127.6 (2 \times CH), 127.4 (C), 121.9 (C), 111.7 (CH), 39.4 (CH_3); IR $\nu_{\text{max}}/\text{cm}^{-1}$ 3068, 3023, 2929, 1616, 1586, 1484, 1377, 1155, 817, 762; HRMS (ES-TOF): m/z : calcd. for $\text{C}_{19}\text{H}_{16}\text{ClN}_4\text{O}_2\text{S}$: 399.0682 found: 399.0687 $[\text{M}+\text{H}]^+$.

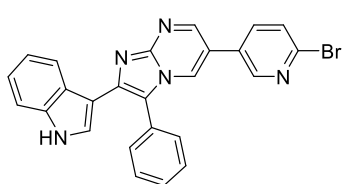
Imidazo[1,2-*a*]pyrimidine 399



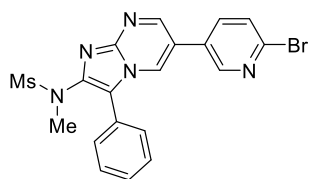
Following **GP8** using ynamide **264** (42.4 mg, 0.20 mmol) and aminide **286** (72.1 mg, 0.24 mmol). After purification by flash chromatography [hexane:ethyl acetate (3:7)] compound **399** was isolated as a white solid (73.2 mg, 85%); mp. 213–214 °C; ^1H NMR (300 MHz, CDCl_3) δ 8.67 (d, J = 2.3 Hz, 1H), 8.66 (d, J = 2.3 Hz, 1H), 7.67–7.62 (m, 2H), 7.62–7.54 (m,

2H), 7.54–7.48 (m, 1H), 3.25 (s, 3H), 3.25 (s, 3H); ^{13}C NMR (101 MHz, CDCl_3) δ 155.1 (CH), 143.4 (C), 142.4 (C), 135.6 (CH), 129.7 (CH), 129.6 (2 \times CH), 129.3 (2 \times CH), 125.9 (C), 119.7 (C), 74.7 (C), 38.8 (CH_3), 37.1 (CH_3); IR $\nu_{\text{max}}/\text{cm}^{-1}$ 3061, 3020, 2934, 1620, 1491, 1472, 1379, 1345, 1154, 968, 742; HRMS (ES-TOF): m/z : calcd. for $\text{C}_{14}\text{H}_{14}\text{N}_4\text{O}_2\text{Si}$: 428.9882, found: 428.9877 $[\text{M}+\text{H}]^+$.

Imidazo[1,2-a]pyrimidine 400

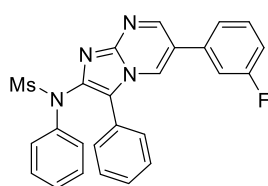


Following **GP10** using alkynylindole **312b** (43.2 mg, 0.20 mmol) and aminide **390** (79.8 mg, 0.24 mmol). After purification by flash chromatography [hexane:ethyl acetate (1:9)] compound **400** was isolated as a yellow solid (46.1 mg, 50%); mp. 220–222°C; ^1H NMR (400 MHz, $\text{DMSO}-\text{D}_6$) δ 11.28 (br., 1H), 8.90 (d, $J = 2.5$ Hz, 1H), 8.81 (d, $J = 2.4$ Hz, 1H), 8.76 (d, $J = 2.4$ Hz, 1H), 8.15 (dd, $J = 8.3, 2.5$ Hz, 1H), 8.11 (d, $J = 7.7$ Hz, 1H), 7.76 (d, $J = 8.3$ Hz, 1H), 7.71 – 7.52 (m, 5H), 7.41 (d, $J = 7.7$ Hz, 1H), 7.17 (d, $J = 2.5$ Hz, 1H), 7.13 (app. t, $J = 7.7$ Hz, 1H), 7.03 (app. t, $J = 7.7$ Hz, 1H); ^{13}C NMR (101 MHz, $\text{DMSO}-\text{D}_6$) δ 149.1 (CH), 148.4 (CH), 147.3 (C), 142.0 (C), 141.3 (C), 138.5 (CH), 136.5 (C), 131.1 (2 \times CH), 130.5 (C), 130.1 (2 \times CH), 129.5 (CH), 129.1 (C), 129.0 (CH), 128.5 (CH), 126.3 (C), 125.0 (CH), 122.1 (CH), 121.9 (CH), 120.0 (CH), 118.2 (C), 118.1 (C), 112.0 (CH), 109.1 (C); IR $\nu_{\text{max}}/\text{cm}^{-1}$ 3155, 3103, 3048, 2973, 2920, 1617, 1561, 1451, 1219, 1091, 737; HRMS (ES-TOF): m/z : calcd. for $\text{C}_{25}\text{H}_{17}^{79}\text{BrN}_5$: 466.0667 found: 466.0675 $[\text{M}+\text{H}]^+$.

Imidazo[1,2-a]pyrimidine 401

Following **GP8** using ynamide **264** (42.1 mg, 0.20 mmol) and aminide **390** (79.5 mg, 0.24 mmol). After purification by flash chromatography [hexane:ethyl acetate (7:3)] compound **401**

was isolated as a white solid (57.0 mg, 62%); mp. 182–184 °C; ^1H NMR (300 MHz, CDCl_3) δ 8.81 (d, $J = 2.5$ Hz, 1H), 8.61 (d, $J = 2.5$ Hz, 1H), 7.57 (d, $J = 2.4$ Hz, 1H), 7.76–7.69 (m, 3H), 7.68–7.50 (m, 4H), 3.31 (s, 3H), 3.31 (s, 3H); ^{13}C NMR (101 MHz, CDCl_3) δ 149.4 (CH), 148.1 (CH), 144.7 (C), 143.2 (C), 142.7 (C), 136.9 (CH), 129.7 (2 \times CH), 129.6 (CH), 129.3 (2 \times CH), 128.7 (CH), 128.5 (CH), 125.7 (C), 120.4 (C), 120.0 (C), 38.9 (CH_3), 37.1 (CH_3); *One resonance for a quaternary carbon was not visible.* IR $\nu_{\text{max}}/\text{cm}^{-1}$ 3083, 3022, 2934, 1623, 1583, 1488, 1452, 1377, 1155, 811, 764; HRMS (ES-TOF): m/z : calcd. for $\text{C}_{19}\text{H}_{17}^{79}\text{BrN}_5\text{O}_2\text{S}$: 458.0284 found: 458.0286 $[\text{M}+\text{H}]^+$.

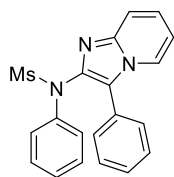
Imidazo[1,2-a]pyrimidine 402

Following **GP8** using ynamide **265** (54.2 mg, 0.20 mmol) and aminide **389** (64.2 mg, 0.24 mmol). After purification by flash chromatography [hexane:ethyl acetate (3:7)] compound **402** was

isolated as a white solid (70.4 mg, 80%); mp. 193–195 °C; ^1H NMR (300 MHz, CDCl_3) δ 8.84 (d, $J = 2.5$ Hz, 1H), 8.53 (d, $J = 2.5$ Hz, 1H), 7.62–7.41 (m, 8H), 7.32–7.21 (m, 4H), 7.21–7.10 (m, 2H), 3.46 (s, 3H); ^{13}C NMR (101 MHz, CDCl_3) δ 163.3 (d, $J_{\text{C-F}} = 248.1$ Hz, CF), 150.3 (CH), 144.7 (C), 142.4 (C), 140.4 (C), 136.0 (d, $J_{\text{C-F}} = 7.5$ Hz, C), 131.2 (d, $J_{\text{C-F}} = 8.4$ Hz, CH), 129.5 (CH), 129.4 (2 \times CH), 129.4 (2 \times CH), 129.1 (2 \times CH), 128.3 (CH), 128.0 (2 \times CH), 127.9 (CH), 125.5 (C), 123.2 (C), 122.8 (CH), 120.7 (C),

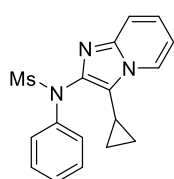
115.8 (d, $J_{C-F} = 21.0$ Hz, CH), 114.2 (d, $J_{C-F} = 22.6$ Hz, CH), 39.0 (CH₃); IR $\nu_{\max}/\text{cm}^{-1}$ 3083, 3067, 3023, 2929, 1614, 1585, 1487, 1383, 1155, 867, 762; HRMS (ES-TOF): m/z : calcd. for C₂₅H₂₀N₄O₂SF: 459.1295, found: 459.1299 [M+H]⁺.

Imidazo[1,2-a]pyridine 403



Following **GP9** using ynamide **265** (54.3 mg, 0.20 mmol) and aminide **384** (41.5 mg, 0.24 mmol). After purification by flash chromatography [hexane:ethyl acetate (3:7)] compound **403** was isolated as a yellow solid (46.9 mg, 65%); mp. 196–198 °C; ¹H NMR (300 MHz, CDCl₃) δ 8.13 (d, $J = 6.9$ Hz, 1H), 7.65 (d, $J = 9.1$ Hz, 1H), 7.59–7.38 (m, 7H), 7.32–7.15 (m, 4H), 6.80 (app. td, $J = 6.9, 1.0$ Hz, 1H), 3.42 (s, 3H); ¹³C NMR (101 MHz, CDCl₃) δ 142.3 (C), 140.8 (C), 140.4 (C), 129.5 (2×CH), 129.0 (2×CH), 129.0 (2×CH), 128.9 (CH), 127.6 (2×CH), 127.4 (CH), 127.1 (C), 125.2 (CH), 123.8 (CH), 121.4 (C), 118.1 (CH), 113.0 (CH), 39.1 (CH₃); IR $\nu_{\max}/\text{cm}^{-1}$ 3096, 3028, 2928, 1612, 1587, 1490, 1378, 1149, 803, 769; HRMS (ES-TOF): m/z : calcd. for C₂₀H₁₈N₃O₂S: 364.1120 found: 364.1123 [M+H]⁺.

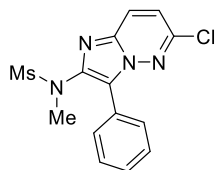
Imidazo[1,2-a]pyridine 404



Following **GP8** using ynamide **279** (47.3 mg, 0.20 mmol) and aminide **384** (41.4 mg, 0.24 mmol). After purification by flash chromatography [hexane:ethyl acetate (1:1)] compound **404** was isolated as a white solid (35.5 mg, 51%); mp. 192–194 °C; ¹H NMR (300 MHz, CDCl₃) δ 8.19 (d, $J = 6.9$ Hz, 1H), 7.74–7.64 (m, 2H), 7.58 (d, $J = 9.1$ Hz, 1H), 7.42–7.31 (m, 2H), 7.30–7.18 (m, 2H), 6.88 (app. td, $J = 6.9$ Hz, 1H), 3.36 (s, 3H), 1.67–1.55 (m, 1H), 1.11–0.99 (m, 2H), 0.94–0.84 (m, 2H); ¹³C NMR (101 MHz, CDCl₃) δ 141.5 (C), 141.0 (C), 140.6 (C), 129.1 (2×CH), 127.5 (2×CH), 127.3 (CH), 124.6 (CH), 123.9 (CH), 120.9 (C), 117.7

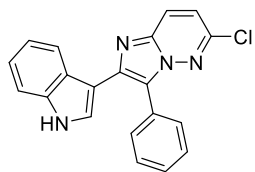
(CH), 112.6 (CH), 39.0 (CH₃), 5.0 (2×CH₂), 2.8 (CH); IR $\nu_{\text{max}}/\text{cm}^{-1}$ 3105, 3047, 2927, 1574, 1412, 1348, 1154, 996, 960, 754; HRMS (ES-TOF): m/z : calcd. for C₁₇H₁₈N₃O₂S: 328.1123 found: 328.1128 [M+H]⁺.

Imidazo[1,2-*b*]pyridazine 405



Following **GP8** using ynamide **264** (42.4 mg, 0.20 mmol) and aminide **382** (50.4 mg, 0.24 mmol). After purification by flash chromatography [hexane:ethyl acetate (3:7)] compound **405** was isolated as a white solid (55.4 mg, 82%); mp. 222–224 °C; ¹H NMR (300 MHz, CDCl₃) δ 8.02–7.95 (m, 2H), 7.87 (d, J = 9.4 Hz, 1H), 7.58–7.49 (m, 2H), 7.49–7.40 (m, 1H), 7.15 (d, J = 9.4 Hz, 1H), 3.26 (s, 3H), 3.26 (s, 3H); ¹³C NMR (101 MHz, CDCl₃) δ 147.3 (C), 142.0 (C), 134.9 (C), 129.1 (CH), 128.8 (2×CH), 128.7 (2×CH), 126.9 (CH), 126.0 (C), 124.5 (C), 119.6 (CH), 38.6 (CH₃), 37.7 (CH₃); IR $\nu_{\text{max}}/\text{cm}^{-1}$ 3096, 3030, 2942, 1578, 1490, 1396, 1241, 1148, 894, 769; HRMS (ES-TOF): m/z : calcd. for C₁₄H₁₄ClN₄O₂S: 337.0526 found: 337.0529 [M+H]⁺.

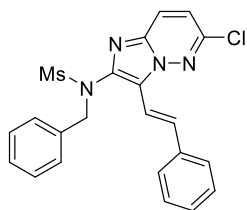
Imidazo[1,2-*b*]pyridazine 406



Following **GP10** using alkynyndole **312b** (43.4 mg, 0.20 mmol) and aminide **382** (49.6 mg, 0.24 mmol). After purification by flash chromatography [hexane:ethyl acetate (1:1)] compound **406** was isolated as a yellow solid (48.9 mg, 71%); mp. 206–208 °C; ¹H NMR (300 MHz, DMSO-*d*₆) δ 11.31 (br., 1H), 8.27 (d, J = 9.4 Hz, 1H), 8.08 (d, J = 7.9 Hz, 1H), 7.69–7.48 (m, 5H), 7.41 (d, J = 8.0 Hz, 1H), 7.37 (d, J = 9.4 Hz, 1H), 7.18 (d, J = 2.7 Hz, 1H), 7.13 (app. t, J = 7.9 Hz, 1H), 7.02 (app. t, J = 8.0 Hz, 1H); ¹³C NMR (101 MHz, DMSO-*d*₆) δ 145.2 (C), 141.0 (C), 137.0 (C), 136.1 (C), 130.4 (2×CH), 128.9 (2×CH),

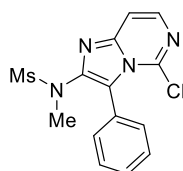
128.7 (CH), 126.4 (C), 125.7 (CH), 124.5 (C), 123.3 (CH), 121.7 (C), 121.2 (CH), 119.5 (CH), 118.0 (CH), 111.6 (CH), 108.5 (C), 79.1 (CH); IR $\nu_{\max}/\text{cm}^{-1}$ 3174, 3100, 3070, 3008, 1588, 1444, 1218, 808, 745; HRMS (ES-TOF): m/z : calcd. for $\text{C}_{20}\text{H}_{14}\text{ClN}_4$: 345.0907 found: 345.0908 $[\text{M}+\text{H}]^+$.

Imidazo[1,2-b]pyridazine 407



Following **GP8** using ynamide **278** (62.2 mg, 0.20 mmol) and aminide **382** (50.4 mg, 0.24 mmol). After purification by flash chromatography [hexane:ethyl acetate (1:4)] compound **407** was isolated as a white solid (73.1 mg, 83%); mp. 204–206 °C; ^1H NMR (300 MHz, CDCl_3) δ 7.85 (d, $J = 16.7$ Hz, 1H), 7.84 (d, $J = 9.4$ Hz, 1H), 7.48 (d, $J = 7.1$ Hz, 2H), 7.36 (app. t, $J = 7.1$ Hz, 2H), 7.33–7.27 (m, 3H), 7.24–7.15 (m, 3H), 7.10 (d, $J = 9.4$ Hz, 1H), 7.04 (d, $J = 16.7$ Hz, 1H), 4.94 (s, 2H), 3.19 (s, 3H); ^{13}C NMR (101 MHz, CDCl_3) δ 147.3 (C), 140.7 (C), 137.2 (C), 135.5 (C), 135.2 (C), 132.1 (CH), 129.0 (2 \times CH), 128.6 (2 \times CH), 128.5 (2 \times CH), 128.2 (CH), 128.1 (CH), 126.9 (2 \times CH), 126.5 (CH), 125.1 (C), 119.1 (CH), 111.7 (CH), 55.2 (CH_2), 38.3 (CH_3); IR $\nu_{\max}/\text{cm}^{-1}$ 3103, 3034, 2929, 1527, 1338, 1296, 1157, 966, 820, 744; HRMS (ES-TOF): m/z : calcd. for $\text{C}_{22}\text{H}_{20}\text{ClN}_4\text{O}_2\text{S}$: 439.0995 found: 439.0991 $[\text{M}+\text{H}]^+$.

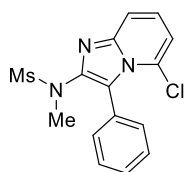
Imidazo[1,2-c]pyrimidine 408



Following **GP9** using ynamide **264** (42.4 mg, 0.20 mmol) and aminide **381** (50.4 mg, 0.24 mmol) for 1.5 h. After purification by flash chromatography [hexane:ethyl acetate (3:7)] compound **408** was isolated as a white solid (64.2 mg, 95%); mp. 110–112 °C; ^1H NMR (300 MHz, CDCl_3) δ 7.87 (d, $J = 6.3$ Hz, 1H), 7.54–7.44 (m, 6H), 3.15 (s, 3H), 3.13 (s, 3H); ^{13}C NMR (101

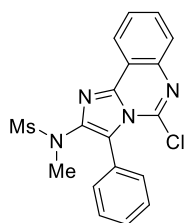
MHz, CDCl₃) δ 144.1 (C), 143.5 (C), 139.1 (CH), 137.5 (C), 132.2 (2 \times CH), 129.6 (CH), 127.8 (2 \times CH), 127.5 (C), 121.9 (C), 111.5 (CH), 38.5 (CH₃), 37.8 (CH₃); IR $\nu_{\max}/\text{cm}^{-1}$ 2929, 1617, 1566, 1478, 1342, 1263, 1150, 964, 911; HRMS (ES-TOF): m/z : calcd. for C₁₄H₁₄N₄O₂SCl: 337.0526 found: 337.0538 [M+H]⁺.

Imidazo[1,2-*a*]pyridine 417



Following **GP9** using ynamide **264** (42.0 mg, 0.20 mmol) and aminide **411** (49.5 mg, 0.24 mmol) for 24 h. After purification by flash chromatography [hexane:ethyl acetate (1:4)] compound **417** was isolated as a white solid (47.2 mg, 70%); mp. 178–180 °C; ¹H NMR (300 MHz, CDCl₃) δ 7.59 (dd, J = 9.0, 1.1 Hz, 1H), 7.56–7.50 (m, 2H), 7.49–7.42 (m, 3H), 7.22 (dd, J = 9.0, 7.3 Hz, 1H), 6.88 (dd, J = 7.3, 1.1 Hz, 1H), 3.19 (s, 3H), 3.17 (s, 3H); ¹³C NMR (101 MHz, CDCl₃) δ 144.1 (C), 142.2 (C), 132.2 (2 \times CH), 129.0 (CH), 128.8 (C), 127.6 (C), 127.4 (2 \times CH), 125.1 (CH), 116.4 (CH), 114.6 (CH), 38.7 (CH₃), 37.6 (CH₃); *One resonance for a quaternary carbon was not visible.* IR $\nu_{\max}/\text{cm}^{-1}$ 3071, 3005, 2922, 1630, 1561, 1488, 1338, 1146, 1098, 957; HRMS (ES-TOF): m/z : calcd. for C₁₅H₁₅N₃O₂SCl: 336.0574 found: 336.0573 [M+H]⁺.

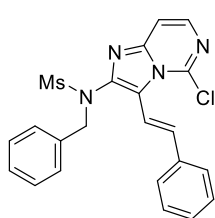
Imidazo[1,2-*c*]quinazoline 418



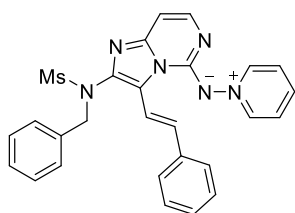
Following **GP9** using ynamide **264** (41.6 mg, 0.20 mmol) and aminide **412** (62.0 mg, 0.24 mmol) for 18 h. After purification by flash chromatography [hexane:ethyl acetate (7:3)] compound **418** was isolated as a white solid (56.8 mg, 73%); mp. 267–269 °C; ¹H NMR (300 MHz, CDCl₃) δ 8.50 (dd, J = 7.3, 1.8 Hz, 1H), 7.87 (dd, J = 7.5, 1.4 Hz, 1H), 7.73 (app. td, J = 7.3, 1.4 Hz, 1H), 7.67 (app. td, J = 7.5, 1.8 Hz, 1H), 7.58–7.51 (m, 2H),

7.51–7.45 (m, 3H), 3.22 (s, 3H), 3.17 (s, 3H); ^{13}C NMR (101 MHz, CDCl_3) δ 142.7 (C), 141.6 (C), 140.4 (C), 134.6 (C), 132.0 (2 \times CH), 131.0 (CH), 129.5 (CH), 128.8 (CH), 127.9 (2 \times CH), 127.8 (C), 127.5 (CH), 124.1 (C), 123.0 (CH), 118.2 (C), 38.7 (CH_3), 37.9 (CH_3); IR $\nu_{\text{max}}/\text{cm}^{-1}$ 2927, 1618, 1603, 1368, 1341, 1251, 1151, 949; HRMS (ES-TOF): m/z : calcd. for $\text{C}_{18}\text{H}_{16}\text{N}_4\text{O}_2\text{SCl}$: 387.0682 found: 387.0678 $[\text{M}+\text{H}]^+$.

Imidazo[1,2-c]pyrimidine 423



Following **GP9** using ynamide **278** (200.1 mg, 0.64 mmol) and aminide **381** (159.8 mg, 0.72 mmol). After purification by flash chromatography [hexane:ethyl acetate (3:2)] compound **423** was isolated as a white solid (234.8 mg, 84%); mp. 150–152 °C; ^1H NMR (400 MHz, CDCl_3) δ 7.79 (d, J = 6.3 Hz, 1H), 7.41–7.36 (m, 5H), 7.36–7.29 (m, 1H), 7.25–7.20 (m, 1H), 7.19–7.12 (m, 4H), 7.00 (d, J = 16.2 Hz, 1H), 6.95 (d, J = 16.2 Hz, 1H), 4.82 (s, 2H), 3.23 (s, 3H); ^{13}C NMR (101 MHz, CDCl_3) δ 144.1 (C), 140.7 (C), 139.1 (CH), 137.6 (C), 136.6 (C), 135.9 (CH), 134.7 (C), 129.4 (2 \times CH), 128.7 (2 \times CH), 128.4 (CH), 128.3 (2 \times CH), 128.1 (CH), 126.9 (2 \times CH), 122.7 (C), 113.0 (CH), 111.5 (CH), 55.1 (CH_2), 38.7 (CH_3); IR $\nu_{\text{max}}/\text{cm}^{-1}$ 3031, 2924, 1621, 1478, 1344, 1217, 1150, 1052, 967; HRMS (ES-TOF): m/z : calcd. for $\text{C}_{22}\text{H}_{19}\text{N}_4\text{O}_2\text{SClNa}$: 461.0811 found: 461.0815 $[\text{M}+\text{Na}]^+$.

Aminide 424

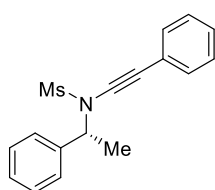
Following **GP5** using *N*-aminopyridinium iodide (87.0 mg, 0.39 mmol) and imidazo[1,2-*c*]pyrimidine **423** (180.6 mg, 0.41 mmol) and potassium carbonate (150.1 mg, 1.09 mmol) for 3 h. After purification by flash chromatography [CH_2Cl_2 :MeOH

(9:1)] aminide **424** was isolated as a bright orange solid (190.2 mg, 98%); mp: 266–268 °C; ^1H NMR (400 MHz, CDCl_3) δ 8.76 (d, J = 6.1 Hz, 2H), 7.97 (d, J = 16.6 Hz, 1H), 7.88 (t, J = 7.7 Hz, 1H), 7.66 (app. t, J = 7.2 Hz, 2H), 7.38 (d, J = 7.4 Hz, 2H), 7.36–7.26 (m, 5H), 7.24–7.16 (m, 5H), 6.56 (d, J = 6.3 Hz, 1H), 4.91 (s, 2H), 3.26 (s, 3H); ^{13}C NMR (101 MHz, CDCl_3) δ 155.2 (C), 145.4 (C), 143.4 (2 \times CH), 140.5 (CH), 138.6 (C), 138.2 (C), 136.5 (CH), 135.6 (C), 129.5 (2 \times CH), 129.1 (CH), 128.3 (2 \times CH), 128.1 (2 \times CH), 127.8 (CH), 126.8 (CH), 126.6 (2 \times CH), 126.5 (2 \times CH), 121.9 (C), 117.8 (CH), 99.3 (CH), 55.0 (CH_2), 38.7 (CH_3); IR $\nu_{\text{max}}/\text{cm}^{-1}$ 3130, 3014, 1572, 1498, 1352, 1183, 1074, 957, 1052, 864, 795; HRMS (ES-TOF): m/z : calcd. for $\text{C}_{27}\text{H}_{25}\text{N}_6\text{O}_2\text{S}$: 497.1760, found: 497.1758 $[\text{M}+\text{H}]^+$.

5.4 Precursors for Chapter 4

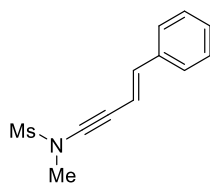
5.4.1 Preparation of ynamides

Ynamides **537** (Dr Raju Jannapureddy, UoB), **542** and **543** (Joshua Priest, UoB) were prepared and characterised by other members of the Davies Group.

(*R*)-*N*-(1-Phenylethyl)-*N*-(phenylethynyl)methanesulfonamide (538)

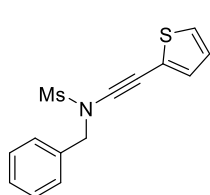
Following **GP3** using (*R*)-*N*-(1-Phenylethyl)methanesulfonamide (1.00 g, 5.0 mmol) and (bromoethynyl)benzene (10.8 g, 6.0 mmol).

After purification by flash chromatography [hexane:ethyl acetate (9:1)] ynamide **538** was isolated as a white solid (0.79 g, 53%); mp: 60–62 °C (lit.^{34b} 62–64 °C); ¹H NMR (300 MHz, CDCl₃) δ 7.56–7.50 (m, 2H), 7.47–7.29 (m, 8H), 5.23 (q, *J* = 7.1 Hz, 1H), 2.75 (s, 3H), 1.78 (d, *J* = 7.1 Hz, 3H); IR ν_{max} /cm⁻¹ 2988, 2924, 2236, 1354, 1162, 962, 798, 694; Analytical data matches that reported in the literature.^{34b}

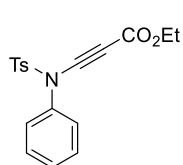
(*E*)-*N*-Methyl-*N*-(4-phenylbut-3-en-1-yn-1-yl)methanesulfonamide (539)

Following **GP3** using *N*-methylmethanesulfonamide (0.57 g, 5.1 mmol) and (*E*)-(4-bromobut-1-en-3-yn-1-yl)benzene (1.19 g, 6.3 mmol). After purification by flash chromatography [hexane:ethyl

acetate (4:1)] ynamide **539** was isolated as a yellow solid (691.3 mg, 60%); ¹H NMR (300 MHz, CDCl₃) δ 7.36–7.25 (m, 5H), 6.87 (d, *J* = 16.0 Hz, 1H), 6.22 (d, *J* = 16.0 Hz, 1H), 3.24 (s, 3H), 3.08 (s, 3H); ¹³C NMR (101 MHz, CDCl₃) δ 140.1 (CH), 136.2 (C), 128.7 (2×CH), 128.5 (CH), 126.1 (2×CH), 107.1 (CH), 84.9 (C), 69.1 (C), 39.2 (CH₃), 36.9 (CH₃); IR ν_{max} /cm⁻¹ 3034, 2941, 2250, 1431, 1279, 1160, 964, 755; Analytical data matches that reported in the literature.¹²⁰

***N*-Benzyl-*N*-(thiophen-2-ylethynyl)methanesulfonamide (**540**)**

Following **GP1** using *N*-benzylmethanesulfonamide (0.26 g, 1.3 mmol) and 2-(2,2-dibromovinyl)thiophene (0.54 g, 2.0 mmol). After purification by flash chromatography [hexane:ethyl acetate (9:1)] ynamide **540** was isolated as a pale yellow solid (342.0 mg, 87%); mp: 72–74 °C; ¹H NMR (300 MHz, CDCl₃) δ 7.49–7.46 (m, 2H), 7.43–7.37 (m, 3H), 7.28 (dd, *J* = 5.2, 1.1 Hz, 1H), 7.19 (dd, *J* = 3.6, 1.1 Hz, 1H), 6.97 (dd, *J* = 5.2, 3.6 Hz, 1H), 4.72 (s, 2H), 2.93 (s, 3H); ¹³C NMR (101 MHz, CDCl₃) δ 134.6 (CH), 133.4 (C), 129.1 (2×CH), 129.0 (2×CH), 128.9 (CH), 128.2 (CH), 127.2 (CH), 122.6 (C), 85.7 (C), 65.0 (C), 56.2 (CH₂), 39.4 (CH₃); IR ν_{max} /cm⁻¹ 3016, 1363, 1215, 1163, 1007, 962, 748; HR-MS (EI-TOF): *m/z*: calcd. for C₁₄H₁₃NO₂S₂: 291.0388 found: 291.0386 [M]⁺.

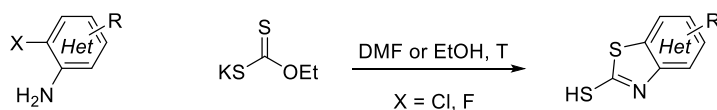
Ethyl 3-((4-methyl-*N*-phenylphenyl)sulfonamido)propiolate (**541**)

Following a reported procedure,^{34b} *n*-BuLi (7.80 mL, 8.3 mmol) was added dropwise to a solution of *N*-(2,2-dichlorovinyl)-4-methyl-*N*-phenylbenzenesulfonamide (1.29 g, 3.8 mmol) in THF (60 mL) at -78 °C. After stirring for 30 min. at -78 °C the reaction mixture was allowed to reach -40 °C and stirred for additional 30 min. Ethyl 2-chloroacetate (1.44 mL, 15.1 mmol) was added and the mixture moved to an ice-cooled bath for 30 min. The mixture was poured into a saturated aqueous solution of NH₄Cl (100 mL) and extracted with ethyl acetate (3×50 mL), dried over MgSO₄, filtered-off and concentrated under reduced pressure. After purification by flash chromatography [hexane:ethyl acetate (4:1)] ynamide **541** was isolated as a white solid (0.82 g, 63%); mp: 117–119 °C (lit.^{34b} 117–119 °C); ¹H NMR (300 MHz, CDCl₃) δ 7.63 (d, *J* = 8.3 Hz, 2H), 7.39–7.29 (m, 5H), 7.23–7.16 (m,

2H), 4.23 (q, $J = 7.1$ Hz, 2H), 2.45 (s, 3H), 1.30 (t, $J = 7.1$ Hz, 3H); IR $\nu_{\text{max}}/\text{cm}^{-1}$ 2966, 2856, 2212, 1702, 1607, 1592, 1515, 1379, 1236, 1119; Analytical data matches that reported in the literature.^{34b}

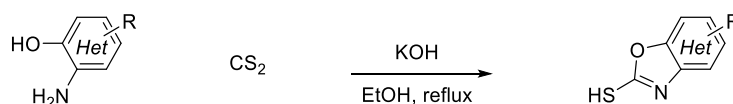
5.4.2 Preparation of precursors for the formation of aminides

General Procedure 11 (GP11)



Adapted from literature procedures.^{113a,113d,121} A mixture of 2-halo(hetero)aryl amine (1.0 eq.) and potassium ethyl xanthate (2.2 eq.) in DMF or EtOH [1.55 M relative to the amount of 2-halo(hetero)aryl amine] was stirred at the indicated temperature for the given time. Subsequently, the mixture was allowed to cool to room temperature. Water (10 mL) and $\text{HCl}_{(\text{aq})}$ [1 M, 20 mL] were then added, precipitating a solid. The suspension was stirred for an additional 30 min, and then filtered off. The resulting cake was washed with water before being dissolved in ethyl acetate, dried over MgSO_4 , filtered off and concentrated under reduced pressure to afford the desired product which was used without further purification in the next step.

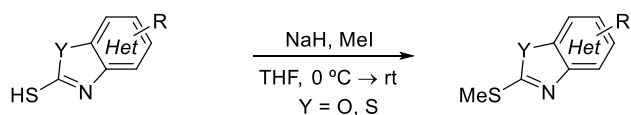
General Procedure 12 (GP12)



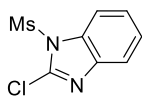
Adapted from literature procedures.^{113a,122} Ground potassium hydroxide (1.5 eq.) was added to a solution of the corresponding 2-hydroxy(hetero)aryl amine (1.0 eq.) in ethanol [0.5 M relative to the amount of 2-hydroxy(hetero)aryl amine]. Carbon disulfide

(8.0 eq.) was added and the reaction mixture stirred at reflux for the given time. Subsequently, the solution was allowed to cool to room temperature and the solvent was removed under reduced pressure. The residue was dissolved in water and neutralised with acetic acid, precipitating a solid. This was filtered off and the resulting cake was washed with water, dissolved in ethyl acetate, dried over MgSO_4 , filtered off and concentrated under reduced pressure, to afford the desired product which was used without further purification in the next step.

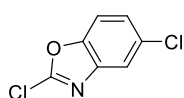
General Procedure 13 (GP13)



Adapted from literature procedures.^{113d,122} A mixture of benzo(thia/oxa)zole-2-thiol or aza-analogue (1.0 eq.) in dry THF [0.25 M] was cooled down into an ice-bath before the portionwise addition of sodium hydride (60% in mineral oil, 1.1 eq.) or potassium carbonate (1.1 eq.) over 10 min. The reaction mixture was stirred for 30 min, before the dropwise addition of methyl iodide (1.2 eq.). The cooling bath was removed and the solution stirred for 8 h at room temperature. The mixture was quenched with $\text{NH}_4\text{Cl}_{(\text{aq})}$ (sat.), and the resulting mixture was extracted with ethyl acetate (2×15 mL), washed with brine (10 mL), dried over MgSO_4 , filtered off and concentrated under reduced pressure to afford the desired product which was used without further purification in the next step unless otherwise specified.

2-Chloro-1-(methylsulfonyl)-1H-benzo[d]imidazole (442)

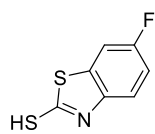
A suspension of 2-chlorobenzimidazole (0.40 g, 2.6 mmol) and sodium carbonate (0.41 g, 3.9 mmol) in dry DMF (5 mL) was stirred at 0 °C for 5 min before the dropwise addition of mesyl chloride (0.22 mL, 2.9 mmol). The mixture was stirred at room temperature for 2 h. Water (5 mL) was then added precipitating a white solid that was filtered off and washed with water (10 mL). The air-dried residue was purified by flash chromatography [hexane:ethyl acetate (4:1)], to afford compound **442** as a white solid (348.1 mg, 58%); mp. 138–140 °C; ^1H NMR (300 MHz, CDCl_3) δ 7.98–7.91 (m, 1H), 7.77–7.70 (m, 1H), 7.47–7.38 (m, 2H), 3.43 (s, 3H); ^{13}C NMR (101 MHz, CDCl_3) δ 140.8 (C), 137.9 (C), 133.7 (C), 125.8 (CH), 125.4 (CH), 120.1 (CH), 113.6 (CH), 42.7 (CH_3); IR $\nu_{\text{max}}/\text{cm}^{-1}$ 3000, 2917, 1500, 1446, 1371, 1229, 1143, 1038, 967; HRMS (ES-TOF): m/z : calcd. for $\text{C}_8\text{H}_8\text{N}_2\text{O}_2\text{SCl}$: 230.9995 found: 230.9987 $[\text{M}+\text{H}]^+$.

2,5-Dichlorobenzo[d]oxazole (471)

Following a literature procedure,¹¹² a suspension of 5-chloro-2-mercaptobenzoxazole (0.50 g, 2.7 mmol) in POCl_3 (2.20 mL, 24.0 mmol) was stirred at room temperature for 5 min. PCl_5 (0.66 g, 3.2 mmol) and CH_2Cl_2 (2.2 mL) were then added and the reaction mixture was stirred for 1.5 h. The mixture was slowly quenched over an ice-cooled solution of Na_2CO_3 (sat.) until no further gas was evolved. The mixture was extracted with CH_2Cl_2 (2×20 mL) and the combined organic extracts were washed with brine (10 mL), dried over MgSO_4 , filtered off and concentrated under reduced pressure. Compound **471** was isolated after flash chromatography [hexane: CH_2Cl_2 (7:3)] as a white solid (100.5 mg, 20%); ^1H NMR (300

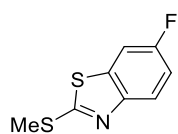
MHz, CDCl₃) δ 7.67 (d, J = 2.1 Hz, 1H), 7.44 (d, J = 8.8 Hz, 1H), 7.34 (dd, J = 8.8, 2.1 Hz, 1H); ¹³C NMR (101 MHz, CDCl₃) δ 152.3 (C), 150.1 (C), 142.1 (C), 130.8 (C), 125.9 (CH), 119.8 (CH), 111.2 (CH); IR $\nu_{\text{max}}/\text{cm}^{-1}$ 3150, 3053, 1767, 1619, 1478, 1298, 1259, 1151; HRMS (EI-TOF): m/z : calcd. for C₇H₃NOCl₂: 186.9592 found: 186.9593 [M]⁺. Analytical data matches that reported in the literature.¹²³

6-Fluoro-2-mercaptobenzothiazole (478)



Following **GP11**, using 2,4-difluoroaniline (1.01 mL, 10.0 mmol) and potassium ethyl xanthate (3.5 g, 22.0 mmol) in DMF (6.5 mL) at 95 °C for 4 h. Compound **478** was isolated as a pale pink solid (1.54 g, 83%); mp. 218–220 °C; ¹H NMR (300 MHz, DMSO-d₆) δ 13.82 (s, 1H), 7.66 (ddd, J = 8.4, 2.2, 0.6 Hz, 1H), 7.31–7.24 (m, 2H); ¹³C NMR (101 MHz, DMSO-d₆) δ 190.4 (C), 159.6 (d, $J_{\text{C-F}}$ = 241.3 Hz, C), 138.5 (C), 131.2 (d, $J_{\text{C-F}}$ = 11.1 Hz, C), 115.2 (d, $J_{\text{C-F}}$ = 24.6 Hz, CH), 113.8 (d, $J_{\text{C-F}}$ = 8.9 Hz, CH), 109.3 (d, $J_{\text{C-F}}$ = 27.7 Hz, CH). Analytical data matches that reported in the literature.¹²¹

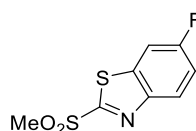
6-Fluoro-2-(methylthio)benzo[d]thiazole (479)



Following **GP13**, compound **478** (1.64 g, 8.1 mmol), methyl iodide (0.60 mL, 8.9 mmol) and sodium hydride (0.36 g, 9.7 mmol) in dry THF (32 mL) for 9 h. Compound **479** was isolated as an orange solid (1.60 g, 99%); ¹H NMR (300 MHz, DMSO-d₆) δ 7.96 (dd, J = 8.7, 2.7 Hz, 1H), 7.86 (dd, J = 8.9, 4.9 Hz, 1H), 7.33 (app. td, J = 9.0, 2.7 Hz, 1H), 2.79 (s, 3H); ¹³C NMR (101 MHz, DMSO-d₆) δ 168.3 (C), 159.4 (d, $J_{\text{C-F}}$ = 241.8 Hz, C), 150.2 (C), 136.2 (d, $J_{\text{C-F}}$ = 12.0 Hz, C), 122.5 (d, $J_{\text{C-F}}$ = 9.4 Hz, CH), 115.0 (d, $J_{\text{C-F}}$ = 24.6 Hz, CH), 108.9 (d,

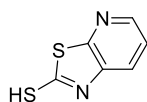
$J_{C-F} = 27.6$ Hz, CH), 16.0 (CH₃); IR $\nu_{\max}/\text{cm}^{-1}$ 2924, 1853, 1596, 1567, 1441, 1189, 1005, 903, 809. Analytical data matches that reported in the literature.^{113d}

6-Fluoro-2-(methylsulfonyl)benzo[d]thiazole (481)



Following a literature procedure,¹¹⁴ H₂O_{2(aq)} (30%, 0.16 mL, 2.0 mmol) was added over a mixture of compound **479** (200.1 mg, 1.0 mmol) and cyanuric chloride (184.4 mg, 1.0 mmol) in acetonitrile (5 mL). The mixture was stirred at room temperature for 5 h. Water (10 mL) was then added to the mixture followed by extraction with ethyl acetate (4×5 mL). The combined organic extracts were dried over MgSO₄, filtered and concentrated under reduced pressure. Purification by flash chromatography [hexane:ethyl acetate (7:3)] afforded compound **481** as a white solid (123.5 mg, 53%); mp. 134–136 °C; ¹H NMR (300 MHz, CDCl₃) δ 8.01 (dd, $J = 9.0, 4.7$ Hz, 1H), 7.69 (dd, $J = 7.9, 2.5$ Hz, 1H), 7.31 (app. td, $J = 8.9, 2.5$ Hz, 1H), 3.07 (s, 3H); ¹³C NMR (101 MHz, CDCl₃) δ 178.0 (C), 160.9 (d, $J_{C-F} = 248.9$ Hz, C), 159.7 (C), 150.5 (C), 137.2 (d, $J_{C-F} = 11.2$ Hz, C), 125.2 (d, $J_{C-F} = 9.6$ Hz, CH), 116.1 (d, $J_{C-F} = 25.1$ Hz, CH), 108.6 (d, $J_{C-F} = 26.9$ Hz, CH), 43.2 (CH₃); IR $\nu_{\max}/\text{cm}^{-1}$ 3062, 1600, 1503, 1468, 1449, 1187, 761; HRMS (ES-TOF): m/z : calcd. for C₈H₇NO₂FS₂: 231.9902 found: 231.9907 [M+H]⁺.

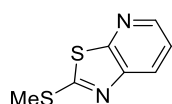
Thiazolo[5,4-*b*]pyridine-2-thiol (493)



Following **GP11**, 3-amino-2-chloropyridine (1.28 g, 10.0 mmol) and potassium ethyl xanthate (3.5 g, 21.9 mmol) were stirred in DMF (6.5 mL) at 130 °C for 24 h, to afford compound **493** as a beige solid (1.55 g, 92%); ¹H NMR (300 MHz, DMSO-*d*₆) δ 13.95 (br., 1H), 8.41 (dd, $J = 4.8, 1.4$ Hz, 1H), 7.63 (dd, $J = 8.2, 1.4$ Hz, 1H), 7.43 (dd, $J = 8.2, 4.8$ Hz, 1H); ¹³C NMR (101 MHz, DMSO-*d*₆) δ

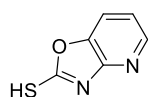
189.2 (C), 151.8 (C), 146.1 (CH), 136.7 (C), 122.8 (CH), 119.9 (CH); IR $\nu_{\max}/\text{cm}^{-1}$ 3080, 2536, 1594, 1520, 1391, 1300, 1029; Analytical data matches that reported in the literature.¹²²

2-(Methylthio)thiazolo[5,4-*b*]pyridine (497)

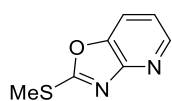


Following **GP13**, compound **493** (1.20 g, 7.1 mmol), methyl iodide (0.53 mL, 8.6 mmol) and sodium hydride (0.31 g, 7.9 mmol) were stirred in dry THF (32 mL) for 24 h, affording compound **497** as an orange solid (1.15 g, 88%); ¹H NMR (300 MHz, DMSO-*d*₆) δ 8.49 (dd, *J* = 4.7, 1.5 Hz, 1H), 8.22 (dd, *J* = 8.2, 1.5 Hz, 1H), 7.53 (dd, *J* = 8.2, 4.7 Hz, 1H), 2.81 (s, 3H); ¹³C NMR (101 MHz, DMSO) δ 169.4 (C), 158.2 (C), 146.4 (C), 146.3 (CH), 128.5 (CH), 122.3 (CH), 15.5 (CH₃); IR $\nu_{\max}/\text{cm}^{-1}$ 3049, 2922, 2852, 1552, 1433, 1374, 1216, 1006; Analytical data matches that reported in the literature.¹²²

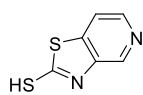
Oxazolo[4,5-*b*]pyridine-2-thiol (494)



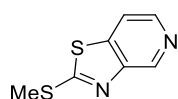
Following **GP12**, 2-amino-3-hydroxypyridine (2.20 g, 20.0 mmol), potassium hydroxide (2.00 g, 29.0 mmol) and carbon disulfide (9.60 mL, 160.0 mmol) in ethanol (40 mL) were stirred under reflux for 8 h to afford compound **494** as a beige solid (2.12 g, 70%); mp. 254–256 °C; ¹H NMR (300 MHz, DMSO-*d*₆) δ 14.53 (br., 1H), 8.23 (dd, *J* = 5.2, 1.3 Hz, 1H), 7.88 (dd, *J* = 8.1, 1.3 Hz, 1H), 7.27 (dd, *J* = 8.1, 5.2 Hz, 1H); ¹³C NMR (101 MHz, DMSO-*d*₆) δ 181.8 (C), 147.5 (C), 144.7 (CH), 142.1 (C), 119.6 (CH), 117.5 (CH); IR $\nu_{\max}/\text{cm}^{-1}$ 3048–2570 (br), 1631, 1607, 1481, 1430, 1366; 1248, 1134. Analytical data matches that reported in the literature.¹²²

2-(Methylthio)oxazolo[4,5-b]pyridine (498)

Following a modification of **GP13**, compound **494** (2.00 g, 13.2 mmol), methyl iodide (0.98 mL, 15.8 mmol) and potassium carbonate (1.8 g, 13.2 mmol) were stirred in dry DMF (33 mL) for 1 h. After purification by flash chromatography [hexane:ethyl acetate (3:2)] compound **498** was isolated as a white solid (1.73 g, 79%); mp. 55–57 °C; ^1H NMR (300 MHz, CDCl_3) δ 8.41 (dd, $J = 5.0, 1.4$ Hz, 1H), 7.65 (dd, $J = 8.1, 1.4$ Hz, 1H), 7.13 (dd, $J = 8.1, 5.0$ Hz, 1H), 2.77 (s, 3H); ^{13}C NMR (101 MHz, CDCl_3) δ 170.3 (C), 156.1 (C), 145.8 (CH), 144.2 (C), 118.8 (CH), 117.1 (CH), 14.7 (CH_3); IR $\nu_{\text{max}}/\text{cm}^{-1}$ 3065, 2929, 1617, 1493, 1400, 1250, 1125, 1093. Analytical data matches that reported in the literature.¹²²

Thiazolo[4,5-c]pyridine-2-thiol (495)

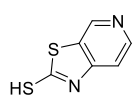
Following **GP11** using 3-amino-4-chloropyridine (0.50 g, 3.9 mmol) and potassium ethyl xanthate (1.34 g, 8.6 mmol) were stirred in DMF (2.5 mL) at 130 °C for 24 h, to afford compound **495** as a brown solid (337.8 mg, 52%); mp. 280 °C (degradation); ^1H NMR (300 MHz, DMSO-d_6) δ 11.86 (br., 1H), 8.62 (s, 1H), 8.49 (d, $J = 5.7$ Hz, 1H), 8.05 (d, $J = 5.7$ Hz, 1H); ^{13}C NMR (101 MHz, DMSO-d_6) δ 144.4 (C), 140.3 (CH), 140.3 (CH), 131.4 (C), 131.3 (C), 118.5 (CH); IR $\nu_{\text{max}}/\text{cm}^{-1}$ 3087, 1527, 1452, 1289, 1029, 814; HRMS (ES-TOF): m/z : calcd. for $\text{C}_6\text{H}_5\text{N}_2\text{S}_2$: 168.9894 found: 168.9891 $[\text{M}+\text{H}]^+$.

2-(Methylthio)thiazolo[4,5-c]pyridine (499)

Following **GP13**, compound **495** (280.5 mg, 1.7 mmol), methyl iodide (0.12 mL, 2.1 mmol) and sodium hydride (73.5 mg, 1.8 mmol) were

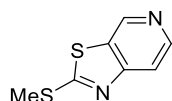
stirred in dry THF (7 mL) for 5 h. Purification by flash chromatography [hexane:ethyl acetate (1:1)] afforded compound **499** as a white solid (172.2 mg, 57%); mp. 87–89 °C; ^1H NMR (300 MHz, CDCl_3) δ 9.14 (d, J = 0.7 Hz, 1H), 8.43 (d, J = 5.4 Hz, 1H), 7.71 (dd, J = 5.4, 0.7 Hz, 1H), 2.83 (s, 3H); ^{13}C NMR (101 MHz, CDCl_3) δ 169.9 (C), 150.1 (C), 143.6 (C), 143.2 (CH), 143.1 (CH), 116.1 (CH), 16.1 (CH_3); IR $\nu_{\text{max}}/\text{cm}^{-1}$ 2996, 1572, 1456, 1438, 1415, 978; HRMS (EI-TOF): m/z : calcd. for $\text{C}_7\text{H}_6\text{N}_2\text{S}_2$: 181.9972 found: 181.9967 $[\text{M}]^+$.

Thiazolo[5,4-*c*]pyridine-2-thiol (496)



Following **GP11** using 4-amino-3-fluoropyridine (0.40 g, 3.6 mmol) and potassium ethyl xanthate (1.30 g, 7.9 mmol) were stirred in DMF (2.3 mL) at 130 °C for 6 h, to afford compound **496** as a yellow solid (590.2 mg, 98%); mp. 305 °C (degradation) (lit.¹²² >290 °C); ^1H NMR (300 MHz, $\text{DMSO}-d_6$) δ 14.25 (br., 1H), 8.82 (d, J = 0.8 Hz 1H), 8.40 (d, J = 6.1 Hz, 1H), 7.45 (dd, J = 6.1, 0.8 Hz, 1H); IR $\nu_{\text{max}}/\text{cm}^{-1}$ 3077, 3029, 1607, 1513, 1448, 1399, 1320, 1246, 1040. Analytical data matches that reported in the literature.¹²²

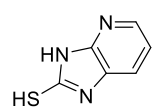
2-(Methylthio)thiazolo[5,4-*c*]pyridine (500)



Following **GP13**, compound **496** (0.40 g, 1.8 mmol), methyl iodide (0.13 mL, 2.1 mmol) and sodium hydride (86.4 mg, 2.1 mmol) were stirred in dry THF (7 mL) for 5 h, to afford compound **500** as a white solid (139.0 mg, 45%); mp. 162–164 °C; ^1H NMR (300 MHz, CDCl_3) δ 9.02 (d, J = 0.7 Hz, 1H), 8.57 (d, J = 5.6 Hz, 1H), 7.73 (dd, J = 5.6, 0.7 Hz, 1H), 2.83 (s, 3H); ^{13}C NMR (101 MHz, CDCl_3) δ 174.9 (C), 158.2 (C), 146.0 (CH), 143.0 (CH), 132.4 (C), 115.7 (CH), 16.1

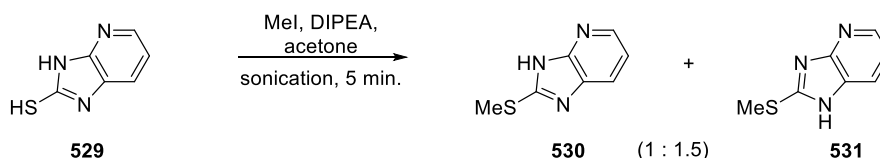
(CH₃); IR $\nu_{\text{max}}/\text{cm}^{-1}$ 2916, 1578, 1427, 1397, 1006, 978; HRMS (EI-TOF): m/z : calcd. for C₇H₆N₂S₂: 181.9972 found: 181.9970 [M]⁺.

3*H*-Imidazo[4,5-*b*]pyridine-2-thiol (**529**)



Following and adaptation of **GP12**, 2,3-diaminopyridine (1.01 g, 9.2 mmol), potassium hydroxide (0.74 g, 13.3 mmol) and carbon disulfide (4.4 mL, 73.3 mmol) in EtOH (18 mL) were stirred under reflux for 5 h, to afford compound **529** as brown solid (1.11 g, 80%); mp. 310–312 °C (lit.¹²⁴ 315–316 °C); ¹H NMR (300 MHz, DMSO-*d*₆) δ 13.13 (br., 1H), 12.73 (br., 1H), 8.10 (dd, J = 5.0, 1.4 Hz, 1H), 7.48 (dd, J = 7.9, 1.4 Hz, 1H), 7.13 (dd, J = 7.9, 5.1 Hz, 1H); ¹³C NMR (101 MHz, DMSO-*d*₆) δ 170.3 (C), 146.9 (C), 142.8 (CH), 125.9 (C), 118.6 (CH), 116.7 (CH). Analytical data matches the reported in the literature.¹²⁵

1-(methylsulfonyl)-2-(methylthio)-1*H*-imidazo[4,5-*b*]pyridine (**533**)

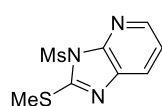


A mixture of **529** (0.96 g, 6.3 mmol), methyl iodide (0.39 mL, 6.3 mmol) and *N,N*-diisopropylethylamine (1.09 mL, 6.3 mmol) in acetone (3.2 mL) was sonicated for 5 minutes, leading to the dissolution of the thiol and immediate precipitation of the product as a white solid. This was extracted with ethyl acetate (20 mL) and washed with brine (2×10 mL). The solution was dried over MgSO₄, filtered off and concentrated under reduced pressure. The residue was recrystallized in ethyl acetate affording the product as a mixture of tautomers **530** and **531** (1 : 1.5). Beige solid (514.0 mg, 49%); mp. 211–213 °C (lit.¹²⁴ 210–212 °C); ¹H NMR (300 MHz, DMSO-*d*₆) δ 13.14 and 12.78

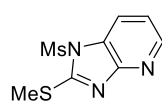
(br., 1H), 8.17 (m, 1H), 7.98–7.67 (m, 1H), 7.27–7.05 (m, 1H), 2.71 (s, 3H); IR $\nu_{\max}/\text{cm}^{-1}$ 3067, 2978, 2931, 1513, 1457, 1393, 1298, 1271, 950. Analytical data matches that reported in the literature.¹²⁵



Part of the mixture obtained in the previous step (250.2 mg, 1.5 mmol) was taken into a flame-dried flask. Mesyl chloride (0.18 mL, 2.3 mmol), *N,N*-diisopropylethylamine (0.39 mL, 2.3 mmol), 4-dimethylaminopyridine (9 mg, 0.1 mmol) and DMF (3 mL) were sequentially added and the resulting mixture was stirred at room temperature for 24 h. The reaction mixture was diluted with brine (5 mL) and extracted with ethyl acetate (2×10 mL). The organic phases were combined, dried over MgSO_4 , filtered off and concentrated under reduced pressure, affording a mixture of regioisomers **532** and **533** (1 : 5.6) that were separated by flash chromatography [hexane:ethyl acetate (1:1)].



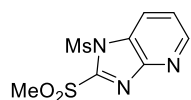
Compound **532**: White solid (30.3 mg, 8%). mp. 140–142 °C; ^1H NMR (300 MHz, CDCl_3) δ 8.28 (dd, $J = 4.9, 1.5$ Hz, 1H), 7.84 (dd, $J = 8.0, 1.5$ Hz, 1H), 7.22 (dd, $J = 8.0, 4.9$ Hz, 1H), 3.56 (s, 3H), 2.65 (s, 3H); ^{13}C NMR (101 MHz, CDCl_3) δ 155.5 (C), 148.0 (C), 143.6 (CH), 135.6 (C), 126.0 (CH), 120.4 (CH), 42.4 (CH₃), 14.9 (CH₃); IR $\nu_{\max}/\text{cm}^{-1}$ 3020, 2989, 2910, 1597, 1439, 1402, 1353, 1227, 1151, 1032. HRMS (ES-TOF): m/z : calcd. for $\text{C}_8\text{H}_{10}\text{N}_3\text{O}_2\text{S}_2$: 244.0214 found: 244.0215 $[\text{M}+\text{H}]^+$.



Compound **533**: White solid (164.5 mg, 45%). mp. 166–168 °C; ^1H NMR (300 MHz, CDCl_3) δ 8.45 (dd, $J = 4.9, 1.5$ Hz, 1H), 8.03 (dd, $J = 8.1, 1.5$ Hz, 1H), 7.16 (dd, $J = 8.1, 4.9$ Hz, 1H), 3.23 (s, 3H), 2.76

(s, 3H); ^{13}C NMR (101 MHz, CDCl_3) δ 157.6 (C), 155.3 (C), 146.5 (CH), 127.1 (C), 120.5 (CH), 118.9 (CH), 41.2 (CH_3), 15.5 (CH_3); IR $\nu_{\text{max}}/\text{cm}^{-1}$ 3014, 2997, 2905, 1599, 1461, 1394, 1361, 1320, 1210, 1145, 1035. HRMS (ES-TOF): m/z : calcd. for $\text{C}_8\text{H}_{10}\text{N}_3\text{O}_2\text{S}_2$: 244.0214 found: 244.0216 $[\text{M}+\text{H}]^+$.

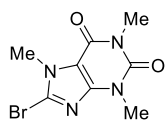
1,2-bis(methylsulfonyl)-1H-imidazo[4,5-b]pyridine (534)



m-Chloroperbenzoic acid (70%, 353.5 mg, 2.1 mmol,) was added into an ice-cooled solution of **533** (200.7 mg, 0.8 mmol) in CH_2Cl_2 (4 mL).

The mixture was stirred at room temperature for 40 min. Then, washed with a saturated aqueous solution of $\text{Na}_2\text{S}_2\text{O}_3$ (10 mL), and concentrated under reduced pressure. The resulting product was directly taken into the aminide-forming step due to its quick degradation over time.

8-Bromocaffeine (537)

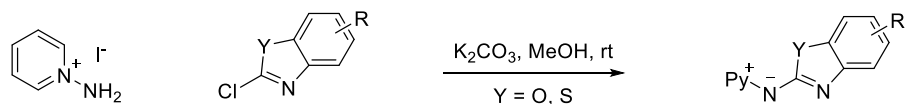


Following the reported procedure,¹²⁶ caffeine (0.97 g, 5.0 mmol) and aged NBS (1.78 g, 10.0 mmol) were combined and dissolved in dry CH_2Cl_2 (30 mL). Water was then added and the resulting mixture was

vigorously stirred at room temperature for 5 days. The mixture was then washed with NaOH [2 M] (100 mL) followed by water (2×50 mL). The organic phase was dried over MgSO_4 , filtered off, concentrated under reduced pressure and purified by flash chromatography [hexane:ethyl acetate (1:1)] to afford compound **537** as a white solid (1.1 g, 80%); mp. 194–196 °C; ^1H NMR (300 MHz, CDCl_3) δ 3.97 (s, 3H), 3.56 (s, 3H), 3.40 (s, 3H); IR $\nu_{\text{max}}/\text{cm}^{-1}$ 2953, 1701, 1653, 1448, 1341, 972, 743. Analytical data matches that reported in the literature.¹²⁶

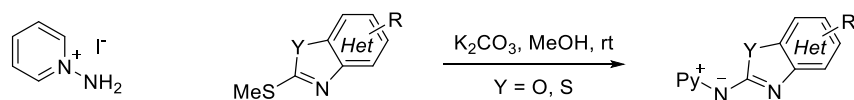
5.4.3 Preparation of aminides

General Procedure 14 (GP14)



Following a modification of **GP5** a mixture of *N*-aminopyridinium iodide (1.0 eq.) and potassium carbonate (2.8 eq.) in methanol [0.1 M relative to the amount of *N*-aminopyridinium iodide] was stirred at room temperature for 30 min until a permanent purple suspension appeared. The corresponding 2-halobenzoheterocycle (1.04 eq.) was added and the reaction mixture was stirred at room temperature for the indicated period of time. The solvent was removed under reduced pressure and the residue redissolved in CH_2Cl_2 and washed with a solution of NaOH [2.5 M]. The aqueous phase was extracted with CH_2Cl_2 and the combined organic phases were dried over MgSO_4 , filtered off and the solvent removed under reduced pressure. The residue was purified by flash chromatography over silica gel.

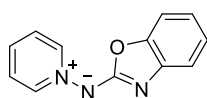
General Procedure 15 (GP15)



Following an adaptation of **GP14**, a mixture of *N*-aminopyridinium iodide (1.0 eq.) and potassium carbonate (2.8 eq.) in methanol [0.1 M relative to the amount of *N*-aminopyridinium iodide] was stirred at room temperature for 30 min until a permanent purple suspension appeared. The corresponding 2-methylthiobenzo(thio/oxa)zole (1.04 eq.) was added and the reaction mixture was stirred at room temperature for the indicated period of time. The solvent was removed under reduced pressure and the

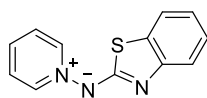
residue dissolved in CH_2Cl_2 and washed with a solution of NaOH [2.5 M]. The aqueous phase was extracted with CH_2Cl_2 and the combined organic phases were dried over MgSO_4 , filtered off and the solvent removed under reduced pressure. The residue was purified by flash chromatography over silica gel.

Pyridinium N-(benzo[d]oxazol-2-yl) amide (436)



Following **GP14** using *N*-aminopyridinium iodide (0.40 g, 2.0 mmol), 2-chlorobenzoxazole (0.23 mL, 2.1 mmol) and potassium carbonate (0.80 g, 5.6 mmol) for 16 h. After purification by flash chromatography [CH_2Cl_2 :methanol (95:5)] aminide **436** was isolated as a bright yellow solid (405.2 mg, 96%); mp. 200–202 °C; ^1H NMR (300 MHz, CDCl_3) δ 9.60–9.54 (m, 2H), 7.63–7.53 (m, 3H), 7.35 (dd, $J = 7.7, 0.9$ Hz, 1H), 7.29 (dd, $J = 7.5, 1.1$ Hz, 1H), 7.15 (app. td, $J = 7.5, 0.9$ Hz, 1H), 7.04 (app. td, $J = 7.7, 1.1$ Hz, 1H); ^{13}C NMR (101 MHz, CDCl_3) δ 166.1 (C), 147.4 (C), 143.5 (C), 138.6 (2 \times CH), 131.3 (CH), 126.1 (2 \times CH), 123.1 (CH), 120.8 (CH), 115.3 (CH), 108.5 (CH); IR $\nu_{\text{max}}/\text{cm}^{-1}$ 3069, 3046, 1626, 1604, 1526, 1469, 1300, 1236, 1192, 1002; HRMS (ES-TOF): m/z : calcd. for $\text{C}_{12}\text{H}_9\text{N}_3\text{ONa}$: 234.0643 found: 234.0641 $[\text{M}+\text{Na}]^+$.

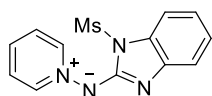
Pyridinium N-(benzo[d]thiazol-2-yl) amide (437)



Following **GP14** using *N*-aminopyridinium iodide (0.40 g, 2.0 mmol), 2-chlorobenzoxothiazole (0.30 mL, 2.1 mmol) and potassium carbonate (0.80 g, 5.6 mmol) for 16 h. After purification by flash chromatography [CH_2Cl_2 :methanol (95:5)] aminide **437** was isolated as a bright yellow solid (434.4 mg, 95%); mp. 174–176 °C; ^1H NMR (300 MHz, CDCl_3) δ 9.64–9.55 (m, 2H), 7.62–7.41 (m, 5H), 7.30–7.18 (m, 1H), 7.03 (app. td, $J = 7.6, 1.1$ Hz, 1H); ^{13}C NMR (101 MHz,

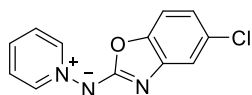
CDCl₃) δ 172.3 (C), 153.3 (C), 138.3 (2 \times CH), 131.0 (C), 131.0 (CH), 125.9 (2 \times CH), 125.3 (CH), 121.2 (CH), 120.5 (CH), 118.0 (CH); IR $\nu_{\max}/\text{cm}^{-1}$ 3070, 3050, 1590, 1551, 1467, 1351, 1290, 1193, 1012, 754; HRMS (ES-TOF): m/z : calcd. for C₁₂H₁₀N₃OS: 228.0595 found: 228.0598 [M+H]⁺.

Pyridinium N-(1-(Methylsulfonyl)-1H-benzo[d]imidazol-2-yl) amide (443)



Following **GP14** using *N*-aminopyridinium iodide (278.5 mg, 1.3 mmol), compound **442** (301.2 mg, 1.3 mmol) and potassium carbonate (483.7 mg, 3.5 mmol) for 17 h. After purification by flash chromatography [CH₂Cl₂:methanol (95:5)] aminide **443** was isolated as a bright yellow solid (105.3 mg, 37%); mp. 135–137 °C; ¹H NMR (300 MHz, CDCl₃) δ 9.51–9.44 (m, 2H), 7.82 (dd, J = 8.2, 1.3 Hz, 1H), 7.68–7.52 (m, 3H), 7.29 (dd, J = 7.7, 1.2 Hz, 1H), 7.16 (app. td, J = 7.7, 1.3 Hz, 1H), 7.02 (app. td, J = 8.2, 1.2 Hz, 1H), 3.53 (s, 3H); ¹³C NMR (101 MHz, CDCl₃) δ 157.1 (C), 142.7 (C), 139.7 (2 \times CH), 132.2 (CH), 131.4 (C), 126.0 (2 \times CH), 123.8 (CH), 120.7 (CH), 115.6 (CH), 112.5 (CH), 41.4 (CH₃); IR $\nu_{\max}/\text{cm}^{-1}$ 3018, 1601, 1523, 1466, 1352, 1282, 1214, 746, 667; HRMS (ES-TOF): m/z : calcd. for C₁₃H₁₃N₄O₂S: 289.0759 found: 289.0748 [M+H]⁺.

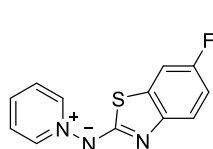
Pyridinium N-(5-Chlorobenzo[d]oxazol-2-yl) amide (472)



Following **GP14** using *N*-aminopyridinium iodide (248.2 mg, 1.1 mmol), compound **471** (231.3 mg, 1.2 mmol) and potassium carbonate (464.4 mg, 3.4 mmol) for 16 h. After purification by flash chromatography [CH₂Cl₂:methanol (95:5)] aminide **472** was isolated as a bright yellow solid (208.6 mg, 76%); mp. 218–220 °C; ¹H NMR (300 MHz, CDCl₃) δ 9.49 (dd, J = 6.9, 1.3 Hz, 2H), 7.69–7.55 (m, 3H), 7.26 (br., 1H), 7.14 (d, J = 8.3 Hz, 1H), 6.96 (dd, J = 8.3, 2.1 Hz,

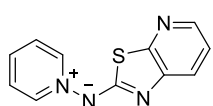
^1H); ^{13}C NMR (101 MHz, CDCl_3) δ 167.2 (C), 146.2 (C), 145.0 (C), 139.0 (CH), 132.1 (CH), 128.3 (C), 126.2 (2 \times CH), 120.3 (2 \times CH), 115.3 (CH), 108.9 (CH); IR $\nu_{\text{max}}/\text{cm}^{-1}$ 3061, 3039, 1603, 1519, 1453, 1188; HRMS (ES-TOF): m/z : calcd. for $\text{C}_{12}\text{H}_9\text{N}_3\text{OCl}$: 246.0434 found: 246.0432 $[\text{M}+\text{H}]^+$.

Pyridinium N-(6-fluorobenzo[d]thiazol-2-yl) amide (480)



Following **GP15** using *N*-aminopyridinium iodide (73.0 mg, 0.33 mmol), compound **481** (80.2 mg, 0.35 mmol) and potassium carbonate (129.3 mg, 0.93 mmol) for 16 h. After purification by flash chromatography [CH_2Cl_2 :methanol (95:5)] aminide **480** was isolated as a bright yellow solid (63.6 mg, 74%); mp. 168–170 °C; ^1H NMR (300 MHz, CDCl_3) δ 9.63–9.55 (m, 2H), 7.59–7.49 (m, 3H), 7.36 (dd, J = 8.9, 4.8 Hz, 1H), 7.28 (dd, J = 8.3, 2.7 Hz, 1H), 6.94 (app. td, J = 9.0, 2.7 Hz, 1H); ^{13}C NMR (101 MHz, CDCl_3) δ 171.9 (C), 158.1 (d, $J_{\text{C-F}}$ = 239.1 Hz, C), 149.8 (C), 138.2 (2 \times CH), 131.8 (d, $J_{\text{C-F}}$ = 10.2 Hz, C), 130.9 (CH), 125.9 (2 \times CH), 118.2 (d, $J_{\text{C-F}}$ = 8.6 Hz, CH), 112.6 (d, $J_{\text{C-F}}$ = 23.6 Hz, CH), 107.2 (d, $J_{\text{C-F}}$ = 26.8 Hz, CH); IR $\nu_{\text{max}}/\text{cm}^{-1}$ 3062, 3034, 1600, 1503, 1468, 1448, 1188; HRMS (ES-TOF): m/z : calcd. for $\text{C}_{12}\text{H}_9\text{N}_3\text{SF}$: 246.0501 found: 246.0503 $[\text{M}+\text{H}]^+$.

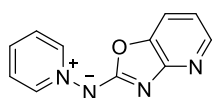
Pyridinium N-(thiazolo[5,4-*b*]pyridin-2-yl) amide (501)



Following **GP15** using *N*-aminopyridinium iodide (235.0 mg, 1.10 mmol), compound **497** (200.6 mg, 1.04 mmol) and potassium carbonate (410.5 mg, 3.01 mmol) for 24 h. After purification by flash chromatography [CH_2Cl_2 :methanol (95:5)] aminide **501** was isolated as a bright yellow solid (193.7 mg, 80%); mp. 194–196 °C; ^1H NMR (300 MHz, CDCl_3) δ 9.49 (dd, J = 7.1, 1.2 Hz, 2H), 8.10 (dd, J = 4.8, 1.5 Hz, 1H), 7.66 (t, J = 7.5 Hz, 1H), 7.61–7.55 (m, 2H), 7.51 (dd, J =

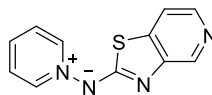
8.0, 1.5 Hz, 1H), 7.11 (dd, $J = 8.0, 4.8$ Hz, 1H); ^{13}C NMR (101 MHz, CDCl_3) δ 171.8 (C), 156.0 (C), 147.6 (C), 141.7 (CH), 139.5 (2 \times CH), 132.8 (CH), 126.1 (2 \times CH), 122.7 (CH), 120.5 (CH); IR $\nu_{\text{max}}/\text{cm}^{-1}$ 3109, 3069, 1573, 1550, 1467, 1141; HRMS (ES-TOF): m/z : calcd. for $\text{C}_{11}\text{H}_9\text{N}_4\text{S}$: 229.0548 found: 229.0551 $[\text{M}+\text{H}]^+$.

Pyridinium *N*-(oxazolo[4,5-*b*]pyridin-2-yl) amide (502)



Following **GP15** using *N*-aminopyridinium iodide (222.0 mg, 1.01 mmol), compound **498** (173.2 mg, 1.05 mmol) and potassium carbonate (389.8 mg, 2.82 mmol) for 22 h. After purification by flash chromatography [CH_2Cl_2 :methanol (9:1)] aminide **502** was isolated as a yellow solid (168.3 mg, 79%); mp. 189–191 °C; ^1H NMR (300 MHz, CDCl_3) δ 9.55 (dd, $J = 7.1, 1.2$ Hz, 2H), 8.14 (dd, $J = 5.2, 1.4$ Hz, 1H), 7.73 (tt, $J = 7.5, 2.1$ Hz, 1H), 7.66–7.59 (m, 2H), 7.39 (dd, $J = 7.7, 1.4$ Hz, 1H), 6.87 (dd, $J = 7.7, 5.2$ Hz, 1H); ^{13}C NMR (101 MHz, CDCl_3) δ 167.8 (C), 158.7 (C), 143.5 (CH), 140.3 (C), 139.9 (CH), 133.5 (CH), 126.2 (2 \times CH), 115.6 (2 \times CH), 114.1 (CH); IR $\nu_{\text{max}}/\text{cm}^{-1}$ 3109, 3044, 1596, 1528, 1470, 1400, 1298, 1250, 1181; HRMS (ES-TOF): m/z : calcd. for $\text{C}_{11}\text{H}_9\text{N}_4\text{O}$: 213.0776 found: 213.0775 $[\text{M}+\text{H}]^+$.

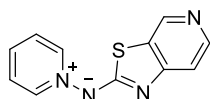
Pyridinium *N*-(thiazolo[4,5-*c*]pyridin-2-yl) amide (503)



Following **GP15** using *N*-aminopyridinium iodide (176.2 mg, 0.79 mmol), compound **499** (150.9 mg, 0.82 mmol), and potassium carbonate (307.2 mg, 2.22 mmol) for 17 h. After purification by flash chromatography [CH_2Cl_2 :methanol (95:5)] aminide **503** was isolated as a yellow solid (140.5 mg, 78%); mp. 193–195 °C; ^1H NMR (300 MHz, CDCl_3) δ 9.57–9.50 (m, 2H), 8.65 (s, 1H), 8.16 (d, $J = 5.2$ Hz, 1H), 7.71–7.55 (m, 3H), 7.49 (d, $J = 5.2$ Hz, 1H); ^{13}C NMR (101 MHz, CDCl_3) δ 172.7 (C), 150.7 (C), 140.7 (2 \times CH), 140.1 (C), 139.2 (CH), 138.8 (CH),

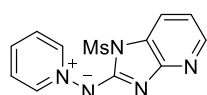
132.7 (CH), 126.2 (2×CH), 115.7 (CH); IR $\nu_{\max}/\text{cm}^{-1}$ 3032, 1574, 1498, 1461, 1409, 916; HRMS (ES-TOF): m/z : calcd. for $\text{C}_{11}\text{H}_9\text{N}_4\text{S}$: 229.0548 found: 229.0549 $[\text{M}+\text{H}]^+$.

Pyridinium *N*-(thiazolo[5,4-*c*]pyridin-2-yl) amide (504)



Following **GP15** using *N*-aminopyridinium iodide (117.5 mg, 0.53 mmol), compound **500** (100.3 mg, 0.55 mmol) and potassium carbonate (206.2 mg, 1.49 mmol) for 22 h. After purification by flash chromatography [CH_2Cl_2 :methanol (9:1)] aminide **504** was isolated as a yellow solid (108.8 mg, 90%); mp. 223–225 °C; ^1H NMR (300 MHz, CDCl_3) δ 9.38 (d, $J = 5.9$ Hz, 2H), 8.65 (s, 1H), 8.30 (d, $J = 5.6$ Hz, 1H), 7.78 (t, $J = 7.6$ Hz, 1H), 7.65 (app. t, $J = 7.0$ Hz, 2H), 7.19 (d, $J = 5.6$ Hz, 1H); ^{13}C NMR (101 MHz, CDCl_3) δ 176.3 (C), 159.5 (C), 145.5 (CH), 141.1 (2×CH), 140.1 (CH), 134.2 (CH), 128.7 (C), 126.3 (2×CH), 112.2 (CH); IR $\nu_{\max}/\text{cm}^{-1}$ 3027, 1478, 1439, 1320, 1195, 809; HRMS (ES-TOF): m/z : calcd. for $\text{C}_{11}\text{H}_9\text{N}_4\text{S}$: 229.0548 found: 229.0550 $[\text{M}+\text{H}]^+$.

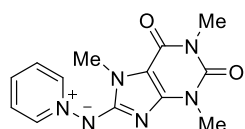
Pyridinium *N*-(1-(Methylsulfonyl)-1*H*-imidazo[5,4-*b*]pyridin-2-yl) amide (535)



Following **GP15** using *N*-aminopyridinium iodide (202.4 mg, 0.90 mmol), sulfone **534** (260.6 mg, 0.94 mmol) and potassium carbonate (352.2 mg, 2.53 mmol) for 22 h. After purification by flash chromatography [CH_2Cl_2 :MeOH (92:8)] aminide **535** was isolated as a yellow solid (38.5 mg, 15%); mp. 199–201 °C; ^1H NMR (300 MHz, CDCl_3) δ 9.45 (d, $J = 6.2$ Hz, 2H), 8.17 (dd, $J = 5.1$, 1.3 Hz, 1H), 7.91 (dd, $J = 7.9$, 1.3 Hz, 1H), 7.77 (t, $J = 7.5$ Hz, 1H), 7.63 (app. t, $J = 7.0$ Hz, 2H), 6.87 (dd, $J = 7.9$, 5.1 Hz, 1H), 3.54 (s, 3H); ^{13}C NMR (101 MHz, CDCl_3) δ 158.9 (C), 156.2 (C), 144.1 (CH), 140.9 (2×CH), 134.4 (CH), 126.2 (2×CH), 124.9 (C), 118.8 (CH), 115.5 (CH), 41.5 (CH_3); IR $\nu_{\max}/\text{cm}^{-1}$ 2994, 2909, 1581, 1513, 1466, 1397,

1351, 1293, 1155; HRMS (ES-TOF): m/z : calcd. for $C_{12}H_{12}N_5O_2S$: 290.0712 found: 290.0710 $[M+H]^+$.

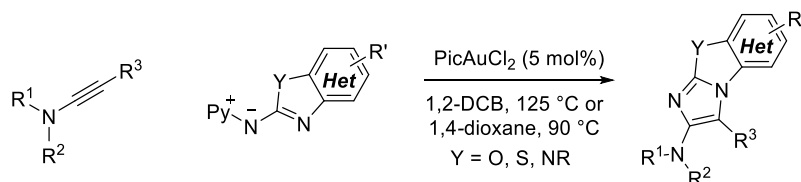
Pyridinium *N*-(1,3,7-trimethyl-2,6-dioxo-2,3,6,7-tetrahydro-1*H*-purin-8-yl) aminide (538)



Following **GP14** using *N*-aminopyridinium iodide (200.2 mg, 0.90 mmol), **537** (255.3 mg, 0.93 mmol) and potassium carbonate (375.3 mg, 2.72 mmol) for 24 h. After purification by flash chromatography [CH_2Cl_2 :methanol (95:5)] aminide **538** was isolated as a bright orange solid (221.3 mg, 86%); mp. 226–228 °C; 1H NMR (300 MHz, $CDCl_3$) δ 9.32 (dd, J = 5.6, 2.8 Hz, 2H), 7.47–7.43 (m, 3H), 3.73 (s, 3H), 3.53 (s, 3H), 3.40 (s, 3H); ^{13}C NMR (101 MHz, $CDCl_3$) δ 155.8 (C), 154.1 (C), 151.9 (C), 147.9 (C), 137.3 (2 \times CH), 129.2 (CH), 125.8 (2 \times CH), 102.7 (C), 30.0 (CH_3), 29.7 (CH_3), 27.6 (CH_3); IR ν_{max}/cm^{-1} 3057, 2945, 1687, 1646, 1486, 1444, 1214, 1140; HRMS (ES-TOF): m/z : calcd. for $C_{13}H_{14}N_6O_2Na$: 309.1076 found: 309.1075 $[M+Na]^+$.

5.5 Cycloaddition products for Chapter 4

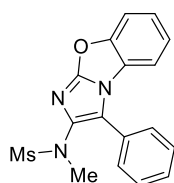
General Procedure 16 (GP16)



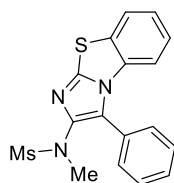
A heat gun-dried Schlenk tube was charged with the corresponding ynamide (1.0 eq.) [if the ynamide was an oil it was added as a stock solution in the reaction solvent], heterocyclic aminide (1.2 eq.) and dichloro(2-pyridinecarboxylate)gold (PicAuCl₂)

(5 mol%) under an argon atmosphere. Dry solvent (1,2-dichlorobenzene or 1,4-dioxane, [0.1 M relative to the amount of ynamide] was then added and the mixture was stirred under argon at the specified temperature (90 or 125 °C) for the indicated period of time. The reaction mixture was then allowed to cool and either (A) added directly onto a silica gel column to be purified by flash chromatography (when using 1,2-dichlorobenzene), or (B) concentrated under reduced pressure and the residue purified by silica gel flash chromatography (when using 1,4-dioxane).

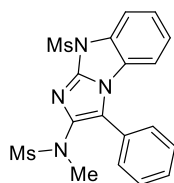
Imidazo[2,1-*b*]benzoxazole **451**



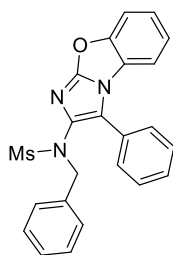
Following **GP16** using ynamide **264** (41.5 mg, 0.20 mmol) and aminide **436** (51.2 mg, 0.24 mmol) in 1,2-DCB for 6 h. After purification by flash chromatography [hexane:ethyl acetate (3:2)] compound **451** was isolated as a pale yellow solid (57.0 mg, 84%); mp. 170–172 °C; ^1H NMR (300 MHz, CDCl_3) δ 7.83 (d, $J = 7.0$ Hz, 2H), 7.61–7.51 (m, 3H), 7.51–7.43 (m, 2H), 7.35 (app. td, $J = 8.0, 1.2$ Hz, 1H), 7.31–7.23 (m, 1H), 3.26 (s, 3H), 3.22 (s, 3H); ^{13}C NMR (101 MHz, CDCl_3) δ 151.9 (C), 150.2 (C), 135.7 (C), 128.9 (2 \times CH), 128.7 (CH), 128.4 (2 \times CH), 127.2 (C), 126.8 (C), 124.9 (CH), 124.1 (CH), 121.5 (C), 112.5 (CH), 112.3 (CH), 39.0 (CH₃), 36.8 (CH₃); IR $\nu_{\text{max}}/\text{cm}^{-1}$ 2989, 1636, 1588, 1554, 1475, 1407, 1381, 1232, 1147, 1090; HRMS (ES-TOF): m/z : calcd. for $\text{C}_{17}\text{H}_{15}\text{N}_3\text{O}_3\text{SNa}$: 364.0732 found: 364.0734 $[\text{M}+\text{Na}]^+$.

Imidazo[2,1-*b*]benzothiazole 452

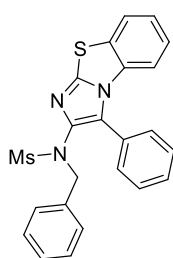
Following **GP16** using ynamide **264** (41.2 mg, 0.20 mmol) and aminide **437** (55.3 mg, 0.24 mmol) in 1,2-DCB for 8 h. After purification by flash chromatography [hexane:ethyl acetate (1:1)] compound **452** was isolated as a white solid (61.2 mg, 87%); mp. 180–182 °C; ^1H NMR (300 MHz, CDCl_3) δ 7.68–7.56 (m, 3H), 7.51–7.43 (m, 3H), 7.28–7.20 (m, 1H), 7.16–7.09 (m, 2H), 3.14 (s, 3H), 3.11 (s, 3H); ^{13}C NMR (101 MHz, CDCl_3) δ 144.7 (C), 140.5 (C), 133.1 (C), 130.3 (2 \times CH), 129.6 (C), 129.4 (CH), 128.8 (2 \times CH), 127.3 (C), 125.9 (CH), 125.8 (C), 125.0 (CH), 124.1 (CH), 114.0 (CH), 39.1 (CH_3), 36.9 (CH_3); IR $\nu_{\text{max}}/\text{cm}^{-1}$ 3026, 1487, 1361, 1327, 1146, 975; HRMS (ES-TOF): m/z : calcd. for $\text{C}_{17}\text{H}_{15}\text{N}_3\text{O}_2\text{S}_2\text{Na}$: 380.0503 found: 380.0501 $[\text{M}+\text{Na}]^+$.

Imidazo[1,2-*a*]benzimidazole 446

Following **GP16** using ynamide **264** (29.4 mg, 0.14 mmol) and aminide **443** (48.2 mg, 0.17 mmol) in 1,2-DCB for 24 h. After purification by flash chromatography [hexane:ethyl acetate (3:2)] compound **446** was isolated as an off-white foam (20.4 mg, 35%); ^1H NMR (300 MHz, CDCl_3) δ 8.04 (d, J = 8.4 Hz, 1H), 7.79–7.73 (m, 2H), 7.59–7.44 (m, 3H), 7.42–7.32 (m, 2H), 7.25 (app. td, J = 7.8, 1.1 Hz, 1H), 3.44 (s, 3H), 3.23 (s, 3H), 3.22 (s, 3H); ^{13}C NMR (101 MHz, CDCl_3) δ 141.5 (C), 137.7 (C), 132.3 (C), 129.1 (2 \times CH), 129.1 (CH), 128.9 (2 \times CH), 126.9 (C), 126.3 (C), 125.3 (CH), 124.5 (CH), 121.9 (C), 115.1 (CH), 112.4 (CH), 40.7 (CH_3), 39.1 (CH_3), 37.4 (CH_3); IR $\nu_{\text{max}}/\text{cm}^{-1}$ 3029, 2929, 1602, 1572, 1474, 1366, 1339, 964, 908; HRMS (ES-TOF): m/z : calcd. for $\text{C}_{18}\text{H}_{18}\text{N}_4\text{O}_4\text{S}_2\text{Na}$: 441.0667 found: 441.0666 $[\text{M}+\text{Na}]^+$.

Imidazo[2,1-*b*]benzoxazole 453

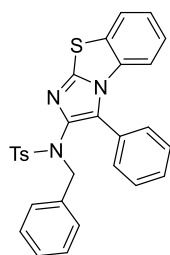
Following **GP16** using ynamide **266** (57.4 mg, 0.20 mmol) and aminide **436** (50.8 mg, 0.24 mmol) in 1,2-DCB for 1 h. After purification by flash chromatography [hexane:ethyl acetate (3:2)] compound **453** was isolated as a white solid (77.3 mg, 92%); mp. 56–58 °C; ¹H NMR (300 MHz, CDCl₃) δ 7.51 (d, *J* = 7.9 Hz, 1H), 7.41–7.33 (m, 5H), 7.33–7.22 (m, 2H), 7.21–7.13 (m, 1H), 7.10–7.02 (m, 1H), 7.01–6.92 (m, 4H), 4.69 (s, 2H), 3.28 (s, 3H); ¹³C NMR (101 MHz, CDCl₃) δ 151.8 (C), 150.1 (C), 134.7 (C), 133.2 (C), 129.1 (2×CH), 128.6 (2×CH), 128.4 (CH), 128.4 (2×CH), 127.9 (2×CH), 127.6 (CH), 126.9 (C), 126.7 (C), 124.8 (CH), 124.0 (CH), 123.4 (C), 112.4 (CH), 112.2 (CH), 55.3 (CH₂), 38.3 (CH₃); IR ν_{max} /cm⁻¹ 3029, 1735, 1631, 1604, 1577, 1477, 1384, 1281, 1185, 1043, 1025; HRMS (ES-TOF): *m/z*: calcd. for C₂₃H₁₉N₃O₃SNa: 440.1045 found: 440.1060 [M+Na]⁺.

Imidazo[2,1-*b*]benzothiazole 454

Following **GP16** using ynamide **266** (57.1 mg, 0.20 mmol) and aminide **437** (54.5 mg, 0.24 mmol) in 1,2-DCB for 3 h. After purification by flash chromatography [hexane:ethyl acetate (3:2)] compound **454** was isolated as a white solid (80.6 mg, 93%); mp. 128–130 °C; ¹H NMR (300 MHz, CDCl₃) δ 7.66 (dd, *J* = 8.0, 0.8 Hz, 1H), 7.45–7.38 (m, 1H), 7.34 (app. t, *J* = 7.3 Hz, 2H), 7.29–7.21 (m, 1H), 7.19–7.08 (m, 4H), 7.07–6.94 (m, 5H), 4.70 (s, 2H), 3.25 (s, 3H); ¹³C NMR (101 MHz, CDCl₃) δ 144.5 (C), 138.1 (C), 135.0 (C), 133.0 (C), 130.5 (2×CH), 129.5 (C), 129.1 (2×CH), 128.9 (CH), 128.3 (2×CH), 128.1 (2×CH), 127.7 (C), 127.6 (CH), 126.9 (C), 125.8 (CH), 124.9 (CH), 124.0 (CH), 113.9 (CH),

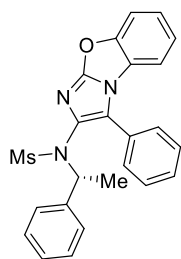
55.1 (CH₂), 38.2 (CH₃); IR $\nu_{\text{max}}/\text{cm}^{-1}$ 2991, 1608, 1581, 1488, 1379, 1255, 1160, 1028, 879; HRMS (ES-TOF): m/z : calcd. for C₂₃H₁₉N₃O₂S₂Na: 456.0816 found: 456.0820 [M+Na]⁺.

*Imidazo[2,1-*b*]benzothiazole 455*

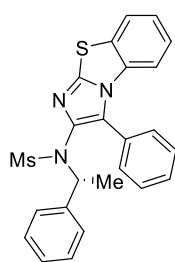


Following **GP16** using ynamide **537** (72.3 mg, 0.20 mmol) and aminide **437** (54.4 mg, 0.24 mmol) in 1,2-DCB for 2 h. After purification by flash chromatography [hexane:ethyl acetate (4:1)] compound **455** was isolated as a white solid (92.9 mg, 91%); mp. 166–168 °C; ¹H NMR (300 MHz, CDCl₃) δ 7.87 (d, J = 7.8 Hz, 2H), 7.65 (d, J = 7.9 Hz, 1H), 7.46 (t, J = 7.3 Hz, 1H), 7.43–7.42 (m, 4H), 7.25–7.16 (m, 3H), 7.11 (app. t, J = 7.9 Hz, 2H), 7.01 (app. t, J = 7.5 Hz, 2H), 6.97–6.89 (m, 3H), 4.51 (s, 2H), 2.48 (s, 3H); ¹³C NMR (101 MHz, CDCl₃) δ 144.2 (C), 143.7 (C), 137.9 (C), 135.9 (C), 135.1 (C), 133.0 (C), 130.7 (2×CH), 129.7 (C), 129.6 (2×CH), 129.1 (2×CH), 128.9 (C), 128.6 (2×CH), 128.2 (2×CH), 128.0 (CH), 128.0 (2×CH), 127.4 (CH), 127.3 (C), 125.7 (CH), 124.7 (CH), 123.9 (CH), 113.9 (CH), 54.4 (CH₂), 21.7 (CH₃); IR $\nu_{\text{max}}/\text{cm}^{-1}$ 3030, 1594, 1583, 1484, 1362, 1346, 1237, 1153, 1074; HRMS (ES-TOF): m/z : calcd. for C₂₉H₂₄N₃O₂S₂: 510.1310 found: 510.1315 [M+H]⁺.

This reaction was also performed using ynamide **537** (0.90 g, 2.49 mmol), aminide **437** (0.68 g, 2.99 mmol) and dichloro(2-pyridinecarboxylate)gold (PicAuCl₂) (48.5 mg, 0.13 mmol) in 1,2-DCB (25 mL) for 1 h. After this time, solvent was removed under reduced pressure and the residue purified as above, to afford **455** (1.08 g, 85%).

(R)-(-)-Imidazo[2,1-b]benzoxazole 456

Following **GP16** using ynamide **538** (60.1 mg, 0.20 mmol) and aminide **436** (50.7 mg, 0.24 mmol) in 1,2-DCB for 2 h. After purification by flash chromatography [hexane:ethyl acetate (4:1)] compound **456** was isolated as an off-white foam (44.0 mg, 51% at ~95% purity estimated by ^1H NMR); $[\alpha]_D^{24} = -43.9$ (c 1.0, CH_2Cl_2); *Some resonances are broadened due to restricted rotation.* ^1H NMR (300 MHz, CDCl_3) δ 7.68–6.76 (m, 14H), 5.39–5.08 (m, 1H), 3.00 (br., 3H), 1.37 (br., 3H); ^{13}C NMR (101 MHz, CDCl_3) δ 151.5 (C), 150.2 (C), 139.6 (C), 131.0 (C), 128.7 (2 \times CH), 128.6 (CH), 128.5 (CH), 128.1 (2 \times CH), 127.9 (CH), 127.8 (CH), 127.4 (C), 126.8 (C), 124.8 (2 \times CH), 124.4 (C), 123.9 (2 \times CH), 112.4 (CH), 112.3 (CH), 59.7 (CH), 41.0 (CH_3), 29.7 (CH_3); IR $\nu_{\text{max}}/\text{cm}^{-1}$ 3069, 3033, 2983, 1630, 1576, 1477, 1339, 1185, 1160; HRMS (ES-TOF): m/z: calcd. for $\text{C}_{24}\text{H}_{21}\text{N}_3\text{O}_3\text{SNa}$: 454.1201 found: 454.1196 $[\text{M}+\text{Na}]^+$.

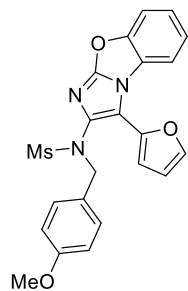
(R)-(-)-Imidazo[2,1-b]benzothiazole 457

Following **GP16** using ynamide **538** (60.2 mg, 0.20 mmol) and aminide **437** (54.4 mg, 0.24 mmol) in 1,2-DCB for 15 h. After purification by flash chromatography [hexane:ethyl acetate (4:1)] compound **457** was isolated as an off-white foam (51.0 mg, 57% at ~90% purity estimated by ^1H NMR); $[\alpha]_D^{24} = -58.3$ (c 1.0, CH_2Cl_2); *Some resonances are broadened due to restricted rotation.* ^1H NMR (300 MHz, CDCl_3) δ 7.76–6.90 (m, 14H), 5.25 (q, $J = 7.1$ Hz, 1H), 3.03 (br., 3H), 1.47 (br., 3H); ^{13}C NMR (101 MHz, CDCl_3) δ 144.1 (C), 140.0 (C), 135.9 (C), 133.1 (C), 130.5 (CH), 129.7 (C), 128.9 (CH), 128.7 (C), 128.4 (CH), 128.2 (2 \times CH), 128.1 (2 \times CH), 127.7 (CH), 127.4 (C), 125.8 (CH), 124.9 (2 \times CH), 124.0

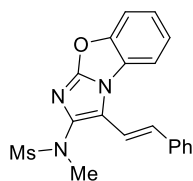
(2×CH), 114.1 (CH), 59.4 (CH), 40.8 (CH₃), 29.7 (CH₃); IR $\nu_{\text{max}}/\text{cm}^{-1}$ 3026, 2854, 1487, 1341, 1220, 1160, 968, 754; HRMS (ES-TOF): m/z : calcd. for C₂₄H₂₁N₃O₂S₂Na: 470.0973 found: 470.0977 [M+Na]⁺.

The reaction was also carried out following **GP16** using ynamide **538** (30.1 mg, 0.10 mmol) and aminide **437** (27.2 mg, 0.12 mmol) in 1,4-dioxane at 90 °C for 24 h, affording **457** (34.2 mg, 76%).

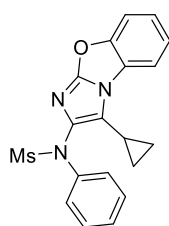
*Imidazo[2,1-*b*]benzoxazole 459*



Following **GP16** using ynamide **276** (61.2 mg, 0.20 mmol) and aminide **436** (50.7 mg, 0.24 mmol) in 1,2-DCB for 1 h. After purification by flash chromatography [hexane:ethyl acetate (3:2)] compound **459** was isolated as a white solid (75.7 mg, 86%); mp. 164–166 °C; ¹H NMR (300 MHz, CDCl₃) 7.89–7.81 (m, 1H), 7.57–7.47 (m, 2H), 7.39–7.28 (m, 2H), 7.07 (d, *J* = 8.7 Hz, 2H), 6.90 (dd, *J* = 3.5, 0.6 Hz, 1H), 6.65 (d, *J* = 8.7 Hz, 2H), 6.50 (dd, *J* = 3.5, 1.8 Hz, 1H), 4.75 (s, 2H), 3.71 (s, 3H), 3.17 (s, 3H); ¹³C NMR (101 MHz, CDCl₃) δ 159.2 (C), 151.7 (C), 150.1 (C), 141.9 (C), 141.5 (CH), 133.0 (C), 130.3 (2×CH), 127.1 (C), 126.8 (C), 125.0 (CH), 124.3 (CH), 115.4 (C), 113.9 (CH), 113.5 (2×CH), 112.2 (CH), 112.0 (CH), 109.7 (CH), 55.1 (CH₃), 54.5 (CH₂), 38.2 (CH₃); IR $\nu_{\text{max}}/\text{cm}^{-1}$ 2931, 1630, 1578, 1472, 1342, 1155; HRMS (ES-TOF): m/z : calcd. for C₂₂H₁₉N₃O₅SNa: 460.0943 found: 460.0945 [M+Na]⁺.

Imidazo[2,1-*b*]benzoxazole 462

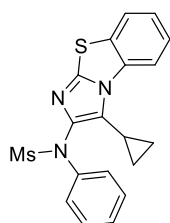
Following **GP16** using ynamide **539** (46.9 mg, 0.20 mmol) and aminide **436** (50.6 mg, 0.24 mmol) in 1,4-dioxane at 90 °C for 45 min. After cooling down the reaction mixture, the product precipitated and was filtered off and washed with ice-cooled diethyl ether followed by hexane and dried under air, to afford the pure compound **462** as a pale brown solid (55.4 mg, 75%); mp. 255 °C (degradation); ^1H NMR (300 MHz, CDCl_3) δ 7.83–7.76 (m, 1H), 7.60–7.53 (m, 3H), 7.44–7.24 (m, 7H), 3.35 (s, 3H), 3.14 (s, 3H); ^{13}C NMR (101 MHz, CDCl_3) δ 150.1 (C), 136.9 (C), 136.6 (C), 130.3 (CH), 128.8 (2 \times CH), 128.2 (CH), 127.1 (C), 126.6 (2 \times CH), 124.9 (CH), 124.4 (CH), 121.1 (C), 113.3 (CH), 112.7 (CH), 112.5 (CH), 38.6 (CH_3), 36.3 (CH_3); *One resonance for a quaternary carbon was not visible*; IR $\nu_{\text{max}}/\text{cm}^{-1}$ 3025, 1636, 1584, 1469, 1333, 1147, 732; HRMS (ES-TOF): m/z : calcd. for $\text{C}_{19}\text{H}_{17}\text{N}_3\text{O}_3\text{SNa}$: 390.0888 found: 390.0889 $[\text{M}+\text{Na}]^+$.

Imidazo[2,1-*b*]benzoxazole 463

Following **GP16** using ynamide **279** (47.6 mg, 0.20 mmol) and aminide **436** (50.7 mg, 0.24 mmol) in 1,2-DCB for 4 h. After purification by flash chromatography [hexane:ethyl acetate (3:2)] compound **463** was isolated as a pale yellow solid (50.0 mg, 68%); mp. 200–202 °C; ^1H NMR (300 MHz, CDCl_3) δ 7.79–7.65 (m, 3H), 7.59–7.51 (m, 1H), 7.45–7.26 (m, 5H), 3.28 (s, 3H), 1.91 (tt, J = 8.2, 5.3 Hz, 1H), 1.16–0.96 (m, 4H); ^{13}C NMR (101 MHz, CDCl_3) δ 150.7 (C), 150.0 (C), 141.1 (C), 135.5 (C), 129.2 (2 \times CH), 127.4 (CH), 127.3 (2 \times CH), 126.9 (C), 124.5 (CH), 124.2 (CH), 122.5 (C), 112.4 (CH), 111.9 (CH), 38.5 (CH_3), 5.9

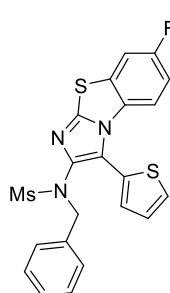
(2×CH₂), 3.8 (CH); IR $\nu_{\text{max}}/\text{cm}^{-1}$ 2922, 1628, 1568, 479, 1395, 1165, 1092, 742; HRMS (ES-TOF): m/z : calcd. for C₁₉H₁₈N₃O₃S: 368.1069 found: 368.1061 [M+H]⁺.

*Imidazo[2,1-*b*]benzothiazole 464*



Following **GP16** using ynamide **279** (47.6 mg, 0.20 mmol) and aminide **437** (54.7 mg, 0.24 mmol) in 1,2-DCB for 4 h. After purification by flash chromatography [hexane:ethyl acetate (3:2)] compound **464** was isolated as a pale yellow solid (50.6 mg, 66%); mp. 174–176 °C; ¹H NMR (300 MHz, CDCl₃) δ 8.13 (d, J = 8.0 Hz, 1H), 7.82–7.66 (m, 3H), 7.50–7.26 (m, 3H), 3.30 (s, 3H), 1.93 (app. quin, J = 5.5 Hz, 1H), 1.23–1.07 (m, 4H); ¹³C NMR (101 MHz, CDCl₃) δ 143.3 (C), 141.2 (C), 139.8 (C), 133.5 (C), 129.6 (C), 129.2 (2×CH), 127.3 (CH), 127.3 (2×CH), 126.8 (C), 126.1 (CH), 124.8 (CH), 124.0 (CH), 114.2 (CH), 38.6 (CH₃), 6.9 (2×CH₂), 4.7 (CH); IR $\nu_{\text{max}}/\text{cm}^{-1}$ 3027, 2931, 1582, 1487, 1377, 1343, 1288, 1166, 774; HRMS (ES-TOF): m/z : calcd. for C₁₉H₁₈N₃O₂S₂: 384.0840 found: 384.0840 [M+H]⁺.

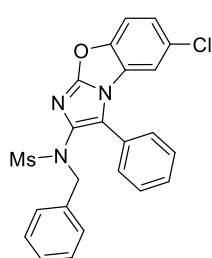
*Imidazo[2,1-*b*]benzothiazole 505*



Following **GP16** using ynamide **540** (58.6 mg, 0.20 mmol) and aminide **480** (58.7 mg, 0.24 mmol) in 1,2-DCB for 1 h. After purification by flash chromatography [hexane:ethyl acetate (4:1)] compound **505** was isolated as a pale green solid (72.5 mg, 79%); mp. 182–184 °C; ¹H NMR (300 MHz, CDCl₃) δ 7.49 (dd, J = 5.2, 1.2 Hz, 1H), 7.40 (dd, J = 7.9, 2.5 Hz, 1H), 7.20–7.07 (m, 5H), 7.05 (d, J = 4.5 Hz, 1H), 6.98–6.88 (m, 2H), 4.75 (s, 3H), 3.19 (s, 3H); ¹³C NMR (101 MHz, CDCl₃) δ 159.7 (d, $J_{\text{C-F}}$ = 246.5 Hz, C), 144.9 (C), 140.1 (C), 135.3 (C), 131.5 (CH), 130.9 (d, $J_{\text{C-F}}$ = 10.0 Hz, C), 129.4 (C), 129.0

(CH), 128.9 (2×CH), 128.3 (2×CH), 127.7 (CH), 127.2 (CH), 126.0 (C), 120.5 (C), 114.8 (d, J_{C-F} = 8.8 Hz, CH), 113.7 (d, J_{C-F} = 24.2 Hz, CH), 111.1 (d, J_{C-F} = 27.2 Hz, CH), 54.9 (CH₃), 38.1 (CH₃); IR $\nu_{\max}/\text{cm}^{-1}$ 3082, 2924, 1609, 1579, 1488, 1338, 1155; HRMS (ES-TOF): m/z : calcd. for C₂₁H₁₆N₃O₂S₃FNa: 480.0286 found: 480.0283 [M+Na]⁺.

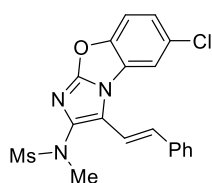
Imidazo[2,1-*b*]benzoxazole 506



Following **GP16** using ynamide **266** (57.5 mg, 0.20 mmol) and aminide **472** (58.6 mg, 0.24 mmol) in 1,2-DCB for 1 h. After purification by flash chromatography [hexane:ethyl acetate (3:1)] compound **506** was isolated as a white solid (78.4 mg, 87%); mp.

168–170 °C; ¹H NMR (400 MHz, CDCl₃) δ 7.46 (d, J = 8.8 Hz, 1H), 7.41–7.36 (m, 3H), 7.36–7.31 (m, 2H), 7.28 (dd, J = 8.8, 2.1 Hz, 1H), 7.22 (d, J = 2.1 Hz, 1H), 7.10–7.03 (m, 1H), 7.00–6.93 (m, 4H), 4.68 (s, 2H), 3.27 (s, 3H); ¹³C NMR (101 MHz, CDCl₃) δ 152.1 (C), 148.6 (C), 134.6 (C), 133.7 (C), 129.6 (C), 129.1 (2×CH), 128.8 (CH), 128.6 (2×CH), 128.5 (2×CH), 127.9 (2×CH), 127.7 (CH), 127.4 (C), 126.5 (C), 124.8 (CH), 123.6 (C), 113.2 (CH), 112.5 (CH), 55.2 (CH₂), 38.3 (CH₃); IR $\nu_{\max}/\text{cm}^{-1}$ 3004, 2923, 1634, 1582, 1335, 1145; HRMS (ES-TOF): m/z : calcd. for C₂₃H₁₈N₃O₃SClNa: 474.0655 found: 474.0648 [M+Na]⁺.

Imidazo[2,1-*b*]benzoxazole 507

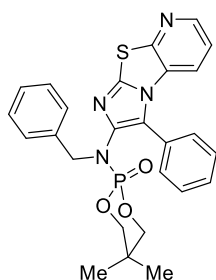


Following **GP16** using ynamide **539** (46.8 mg, 0.20 mmol) and aminide **472** (59.0 mg, 0.24 mmol) in 1,4-dioxane at 90 °C for 1 h.

After cooling down to room temperature the resulting precipitate was filtered off, washed with cold diethyl ether followed by hexane and dried under air, to

afford the pure compound **507** as a white solid (60.3 mg, 75%); mp. 270 °C (degradation); ^1H NMR (400 MHz, CDCl_3) δ 7.74 (d, J = 2.0 Hz, 1H), 7.57 (d, J = 7.7 Hz, 2H), 7.50 (d, J = 9.0 Hz, 1H), 7.41 (app. t, J = 7.7 Hz, 2H), 7.37 (dd, J = 9.0, 2.0 Hz, 1H), 7.35–7.30 (m, 1H), 7.28 (d, J = 16.6 Hz, 1H), 7.19 (d, J = 16.6 Hz, 1H), 3.33 (s, 3H), 3.13 (s, 3H); ^{13}C NMR (101 MHz, CDCl_3) δ 152.4 (C), 148.6 (C), 137.1 (C), 136.3 (C), 131.0 (CH), 129.9 (C), 128.9 (2 \times CH), 128.4 (CH), 127.7 (C), 126.7 (2 \times CH), 125.0 (CH), 121.2 (C), 113.4 (CH), 112.9 (CH), 112.8 (CH), 38.5 (CH_3), 36.3 (CH_3); IR $\nu_{\text{max}}/\text{cm}^{-1}$ 3004, 1632, 1570, 1482, 1335, 1148; HRMS (ES-TOF): m/z : calcd. for $\text{C}_{19}\text{H}_{16}\text{N}_3\text{O}_3\text{SClNa}$: 424.0499 found: 424.0496 $[\text{M}+\text{Na}]^+$.

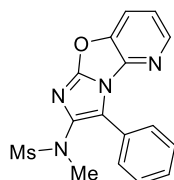
Imidazo[2',1':2,3]thiazolo[5,4-b]pyridine 508



Following **GP16** using ynamide **542** (71.5 mg, 0.20 mmol) and aminide **501** (54.6 mg, 0.24 mmol) in 1,2-DCB for 1 h. After purification by flash chromatography [hexane:ethyl acetate (1:1)] compound **508** was isolated as a white solid (93.3 mg, 92%); mp. 196–198 °C; ^1H NMR (300 MHz, CDCl_3) δ 8.36 (dd, J = 4.8, 1.5 Hz, 1H), 7.46–7.32 (m, 3H), 7.24–7.14 (m, 3H), 7.14–7.00 (m, 6H), 4.56 (d, J = 7.0 Hz, 2H), 4.33 (dd, J = 11.0, 4.6 Hz, 2H), 3.91 (dd, J = 19.3, 11.0 Hz, 2H), 1.12 (s, 3H), 0.92 (s, 3H); ^{13}C NMR (101 MHz, CDCl_3) δ 153.3 (C), 145.5 (CH), 142.5 (C), 139.3 (d, $J_{\text{C-P}}$ = 4.1 Hz, C), 136.7 (d, $J_{\text{C-P}}$ = 4.8 Hz, C), 130.2 (2 \times CH), 129.0 (CH), 128.8 (2 \times CH), 128.5 (2 \times CH), 128.1 (2 \times CH), 127.4 (C), 127.3 (CH), 125.1 (d, $J_{\text{C-P}}$ = 6.4 Hz, C), 120.0 (CH), 119.8 (CH), 76.6 (d, $J_{\text{C-P}}$ = 5.3 Hz, 2 \times CH_2), 53.7 (d, $J_{\text{C-P}}$ = 5.4 Hz, CH_2), 32.1 (d, J = 5.3 Hz, C), 22.1 (CH_3), 21.0 (CH_3); *One resonance for a quaternary carbon was not visible.* IR

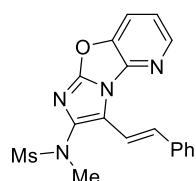
$\nu_{\max}/\text{cm}^{-1}$ 2965, 1487, 1381, 1255, 1056, 1006; HRMS (ES-TOF): m/z : calcd. for $\text{C}_{26}\text{H}_{25}\text{N}_4\text{O}_3\text{S}^{31}\text{PNa}$: 527.1283 found: 527.1281 $[\text{M}+\text{Na}]^+$.

Imidazo[2',1':2,3]oxazolo[4,5-b]pyridine 509



Following **GP16** using ynamide **264** (41.7 mg, 0.20 mmol) and aminide **502** (51.0 mg, 0.24 mmol) in 1,2-DCB for 1 h. After purification by flash chromatography [hexane:ethyl acetate (1:1)] compound **509** was isolated as a white solid (65.4 mg, 95%); mp. 240–242 °C; ^1H NMR (400 MHz, CDCl_3) δ 8.35 (dd, $J = 5.1, 1.2$ Hz, 1H), 8.21 (d, $J = 7.3$ Hz, 2H), 7.83 (dd, $J = 8.2, 1.2$ Hz, 1H), 7.52 (app. t, $J = 7.5$ Hz, 2H), 7.41 (t, $J = 7.4$ Hz, 1H), 7.34 (dd, $J = 8.2, 5.1$ Hz, 1H), 3.27 (s, 3H), 3.21 (s, 3H); ^{13}C NMR (101 MHz, CDCl_3) δ 151.7 (C), 143.7 (CH), 143.6 (C), 141.9 (C), 136.3 (C), 128.5 (2 \times CH), 128.5 (CH), 128.3 (2 \times CH), 126.5 (C), 123.1 (C), 120.2 (CH), 119.5 (CH), 38.7 (CH_3), 37.1 (CH_3); HRMS (ES-TOF): m/z : calcd. for $\text{C}_{16}\text{H}_{14}\text{N}_4\text{O}_3\text{SNa}$: 365.0684 found: 365.0686 $[\text{M}+\text{Na}]^+$.

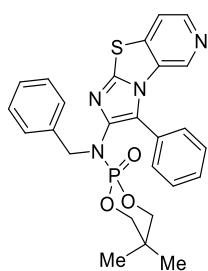
Imidazo[2',1':2,3]oxazolo[4,5-b]pyridine 510



Following **GP16** using ynamide **539** (47.14 mg, 0.20 mmol) and aminide **502** (50.97 mg, 0.24 mmol) in 1,4-dioxane at 90 °C for 1 h. After purification by flash chromatography [hexane:ethyl acetate (1:1)] compound **510** was isolated as a white solid (55.83 mg, 76%); mp. 246–248 °C; ^1H NMR (300 MHz, CDCl_3) δ 8.49–8.35 (m, 2H), 7.84 (dd, $J = 8.2, 1.3$ Hz, 1H), 7.63 (d, $J = 7.3$ Hz, 2H), 7.42–7.34 (m, 3H), 7.32–7.29 (m, 1H), 7.28–7.24 (m, 1H), 3.37 (s, 3H), 3.12 (s, 3H); ^{13}C NMR (101 MHz, CDCl_3) δ 152.1 (C), 143.7 (CH), 143.5 (C), 141.7 (C), 137.4 (C), 137.2 (C), 131.4 (CH), 128.6 (2 \times CH), 127.8 (CH), 126.9 (2 \times CH), 123.9 (C), 120.2 (CH), 119.5 (CH), 112.6 (CH), 38.7 (CH_3), 36.2 (CH_3); IR $\nu_{\max}/\text{cm}^{-1}$ 3093,

3021, 1633, 1581, 1471, 1453, 1341, 1149, 959; HRMS (ES-TOF): m/z : calcd. for $C_{18}H_{16}N_4O_3SNa$: 391.0841 found: 391.0839 $[M+Na]^+$.

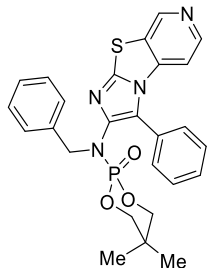
Imidazo[2',1':2,3]thiazolo[4,5-c]pyridine 511



Following **GP16** using ynamide **542** (70.9 mg, 0.20 mmol) and aminide **503** (54.7 mg, 0.24 mmol) in 1,2-DCB for 8 h. After purification by flash chromatography [ethyl acetate:methanol (95:5)] compound **511** was isolated as a white solid (65.8 mg, 65%); mp.

119–121 °C; 1H NMR (300 MHz, $CDCl_3$) δ 8.41 (d, $J = 5.3$ Hz, 1H), 8.31 (d, $J = 0.4$ Hz, 1H), 7.63 (dd, $J = 5.3, 0.4$ Hz, 1H), 7.49–7.32 (m, 3H), 7.24–7.17 (m, 2H), 7.17–7.01 (m, 5H), 4.56 (d, $J = 7.1$ Hz, 2H), 4.34 (dd, $J = 10.9, 4.1$ Hz, 2H), 3.89 (dd, $J = 19.8, 10.9$ Hz, 2H), 1.12 (s, 3H), 0.90 (s, 3H); ^{13}C NMR (101 MHz, $CDCl_3$) δ 144.2 (CH), 143.1 (C), 142.8 (C), 140.1 (d, $J_{C-P} = 3.5$ Hz, C), 139.6 (CH), 136.7 (d, $J_{C-P} = 4.7$ Hz, C), 134.6 (CH), 130.6 (C), 130.2 (2 \times CH), 129.2 (C), 128.8 (2 \times CH), 128.7 (2 \times CH), 128.1 (2 \times C), 127.3 (CH), 125.5 (d, $J_{C-P} = 6.2$ Hz, C), 118.7 (CH), 76.6 (d, $J_{C-P} = 6.1$ Hz, 2 \times CH₂), 53.8 (d, $J = 5.3$ Hz, CH₂), 32.1 (d, $J_{C-P} = 5.2$ Hz, C), 22.2 (CH₃), 20.9 (CH₃); IR ν_{max}/cm^{-1} 2922, 1577, 1489, 1251, 1056, 1001; HRMS (ES-TOF): m/z : calcd. for $C_{26}H_{25}N_4O_3S^{31}PNa$: 527.1283 found: 527.1284 $[M+Na]^+$.

Imidazo[2',1':2,3]thiazolo[5,4-c]pyridine 512

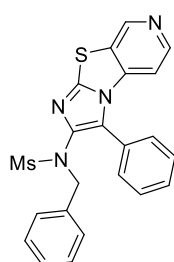


Following **GP16** using ynamide **542** (71.2 mg, 0.20 mmol) and aminide **504** (55.2 mg, 0.24 mmol) in 1,2-DCB for 22 h. After purification by flash chromatography [ethyl acetate:methanol (9:1)] compound **512** was isolated as a white solid (21.9 mg, 22%); mp.

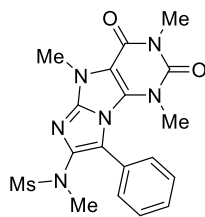
100–102 °C; 1H NMR (300 MHz, $CDCl_3$) δ 8.90 (s, 1H), 8.35 (d, $J = 5.6$ Hz, 1H), 7.53–

7.36 (m, 3H), 7.24–7.01 (m, 7H), 6.90 (d, $J = 5.6$ Hz, 1H), 4.58 (d, $J = 7.1$ Hz, 2H), 4.37 (dd, $J = 10.9, 4.2$ Hz, 2H), 3.92 (dd, $J = 19.7, 10.9$ Hz, 2H), 1.15 (s, 3H), 0.93 (s, 3H); ^{13}C NMR (101 MHz, CDCl_3) δ 146.1 (CH), 145.1 (CH), 144.8 (C), 140.8 (d, $J_{\text{C-P}} = 3.2$ Hz, C), 138.6 (C), 136.6 (d, $J_{\text{C-P}} = 5.0$ Hz, C), 130.3 (2 \times CH), 129.2 (CH), 128.8 (2 \times CH), 128.5 (2 \times CH), 128.1 (2 \times CH), 127.3 (CH), 127.1 (d, $J_{\text{C-P}} = 8.3$ Hz, C), 125.4 (d, $J_{\text{C-P}} = 5.9$ Hz, C), 108.2 (CH), 76.6 (d, $J_{\text{C-P}} = 5.3$ Hz, 2 \times CH₂), 53.7 (d, $J_{\text{C-P}} = 5.2$ Hz, CH₂), 32.1 (d, $J_{\text{C-P}} = 5.1$ Hz, C), 22.1 (CH₃), 20.9 (CH₃); *One resonance for a quaternary carbon was not visible*; IR $\nu_{\text{max}}/\text{cm}^{-1}$ 2935, 1706, 1569, 1489, 1248, 1052; HRMS (ES-TOF): m/z : calcd. for $\text{C}_{26}\text{H}_{25}\text{N}_4\text{O}_3\text{S}^{31}\text{PNa}$: 527.1283 found: 527.1285 $[\text{M}+\text{Na}]^+$.

Imidazo[2',1':2,3]thiazolo[5,4-c]pyridine 513



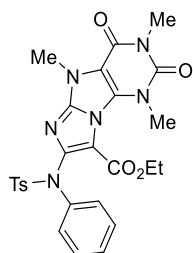
Following **GP16** using ynamide **266** (56.0 mg, 0.20 mmol) and aminide **504** (54.8 mg, 0.24 mmol) in 1,2-DCB for 22 h. After purification by flash chromatography [hexane:ethyl acetate (3:7)] compound **513** was isolated as a white solid (25.0 mg, 29%); mp. 102–104 °C; ^1H NMR (300 MHz, CDCl_3) δ 8.93 (s, 1H), 8.35 (d, $J = 5.6$ Hz, 1H), 7.51–7.43 (m, 1H), 7.36 (app. t, $J = 7.4$ Hz, 2H), 7.18–7.09 (m, 3H), 7.03 (app. t, $J = 7.4$ Hz, 2H), 7.06–6.96 (m, 2H), 6.90 (d, $J = 5.6$ Hz, 1H), 4.69 (s, 2H), 3.25 (s, 3H); ^{13}C NMR (101 MHz, CDCl_3) δ 147.7 (C), 146.3 (CH), 145.2 (CH), 139.3 (C), 138.5 (C), 134.8 (C), 130.3 (2 \times CH), 129.4 (CH), 129.1 (2 \times CH), 128.5 (2 \times CH), 128.2 (2 \times CH), 127.7 (CH), 127.0 (C), 126.2 (C), 108.4 (CH), 55.1 (CH₂), 38.3 (CH₃); *One resonance for a quaternary carbon was not visible*; IR $\nu_{\text{max}}/\text{cm}^{-1}$ 2923, 1572, 1491, 1339, 1151, 960; HRMS (ES-TOF): m/z : calcd. for $\text{C}_{22}\text{H}_{18}\text{N}_4\text{O}_2\text{S}_2\text{Na}$: 457.0769 found: 457.0775 $[\text{M}+\text{Na}]^+$.

Imidazo[1,2-*e*]purine 539

Following **GP16** using ynamide **264** (41.8 mg, 0.20 mmol) and aminide **538** (68.8 mg, 0.24 mmol) in 1,4-dioxane at 90 °C for 24 h.

After purification by flash chromatography [ethyl acetate (100%)] compound **539** was isolated as a white solid (53.2 mg, 64%); mp.

280–282 °C; ^1H NMR (300 MHz, CDCl_3) δ 7.56–7.51 (m, 2H), 7.49–7.45 (m, 3H), 3.98 (s, 3H), 3.42 (s, 3H), 3.16 (s, 3H), 3.11 (s, 3H), 2.92 (s, 3H); ^{13}C NMR (101 MHz, CDCl_3) δ 155.4 (C), 150.5 (C), 145.6 (C), 141.6 (C), 131.1 (2 \times CH), 130.6 (C), 129.7 (CH), 129.1 (2 \times CH), 128.9 (C), 118.3 (C), 107.1 (C), 38.6 (CH_3), 37.3 (CH_3), 35.5 (CH_3), 31.1 (CH_3), 28.4 (CH_3); IR $\nu_{\text{max}}/\text{cm}^{-1}$ 2956, 1706, 1670, 1642, 1343, 1153; HRMS (ES-TOF): m/z : calcd. for $\text{C}_{18}\text{H}_{20}\text{N}_6\text{O}_4\text{SNa}$: 439.1164 found: 439.1160 $[\text{M}+\text{Na}]^+$.

Imidazo[1,2-*e*]purine 540

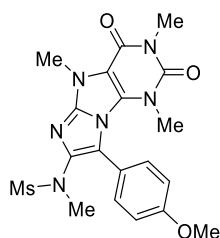
Following **GP16** using ynamide **541** (69.4 mg, 0.20 mmol) and aminide **538** (69.3 mg, 0.24 mmol) in 1,4-dioxane at 90 °C for 24 h.

After purification by flash chromatography [hexane:ethyl acetate (3:2)] compound **540** was isolated as a white solid (54.0 mg, 49%); mp. 208–

210 °C; ^1H NMR (300 MHz, CDCl_3) δ 7.70 (d, J = 8.3 Hz, 2H), 7.47–7.41 (m, 2H), 7.28–7.22 (m, 5H), 4.42 (q, J = 7.1 Hz, 2H), 3.98 (s, 3H), 3.64 (s, 3H), 3.44 (s, 3H), 2.42 (s, 3H), 1.50 (t, J = 7.1 Hz, 3H); ^{13}C NMR (101 MHz, CDCl_3) δ 159.7 (C), 155.4 (C), 151.0 (C), 150.1 (C), 146.5 (C), 143.7 (C), 139.8 (C), 136.2 (C), 132.1 (C), 129.1 (2 \times CH), 128.8 (2 \times CH), 128.7 (2 \times CH), 128.1 (2 \times CH), 127.7 (CH), 112.5 (C), 107.7 (C), 61.8 (CH_2), 36.5 (CH_3), 31.4 (CH_3), 28.4 (CH_3), 21.6 (CH_3), 14.4 (CH_3); IR

$\nu_{\max}/\text{cm}^{-1}$ 2985, 1707, 1666, 1638, 1497, 1090; HRMS (ES-TOF): m/z : calcd. for $\text{C}_{26}\text{H}_{26}\text{N}_6\text{O}_6\text{SNa}$: 573.1532 found: 573.1534 $[\text{M}+\text{Na}]^+$.

*Imidazo[1,2-*e*]purine 541*



Following **GP16** using ynamide **543** (47.7 mg, 0.20 mmol) and aminide **538** (68.5 mg, 0.24 mmol) in 1,4-dioxane at 90 °C for 4 h.

After purification by flash chromatography [ethyl acetate (100%)]

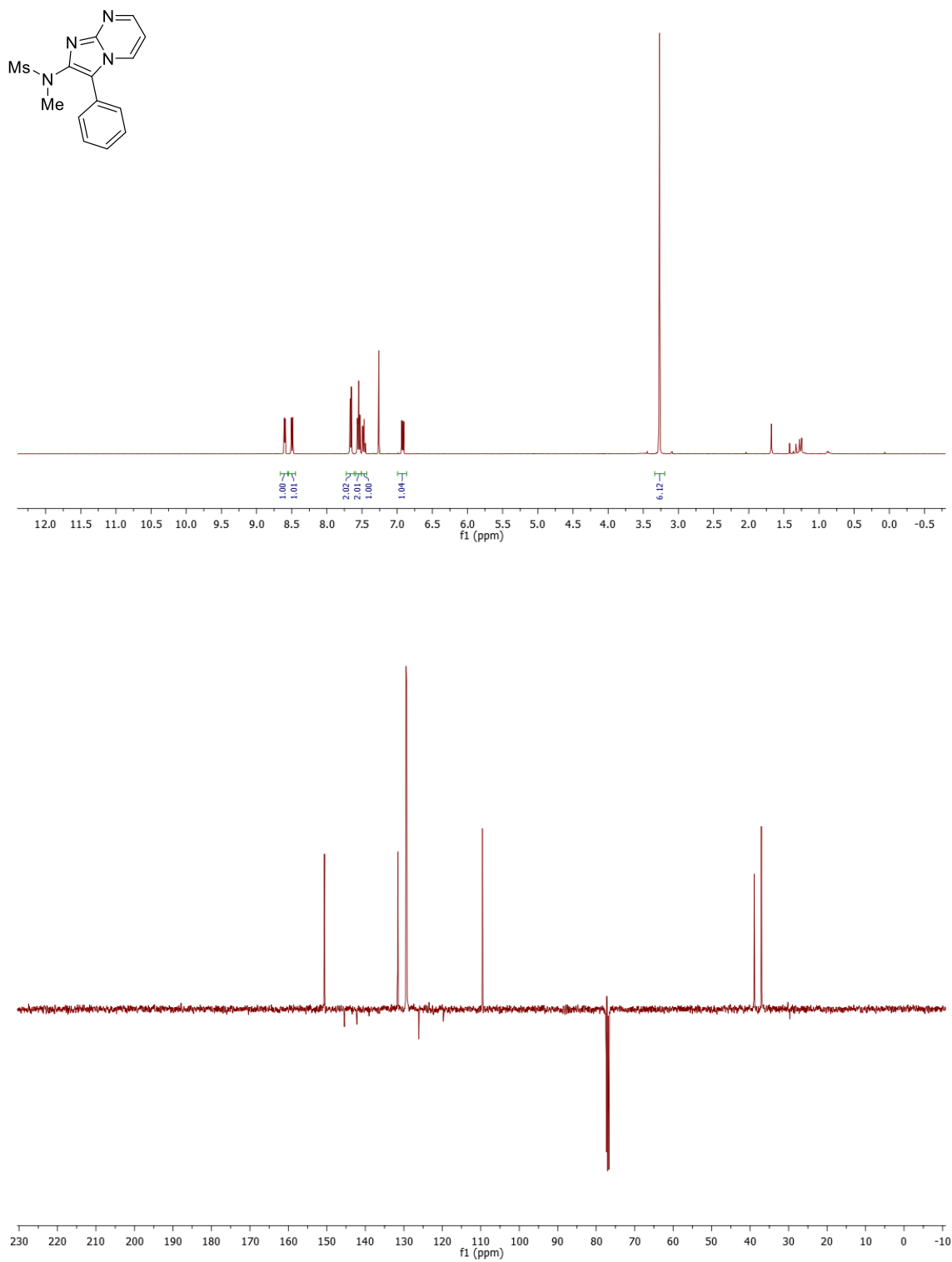
compound **541** was isolated as a white solid (67.5 mg, 75%); mp.

258–260 °C; ^1H NMR (300 MHz, CDCl_3) δ 7.44 (d, J = 8.8 Hz, 2H), 6.98 (d, J = 8.8 Hz, 2H), 3.97 (s, 3H), 3.86 (s, 3H), 3.42 (s, 3H), 3.16 (s, 3H), 3.12 (s, 3H), 2.97 (s, 3H); ^{13}C NMR (101 MHz, CDCl_3) δ 160.6 (C), 155.4 (C), 150.4 (C), 145.4 (C), 141.5 (C), 132.7 (2 \times CH), 130.7 (C), 120.8 (C), 118.2 (C), 114.5 (2 \times CH), 106.9 (C), 55.3 (CH₃), 38.6 (CH₃), 37.3 (CH₃), 35.5 (CH₃), 31.1 (CH₃), 28.4 (CH₃); IR $\nu_{\max}/\text{cm}^{-1}$ 3029, 2945, 1706, 1670, 1640, 1489, 1333; HRMS (ES-TOF): m/z : calcd. for $\text{C}_{19}\text{H}_{22}\text{N}_6\text{O}_5\text{SNa}$: 469.1270 found: 469.1269 $[\text{M}+\text{Na}]^+$.

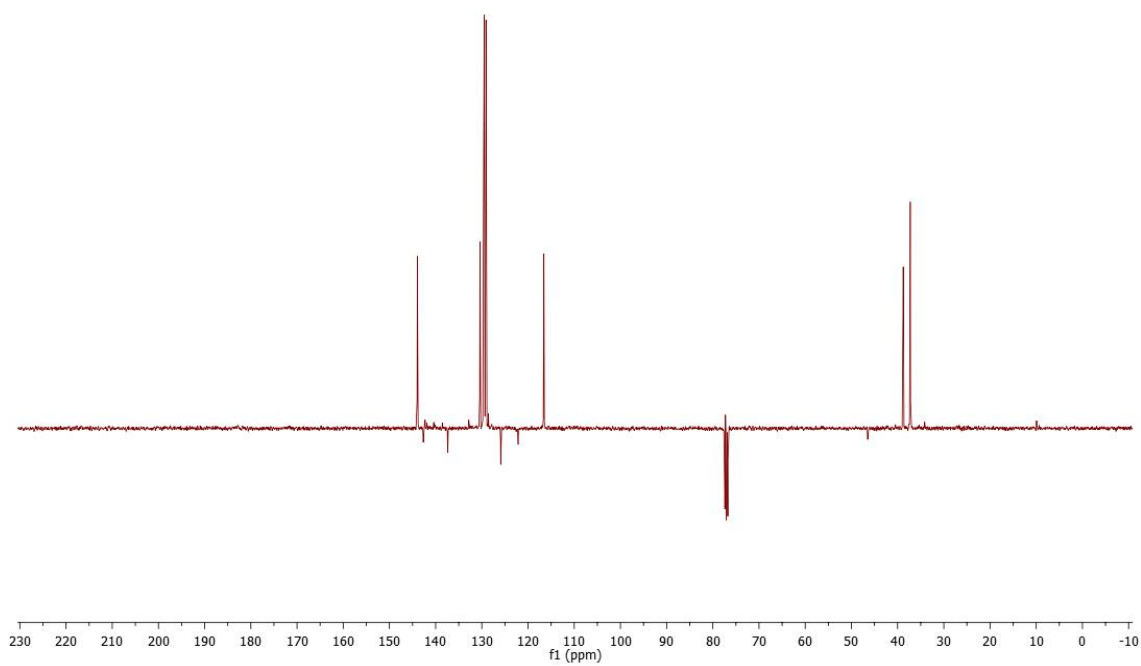
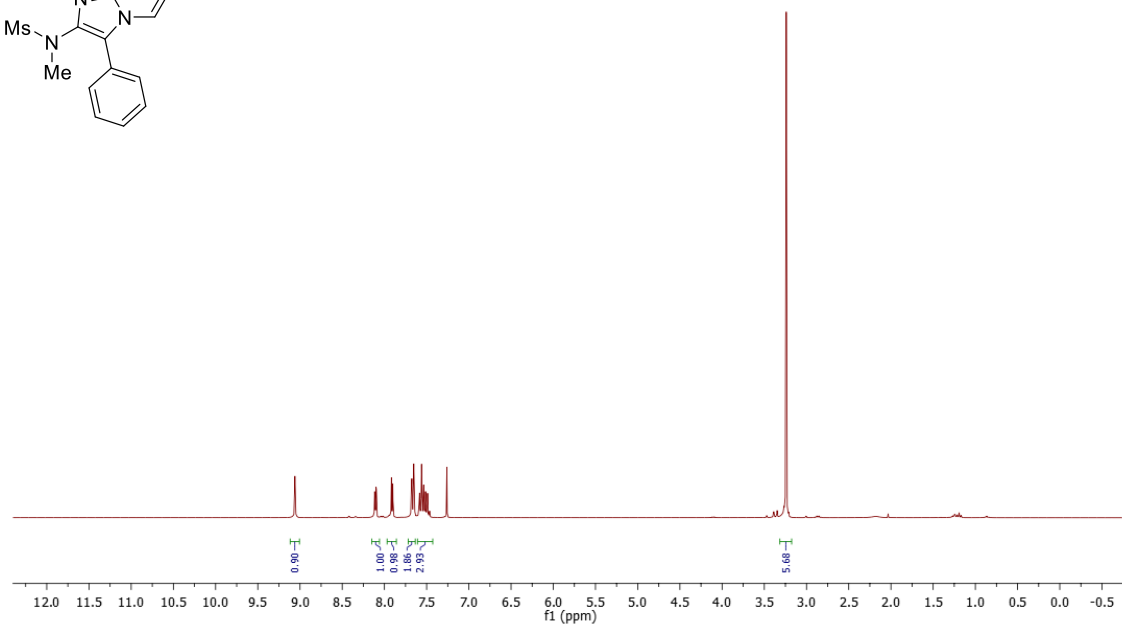
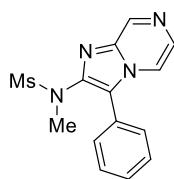
Appendix 1

Appendix 1.1 Selected NMR Spectra

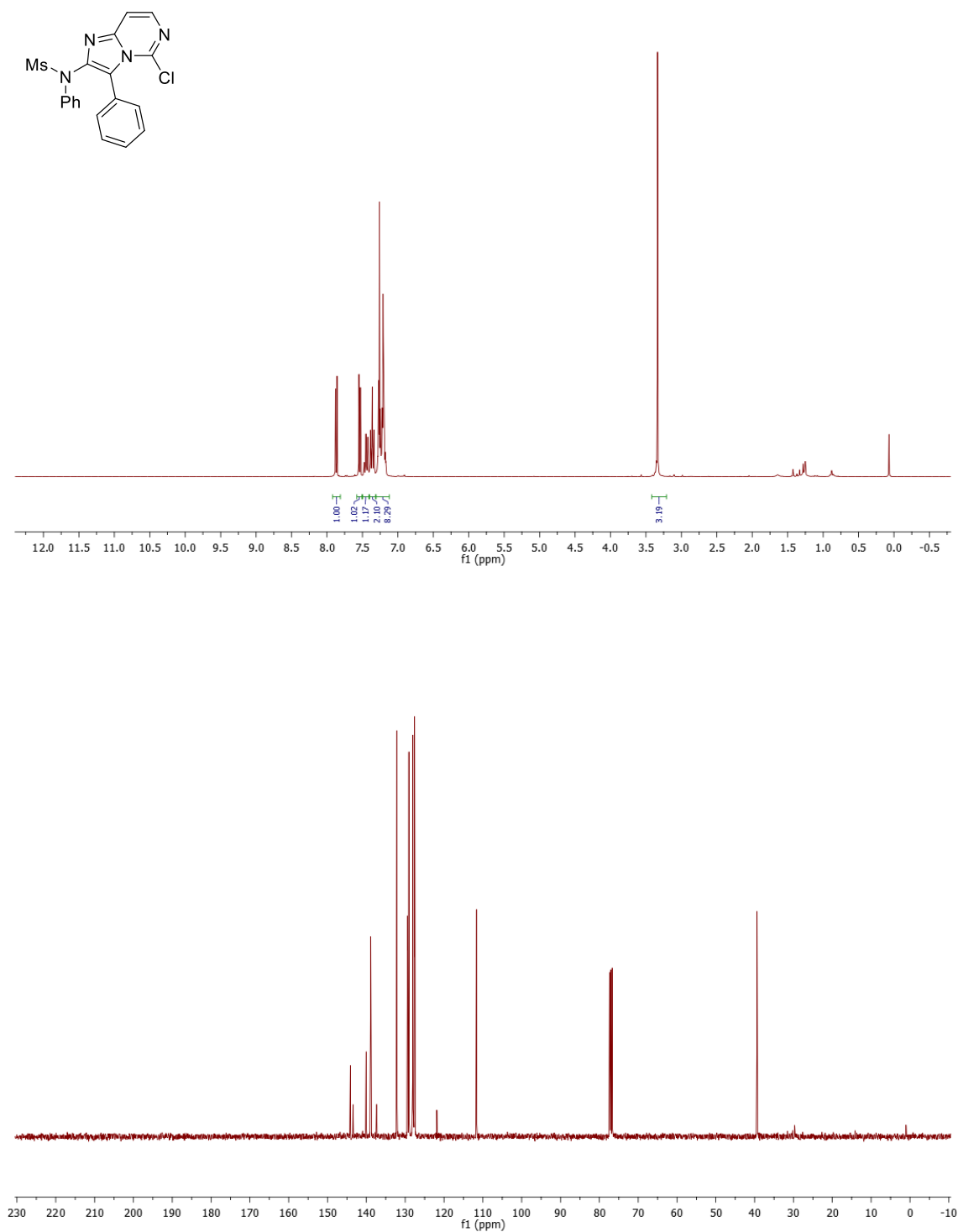
284 - ^1H -NMR (300 MHz, CDCl_3) and ^{13}C -NMR (Pendant, 101 MHz, CDCl_3)



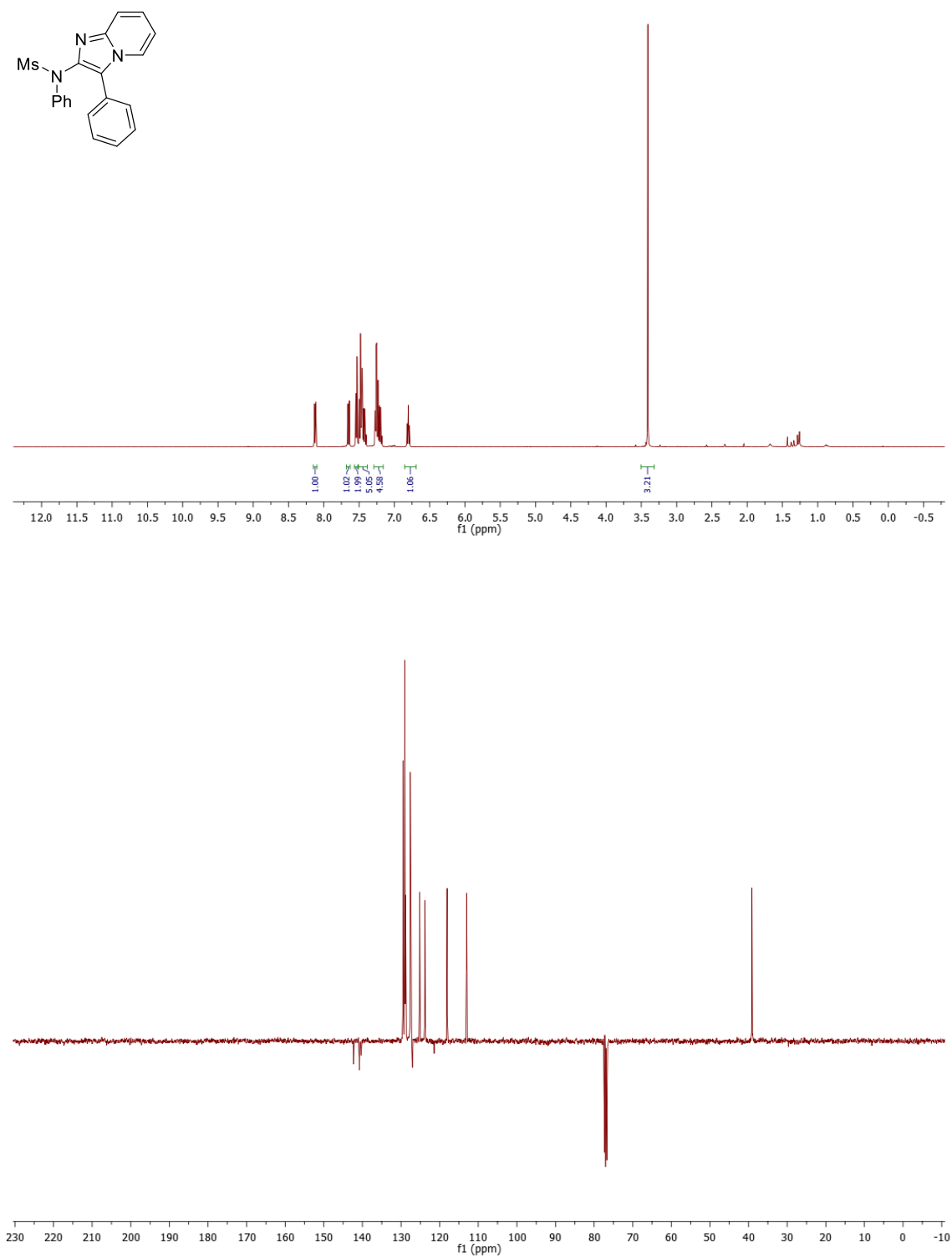
396 - ^1H -NMR (300 MHz, CDCl_3) and ^{13}C -NMR (Pendant, 101 MHz, CDCl_3)



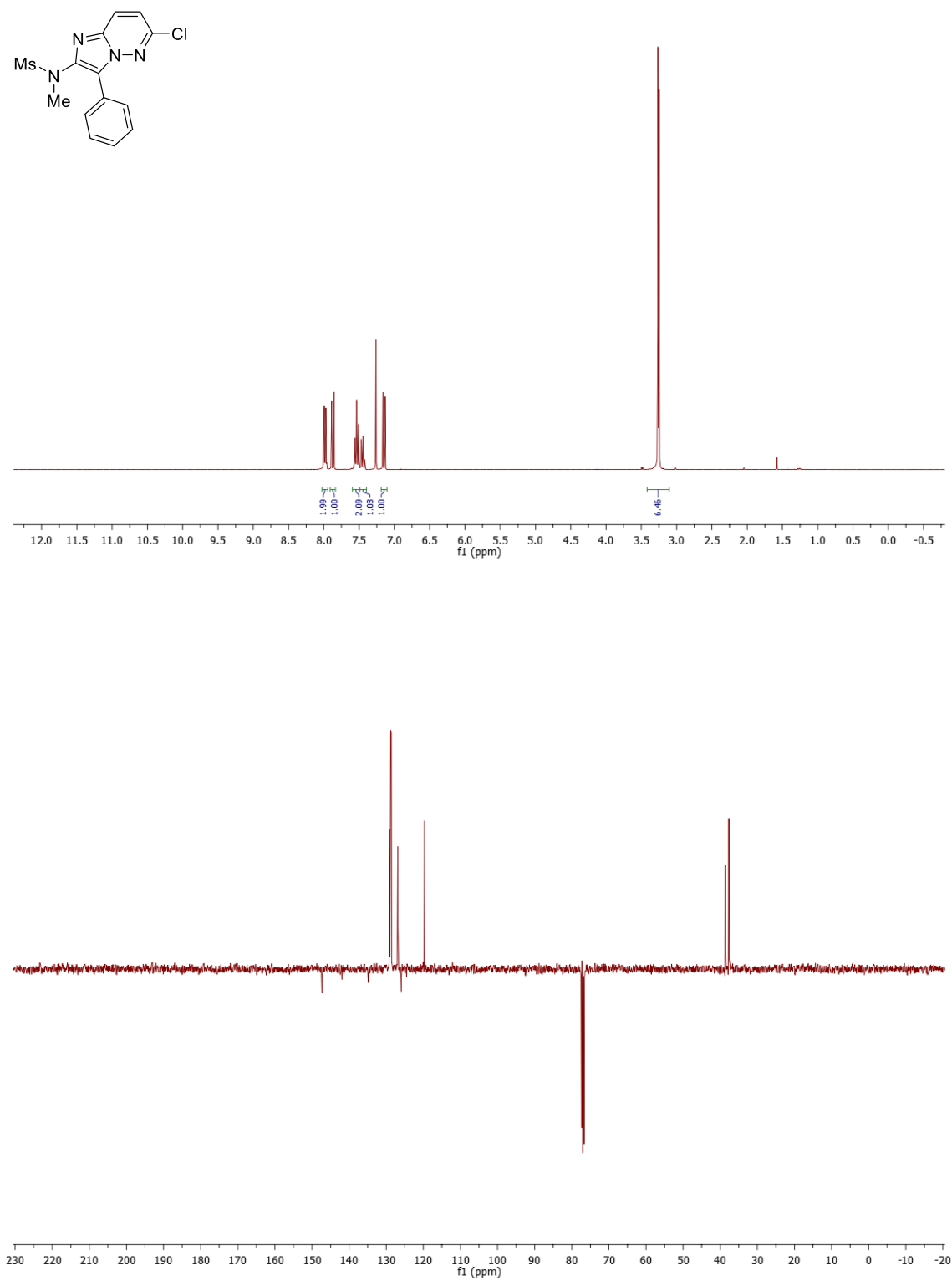
398 - ^1H -NMR (300 MHz, CDCl_3) and ^{13}C -NMR (UDEFT, 101 MHz, CDCl_3)



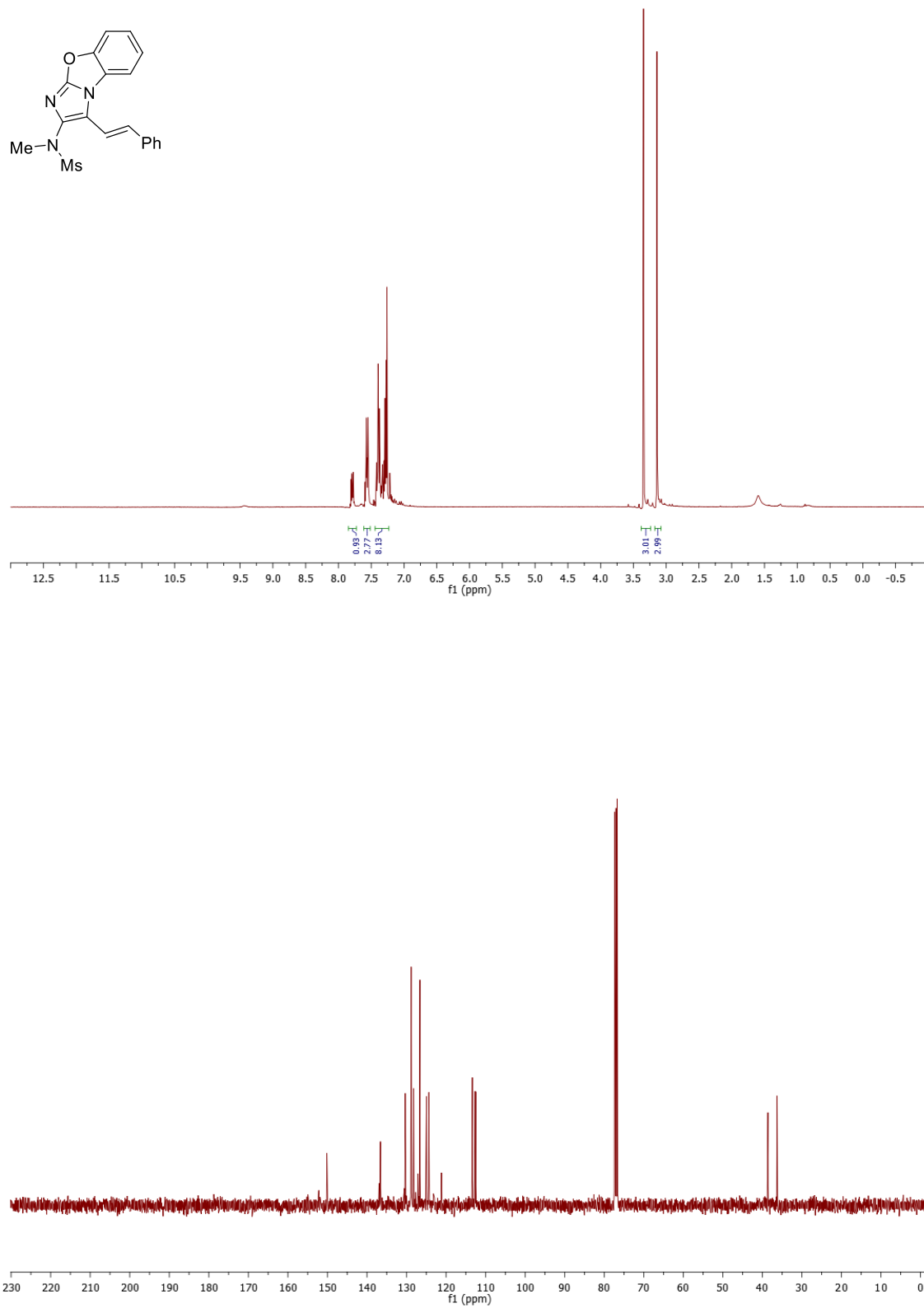
403 - ^1H -NMR (300 MHz, CDCl_3) and ^{13}C -NMR (Pendant, 101 MHz, CDCl_3)



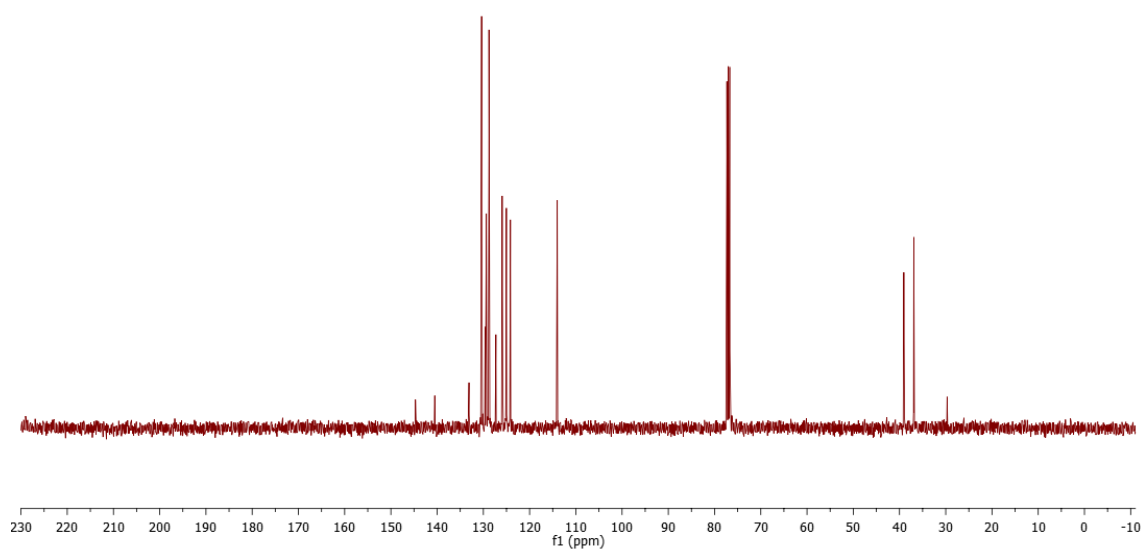
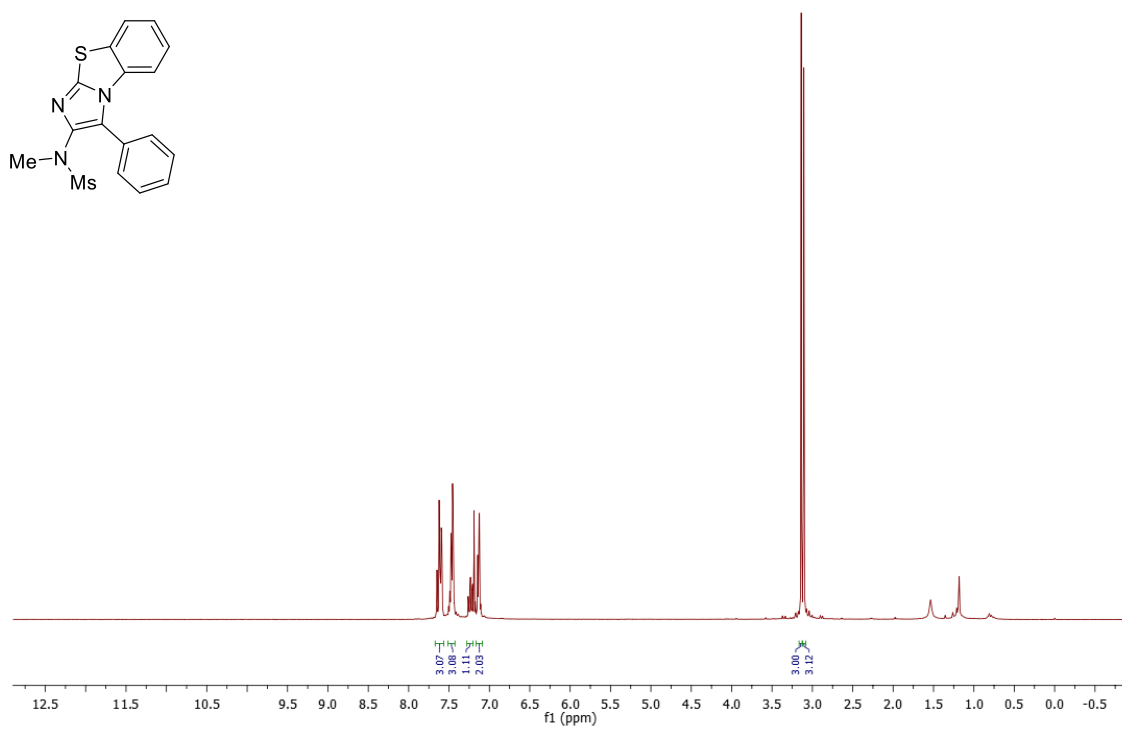
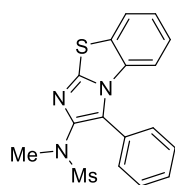
405 - ^1H -NMR (300 MHz, CDCl_3) and ^{13}C -NMR (Pendant, 101 MHz, CDCl_3)



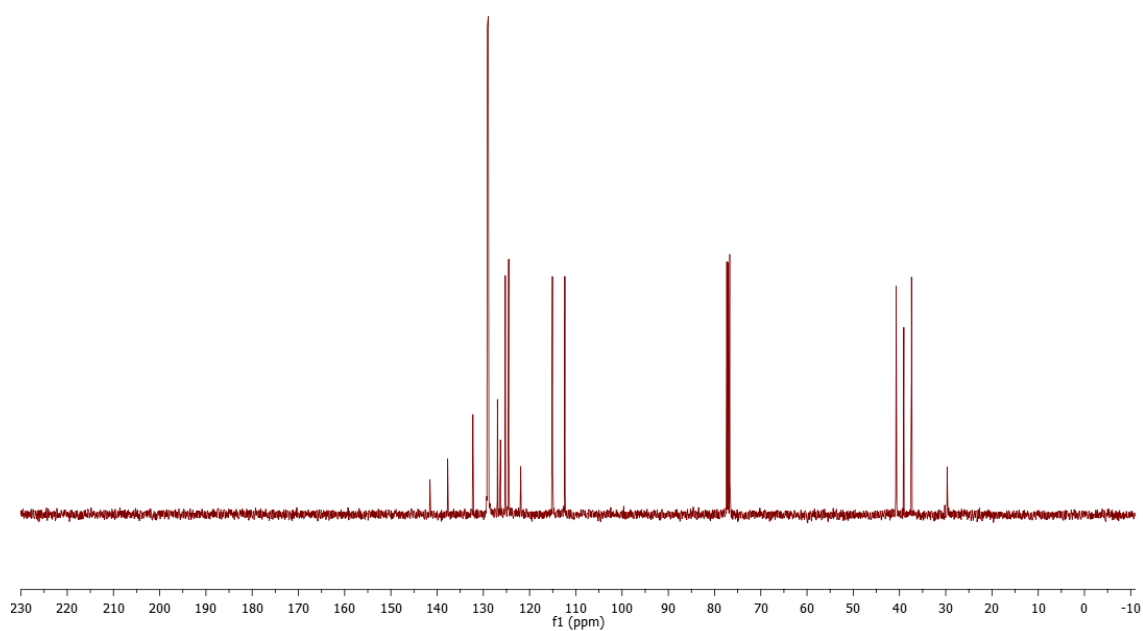
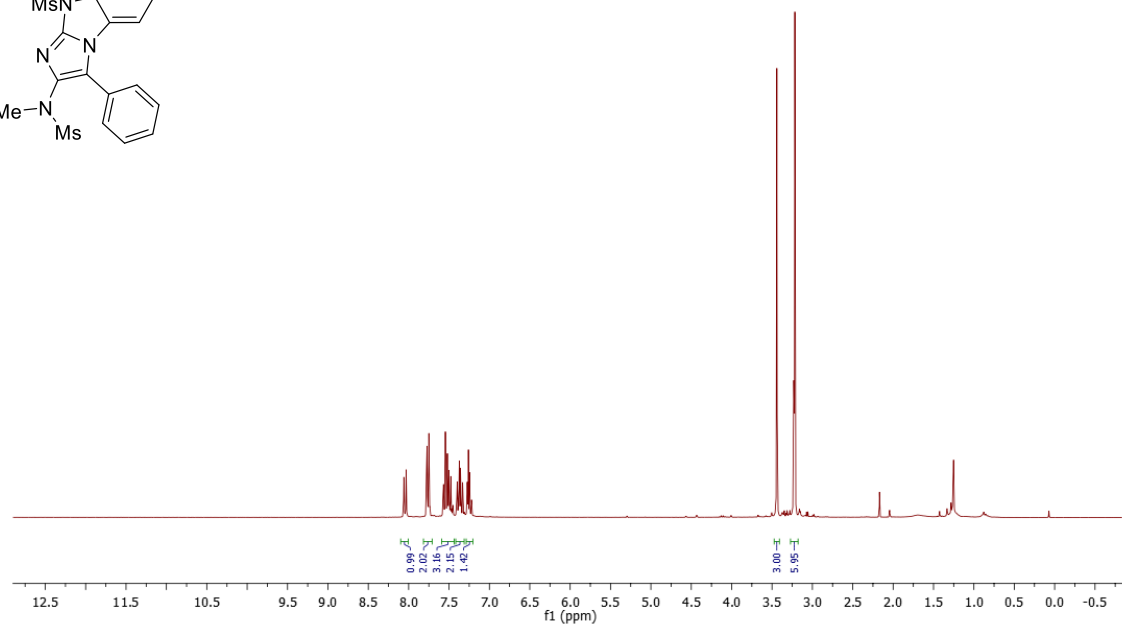
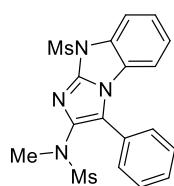
462 - ^1H -NMR (300 MHz, CDCl_3) and ^{13}C -NMR (UDEFT, 101 MHz, CDCl_3)



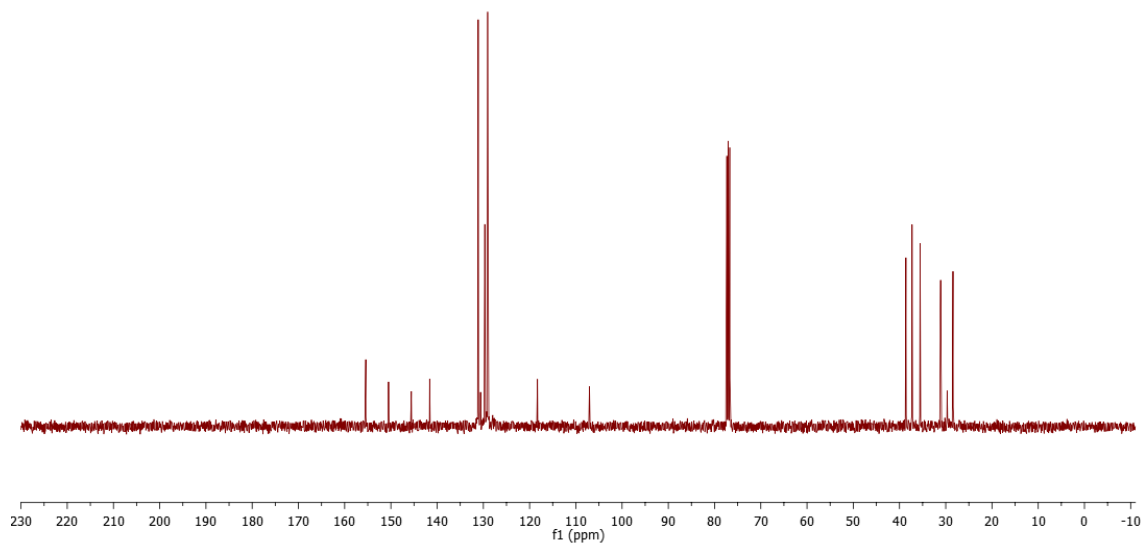
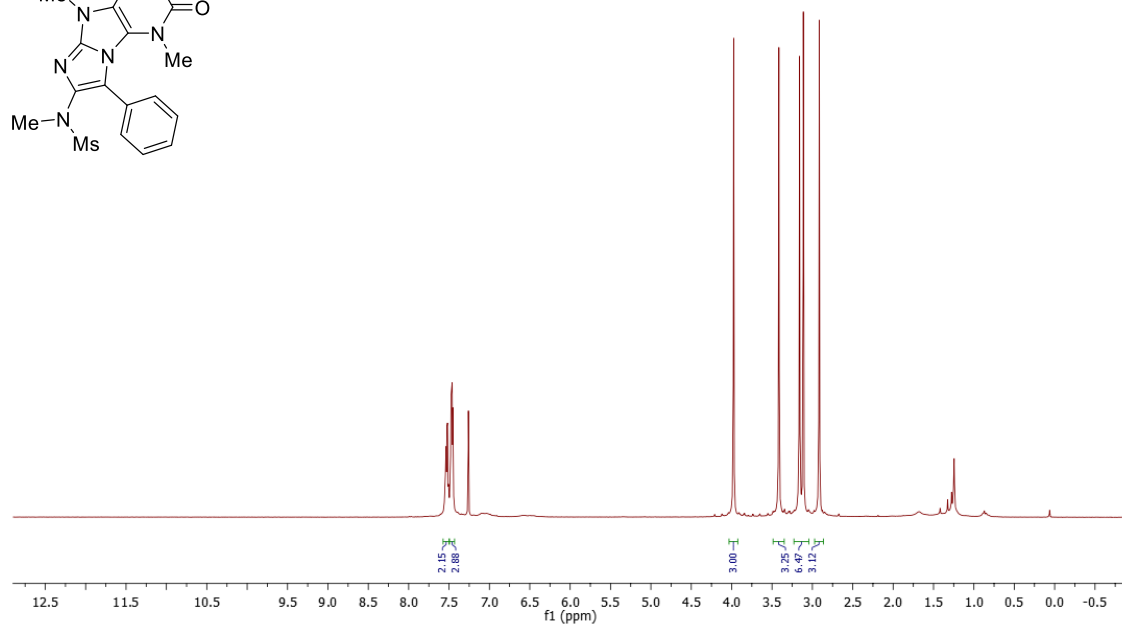
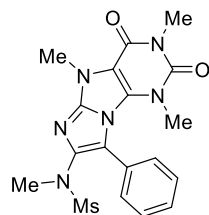
452 - ^1H -NMR (300 MHz, CDCl_3) and ^{13}C -NMR (UDEFT, 101 MHz, CDCl_3)



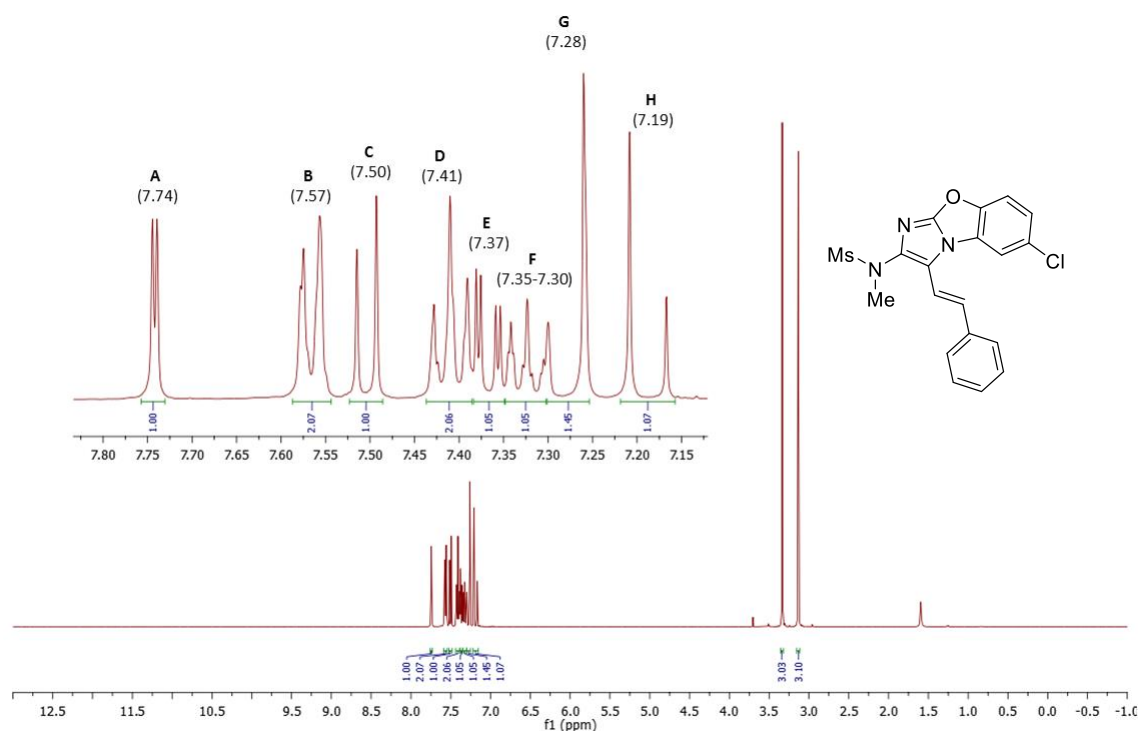
446 - ^1H -NMR (300 MHz, CDCl_3) and ^{13}C -NMR (UDEFT, 101 MHz, CDCl_3)



539 - ^1H -NMR (300 MHz, CDCl_3) and ^{13}C -NMR (UDEFT, 101 MHz, CDCl_3)



Appendix 1.2 Assignment of the structure for compound 507

 $^1\text{H-NMR}$:Figure 15: $^1\text{H-NMR}$ spectrum for compound 507

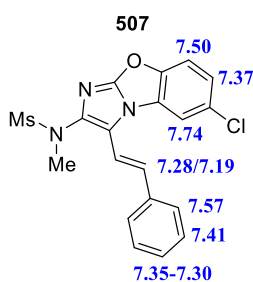
$^1\text{H NMR}$ (300 MHz, CDCl_3) δ 7.74 (d, $J = 2.0$ Hz, 1H), 7.57 (d, $J = 7.7$ Hz, 2H), 7.50 (d, $J = 9.0$ Hz, 1H), 7.41 (app. t, $J = 7.7$ Hz, 2H), 7.37 (dd, $J = 9.0, 2.0$ Hz, 1H), 7.35–7.30 (m, 1H), 7.28 (d, $J = 16.6$ Hz, 1H), 7.19 (d, $J = 16.6$ Hz, 1H), 3.33 (s, 3H), 3.13 (s, 3H)

Key correlations from $^1\text{H-NMR}$ spectrum; Resonances in the spectra have been labelled with letters for clarity:

- A (δ 7.74): aromatic proton splitted as a doublet with a J value of 2.0 Hz. This is the H surrounded by the chlorine atom and the oxazole ring in the imidazo[2,1-

a]benzoxazole core. The small splitting is due to the 4J coupling with **E** (δ 7.37), which is also coupled with **C** (δ 7.50) with a $^3J = 9.0$ Hz.

- **B** (δ 7.57): two equivalent aromatic protons from the phenyl fragment. The splitting as an apparent doublet ($^3J = 7.6$ Hz) points towards the atoms in *ortho* position of the ring. Therefore, **D** (δ 7.41) corresponds to the two protons in *meta*-position and **F** (δ 7.35–7.30) to the one in *para*-position.
- **G** (δ 7.28) and **H** (δ 7.19) correspond to the olefinic system and are coupled between themselves with a $^3J_{\text{Trans}} = 16.6$ Hz. The resonance for the residual CHCl_3 is merged into **G**. The assignment of **G** and **H** was done through 2D-experiments.



HSQC:

^{13}C NMR (101 MHz, CDCl_3) δ 152.4 (C), 148.6 (C), 137.1 (C), 136.3 (C), 131.0 (CH), 129.9 (C), 128.9 (2 \times CH), 128.4 (CH), 127.7 (C), 126.7 (2 \times CH), 125.0 (CH), 121.2 (C), 113.4 (CH), 112.9 (CH), 112.8 (CH), 38.5 (CH_3), 36.3 (CH_3)

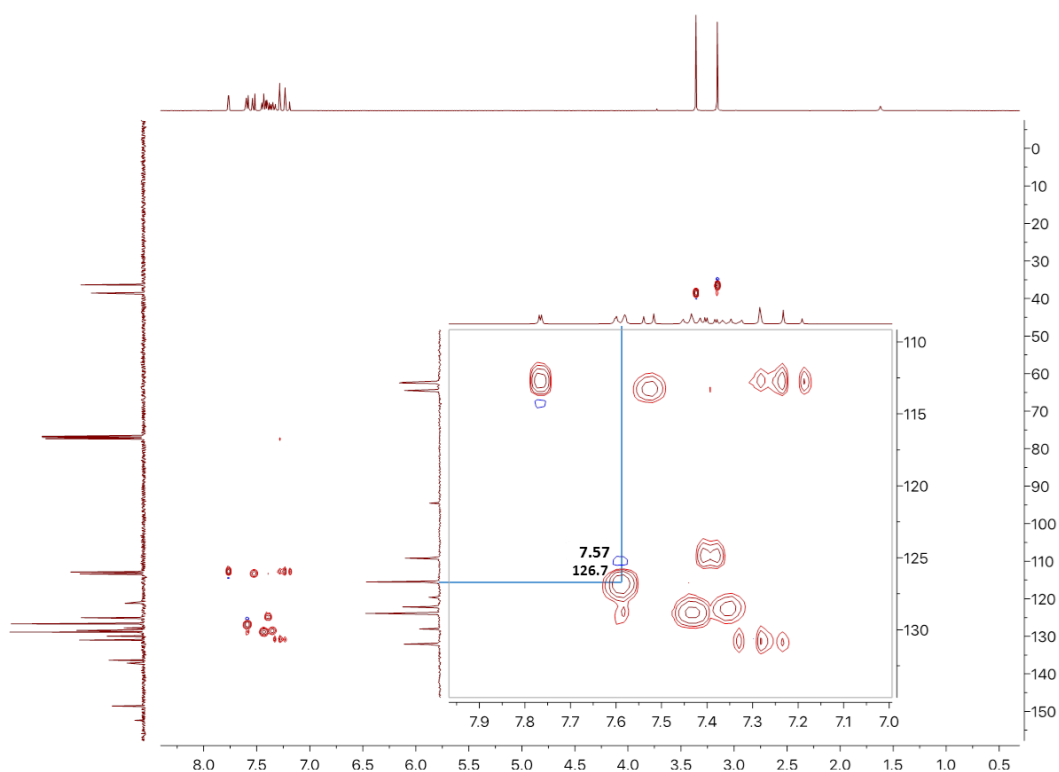
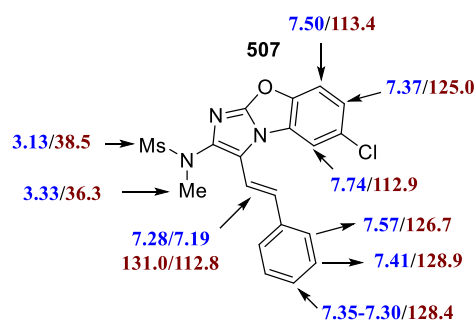


Figure 16: HSQC spectroscopy experiment for compound 507

HSQC spectroscopic experiments indicate the $^1J_{\text{C-H}}$ coupling. For instance, the aromatic proton at 7.57 ppm (**B**) can be seen directly connected to the carbon at 126.7 ppm as shown in the figure with the blue lines. Following the same analysis for every resonance, each proton was matched with its corresponding carbon.



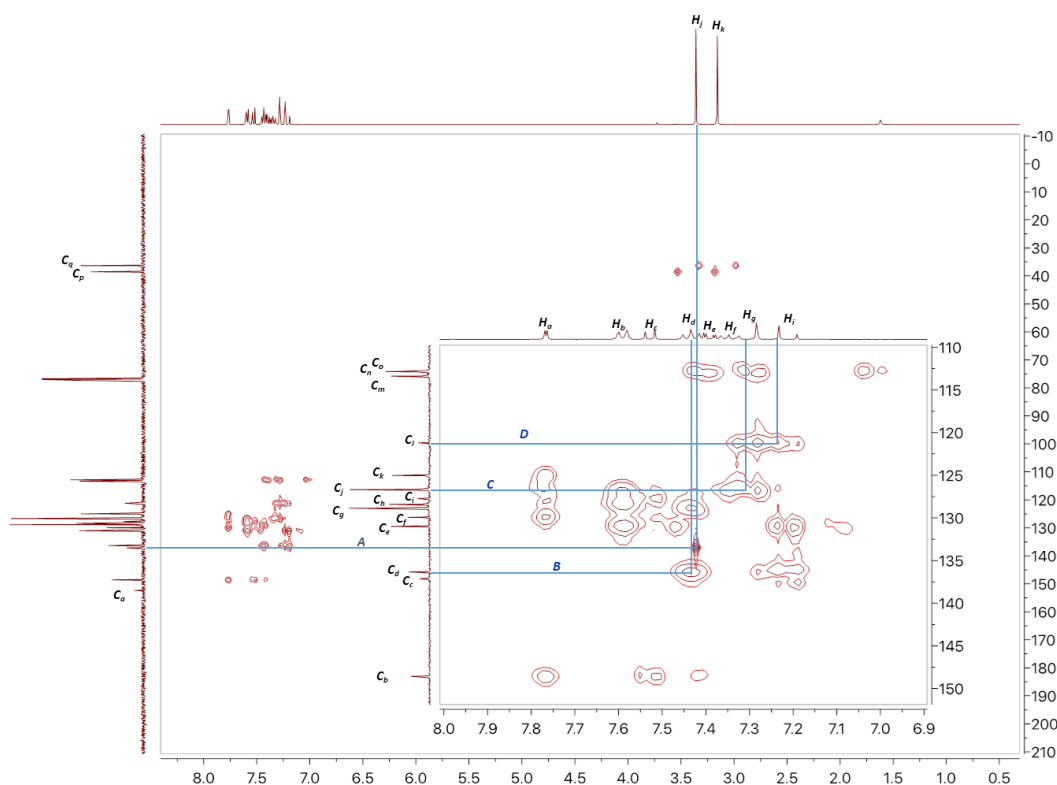
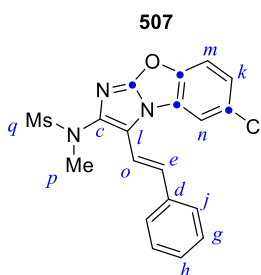
HMBC:

Figure 17: HMBC spectroscopy experiment for compound **507**

HMBC spectroscopic experiments indicate the $^3J_{\text{C-H}}$ coupling and in occasions, $^2J_{\text{C-H}}$ and $^1J_{\text{C-H}}$. Key correlations for the assignment of the carbocyclic scaffold of **507** (indicated with blue lines); Resonances in both axes of the spectra have been labelled with letters relative to the order in which they appear:

- The methyl protons in $\underline{H_j}$ correlates with $\underline{C_c}$. This indicates that the sulfonamide group is attached to $\underline{C_c}$ in the imidazo[2,1-*a*]benzoxazole core.
- Correlation $\underline{H_d} - \underline{C_d}$. Carbon $\underline{C_d}$ corresponds to the *ipso*-position in the phenyl fragment.
- Correlation $\underline{H_g} - \underline{C_j}$. This allows discerning between the two olefinic signals. $\underline{H_g}$ is the closest to the phenyl group.

- Correlation $\underline{H}_j - \underline{C}_j$. Carbon \underline{C}_j is attached to the olefinic fragment.



For the assignment of the remaining quaternary carbon atoms (indicated with a blue spot) the ^{13}C -NMR spectrum of **507** was compared with that from analogous structures and tabulated values for the benzoxazole ring.

- \underline{C}_a is the most shifted carbon and, therefore it corresponds to the bridgehead between the imidazole and the oxazole rings.
- Comparison of the spectra of **507** and **462** show a strong similarity between both. The main difference is that \underline{C}_f (129.9 ppm) is a quaternary carbon in **462** which disappears in the spectrum of **507** while a new CH appears at 124.4 ppm. Hence, \underline{C}_f corresponds to the carbon atom connected to the chlorine.

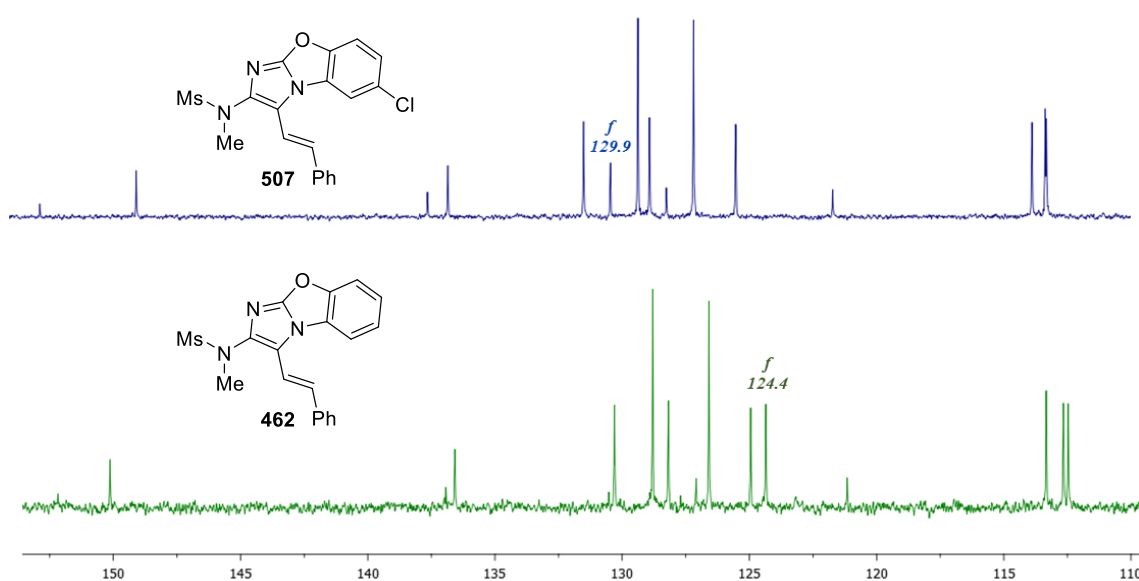


Figure 18: Comparison of the ^{13}C -NMR spectra for compounds **507** and **462**

- Tabulated values for ^{13}C -chemical shifts in oxazoles indicate that the 5-position of the oxazole is more shifted than the 4- (138.1 ppm vs 125.4 ppm). By analogy, \underline{C}_b is assigned to the carbon directly connected to the oxygen in the benzoxazole part of the molecule.

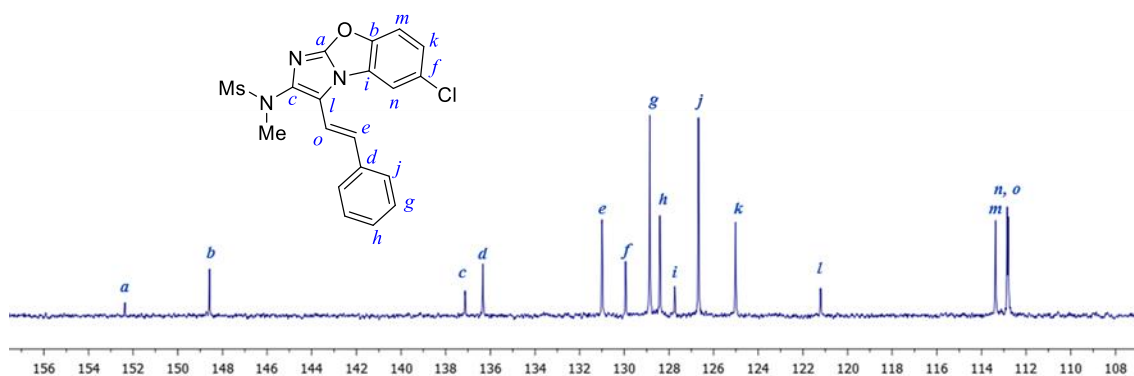


Figure 19: Assignment of the carbocyclic scaffold for 507

Appendix 2

Appendix 2.1 X-Ray crystal structure data

Data was obtained and solved by Dr Louise Male.

Appendix 2.1.1 Imidazo[1,2-*c*]pyrimidine 398

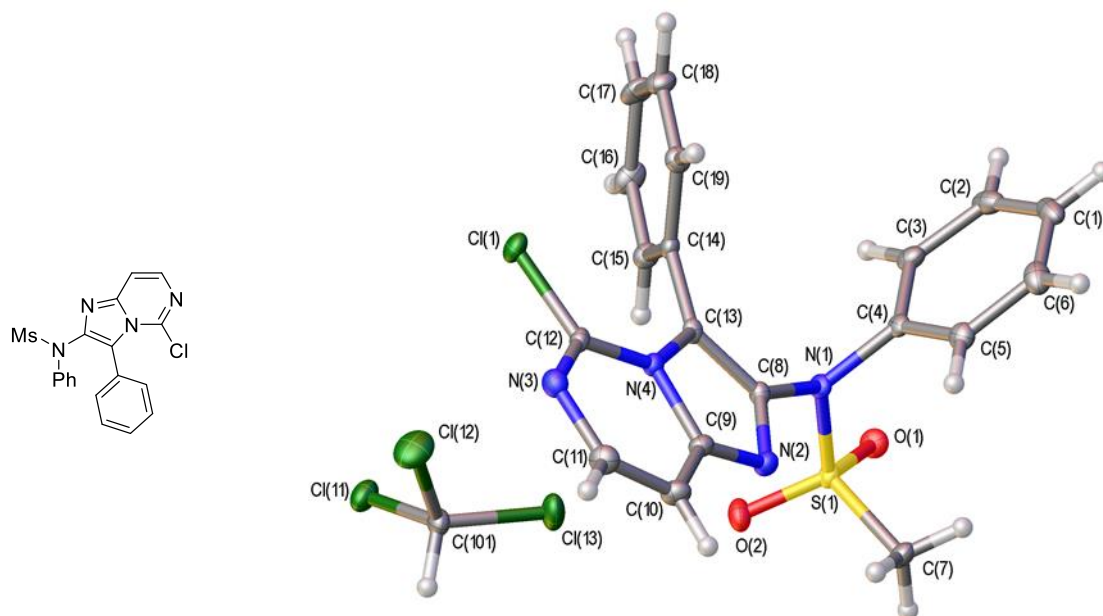


Table 1. Crystal data and structure refinement for 398.

Identification code	398		
Empirical formula	$\text{C}_{19}\text{H}_{15}\text{Cl N}_4\text{O}_2\text{S}$, CHCl_3		
Formula weight	518.23		
Temperature	100.00(10) K		
Wavelength	1.5418 Å		
Crystal system	Monoclinic		
Space group	$P 2_1/c$		
Unit cell dimensions	a = 10.9178(2) Å	$\alpha = 90^\circ$.	
	b = 13.2275(2) Å	$\beta = 95.469(2)^\circ$.	
	c = 15.1914(3) Å	$\gamma = 90^\circ$.	
Volume	2183.88(7) Å ³		

Z	4
Density (calculated)	1.576 Mg/m ³
Absorption coefficient	6.051 mm ⁻¹
F(000)	1056
Crystal size	0.250 x 0.180 x 0.060 mm ³
Theta range for data collection	4.441 to 74.455°.
Index ranges	-13<=h<=13, -16<=k<=14, -18<=l<=10
Reflections collected	8852
Independent reflections	4329 [R(int) = 0.0251]
Completeness to theta = 67.684°	99.9 %
Absorption correction	Semi-empirical from equivalents
Max. and min. transmission	1.00000 and 0.60334
Refinement method	Full-matrix least-squares on F ²
Data / restraints / parameters	4329 / 0 / 281
Goodness-of-fit on F ²	1.045
Final R indices [I>2sigma(I)]	R1 = 0.0308, wR2 = 0.0755
R indices (all data)	R1 = 0.0356, wR2 = 0.0794
Extinction coefficient	n/a
Largest diff. peak and hole	0.416 and -0.589 e.Å ⁻³

Notes:

The hydrogen atoms have been fixed as riding models.

Table 2. Atomic coordinates (x 10⁴) and equivalent isotropic displacement parameters (Å²x 10³) for 398. U(eq) is defined as one third of the trace of the orthogonalized U^{ij} tensor.

<i>Atom</i>	<i>x</i>	<i>y</i>	<i>z</i>	<i>U(eq)</i>
C(1)	10265(2)	1466(2)	8782(1)	22(1)
C(2)	10643(2)	2447(2)	8628(1)	22(1)
C(3)	9934(2)	3080(2)	8055(1)	17(1)
C(4)	8855(2)	2705(1)	7610(1)	13(1)
C(5)	8484(2)	1714(2)	7742(1)	16(1)

C(6)	9182(2)	1101(2)	8342(1)	22(1)
C(7)	8179(2)	2291(2)	5433(1)	17(1)
C(8)	6876(2)	3513(1)	7087(1)	12(1)
C(9)	4932(2)	3311(1)	6912(1)	13(1)
C(10)	3700(2)	3034(2)	6685(1)	18(1)
C(11)	2810(2)	3526(2)	7083(1)	19(1)
C(12)	4195(2)	4532(1)	7899(1)	13(1)
C(13)	6462(2)	4181(1)	7679(1)	11(1)
C(14)	7201(2)	4848(1)	8298(1)	12(1)
C(15)	7995(2)	5533(1)	7950(1)	15(1)
C(16)	8772(2)	6128(2)	8511(1)	20(1)
C(17)	8757(2)	6046(2)	9421(1)	21(1)
C(18)	7967(2)	5364(2)	9772(1)	19(1)
C(19)	7194(2)	4762(1)	9214(1)	15(1)
N(1)	8143(1)	3349(1)	6983(1)	12(1)
N(2)	5965(1)	2980(1)	6617(1)	14(1)
N(3)	3062(1)	4294(1)	7686(1)	16(1)
N(4)	5181(1)	4061(1)	7568(1)	11(1)
O(1)	9908(1)	3502(1)	6073(1)	17(1)
O(2)	7882(1)	4231(1)	5538(1)	20(1)
S(1)	8595(1)	3438(1)	5973(1)	13(1)
Cl(1)	4494(1)	5521(1)	8617(1)	17(1)
C(101)	5008(2)	6692(2)	5487(1)	17(1)
Cl(11)	5609(1)	7936(1)	5429(1)	23(1)
Cl(12)	4133(1)	6601(1)	6397(1)	33(1)
Cl(13)	6200(1)	5804(1)	5558(1)	25(1)

Table 3. Bond lengths [Å] and angles [°] for 398.

C(1)-C(6)	1.388(3)	C(1)-C(2)	1.389(3)
-----------	----------	-----------	----------

Appendix 2

C(1)-H(1)	0.9500	C(14)-C(15)	1.392(2)
C(2)-C(3)	1.389(3)	C(14)-C(19)	1.398(2)
C(2)-H(2)	0.9500	C(15)-C(16)	1.389(3)
C(3)-C(4)	1.393(3)	C(15)-H(15)	0.9500
C(3)-H(3)	0.9500	C(16)-C(17)	1.388(3)
C(4)-C(5)	1.392(3)	C(16)-H(16)	0.9500
C(4)-N(1)	1.448(2)	C(17)-C(18)	1.389(3)
C(5)-C(6)	1.392(3)	C(17)-H(17)	0.9500
C(5)-H(5)	0.9500	C(18)-C(19)	1.389(3)
C(6)-H(6)	0.9500	C(18)-H(18)	0.9500
C(7)-S(1)	1.7625(19)	C(19)-H(19)	0.9500
C(7)-H(7A)	0.9800	N(1)-S(1)	1.6606(15)
C(7)-H(7B)	0.9800	O(1)-S(1)	1.4298(13)
C(7)-H(7C)	0.9800	O(2)-S(1)	1.4302(14)
C(8)-N(2)	1.364(2)	C(101)-Cl(13)	1.7486(19)
C(8)-C(13)	1.368(2)	C(101)-Cl(12)	1.7585(19)
C(8)-N(1)	1.424(2)	C(101)-Cl(11)	1.777(2)
C(9)-N(2)	1.327(2)	C(101)-H(101)	1.0000
C(9)-C(10)	1.406(2)	C(6)-C(1)-C(2)	119.82(19)
C(9)-N(4)	1.414(2)	C(6)-C(1)-H(1)	120.1
C(10)-C(11)	1.359(3)	C(2)-C(1)-H(1)	120.1
C(10)-H(10)	0.9500	C(3)-C(2)-C(1)	120.79(19)
C(11)-N(3)	1.378(3)	C(3)-C(2)-H(2)	119.6
C(11)-H(11)	0.9500	C(1)-C(2)-H(2)	119.6
C(12)-N(3)	1.288(2)	C(2)-C(3)-C(4)	119.01(19)
C(12)-N(4)	1.380(2)	C(2)-C(3)-H(3)	120.5
C(12)-Cl(1)	1.7140(18)	C(4)-C(3)-H(3)	120.5
C(13)-N(4)	1.402(2)	C(5)-C(4)-C(3)	120.63(17)
C(13)-C(14)	1.472(2)	C(5)-C(4)-N(1)	120.26(16)

C(3)-C(4)-N(1)	119.08(17)	C(8)-C(13)-C(14)	127.67(16)
C(6)-C(5)-C(4)	119.63(18)	N(4)-C(13)-C(14)	128.70(15)
C(6)-C(5)-H(5)	120.2	C(15)-C(14)-C(19)	119.63(16)
C(4)-C(5)-H(5)	120.2	C(15)-C(14)-C(13)	118.08(15)
C(1)-C(6)-C(5)	120.1(2)	C(19)-C(14)-C(13)	122.12(16)
C(1)-C(6)-H(6)	120.0	C(16)-C(15)-C(14)	120.09(17)
C(5)-C(6)-H(6)	120.0	C(16)-C(15)-H(15)	120.0
S(1)-C(7)-H(7A)	109.5	C(14)-C(15)-H(15)	120.0
S(1)-C(7)-H(7B)	109.5	C(17)-C(16)-C(15)	120.19(18)
H(7A)-C(7)-H(7B)	109.5	C(17)-C(16)-H(16)	119.9
S(1)-C(7)-H(7C)	109.5	C(15)-C(16)-H(16)	119.9
H(7A)-C(7)-H(7C)	109.5	C(16)-C(17)-C(18)	119.98(18)
H(7B)-C(7)-H(7C)	109.5	C(16)-C(17)-H(17)	120.0
N(2)-C(8)-C(13)	114.13(15)	C(18)-C(17)-H(17)	120.0
N(2)-C(8)-N(1)	122.01(15)	C(19)-C(18)-C(17)	120.08(17)
C(13)-C(8)-N(1)	123.82(16)	C(19)-C(18)-H(18)	120.0
N(2)-C(9)-C(10)	130.92(17)	C(17)-C(18)-H(18)	120.0
N(2)-C(9)-N(4)	110.97(15)	C(18)-C(19)-C(14)	120.02(17)
C(10)-C(9)-N(4)	118.11(16)	C(18)-C(19)-H(19)	120.0
C(11)-C(10)-C(9)	118.30(18)	C(14)-C(19)-H(19)	120.0
C(11)-C(10)-H(10)	120.8	C(8)-N(1)-C(4)	118.84(14)
C(9)-C(10)-H(10)	120.8	C(8)-N(1)-S(1)	118.02(12)
C(10)-C(11)-N(3)	122.90(17)	C(4)-N(1)-S(1)	117.47(11)
C(10)-C(11)-H(11)	118.6	C(9)-N(2)-C(8)	104.61(14)
N(3)-C(11)-H(11)	118.6	C(12)-N(3)-C(11)	118.31(16)
N(3)-C(12)-N(4)	124.15(16)	C(12)-N(4)-C(13)	135.13(15)
N(3)-C(12)-Cl(1)	117.88(14)	C(12)-N(4)-C(9)	118.05(14)
N(4)-C(12)-Cl(1)	117.95(13)	C(13)-N(4)-C(9)	106.67(14)
C(8)-C(13)-N(4)	103.62(15)	O(1)-S(1)-O(2)	120.14(8)

O(1)-S(1)-N(1)	106.77(8)	Cl(13)-C(101)-Cl(11)	110.44(10)
O(2)-S(1)-N(1)	106.38(8)	Cl(12)-C(101)-Cl(11)	109.49(10)
O(1)-S(1)-C(7)	108.21(8)	Cl(13)-C(101)-H(101)	108.5
O(2)-S(1)-C(7)	108.16(9)	Cl(12)-C(101)-H(101)	108.5
N(1)-S(1)-C(7)	106.41(9)	Cl(11)-C(101)-H(101)	108.5
Cl(13)-C(101)-Cl(12)	111.23(10)		

Symmetry transformations used to generate equivalent atoms.

Table 4. Anisotropic displacement parameters ($\text{\AA}^2 \times 10^3$) for 398. The anisotropic displacement factor exponent takes the form: $-2\pi^2 [h^2 a^{*2} U^{11} + \dots + 2 h k a^* b^* U^{12}]$

Atom	U^{11}	U^{22}	U^{33}	U^{23}	U^{13}	U^{12}
C(1)	21(1)	32(1)	13(1)	2(1)	4(1)	12(1)
C(2)	14(1)	35(1)	15(1)	-7(1)	0(1)	6(1)
C(3)	15(1)	21(1)	16(1)	-7(1)	3(1)	0(1)
C(4)	12(1)	16(1)	12(1)	-2(1)	4(1)	4(1)
C(5)	13(1)	19(1)	18(1)	-1(1)	5(1)	1(1)
C(6)	23(1)	22(1)	21(1)	5(1)	9(1)	5(1)
C(7)	18(1)	17(1)	18(1)	-6(1)	3(1)	1(1)
C(8)	10(1)	12(1)	14(1)	1(1)	3(1)	1(1)
C(9)	14(1)	14(1)	12(1)	-1(1)	2(1)	-1(1)
C(10)	15(1)	21(1)	17(1)	-3(1)	1(1)	-3(1)
C(11)	13(1)	24(1)	21(1)	0(1)	3(1)	-2(1)
C(12)	14(1)	11(1)	13(1)	1(1)	5(1)	2(1)
C(13)	9(1)	10(1)	14(1)	2(1)	4(1)	0(1)
C(14)	12(1)	10(1)	14(1)	-1(1)	2(1)	2(1)
C(15)	15(1)	15(1)	15(1)	-1(1)	5(1)	-1(1)
C(16)	19(1)	18(1)	25(1)	-3(1)	9(1)	-6(1)
C(17)	17(1)	23(1)	24(1)	-11(1)	1(1)	-5(1)
C(18)	21(1)	22(1)	14(1)	-3(1)	3(1)	0(1)

C(19)	15(1)	15(1)	16(1)	2(1)	3(1)	-1(1)
N(1)	8(1)	16(1)	14(1)	-1(1)	4(1)	2(1)
N(2)	12(1)	14(1)	15(1)	-2(1)	3(1)	-1(1)
N(3)	13(1)	19(1)	18(1)	2(1)	4(1)	1(1)
N(4)	10(1)	11(1)	12(1)	0(1)	3(1)	0(1)
O(1)	10(1)	21(1)	20(1)	-1(1)	4(1)	-1(1)
O(2)	20(1)	17(1)	23(1)	5(1)	6(1)	6(1)
S(1)	12(1)	12(1)	14(1)	0(1)	4(1)	1(1)
Cl(1)	16(1)	15(1)	22(1)	-5(1)	5(1)	2(1)
C(101)	17(1)	17(1)	17(1)	0(1)	3(1)	5(1)
Cl(11)	31(1)	16(1)	22(1)	-2(1)	7(1)	1(1)
Cl(12)	39(1)	35(1)	27(1)	0(1)	18(1)	-2(1)
Cl(13)	21(1)	19(1)	35(1)	-2(1)	-1(1)	8(1)

Table 5. Hydrogen coordinates ($\times 10^4$) and isotropic displacement parameters ($\text{\AA}^2 \times 10^3$) for 398.

Atom	x	y	z	U(eq)
H(1)	10746	1045	9187	27
H(2)	11396	2688	8917	26
H(3)	10181	3759	7969	21
H(5)	7757	1458	7426	20
H(6)	8918	432	8450	26
H(7A)	8409	2314	4826	26
H(7B)	7288	2192	5424	26
H(7C)	8608	1730	5751	26
H(10)	3495	2516	6263	21
H(11)	1977	3332	6939	23
H(15)	8006	5592	7327	18
H(16)	9315	6592	8272	24
H(17)	9286	6457	9803	26

H(18)	7955	5309	10395	23
H(19)	6660	4291	9455	18
H(101)	4457	6558	4935	20

Table 6. Torsion angles [°] for 398.

C(6)-C(1)-C(2)-C(3)	1.7(3)
C(1)-C(2)-C(3)-C(4)	-2.4(3)
C(2)-C(3)-C(4)-C(5)	0.7(3)
C(2)-C(3)-C(4)-N(1)	-177.24(15)
C(3)-C(4)-C(5)-C(6)	1.5(3)
N(1)-C(4)-C(5)-C(6)	179.48(16)
C(2)-C(1)-C(6)-C(5)	0.6(3)
C(4)-C(5)-C(6)-C(1)	-2.2(3)
N(2)-C(9)-C(10)-C(11)	-178.23(19)
N(4)-C(9)-C(10)-C(11)	2.3(3)
C(9)-C(10)-C(11)-N(3)	1.2(3)
N(2)-C(8)-C(13)-N(4)	-0.3(2)
N(1)-C(8)-C(13)-N(4)	-178.13(15)
N(2)-C(8)-C(13)-C(14)	178.45(16)
N(1)-C(8)-C(13)-C(14)	0.6(3)
C(8)-C(13)-C(14)-C(15)	57.7(3)
N(4)-C(13)-C(14)-C(15)	-123.92(19)
C(8)-C(13)-C(14)-C(19)	-117.6(2)
N(4)-C(13)-C(14)-C(19)	60.8(3)
C(19)-C(14)-C(15)-C(16)	-0.2(3)
C(13)-C(14)-C(15)-C(16)	-175.60(17)
C(14)-C(15)-C(16)-C(17)	-0.2(3)
C(15)-C(16)-C(17)-C(18)	0.3(3)
C(16)-C(17)-C(18)-C(19)	0.1(3)

C(17)-C(18)-C(19)-C(14)	-0.6(3)
C(15)-C(14)-C(19)-C(18)	0.7(3)
C(13)-C(14)-C(19)-C(18)	175.83(17)
N(2)-C(8)-N(1)-C(4)	-98.0(2)
C(13)-C(8)-N(1)-C(4)	79.7(2)
N(2)-C(8)-N(1)-S(1)	54.8(2)
C(13)-C(8)-N(1)-S(1)	-127.47(16)
C(5)-C(4)-N(1)-C(8)	56.7(2)
C(3)-C(4)-N(1)-C(8)	-125.35(18)
C(5)-C(4)-N(1)-S(1)	-96.29(17)
C(3)-C(4)-N(1)-S(1)	81.68(18)
C(10)-C(9)-N(2)-C(8)	-179.1(2)
N(4)-C(9)-N(2)-C(8)	0.4(2)
C(13)-C(8)-N(2)-C(9)	0.0(2)
N(1)-C(8)-N(2)-C(9)	177.86(16)
N(4)-C(12)-N(3)-C(11)	-0.7(3)
Cl(1)-C(12)-N(3)-C(11)	177.54(14)
C(10)-C(11)-N(3)-C(12)	-2.1(3)
N(3)-C(12)-N(4)-C(13)	178.93(18)
Cl(1)-C(12)-N(4)-C(13)	0.7(3)
N(3)-C(12)-N(4)-C(9)	4.2(3)
Cl(1)-C(12)-N(4)-C(9)	-174.06(13)
C(8)-C(13)-N(4)-C(12)	-174.71(18)
C(14)-C(13)-N(4)-C(12)	6.6(3)
C(8)-C(13)-N(4)-C(9)	0.46(18)
C(14)-C(13)-N(4)-C(9)	-178.25(17)
N(2)-C(9)-N(4)-C(12)	175.61(15)
C(10)-C(9)-N(4)-C(12)	-4.8(2)
N(2)-C(9)-N(4)-C(13)	-0.5(2)

C(10)-C(9)-N(4)-C(13)	179.01(16)
C(8)-N(1)-S(1)-O(1)	165.52(13)
C(4)-N(1)-S(1)-O(1)	-41.29(15)
C(8)-N(1)-S(1)-O(2)	36.09(15)
C(4)-N(1)-S(1)-O(2)	-170.71(13)
C(8)-N(1)-S(1)-C(7)	-79.07(15)
C(4)-N(1)-S(1)-C(7)	74.12(15)

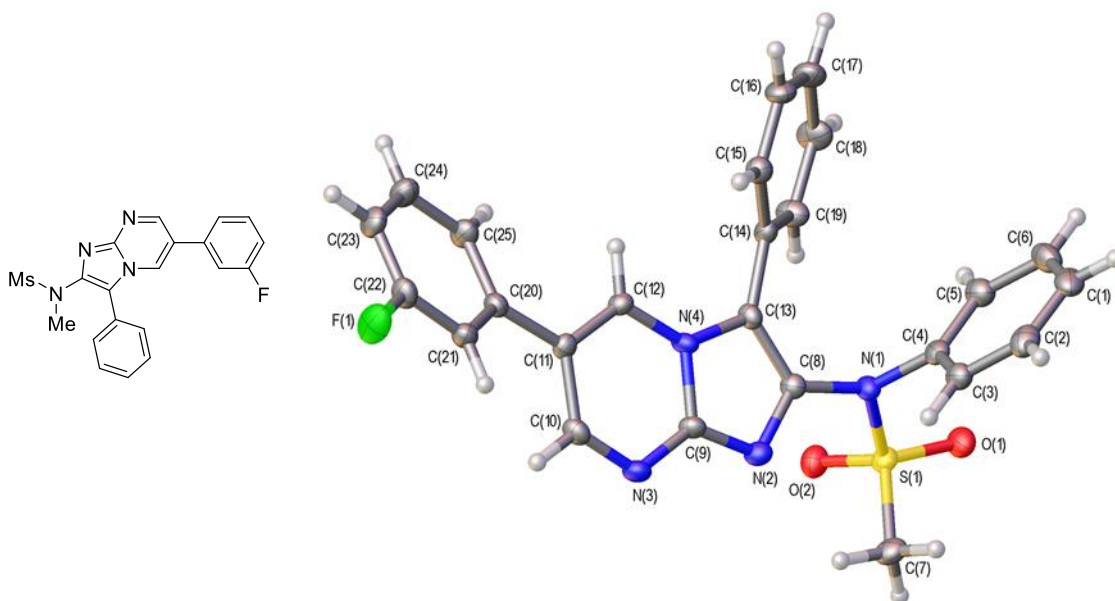
Appendix 2.1.2 Imidazo[1,2-*a*]pyrimidine 402

Table 1. Crystal data and structure refinement for 402

Identification code	402	
Empirical formula	$C_{25}H_{19}FN_4O_2S$	
Formula weight	458.50	
Temperature	101(2) K	
Wavelength	1.5418 Å	
Crystal system	Monoclinic	
Space group	$P 2_1/c$	
Unit cell dimensions	$a = 15.8138(10)$ Å	$\alpha = 90^\circ$.
	$b = 13.1151(8)$ Å	$\beta = 90.830(5)^\circ$.
	$c = 10.3648(6)$ Å	$\gamma = 90^\circ$.
Volume	$2149.4(2)$ Å ³	
Z	4	
Density (calculated)	1.417 Mg/m ³	
Absorption coefficient	1.680 mm ⁻¹	
F(000)	952	

Crystal size	0.320 x 0.020 x 0.010 mm ³
Theta range for data collection	6.538 to 66.567°.
Index ranges	-18<= <i>h</i> <=18, -15<= <i>k</i> <=13, -12<= <i>l</i> <=7
Reflections collected	7206
Independent reflections	3734 [R(int) = 0.0687]
Completeness to theta = 67.684°	95.9 %
Absorption correction	Semi-empirical from equivalents
Max. and min. transmission	1.00000 and 0.88084
Refinement method	Full-matrix least-squares on F ²
Data / restraints / parameters	3734 / 0 / 299
Goodness-of-fit on F ²	1.036
Final R indices [I>2sigma(I)]	R1 = 0.0557, wR2 = 0.1280
R indices (all data)	R1 = 0.0924, wR2 = 0.1504
Extinction coefficient	n/a
Largest diff. peak and hole	0.401 and -0.422 e.Å ⁻³
Notes:	

The hydrogen atoms have been fixed as riding models.

Table 2. Atomic coordinates (x 10⁴) and equivalent isotropic displacement parameters (Å²x 10³) for 402. U(eq) is defined as one third of the trace of the orthogonalized U^{ij} tensor.

Atom	x	y	z	U(eq)
C(1)	5593(2)	5947(3)	3892(3)	32(1)
C(2)	5470(2)	4921(3)	3606(3)	31(1)
C(3)	4762(2)	4612(3)	2909(3)	24(1)
C(4)	4175(2)	5332(3)	2499(3)	22(1)
C(5)	4286(2)	6357(3)	2792(3)	28(1)
C(6)	5003(2)	6657(3)	3494(3)	34(1)
C(7)	3895(2)	4086(3)	-474(3)	28(1)
C(8)	2907(2)	4259(3)	2324(3)	20(1)

C(9)	2342(2)	2808(2)	2629(3)	19(1)
C(10)	1581(2)	1505(3)	3460(3)	22(1)
C(11)	1283(2)	2108(3)	4510(3)	19(1)
C(12)	1546(2)	3086(2)	4558(3)	18(1)
C(13)	2437(2)	4399(3)	3425(3)	19(1)
C(14)	2329(2)	5279(2)	4274(3)	19(1)
C(15)	2392(2)	5207(3)	5613(3)	22(1)
C(16)	2350(2)	6078(3)	6366(3)	29(1)
C(17)	2253(2)	7021(3)	5797(4)	32(1)
C(18)	2172(2)	7104(3)	4470(4)	33(1)
C(19)	2205(2)	6235(3)	3709(3)	28(1)
C(20)	738(2)	1679(2)	5534(3)	20(1)
C(21)	819(2)	659(3)	5900(3)	23(1)
C(22)	338(2)	305(3)	6902(3)	25(1)
C(23)	-218(2)	904(3)	7567(3)	29(1)
C(24)	-300(2)	1912(3)	7191(4)	30(1)
C(25)	164(2)	2297(3)	6183(3)	26(1)
N(1)	3430(2)	5022(2)	1776(3)	21(1)
N(2)	2851(2)	3295(2)	1838(3)	21(1)
N(3)	2084(2)	1830(2)	2550(3)	21(1)
N(4)	2077(2)	3447(2)	3628(2)	18(1)
O(1)	3958(1)	6037(2)	-63(2)	27(1)
O(2)	2557(1)	5215(2)	-226(2)	26(1)
F(1)	419(1)	-689(2)	7239(2)	37(1)
S(1)	3428(1)	5178(1)	182(1)	21(1)

Table 3. Bond lengths [\AA] and angles [$^\circ$] for 402.

C(1)-C(6)	1.378(5)	C(1)-C(2)	1.391(5)
-----------	----------	-----------	----------

Appendix 2

C(1)-H(1)	0.9500	C(14)-C(15)	1.393(4)
C(2)-C(3)	1.385(5)	C(14)-C(19)	1.397(5)
C(2)-H(2)	0.9500	C(15)-C(16)	1.386(5)
C(3)-C(4)	1.387(5)	C(15)-H(15)	0.9500
C(3)-H(3)	0.9500	C(16)-C(17)	1.377(5)
C(4)-C(5)	1.389(5)	C(16)-H(16)	0.9500
C(4)-N(1)	1.446(4)	C(17)-C(18)	1.384(5)
C(5)-C(6)	1.394(5)	C(17)-H(17)	0.9500
C(5)-H(5)	0.9500	C(18)-C(19)	1.387(5)
C(6)-H(6)	0.9500	C(18)-H(18)	0.9500
C(7)-S(1)	1.754(3)	C(19)-H(19)	0.9500
C(7)-H(7A)	0.9800	C(20)-C(21)	1.396(5)
C(7)-H(7B)	0.9800	C(20)-C(25)	1.398(4)
C(7)-H(7C)	0.9800	C(21)-C(22)	1.377(5)
C(8)-N(2)	1.364(4)	C(21)-H(21)	0.9500
C(8)-C(13)	1.383(4)	C(22)-F(1)	1.355(4)
C(8)-N(1)	1.423(4)	C(22)-C(23)	1.373(5)
C(9)-N(2)	1.321(4)	C(23)-C(24)	1.383(5)
C(9)-N(3)	1.349(4)	C(23)-H(23)	0.9500
C(9)-N(4)	1.401(4)	C(24)-C(25)	1.382(5)
C(10)-N(3)	1.314(4)	C(24)-H(24)	0.9500
C(10)-C(11)	1.430(4)	C(25)-H(25)	0.9500
C(10)-H(10)	0.9500	N(1)-S(1)	1.664(3)
C(11)-C(12)	1.349(4)	O(1)-S(1)	1.429(2)
C(11)-C(20)	1.488(4)	O(2)-S(1)	1.435(2)
C(12)-N(4)	1.372(4)	C(6)-C(1)-C(2)	119.9(3)
C(12)-H(12)	0.9500	C(6)-C(1)-H(1)	120.1
C(13)-N(4)	1.389(4)	C(2)-C(1)-H(1)	120.1
C(13)-C(14)	1.462(4)	C(3)-C(2)-C(1)	120.3(4)

C(3)-C(2)-H(2)	119.9	C(12)-C(11)-C(10)	116.8(3)
C(1)-C(2)-H(2)	119.9	C(12)-C(11)-C(20)	121.0(3)
C(2)-C(3)-C(4)	119.5(3)	C(10)-C(11)-C(20)	122.2(3)
C(2)-C(3)-H(3)	120.2	C(11)-C(12)-N(4)	119.6(3)
C(4)-C(3)-H(3)	120.2	C(11)-C(12)-H(12)	120.2
C(5)-C(4)-C(3)	120.7(3)	N(4)-C(12)-H(12)	120.2
C(5)-C(4)-N(1)	119.0(3)	C(8)-C(13)-N(4)	103.4(3)
C(3)-C(4)-N(1)	120.2(3)	C(8)-C(13)-C(14)	132.1(3)
C(4)-C(5)-C(6)	119.1(3)	N(4)-C(13)-C(14)	124.5(3)
C(4)-C(5)-H(5)	120.5	C(15)-C(14)-C(19)	119.1(3)
C(6)-C(5)-H(5)	120.5	C(15)-C(14)-C(13)	122.6(3)
C(1)-C(6)-C(5)	120.5(4)	C(19)-C(14)-C(13)	118.3(3)
C(1)-C(6)-H(6)	119.7	C(16)-C(15)-C(14)	120.1(3)
C(5)-C(6)-H(6)	119.7	C(16)-C(15)-H(15)	119.9
S(1)-C(7)-H(7A)	109.5	C(14)-C(15)-H(15)	119.9
S(1)-C(7)-H(7B)	109.5	C(17)-C(16)-C(15)	120.3(3)
H(7A)-C(7)-H(7B)	109.5	C(17)-C(16)-H(16)	119.8
S(1)-C(7)-H(7C)	109.5	C(15)-C(16)-H(16)	119.8
H(7A)-C(7)-H(7C)	109.5	C(16)-C(17)-C(18)	120.3(3)
H(7B)-C(7)-H(7C)	109.5	C(16)-C(17)-H(17)	119.9
N(2)-C(8)-C(13)	113.3(3)	C(18)-C(17)-H(17)	119.9
N(2)-C(8)-N(1)	122.6(3)	C(17)-C(18)-C(19)	119.8(3)
C(13)-C(8)-N(1)	124.0(3)	C(17)-C(18)-H(18)	120.1
N(2)-C(9)-N(3)	127.5(3)	C(19)-C(18)-H(18)	120.1
N(2)-C(9)-N(4)	111.2(3)	C(18)-C(19)-C(14)	120.4(3)
N(3)-C(9)-N(4)	121.4(3)	C(18)-C(19)-H(19)	119.8
N(3)-C(10)-C(11)	125.2(3)	C(14)-C(19)-H(19)	119.8
N(3)-C(10)-H(10)	117.4	C(21)-C(20)-C(25)	118.9(3)
C(11)-C(10)-H(10)	117.4	C(21)-C(20)-C(11)	120.3(3)

C(25)-C(20)-C(11)	120.7(3)	C(8)-N(1)-C(4)	117.7(3)
C(22)-C(21)-C(20)	118.6(3)	C(8)-N(1)-S(1)	119.3(2)
C(22)-C(21)-H(21)	120.7	C(4)-N(1)-S(1)	118.1(2)
C(20)-C(21)-H(21)	120.7	C(9)-N(2)-C(8)	104.8(3)
F(1)-C(22)-C(23)	118.7(3)	C(10)-N(3)-C(9)	116.8(3)
F(1)-C(22)-C(21)	117.9(3)	C(12)-N(4)-C(13)	132.3(3)
C(23)-C(22)-C(21)	123.5(3)	C(12)-N(4)-C(9)	120.4(3)
C(22)-C(23)-C(24)	117.6(3)	C(13)-N(4)-C(9)	107.3(2)
C(22)-C(23)-H(23)	121.2	O(1)-S(1)-O(2)	118.92(15)
C(24)-C(23)-H(23)	121.2	O(1)-S(1)-N(1)	106.28(14)
C(25)-C(24)-C(23)	121.0(3)	O(2)-S(1)-N(1)	106.57(13)
C(25)-C(24)-H(24)	119.5	O(1)-S(1)-C(7)	108.85(15)
C(23)-C(24)-H(24)	119.5	O(2)-S(1)-C(7)	108.77(16)
C(24)-C(25)-C(20)	120.5(3)	N(1)-S(1)-C(7)	106.82(15)
C(24)-C(25)-H(25)	119.8		
C(20)-C(25)-H(25)	119.8		

Symmetry transformations used to generate equivalent atoms.

Table 4. Anisotropic displacement parameters ($\text{\AA}^2 \times 10^3$) for 402. The anisotropic displacement factor exponent takes the form: $-2\pi^2 [h^2 a^{*2} U^{11} + \dots + 2 h k a^* b^* U^{12}]$

Atom	U^{11}	U^{22}	U^{33}	U^{23}	U^{13}	U^{12}
C(1)	34(2)	43(3)	19(2)	-5(2)	2(2)	-10(2)
C(2)	30(2)	42(2)	21(2)	5(2)	3(1)	-4(2)
C(3)	29(2)	21(2)	24(2)	0(2)	6(1)	-5(1)
C(4)	25(2)	25(2)	16(2)	1(1)	6(1)	-6(1)
C(5)	35(2)	23(2)	26(2)	0(2)	6(2)	-4(2)
C(6)	46(2)	28(2)	28(2)	-4(2)	6(2)	-16(2)
C(7)	35(2)	30(2)	20(2)	1(2)	9(1)	-1(2)
C(8)	24(2)	17(2)	18(2)	2(1)	2(1)	-1(1)
C(9)	25(2)	14(2)	18(2)	-1(1)	2(1)	1(1)

C(10)	28(2)	14(2)	22(2)	1(1)	-2(1)	-2(1)
C(11)	18(2)	18(2)	21(2)	2(1)	2(1)	1(1)
C(12)	22(2)	18(2)	15(1)	0(1)	3(1)	0(1)
C(13)	24(2)	16(2)	18(2)	2(1)	1(1)	-5(1)
C(14)	21(2)	15(2)	21(2)	1(1)	5(1)	-2(1)
C(15)	25(2)	20(2)	23(2)	2(2)	2(1)	-1(1)
C(16)	35(2)	31(2)	20(2)	-7(2)	6(1)	-4(2)
C(17)	40(2)	20(2)	35(2)	-9(2)	9(2)	-1(2)
C(18)	48(2)	15(2)	36(2)	3(2)	8(2)	1(2)
C(19)	42(2)	20(2)	21(2)	2(2)	4(2)	-3(2)
C(20)	23(2)	16(2)	21(2)	-1(1)	1(1)	-4(1)
C(21)	24(2)	19(2)	27(2)	-4(2)	5(1)	-2(1)
C(22)	28(2)	16(2)	32(2)	3(2)	2(1)	-5(1)
C(23)	30(2)	27(2)	30(2)	2(2)	11(2)	-7(2)
C(24)	30(2)	24(2)	36(2)	-3(2)	11(2)	0(2)
C(25)	31(2)	16(2)	32(2)	1(2)	7(2)	-2(1)
N(1)	26(1)	21(2)	16(1)	0(1)	3(1)	-6(1)
N(2)	27(1)	20(2)	17(1)	1(1)	4(1)	0(1)
N(3)	29(1)	16(2)	19(1)	-3(1)	4(1)	0(1)
N(4)	27(1)	13(1)	14(1)	-1(1)	2(1)	-1(1)
O(1)	33(1)	27(1)	22(1)	5(1)	4(1)	-7(1)
O(2)	24(1)	29(1)	24(1)	7(1)	-1(1)	-1(1)
F(1)	42(1)	21(1)	49(1)	14(1)	12(1)	0(1)
S(1)	25(1)	22(1)	16(1)	3(1)	4(1)	-2(1)

Table 5. Hydrogen coordinates ($\times 10^4$) and isotropic displacement parameters ($\text{\AA}^2 \times 10^3$) for 402.

Atom	x	y	z	U(eq)
H(1)	6083	6157	4362	38
H(2)	5874	4430	3891	37
H(3)	4680	3911	2711	29

H(5)	3879	6848	2519	34
H(6)	5085	7356	3698	41
H(7A)	3572	3482	-225	42
H(7B)	4478	4024	-148	42
H(7C)	3898	4142	-1417	42
H(10)	1400	815	3418	26
H(12)	1365	3522	5232	22
H(15)	2463	4559	6010	27
H(16)	2388	6025	7279	34
H(17)	2242	7616	6318	38
H(18)	2094	7754	4081	39
H(19)	2142	6291	2799	33
H(21)	1198	218	5466	28
H(23)	-535	637	8261	35
H(24)	-681	2345	7633	36
H(25)	91	2988	5928	31

Table 6. Torsion angles [°] for 402.

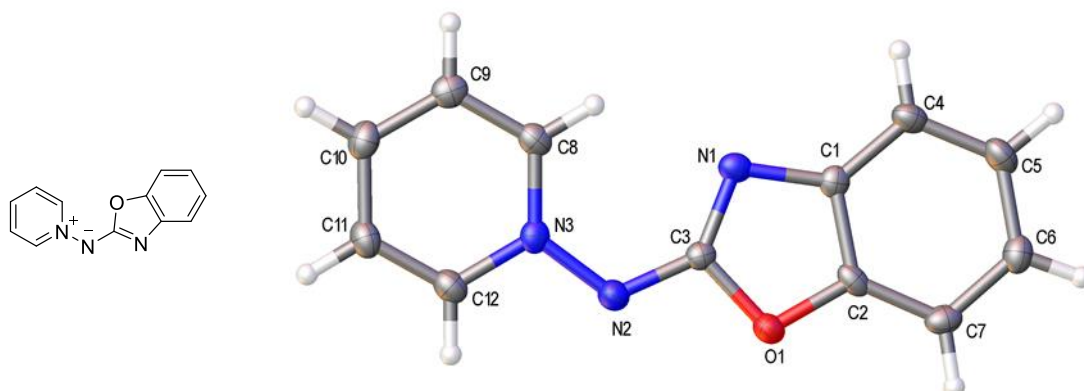
C(6)-C(1)-C(2)-C(3)	0.8(5)
C(1)-C(2)-C(3)-C(4)	-0.2(5)
C(2)-C(3)-C(4)-C(5)	-0.6(5)
C(2)-C(3)-C(4)-N(1)	-179.7(3)
C(3)-C(4)-C(5)-C(6)	0.7(5)
N(1)-C(4)-C(5)-C(6)	179.8(3)
C(2)-C(1)-C(6)-C(5)	-0.7(5)
C(4)-C(5)-C(6)-C(1)	-0.1(5)
N(3)-C(10)-C(11)-C(12)	-0.1(5)
N(3)-C(10)-C(11)-C(20)	-177.8(3)
C(10)-C(11)-C(12)-N(4)	-0.4(5)
C(20)-C(11)-C(12)-N(4)	177.3(3)

N(2)-C(8)-C(13)-N(4)	0.6(4)
N(1)-C(8)-C(13)-N(4)	-176.6(3)
N(2)-C(8)-C(13)-C(14)	178.1(3)
N(1)-C(8)-C(13)-C(14)	0.9(6)
C(8)-C(13)-C(14)-C(15)	-132.3(4)
N(4)-C(13)-C(14)-C(15)	44.7(5)
C(8)-C(13)-C(14)-C(19)	44.2(5)
N(4)-C(13)-C(14)-C(19)	-138.8(3)
C(19)-C(14)-C(15)-C(16)	-1.5(5)
C(13)-C(14)-C(15)-C(16)	174.9(3)
C(14)-C(15)-C(16)-C(17)	-0.5(5)
C(15)-C(16)-C(17)-C(18)	1.9(6)
C(16)-C(17)-C(18)-C(19)	-1.3(6)
C(17)-C(18)-C(19)-C(14)	-0.8(6)
C(15)-C(14)-C(19)-C(18)	2.1(5)
C(13)-C(14)-C(19)-C(18)	-174.5(3)
C(12)-C(11)-C(20)-C(21)	-146.2(3)
C(10)-C(11)-C(20)-C(21)	31.4(5)
C(12)-C(11)-C(20)-C(25)	31.2(5)
C(10)-C(11)-C(20)-C(25)	-151.3(3)
C(25)-C(20)-C(21)-C(22)	-1.1(5)
C(11)-C(20)-C(21)-C(22)	176.3(3)
C(20)-C(21)-C(22)-F(1)	179.5(3)
C(20)-C(21)-C(22)-C(23)	-0.1(6)
F(1)-C(22)-C(23)-C(24)	-178.9(3)
C(21)-C(22)-C(23)-C(24)	0.7(6)
C(22)-C(23)-C(24)-C(25)	-0.1(6)
C(23)-C(24)-C(25)-C(20)	-1.1(6)
C(21)-C(20)-C(25)-C(24)	1.7(5)

C(11)-C(20)-C(25)-C(24)	-175.6(3)
N(2)-C(8)-N(1)-C(4)	-109.5(3)
C(13)-C(8)-N(1)-C(4)	67.4(4)
N(2)-C(8)-N(1)-S(1)	45.3(4)
C(13)-C(8)-N(1)-S(1)	-137.7(3)
C(5)-C(4)-N(1)-C(8)	-124.6(3)
C(3)-C(4)-N(1)-C(8)	54.4(4)
C(5)-C(4)-N(1)-S(1)	80.2(3)
C(3)-C(4)-N(1)-S(1)	-100.8(3)
N(3)-C(9)-N(2)-C(8)	179.3(3)
N(4)-C(9)-N(2)-C(8)	-0.6(4)
C(13)-C(8)-N(2)-C(9)	0.0(4)
N(1)-C(8)-N(2)-C(9)	177.2(3)
C(11)-C(10)-N(3)-C(9)	0.7(5)
N(2)-C(9)-N(3)-C(10)	179.3(3)
N(4)-C(9)-N(3)-C(10)	-0.8(5)
C(11)-C(12)-N(4)-C(13)	179.3(3)
C(11)-C(12)-N(4)-C(9)	0.3(5)
C(8)-C(13)-N(4)-C(12)	180.0(3)
C(14)-C(13)-N(4)-C(12)	2.2(5)
C(8)-C(13)-N(4)-C(9)	-0.9(3)
C(14)-C(13)-N(4)-C(9)	-178.6(3)
N(2)-C(9)-N(4)-C(12)	-179.7(3)
N(3)-C(9)-N(4)-C(12)	0.3(5)
N(2)-C(9)-N(4)-C(13)	1.0(4)
N(3)-C(9)-N(4)-C(13)	-178.9(3)
C(8)-N(1)-S(1)-O(1)	175.7(2)
C(4)-N(1)-S(1)-O(1)	-29.5(3)
C(8)-N(1)-S(1)-O(2)	48.0(3)

C(4)-N(1)-S(1)-O(2)	-157.3(2)
C(8)-N(1)-S(1)-C(7)	-68.2(3)
C(4)-N(1)-S(1)-C(7)	86.6(3)

Appendix 2.1.3 Aminide 436

**Table 1 Crystal data and structure refinement for 436.**

Identification code	436
Empirical formula	C ₁₂ H ₉ N ₃ O
Formula weight	211.22
Temperature/K	100.01(10)
Crystal system	monoclinic
Space group	P2 ₁ /n
a/Å	6.0637(3)
b/Å	18.6004(7)
c/Å	8.8473(3)
α /°	90
β /°	103.992(4)
γ /°	90
Volume/Å ³	968.26(7)
Z	4
$\rho_{\text{calc}}/\text{cm}^3$	1.449
μ/mm^{-1}	0.097
F(000)	440.0
Crystal size/mm ³	0.2414 × 0.179 × 0.0859
Radiation	MoK α (λ = 0.71073)
2 θ range for data collection/°	6.458 to 52.736
Index ranges	-7 ≤ h ≤ 7, -16 ≤ k ≤ 23, -10 ≤ l ≤ 11
Reflections collected	3935

Independent reflections	1979 [$R_{\text{int}} = 0.0286$, $R_{\text{sigma}} = 0.0486$]
Data/restraints/parameters	1979/0/145
Goodness-of-fit on F^2	1.120
Final R indexes [$I \geq 2\sigma(I)$]	$R_1 = 0.0492$, $wR_2 = 0.1157$
Final R indexes [all data]	$R_1 = 0.0685$, $wR_2 = 0.1305$
Largest diff. peak/hole / $e \text{ \AA}^{-3}$	0.48/-0.27

Table 2 Fractional Atomic Coordinates ($\times 10^4$) and Equivalent Isotropic Displacement Parameters ($\text{\AA}^2 \times 10^3$) for 436. U_{eq} is defined as 1/3 of the trace of the orthogonalised U_{ij} tensor.

Atom	x	y	z	U(eq)
C1	4129(3)	1512.3(11)	4965(2)	18.3(5)
C2	2353(4)	1551.8(11)	5708(2)	19.5(5)
C3	4770(3)	736.1(11)	6817(2)	17.4(4)
C4	4115(4)	1966.5(12)	3728(2)	23.3(5)
C5	2321(4)	2439.7(12)	3289(2)	26.1(5)
C6	570(4)	2470.6(11)	4043(2)	24.2(5)
C7	539(4)	2016.7(11)	5287(2)	22.9(5)
C8	8668(3)	-157.6(11)	7096(2)	20.8(5)
C9	10534(4)	-606.9(11)	7370(2)	22.8(5)
C10	11007(4)	-1055.9(11)	8647(2)	24.5(5)
C11	9578(4)	-1041.5(11)	9649(2)	24.4(5)
C12	7736(4)	-594.0(11)	9367(2)	22.9(5)
N1	5668(3)	977.0(9)	5698.3(19)	20.3(4)
N2	5353(3)	252.5(10)	7968(2)	22.9(4)
N3	7285(3)	-155.3(9)	8088.9(19)	19.8(4)
O1	2725(2)	1056.2(8)	6890.5(16)	23.1(4)

Table 3 Anisotropic Displacement Parameters ($\text{\AA}^2 \times 10^3$) for 436. The Anisotropic displacement factor exponent takes the form: $-2\pi^2[h^2a^{*2}U_{11}+2hka^{*}b^{*}U_{12}+\dots]$.

Atom	U_{11}	U_{22}	U_{33}	U_{23}	U_{13}	U_{12}
C1	17.4(10)	17(1)	18.8(10)	-3.1(9)	0.9(8)	-3.0(8)
C2	25.3(11)	18.3(10)	13.6(9)	0.2(8)	2.0(8)	-6.9(9)
C3	16.8(10)	18.1(10)	17.1(10)	-2.9(8)	3.6(8)	-2.0(8)
C4	23.0(11)	27.3(12)	20.5(10)	0.5(9)	7.0(9)	-6.1(10)
C5	29.9(12)	24.8(12)	22.9(11)	6(1)	4.8(9)	-5.6(10)

C6	25.2(11)	20.7(11)	24.0(11)	-1.6(9)	0.7(9)	2.6(9)
C7	20.8(11)	28.0(12)	21(1)	-6.5(9)	7.3(9)	-2.6(9)
C8	23.0(11)	20.4(10)	17.9(10)	-2.0(9)	2.8(8)	-5.8(9)
C9	22.1(11)	22.0(11)	23.6(11)	-6.6(9)	4.2(9)	-4.6(9)
C10	24.5(12)	18.7(11)	28.0(11)	-3.2(9)	2.0(9)	1.6(9)
C11	30.0(12)	19.4(11)	21.8(11)	1.2(9)	2.4(9)	0.4(10)
C12	27.3(12)	21.5(11)	19.6(10)	0.1(9)	5.1(9)	-4.2(10)
N1	18.3(9)	23.6(9)	18.9(8)	-1.7(8)	4.2(7)	-4.4(8)
N2	21.9(9)	26.2(10)	21.0(9)	3.3(8)	6.0(7)	0.6(8)
N3	18.6(9)	19.8(9)	18.6(8)	-1.7(7)	0.0(7)	-1.0(8)
O1	23.3(8)	26.3(8)	20.3(7)	4.6(6)	6.8(6)	0.2(7)

Table 4 Bond Lengths for 436.

Atom	Atom	Length/Å	Atom	Atom	Length/Å
C1	C2	1.393(3)	C5	C6	1.385(3)
C1	C4	1.381(3)	C6	C7	1.391(3)
C1	N1	1.411(3)	C8	C9	1.380(3)
C2	C7	1.378(3)	C8	N3	1.353(3)
C2	O1	1.371(2)	C9	C10	1.378(3)
C3	N1	1.318(3)	C10	C11	1.382(3)
C3	N2	1.341(3)	C11	C12	1.367(3)
C3	O1	1.392(2)	C12	N3	1.368(3)
C4	C5	1.380(3)	N2	N3	1.378(2)

Table 5 Bond Angles for 436.

Atom	Atom	Atom	Angle/°	Atom	Atom	Atom	Angle/°
C2	C1	N1	108.73(17)	C2	C7	C6	115.6(2)
C4	C1	C2	118.99(19)	N3	C8	C9	119.88(19)
C4	C1	N1	132.3(2)	C10	C9	C8	120.7(2)
C7	C2	C1	124.27(19)	C9	C10	C11	118.4(2)
O1	C2	C1	108.74(18)	C12	C11	C10	120.4(2)
O1	C2	C7	127.0(2)	C11	C12	N3	120.4(2)
N1	C3	N2	135.9(2)	C3	N1	C1	103.75(17)
N1	C3	O1	115.12(17)	C3	N2	N3	119.40(17)

N2	C3	O1	108.99(17)	C8	N3	C12	120.25(18)
C5	C4	C1	117.8(2)	C8	N3	N2	126.89(17)
C4	C5	C6	122.3(2)	C12	N3	N2	112.86(17)
C5	C6	C7	121.0(2)	C2	O1	C3	103.65(16)

Table 6 Torsion Angles for 436.

A	B	C	D	Angle/°	A	B	C	D	Angle/°
C1	C2	C7	C6	-0.7(3)	C9	C10	C11	C12	0.4(3)
C1	C2	O1	C3	0.6(2)	C10	C11	C12	N3	0.0(3)
C1	C4	C5	C6	0.0(3)	C11	C12	N3	C8	-0.4(3)
C2	C1	C4	C5	-0.1(3)	C11	C12	N3	N2	179.16(18)
C2	C1	N1	C3	-0.5(2)	N1	C1	C2	C7	-179.68(18)
C3	N2	N3	C8	-4.1(3)	N1	C1	C2	O1	0.0(2)
C3	N2	N3	C12	176.41(17)	N1	C1	C4	C5	-179.9(2)
C4	C1	C2	C7	0.4(3)	N1	C3	N2	N3	-4.1(3)
C4	C1	C2	O1	-179.94(17)	N1	C3	O1	C2	-1.0(2)
C4	C1	N1	C3	179.4(2)	N2	C3	N1	C1	-177.5(2)
C4	C5	C6	C7	-0.4(3)	N2	C3	O1	C2	177.89(16)
C5	C6	C7	C2	0.7(3)	N3	C8	C9	C10	0.1(3)
C7	C2	O1	C3	-179.81(19)	O1	C2	C7	C6	179.70(18)
C8	C9	C10	C11	-0.4(3)	O1	C3	N1	C1	0.9(2)
C9	C8	N3	C12	0.3(3)	O1	C3	N2	N3	177.38(15)
C9	C8	N3	N2	-179.15(18)					

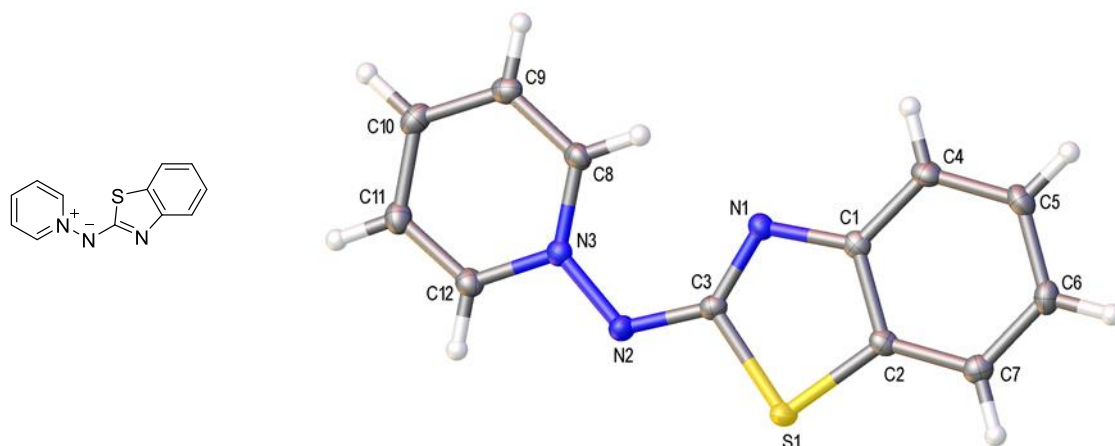
Table 7 Hydrogen Atom Coordinates ($\text{\AA} \times 10^4$) and Isotropic Displacement Parameters ($\text{\AA}^2 \times 10^3$) for 436.

Atom	x	y	z	U(eq)
H4	5301	1954	3196	28
H5	2286	2755	2440	31
H6	-627	2807	3706	29
H7	-656	2026	5811	27
H8	8355	149	6212	25
H9	11503	-607	6672	27

Appendix 2

H10	12284	-1368	8834	29
H11	9878	-1344	10540	29
H12	6763	-588	10063	27

Appendix 2.1.4 Aminide 437

**Table 1** Crystal data and structure refinement for **437**.

Identification code	437
Empirical formula	C ₁₂ H ₉ N ₃ S
Formula weight	227.28
Temperature/K	99.99(10)
Crystal system	monoclinic
Space group	P2 ₁ /c
a/Å	6.0554(3)
b/Å	21.6832(9)
c/Å	8.2470(3)
α /°	90
β /°	108.988(5)
γ /°	90
Volume/Å ³	1023.91(8)
Z	4
$\rho_{\text{calc}}/\text{cm}^3$	1.474
μ/mm^{-1}	0.287
F(000)	472.0
Crystal size/mm ³	0.2247 × 0.2101 × 0.114
Radiation	MoK α (λ = 0.71073)
2 θ range for data collection/°	6.436 to 52.742
Index ranges	-7 ≤ h ≤ 5, -27 ≤ k ≤ 13, -10 ≤ l ≤ 10

Reflections collected	4136
Independent reflections	2101 [$R_{\text{int}} = 0.0212$, $R_{\text{sigma}} = 0.0388$]
Data/restraints/parameters	2101/0/145
Goodness-of-fit on F^2	1.039
Final R indexes [$I \geq 2\sigma(I)$]	$R_1 = 0.0376$, $wR_2 = 0.0785$
Final R indexes [all data]	$R_1 = 0.0491$, $wR_2 = 0.0857$
Largest diff. peak/hole / $e \text{ \AA}^{-3}$	0.30/-0.27

Table 2 Fractional Atomic Coordinates ($\times 10^4$) and Equivalent Isotropic Displacement Parameters ($\text{\AA}^2 \times 10^3$) for 437. U_{eq} is defined as 1/3 of of the trace of the orthogonalised U_{ij} tensor.

Atom	x	y	z	U(eq)
C1	5286(3)	3563.5(9)	10151(2)	14.3(4)
C2	3042(3)	3317.8(9)	9897(2)	15.1(4)
C3	3283(3)	4276.9(9)	8317(2)	14.2(4)
C4	7237(3)	3249.7(9)	11213(2)	17.4(4)
C5	6921(3)	2703.4(9)	11980(2)	19.2(4)
C6	4690(3)	2468.3(9)	11732(2)	18.9(4)
C7	2729(3)	2773.9(9)	10682(2)	17.5(4)
C8	6424(3)	5160.9(9)	7726(2)	16.6(4)
C9	7766(3)	5604.8(9)	7293(2)	18.0(4)
C10	6764(3)	6053.7(10)	6099(2)	19.2(4)
C11	4351(4)	6042.3(9)	5330(2)	19.3(4)
C12	3044(3)	5595.8(9)	5751(2)	17.3(4)
N1	5384(3)	4101.7(7)	9270.4(19)	14.3(3)
N2	2472(3)	4745.6(8)	7225(2)	16.1(4)
N3	4062(3)	5156.4(7)	6949.7(19)	14.1(3)
S1	967.8(8)	3788.4(2)	8469.6(6)	16.95(14)

Table 3 Anisotropic Displacement Parameters ($\text{\AA}^2 \times 10^3$) for 437. The Anisotropic displacement factor exponent takes the form: $-2\pi^2[h^2a^{*2}U_{11}+2hka^*b^*U_{12}+\dots]$.

Atom	U_{11}	U_{22}	U_{33}	U_{23}	U_{13}	U_{12}
C1	16.4(9)	15.1(10)	12.0(9)	-2.9(8)	5.5(7)	1.4(8)
C2	15.0(9)	18.7(10)	11.3(9)	-0.4(8)	3.7(7)	1.6(8)

C3	13.5(9)	15.6(10)	14.4(9)	-1.9(8)	5.8(7)	-0.8(8)
C4	14.6(9)	19.8(11)	15.5(9)	-2.4(8)	1.7(7)	0.1(8)
C5	20.1(10)	19.3(11)	15.9(9)	1.5(8)	2.7(8)	5.2(8)
C6	25.6(10)	14.7(10)	17.8(10)	2.3(8)	8.9(8)	1.6(9)
C7	18(1)	19.3(11)	16.1(9)	-1.1(8)	7.0(8)	-0.6(8)
C8	15.6(9)	15.6(10)	18.0(9)	-0.5(8)	4.8(8)	2.4(8)
C9	16.0(9)	18.0(11)	20.2(10)	-4.2(8)	6.1(8)	-0.9(8)
C10	23(1)	18.7(11)	18.1(10)	-2.4(8)	9.5(8)	-4.9(8)
C11	23.7(10)	16.4(10)	16.2(10)	0.8(8)	4.2(8)	0.4(8)
C12	17.7(9)	17.6(11)	14.9(9)	-0.2(8)	3.1(8)	0.4(8)
N1	14.7(8)	14.4(9)	13.3(8)	0.1(6)	3.7(6)	1.1(7)
N2	14.3(8)	16.0(9)	18.0(8)	2.4(7)	5.2(7)	-0.7(7)
N3	15.4(8)	13.0(8)	14.2(8)	-1.3(6)	5.3(6)	0.2(6)
S1	12.0(2)	19.1(3)	18.4(2)	4.1(2)	3.08(18)	-0.5(2)

Table 4 Bond Lengths for 437.

Atom	Atom	Length/Å	Atom	Atom	Length/Å
C1	C2	1.411(3)	C5	C6	1.395(3)
C1	C4	1.397(3)	C6	C7	1.389(3)
C1	N1	1.386(2)	C8	C9	1.380(3)
C2	C7	1.388(3)	C8	N3	1.363(2)
C2	S1	1.7443(19)	C9	C10	1.377(3)
C3	N1	1.315(2)	C10	C11	1.391(3)
C3	N2	1.341(2)	C11	C12	1.365(3)
C3	S1	1.7939(19)	C12	N3	1.367(2)
C4	C5	1.385(3)	N2	N3	1.384(2)

Table 5 Bond Angles for 437.

Atom	Atom	Atom	Angle/°	Atom	Atom	Atom	Angle/°
C4	C1	C2	119.09(18)	C2	C7	C6	118.51(18)
N1	C1	C2	116.34(16)	N3	C8	C9	119.99(18)
N1	C1	C4	124.54(17)	C10	C9	C8	121.23(19)
C1	C2	S1	109.06(14)	C9	C10	C11	117.82(19)

C7	C2	C1	121.54(17)	C12	C11	C10	120.43(19)
C7	C2	S1	129.38(15)	C11	C12	N3	121.05(18)
N1	C3	N2	133.80(18)	C3	N1	C1	110.99(16)
N1	C3	S1	114.45(14)	C3	N2	N3	118.41(15)
N2	C3	S1	111.75(13)	C8	N3	C12	119.47(16)
C5	C4	C1	119.26(18)	C8	N3	N2	127.38(16)
C4	C5	C6	121.08(18)	C12	N3	N2	113.14(15)
C7	C6	C5	120.51(18)	C2	S1	C3	89.14(9)

Table 6 Torsion Angles for 437.

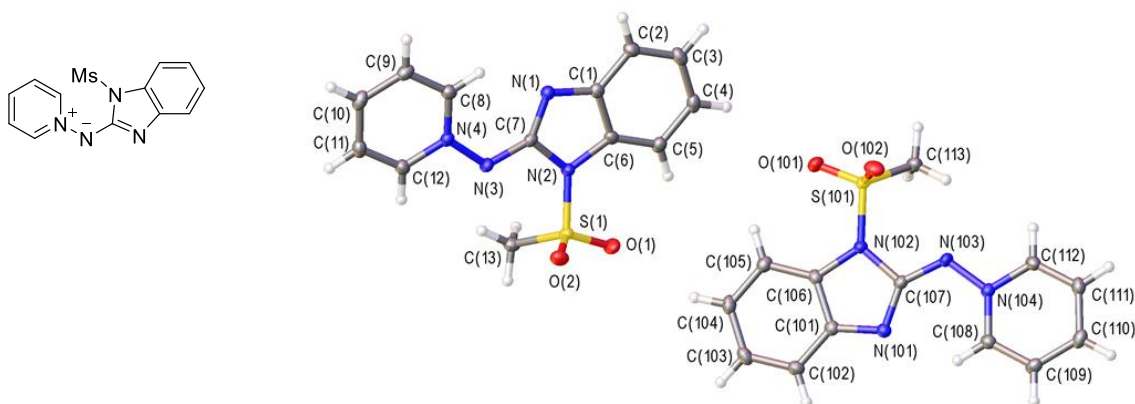
A	B	C	D	Angle/°	A	B	C	D	Angle/°
C1	C2	C7	C6	-0.3(3)	C9	C10	C11	C12	-0.4(3)
C1	C2	S1	C3	0.26(14)	C10	C11	C12	N3	0.9(3)
C1	C4	C5	C6	-1.1(3)	C11	C12	N3	C8	-0.6(3)
C2	C1	C4	C5	0.5(3)	C11	C12	N3	N2	179.41(17)
C2	C1	N1	C3	-1.0(2)	N1	C1	C2	C7	178.64(16)
C3	N2	N3	C8	-3.0(3)	N1	C1	C2	S1	0.3(2)
C3	N2	N3	C12	176.96(16)	N1	C1	C4	C5	-177.80(17)
C4	C1	C2	C7	0.2(3)	N1	C3	N2	N3	0.5(3)
C4	C1	C2	S1	-178.05(14)	N1	C3	S1	C2	-0.86(15)
C4	C1	N1	C3	177.30(17)	N2	C3	N1	C1	-178.14(19)
C4	C5	C6	C7	1.0(3)	N2	C3	S1	C2	178.61(14)
C5	C6	C7	C2	-0.3(3)	N3	C8	C9	C10	0.9(3)
C7	C2	S1	C3	-177.86(18)	S1	C2	C7	C6	177.59(15)
C8	C9	C10	C11	-0.5(3)	S1	C3	N1	C1	1.2(2)
C9	C8	N3	C12	-0.3(3)	S1	C3	N2	N3	-178.84(12)
C9	C8	N3	N2	179.68(17)					

Table 7 Hydrogen Atom Coordinates ($\text{\AA} \times 10^4$) and Isotropic Displacement Parameters ($\text{\AA}^2 \times 10^3$) for 437.

Atom	x	y	z	U(eq)
H4	8762	3409	11406	21
H5	8245	2485	12687	23

H6	4511	2096	12285	23
H7	1208	2614	10506	21
H8	7145	4858	8564	20
H9	9413	5601	7829	22
H10	7691	6361	5810	23
H11	3608	6347	4506	23
H12	1400	5590	5202	21

Appendix 2.1.5 Aminide 443

**Table 1** Crystal data and structure refinement for **443**.

Identification code	443
Empirical formula	C ₁₃ H ₁₂ N ₄ O ₂ S
Formula weight	288.33
Temperature/K	99.9(5)
Crystal system	triclinic
Space group	P-1
a/Å	7.32392(19)
b/Å	8.8468(2)
c/Å	21.5625(5)
α /°	99.806(2)
β /°	90.086(2)
γ /°	113.273(3)
Volume/Å ³	1261.02(6)
Z	4
$\rho_{\text{calc}}/\text{cm}^3$	1.519
μ/mm^{-1}	2.362
F(000)	600.0
Crystal size/mm ³	0.2973 × 0.2478 × 0.1435
Radiation	CuK α (λ = 1.54184)
2 θ range for data collection/°	8.346 to 136.466
Index ranges	-8 ≤ h ≤ 8, -10 ≤ k ≤ 10, -25 ≤ l ≤ 25
Reflections collected	20480

Independent reflections	4617 [$R_{\text{int}} = 0.0163$, $R_{\text{sigma}} = 0.0114$]
Data/restraints/parameters	4617/0/363
Goodness-of-fit on F^2	1.062
Final R indexes [$I \geq 2\sigma(I)$]	$R_1 = 0.0292$, $wR_2 = 0.0776$
Final R indexes [all data]	$R_1 = 0.0310$, $wR_2 = 0.0790$
Largest diff. peak/hole / $e \text{ \AA}^{-3}$	0.28/-0.47

Table 2 Fractional Atomic Coordinates ($\times 10^4$) and Equivalent Isotropic Displacement Parameters ($\text{\AA}^2 \times 10^3$) for 443. U_{eq} is defined as 1/3 of of the trace of the orthogonalised U_{ij} tensor.

Atom	x	y	z	U(eq)
C1	2296(2)	5977.9(18)	4102.7(6)	16.2(3)
C2	2882(2)	7337.5(18)	3794.5(7)	19.3(3)
C3	2133(2)	7074.8(19)	3177.0(7)	21.3(3)
C4	805(2)	5501.7(19)	2868.6(7)	20.2(3)
C5	160(2)	4131.9(18)	3173.0(7)	18.1(3)
C6	938(2)	4401.2(17)	3787.4(6)	15.6(3)
C7	1928(2)	4362.9(17)	4785.8(6)	15.1(3)
C8	4319(2)	6029.2(18)	5947.5(7)	18.0(3)
C9	5277(2)	6703.6(19)	6543.7(7)	20.0(3)
C10	4871(2)	5765(2)	7016.5(7)	21.7(3)
C11	3458(2)	4133.9(19)	6878.7(7)	20.7(3)
C12	2494(2)	3492.4(18)	6288.6(7)	18.0(3)
C13	-2080(2)	734.0(18)	4663.0(7)	20.4(3)
N1	2881.3(17)	5928.0(14)	4710.7(5)	16.0(2)
N2	667.9(18)	3341.6(14)	4233.9(5)	16.4(2)
N3	1848.7(18)	3547.6(14)	5260.0(5)	17.2(2)
N4	2927.5(17)	4424.2(14)	5823.0(5)	15.3(2)
O1	-1442.1(18)	789.5(13)	3475.4(5)	28.2(3)
O2	1114.6(16)	627.1(13)	4164.0(5)	23.6(2)
S1	-382.8(5)	1250.5(4)	4083.9(2)	17.74(10)
C101	6334(2)	-906.6(17)	911.4(6)	16.0(3)
C102	5626(2)	-2245.4(18)	1231.6(7)	18.8(3)
C103	5247(2)	-1928.5(19)	1860.3(7)	20.8(3)
C104	5564(2)	-317.8(19)	2167.2(7)	20.2(3)
C105	6216(2)	1026.9(18)	1850.8(7)	18.6(3)

C106	6572(2)	694.8(17)	1222.0(6)	15.8(3)
C107	7516(2)	665.2(17)	214.3(6)	15.0(3)
C108	8271(2)	-1063.0(17)	-938.4(7)	17.6(3)
C109	8595(2)	-1761.8(18)	-1528.9(7)	19.2(3)
C110	9147(2)	-835.7(19)	-2004.8(7)	20.2(3)
C111	9343(2)	815.9(19)	-1872.4(7)	19.4(3)
C112	8978(2)	1478.4(17)	-1289.5(7)	17.3(3)
C113	7096(2)	4305.4(18)	286.3(7)	19.7(3)
N101	6919.7(17)	-900.2(14)	297.4(5)	15.9(2)
N102	7286.0(17)	1721.9(14)	764.5(5)	16.1(2)
N103	8246.3(18)	1458.6(14)	-262.0(5)	16.8(2)
N104	8462.3(16)	554.2(14)	-821.6(5)	14.9(2)
O101	7447.0(17)	4283.7(13)	1484.5(5)	25.7(2)
O102	10306.4(15)	4454.3(13)	864.6(5)	24.0(2)
S101	8189.8(5)	3810.8(4)	901.3(2)	17.27(10)

Table 3 Anisotropic Displacement Parameters ($\text{\AA}^2 \times 10^3$) for 443. The Anisotropic displacement factor exponent takes the form: $-2\pi^2[\text{h}^2\text{a}^{*2}\text{U}_{11}+2\text{hka}^*\text{b}^*\text{U}_{12}+\dots]$.

Atom	U_{11}	U_{22}	U_{33}	U_{23}	U_{13}	U_{12}
C1	15.3(6)	17.4(7)	17.0(7)	3.1(5)	2.6(5)	7.5(5)
C2	18.1(7)	17.2(7)	21.8(7)	5.1(6)	3.1(6)	5.6(6)
C3	21.3(7)	24.0(8)	22.7(7)	11.9(6)	6.4(6)	10.3(6)
C4	22.4(7)	28.2(8)	14.9(7)	5.9(6)	3.1(5)	14.4(6)
C5	20.0(7)	19.5(7)	16.5(7)	1.5(5)	1.0(5)	10.4(6)
C6	17.4(7)	15.0(7)	16.9(7)	4.0(5)	3.8(5)	8.9(5)
C7	15.4(6)	15.0(7)	14.2(6)	0.0(5)	0.6(5)	6.3(5)
C8	17.9(7)	16.3(7)	19.4(7)	3.1(5)	2.2(5)	6.5(6)
C9	17.0(7)	19.5(7)	20.5(7)	-1.7(6)	-0.4(5)	6.3(6)
C10	18.9(7)	29.9(8)	16.1(7)	-0.9(6)	-2.0(5)	11.8(6)
C11	22.6(7)	26.9(8)	16.3(7)	5.7(6)	2.6(6)	13.2(6)
C12	19.9(7)	17.4(7)	18.0(7)	4.2(5)	3.0(5)	8.5(6)
C13	20.9(7)	16.0(7)	21.6(7)	3.3(6)	1.6(6)	4.8(6)
N1	17.5(6)	15.4(6)	15.0(6)	2.6(5)	0.5(4)	6.4(5)
N2	20.9(6)	13.0(6)	13.5(5)	1.9(4)	-1.3(5)	5.4(5)

N3	20.3(6)	15.0(6)	13.2(6)	0.6(4)	-2.6(4)	4.8(5)
N4	16.1(6)	15.7(6)	14.4(6)	0.8(4)	0.1(4)	7.5(5)
O1	40.4(7)	17.6(5)	18.0(5)	-0.2(4)	-7.4(5)	4.2(5)
O2	29.1(6)	18.1(5)	26.6(6)	4.8(4)	6.1(4)	12.3(4)
S1	23.65(19)	11.97(17)	15.10(17)	0.81(13)	-0.58(13)	5.22(14)
C101	13.9(6)	17.2(7)	16.1(7)	2.6(5)	-0.9(5)	5.7(5)
C102	19.2(7)	16.3(7)	21.3(7)	4.3(6)	0.6(5)	7.3(6)
C103	18.4(7)	24.2(8)	21.3(7)	11.2(6)	2.1(6)	7.3(6)
C104	17.4(7)	27.3(8)	14.6(7)	4.9(6)	1.6(5)	7.1(6)
C105	16.5(7)	19.6(7)	17.3(7)	0.7(6)	0.6(5)	5.7(6)
C106	13.5(6)	16.2(7)	16.3(7)	4.2(5)	-0.5(5)	4.0(5)
C107	14.6(6)	14.7(7)	14.2(6)	0.3(5)	-0.8(5)	5.3(5)
C108	18.1(7)	15.9(7)	18.6(7)	3.8(5)	-0.3(5)	6.5(6)
C109	19.9(7)	18.7(7)	19.1(7)	-0.7(6)	-2.2(5)	9.6(6)
C110	18.6(7)	27.1(8)	14.8(7)	-0.7(6)	-1.0(5)	10.9(6)
C111	18.3(7)	23.6(7)	15.3(7)	5.1(6)	0.6(5)	6.9(6)
C112	17.6(7)	14.9(7)	17.7(7)	4.0(5)	-0.7(5)	4.3(5)
C113	24.2(7)	16.7(7)	19.2(7)	3.1(6)	-0.9(6)	9.5(6)
N101	16.4(6)	14.6(6)	16.1(6)	3.0(5)	0.8(4)	5.3(5)
N102	20.1(6)	12.3(6)	14.2(6)	2.0(4)	1.8(4)	5.0(5)
N103	22.4(6)	14.4(6)	13.0(6)	0.6(4)	2.6(5)	7.4(5)
N104	14.3(6)	15.0(6)	14.0(5)	1.1(4)	-0.2(4)	5.2(5)
O101	40.3(6)	18.3(5)	17.8(5)	0.1(4)	3.5(5)	12.3(5)
O102	20.6(5)	16.7(5)	30.4(6)	5.2(4)	-4.3(4)	2.6(4)
S101	21.53(19)	12.02(17)	15.95(17)	0.73(13)	-1.17(13)	5.07(14)

Table 4 Bond Lengths for 443.

Atom	Atom	Length/Å	Atom	Atom	Length/Å
C1	C2	1.392(2)	C101	C102	1.394(2)
C1	C6	1.406(2)	C101	C106	1.403(2)
C1	N1	1.3919(18)	C101	N101	1.3926(18)
C2	C3	1.385(2)	C102	C103	1.388(2)
C3	C4	1.392(2)	C103	C104	1.393(2)
C4	C5	1.394(2)	C104	C105	1.392(2)

C5	C6	1.3854(19)	C105 C106	1.385(2)
C6	N2	1.4165(18)	C106 N102	1.4153(18)
C7	N1	1.3204(18)	C107 N101	1.3219(18)
C7	N2	1.4336(17)	C107 N102	1.4343(17)
C7	N3	1.3370(18)	C107 N103	1.3356(18)
C8	C9	1.380(2)	C108 C109	1.381(2)
C8	N4	1.3612(18)	C108 N104	1.3596(18)
C9	C10	1.383(2)	C109 C110	1.383(2)
C10	C11	1.384(2)	C110 C111	1.389(2)
C11	C12	1.369(2)	C111 C112	1.367(2)
C12	N4	1.3655(18)	C112 N104	1.3664(18)
C13	S1	1.7505(15)	C113 S101	1.7501(14)
N2	S1	1.6702(12)	N102 S101	1.6696(12)
N3	N4	1.3754(16)	N103 N104	1.3758(16)
O1	S1	1.4333(11)	O101 S101	1.4335(11)
O2	S1	1.4306(11)	O102 S101	1.4324(11)

Table 5 Bond Angles for 443.

Atom	Atom	Atom	Angle/°	Atom	Atom	Atom	Angle/°
C2	C1	C6	119.46(13)	C102	C101	C106	119.60(13)
N1	C1	C2	128.68(13)	N101	C101	C102	128.58(13)
N1	C1	C6	111.86(12)	N101	C101	C106	111.80(12)
C3	C2	C1	118.39(14)	C103	C102	C101	118.29(13)
C2	C3	C4	121.47(14)	C102	C103	C104	121.23(13)
C3	C4	C5	121.13(13)	C105	C104	C103	121.33(13)
C6	C5	C4	116.99(13)	C106	C105	C104	116.98(13)
C1	C6	N2	104.36(12)	C101	C106	N102	104.50(12)
C5	C6	C1	122.53(13)	C105	C106	C101	122.49(13)
C5	C6	N2	133.11(13)	C105	C106	N102	132.95(13)
N1	C7	N2	111.44(12)	N101	C107	N102	111.25(11)
N1	C7	N3	134.43(13)	N101	C107	N103	134.63(13)
N3	C7	N2	114.10(12)	N103	C107	N102	114.11(12)
N4	C8	C9	119.78(13)	N104	C108	C109	119.86(13)
C8	C9	C10	121.05(14)	C108	C109	C110	121.15(13)

C9	C10	C11	118.19(13)	C109	C110	C111	117.86(13)
C12	C11	C10	120.08(14)	C112	C111	C110	120.25(14)
N4	C12	C11	121.19(13)	N104	C112	C111	121.16(13)
C7	N1	C1	106.04(11)	C107	N101	C101	106.09(11)
C6	N2	C7	106.28(11)	C106	N102	C107	106.28(11)
C6	N2	S1	126.22(10)	C106	N102	S101	125.74(9)
C7	N2	S1	125.51(9)	C107	N102	S101	126.46(9)
C7	N3	N4	119.02(11)	C107	N103	N104	119.07(11)
C8	N4	C12	119.70(12)	C108	N104	C112	119.70(12)
C8	N4	N3	127.73(12)	C108	N104	N103	127.67(12)
C12	N4	N3	112.56(11)	C112	N104	N103	112.61(11)
N2	S1	C13	104.24(6)	N102	S101	C113	104.97(6)
O1	S1	C13	109.66(7)	O101	S101	C113	109.10(7)
O1	S1	N2	105.69(6)	O101	S101	N102	105.86(6)
O2	S1	C13	109.59(7)	O102	S101	C113	109.53(7)
O2	S1	N2	109.03(6)	O102	S101	N102	108.77(6)
O2	S1	O1	117.72(7)	O102	S101	O101	117.81(7)

Table 6 Torsion Angles for 443.

A	B	C	D	Angle/°	A	B	C	D	Angle/°
C1	C2	C3	C4	0.9(2)	C101	C102	C103	C104	-0.1(2)
C1	C6	N2	C7	-1.16(14)	C101	C106	N102	C107	-2.66(14)
C1	C6	N2	S1	-165.75(10)	C101	C106	N102	S101	-169.32(10)
C2	C1	C6	C5	0.7(2)	C102	C101	C106	C105	3.0(2)
C2	C1	C6	N2	-179.37(12)	C102	C101	C106	N102	-179.57(12)
C2	C1	N1	C7	-179.86(14)	C102	C101	N101	C107	-178.58(14)
C2	C3	C4	C5	0.7(2)	C102	C103	C104	C105	2.0(2)
C3	C4	C5	C6	-1.6(2)	C103	C104	C105	C106	-1.3(2)
C4	C5	C6	C1	0.9(2)	C104	C105	C106	C101	-1.2(2)
C4	C5	C6	N2	-179.06(14)	C104	C105	C106	N102	-177.75(14)
C5	C6	N2	C7	178.81(15)	C105	C106	N102	C107	174.36(15)
C5	C6	N2	S1	14.2(2)	C105	C106	N102	S101	7.7(2)
C6	C1	C2	C3	-1.5(2)	C106	C101	C102	C103	-2.3(2)
C6	C1	N1	C7	0.00(15)	C106	C101	N101	C107	-0.11(15)

C6 N2 S1 C13	-131.97(12)	C106 N102 S101 C113	-135.65(12)
C6 N2 S1 O1	-16.38(13)	C106 N102 S101 O101	-20.30(13)
C6 N2 S1 O2	111.06(12)	C106 N102 S101 O102	107.20(12)
C7 N2 S1 C13	66.30(12)	C107 N102 S101 C113	60.33(13)
C7 N2 S1 O1	-178.12(11)	C107 N102 S101 O101	175.68(11)
C7 N2 S1 O2	-50.67(13)	C107 N102 S101 O102	-56.82(13)
C7 N3 N4 C8	-9.4(2)	C107 N103 N104 C108	-9.6(2)
C7 N3 N4 C12	171.48(12)	C107 N103 N104 C112	172.11(12)
C8 C9 C10 C11	-0.8(2)	C108 C109 C110 C111	-0.7(2)
C9 C8 N4 C12	-0.2(2)	C109 C108 N104 C112	-0.10(19)
C9 C8 N4 N3	-179.25(13)	C109 C108 N104 N103	-178.23(13)
C9 C10 C11 C12	-0.4(2)	C109 C110 C111 C112	-0.6(2)
C10 C11 C12 N4	1.3(2)	C110 C111 C112 N104	1.6(2)
C11 C12 N4 C8	-1.0(2)	C111 C112 N104 C108	-1.2(2)
C11 C12 N4 N3	178.19(12)	C111 C112 N104 N103	177.19(13)
N1 C1 C2 C3	178.31(14)	N101 C101 C102 C103	176.07(13)
N1 C1 C6 C5	-179.22(12)	N101 C101 C106 C105	-175.61(12)
N1 C1 C6 N2	0.76(15)	N101 C101 C106 N102	1.81(15)
N1 C7 N2 C6	1.26(15)	N101 C107 N102 C106	2.82(15)
N1 C7 N2 S1	165.99(10)	N101 C107 N102 S101	169.36(10)
N1 C7 N3 N4	1.2(2)	N101 C107 N103 N104	1.2(2)
N2 C7 N1 C1	-0.78(15)	N102 C107 N101 C101	-1.68(15)
N2 C7 N3 N4	-177.02(11)	N102 C107 N103 N104	-177.69(11)
N3 C7 N1 C1	-179.01(15)	N103 C107 N101 C101	179.39(15)
N3 C7 N2 C6	179.88(11)	N103 C107 N102 C106	-178.01(11)
N3 C7 N2 S1	-15.39(17)	N103 C107 N102 S101	-11.48(17)
N4 C8 C9 C10	1.1(2)	N104 C108 C109 C110	1.1(2)

Table 7 Hydrogen Atom Coordinates ($\text{\AA} \times 10^4$) and Isotropic Displacement Parameters ($\text{\AA}^2 \times 10^3$) for 443.

Atom	<i>x</i>	<i>y</i>	<i>z</i>	U(eq)
H2	3754	8397	3998	23
H3	2527	7969	2964	26
H4	341	5363	2452	24

Appendix 2

H5	-752	3084	2973	22
H8	4624	6669	5632	22
H9	6211	7807	6629	24
H10	5531	6217	7416	26
H11	3162	3473	7187	25
H12	1527	2402	6203	22
H13A	-1384	1197	5074	31
H13B	-2729	-462	4616	31
H13C	-3060	1184	4617	31
H102	5414	-3323	1029	23
H103	4772	-2808	2081	25
H104	5336	-137	2592	24
H105	6403	2100	2052	22
H108	7922	-1697	-622	21
H109	8440	-2874	-1608	23
H110	9379	-1304	-2401	24
H111	9723	1474	-2182	23
H112	9083	2577	-1210	21
H11A	7472	3880	-110	29
H11B	7545	5499	338	29
H11C	5672	3809	294	29

Bibliography

- [1] (a) R. Hili, A. K. Yudin, *Nat. Chem. Biol.* **2006**, *2*, 284-287; (b) T. Okubo, R. Yoshikawa, S. Chaki, S. Okuyama, A. Nakazato, *Bioorg. Med. Chem.* **2004**, *12*, 423-438; (c) A. N. Jain, *J. Med. Chem.* **2004**, *47*, 947-961; (d) T. Swainston Harrison, G. M. Keating, *CNS Drugs* **2005**, *19*, 65-89.
- [2] (a) M. Balasubramanian, J. G. Keay, in *Comprehensive Heterocyclic Chemistry II* (Ed.: A. R. K. W. R. F. V. Scriven), Pergamon, Oxford, **1996**, pp. 245-300; (b) Z. Jin, *Nat. Prod. Rep.* **2011**, *28*, 1143-1191; (c) A. Ricci, in *Amino Group Chemistry*, Wiley-VCH Verlag GmbH & Co. KGaA, **2008**, pp. I-XIV; (d) A. K. Bagdi, S. Santra, K. Monir, A. Hajra, *Chem. Commun.* **2015**, *51*, 1555-1575
- [3] G. Dequierez, V. Pons, P. Dauban, *Angew. Chem. Int. Ed.* **2012**, *51*, 7384-7395.
- [4] (a) F. Collet, C. Lescot, P. Dauban, *Chem. Soc. Rev.* **2011**, *40*, 1926-1936; (b) B. J. Stokes, T. G. Driver, *Eur. J. Org. Chem.* **2011**, *2011*, 4071-4088.
- [5] C. G. Espino, J. D. Bois, *Angew. Chem. Int. Ed.* **2001**, *40*, 598-600.
- [6] A. Hinman, J. Du Bois, *J. Am. Chem. Soc.* **2003**, *125*, 11510-11511.
- [7] P. Starkov, T. F. Jamison, I. Marek, *Chem. Eur. J.* **2015**, *21*, 5278-5300.
- [8] H. M. L. Davies, J. R. Manning, *Nature* **2008**, *451*, 417-424.
- [9] A. Basha, D. W. Brooks, *J. Chem. Soc., Chem. Commun.* **1987**, 305-306.
- [10] (a) A. Fürstner, P. W. Davies, *Angew. Chem., Int. Ed.* **2007**, *46*, 3410-3449; (b) A. S. K. Hashmi, *Chem. Rev.* **2007**, *107*, 3180-3211; (c) D. J. Gorin, F. D. Toste, *Nature* **2007**, *446*, 395-403.
- [11] (a) A. R. Thornton, V. I. Martin, S. B. Blakey, *J. Am. Chem. Soc.* **2009**, *131*, 2434-2435; (b) A. R. Thornton, S. B. Blakey, *J. Am. Chem. Soc.* **2008**, *130*, 5020-5021; (c) N. Mace, A. R. Thornton, S. B. Blakey, *Angew. Chem.* **2013**, *125*, 5948-5951.
- [12] (a) H.-S. Yeom, S. Shin, *Acc. Chem. Res.* **2014**, *47*, 966-977; (b) L. Fensterbank, M. Malacria, *Acc. Chem. Res.* **2014**, *47*, 953-965; (c) B. Alcaide, P. Almendros, *Acc. Chem. Res.* **2014**, *47*, 939-952; (d) A. Fürstner, *Acc. Chem. Res.* **2014**, *47*, 925-938.
- [13] L. Liu, J. Zhang, *Chem. Soc. Rev.* **2016**, *45*, 506-516.
- [14] (a) P. W. Davies, S. J. C. Albrecht, *Angew. Chem. Int. Ed.* **2009**, *48*, 8372-8375; (b) G. Li, L. Zhang, *Angew. Chem. Int. Ed.* **2007**, *46*, 5156-5159.
- [15] H.-S. Yeom, Y. Lee, J.-E. Lee, S. Shin, *Org. Biomol. Chem* **2009**, *7*, 4744-4752.
- [16] L. Cui, G. Zhang, Y. Peng, L. Zhang, *Org. Lett.* **2009**, *11*, 1225-1228.
- [17] N. Asao, K. Sato, Y. Yamamoto, *Tetrahedron Lett.* **2003**, *44*, 5675-5677.

- [18] (a) W. M. F. Fabian, V. A. Bakulev, C. O. Kappe, *J. Org. Chem.* **1998**, *63*, 5801-5805; (b) B. Japelj, S. Rečnik, P. Čebašek, B. Stanovnik, J. Svete, *J. Heterocycl. Chem.* **2005**, *42*, 1167-1173.
- [19] (a) Y. Wang, M. E. Muratore, A. M. Echavarren, *Chem. Eur. J.* **2015**, *21*, 7332-7339; (b) G. Seidel, A. Fürstner, *Angew. Chem. Int. Ed.* **2014**, *53*, 4807-4811; (c) A. S. K. Hashmi, *Angew. Chem. Int. Ed.* **2010**, *49*, 5232-5241; (d) D. Benitez, N. D. Shapiro, E. Tkatchouk, Y. Wang, W. A. Goddard, F. D. Toste, *Nat. Chem.* **2009**, *1*, 482-486; (e) L. Nunes dos Santos Comprido, J. E. M. N. Klein, G. Knizia, J. Kästner, A. S. K. Hashmi, *Angew. Chem. Int. Ed.* **2015**, *54*, 10336-10340.
- [20] Y. Xi, Y. Su, Z. Yu, B. Dong, E. J. McClain, Y. Lan, X. Shi, *Angew. Chem. Int. Ed.* **2014**, *53*, 9817-9821.
- [21] (a) W. H. Pearson, D. A. Hutta, W.-k. Fang, *J. Org. Chem.* **2000**, *65*, 8326-8332; (b) W. H. Pearson, R. Walavalkar, J. M. Schkeryantz, W. K. Fang, J. D. Blickensdorf, *J. Am. Chem. Soc.* **1993**, *115*, 10183-10194; (c) J. Aubé, G. L. Milligan, *J. Am. Chem. Soc.* **1991**, *113*, 8965-8966; (d) S. Lang, J. A. Murphy, *Chem. Soc. Rev.* **2006**, *35*, 146-156; (e) M. Szostak, L. Yao, J. Aubé, *J. Org. Chem.* **2010**, *75*, 1235-1243.
- [22] W. H. Pearson, D. A. Hutta, W.-k. Fang, *J. Org. Chem.* **2000**, *65*, 8326-8332.
- [23] D. J. Gorin, N. R. Davis, F. D. Toste, *J. Am. Chem. Soc.* **2005**, *127*, 11260-11261.
- [24] For an analogous platinum-catalysed version of this reaction: K. Hiroya, S. Matsumoto, M. Ashikawa, K. Ogiwara, T. Sakamoto, *Org. Lett.* **2006**, *8*, 5349-5352.
- [25] Z. Huo, Y. Yamamoto, *Tetrahedron Lett.* **2009**, *50*, 3651-3653.
- [26] Z.-Y. Yan, Y. Xiao, L. Zhang, *Angew. Chem. Int. Ed.* **2012**, *51*, 8624-8627.
- [27] W. He, C. Li, L. Zhang, *J. Am. Chem. Soc.* **2011**, *133*, 8482-8485.
- [28] (a) A. Wetzel, F. Gagosz, *Angew. Chem. Int. Ed.* **2011**, *50*, 7354-7358; (b) B. Lu, Y. Luo, L. Liu, L. Ye, Y. Wang, L. Zhang, *Angew. Chem. Int. Ed.* **2011**, *50*, 8358-8362.
- [29] For the trapping with propargyl alcohols in a cascade Sauce-Marbet rearrangement/allene hydroamination: N. Li, T.-Y. Wang, L.-Z. Gong, L. Zhang, *Chem. Eur. J.* **2015**, *21*, 3585-3588.
- [30] (a) Y. Tokimizu, S. Oishi, N. Fujii, H. Ohno, *Org. Lett.* **2014**, *16*, 3138-3141; (b) X.-N. Wang, H.-S. Yeom, L.-C. Fang, S. He, Z.-X. Ma, B. L. Kedrowski, R. P. Hsung, *Acc. Chem. Res.* **2014**, *47*, 560-578.

- [31] A. Prechter, G. Henrion, P. Faudot dit Bel, F. Gagosz, *Angew. Chem. Int. Ed.* **2014**, *53*, 4959-4963.
- [32] L. Jin, Y. Wu, X. Zhao, *J. Org. Chem.* **2015**.
- [33] P. W. Davies, A. Cremonesi, L. Dumitrescu, *Angew. Chem. Int. Ed.* **2011**, *50*, 8931-8935.
- [34] (a) E. Chatzopoulou, P. W. Davies, *Chem. Commun.* **2013**, *49*, 8617-8619; (b) A. D. Gillie, R. Jannapu Reddy, P. W. Davies, *Adv. Synth. Catal.* **2016**, *358*, 226-239.
- [35] M. Garzón, P. W. Davies, *Org. Lett.* **2014**, *16*, 4850-4853.
- [36] A.-H. Zhou, Q. He, C. Shu, Y.-F. Yu, S. Liu, T. Zhao, W. Zhang, X. Lu, L.-W. Ye, *Chem. Sci.* **2015**, *6*, 1265-1271.
- [37] L. Zhu, Y. Yu, Z. Mao, X. Huang, *Org. Lett.* **2015**, *17*, 30-33.
- [38] S. K. Pawar, R. L. Sahani, R. S. Liu, *Chem. Eur. J.* **2015**, *21*, 10843-10850.
- [39] Y. Wu, L. Zhu, Y. Yu, X. Luo, X. Huang, *J. Org. Chem.* **2015**, *80*, 11407-11416.
- [40] F. Palacios, A. M. Ochoa de Retana, E. Martinez de Marigorta, J. M. de los Santos, *Eur. J. Org. Chem.* **2001**, *2001*, 2401-2414.
- [41] C. Shu, Y.-H. Wang, B. Zhou, X.-L. Li, Y.-F. Ping, X. Lu, L.-W. Ye, *J. Am. Chem. Soc.* **2015**, *137*, 9567-9570.
- [42] X. Zhang, H. Li, L. You, Y. Tang, R. P. Hsung, *Adv. Synth. Catal.* **2006**, *348*, 2437-2442.
- [43] H. Jin, L. Huang, J. Xie, M. Rudolph, F. Rominger, A. S. K. Hashmi, *Angew. Chem. Int. Ed.* **2016**, *55*, 794-797.
- [44] For reviews on the reactivity of azomethine imines: (a) G. Qiu, Y. Kuang, J. Wu, *Adv. Synth. Catal.* **2014**, *356*, 3483-3504; (b) C. Najera, J. M. Sansano, M. Yus, *Org. Biomol. Chem.* **2015**, *13*, 8596-8636.
- [45] J. González, J. Santamaría, Á. L. Suárez-Sobrino, A. Ballesteros, *Adv. Synth. Catal.* **2016**, 1398-1403.
- [46] (a) L. Ye, L. Cui, G. Zhang, L. Zhang, *J. Am. Chem. Soc.* **2010**, *132*, 3258-3259; (b) L. Ye, W. He, L. Zhang, *J. Am. Chem. Soc.* **2010**, *132*, 8550-8551; (c) B. Lu, C. Li, L. Zhang, *J. Am. Chem. Soc.* **2010**, *132*, 14070-14072.
- [47] P. W. Davies, A. Cremonesi, N. Martin, *Chem. Commun.* **2011**, *47*, 379-381.
- [48] C. Li, L. Zhang, *Org. Lett.* **2011**, *13*, 1738-1741.

- [49] For the intermolecular addition of pyridinium *N*-aminides into terminal alkynes: H.-H. Hung, Y.-C. Liao, R.-S. Liu, *J. Org. Chem.* **2013**, *78*, 7970-7976.
- [50] (a) H. C. Kolb, M. G. Finn, K. B. Sharpless, *Angew. Chem. Int. Ed.* **2001**, *40*, 2004-2021; (b) S. Ma, *Handbook of cyclization reactions*, Wiley-VCH, **2010**.
- [51] (a) M. Mörtl, D. Knausz, Z. Böcskei, Z. Kolos, K. Újszászy, L. Szakács, P. Sohár, *J. Organomet. Chem.* **1995**, *492*, 115-119; (b) K.-U. Clauss, K. Buck, W. Abraham, *Tetrahedron* **1995**, *51*, 7181-7192; (c) K. Buck, D. Jacobi, Y. Plögert, W. Abraham, *J. Prakt. Chem.* **1994**, *336*, 678-685.
- [52] (a) E. Haldón, M. Besora, I. Cano, X. C. Cambeiro, M. A. Pericàs, F. Maseras, M. C. Nicasio, P. J. Pérez, *Chem. Eur. J.* **2014**, *20*, 3463-3474; (b) I. Cano, E. Álvarez, M. C. Nicasio, P. J. Pérez, *J. Am. Chem. Soc.* **2011**, *133*, 191-193.
- [53] R. Carceller, J. L. García-Navío, M. L. Izquierdo, J. Alvarez-Builla, M. Fajardo, P. Gómez-Sal, F. Gago, *Tetrahedron* **1994**, *50*, 4995-5012.
- [54] M. José Reyes, C. Burgos, M. Luisa Izquierdo, J. Alvarez-Builla, *Tetrahedron* **2004**, *60*, 1093-1097.
- [55] K. A. DeKorver, H. Li, A. G. Lohse, R. Hayashi, Z. Lu, Y. Zhang, R. P. Hsung, *Chem. Rev.* **2010**, *110*, 5064-5106.
- [56] G. Evano, A. Coste, K. Jouvin, *Angew. Chem. Int. Ed.* **2010**, *49*, 2840-2859.
- [57] (a) Y. Zhang, R. P. Hsung, X. Zhang, J. Huang, B. W. Slafer, A. Davis, *Org. Lett.* **2005**, *7*, 1047-1050; (b) S. Couty, B. Liegault, C. Meyer, J. Cossy, *Tetrahedron* **2006**, *62*, 3882-3895.
- [58] (a) Z. Xin, S. Kramer, J. Overgaard, T. Skrydstrup, *Chem. Eur. J.* **2014**, *20*, 7926-7930; (b) S. N. Karad, R.-S. Liu, *Angew. Chem. Int. Ed.* **2014**, *53*, 9072-9076; (c) H. V. Adcock, T. Langer, P. W. Davies, *Chem. Eur. J.* **2014**, *20*, 7262-7266; (d) N. Ghosh, S. Nayak, A. K. Sahoo, *Chem. Eur. J.* **2013**, *19*, 9428-9433; (e) S. Kramer, Y. Odabachian, J. Overgaard, M. Rottländer, F. Gagosz, T. Skrydstrup, *Angew. Chem. Int. Ed.* **2011**, *50*, 5090-5094; (f) S. Couty, C. Meyer, J. Cossy, *Tetrahedron* **2009**, *65*, 1809-1832.
- [59] A. Coste, G. Karthikeyan, F. Couty, G. Evano, *Angew. Chem. Int. Ed.* **2009**, *48*, 4381-4385.
- [60] T. Hamada, X. Ye, S. S. Stahl, *J. Am. Chem. Soc.* **2008**, *130*, 833-835.
- [61] (a) Y. Zhang, R. P. Hsung, M. R. Tracey, K. C. M. Kurtz, E. L. Vera, *Org. Lett.* **2004**, *6*, 1151-1154; (b) X. Zhang, Y. Zhang, J. Huang, R. P. Hsung, K. C. M. Kurtz, J. Oppenheimer, M. E. Petersen, I. K. Sagamanova, L. Shen, M. R. Tracey, *J. Org. Chem.* **2006**, *71*, 4170-4177.
- [62] N. B. Desai, N. McKelvie, F. Ramirez, *J. Am. Chem. Soc.* **1962**, *84*, 1745-1747.

- [63] E. J. Corey, P. L. Fuchs, *Tetrahedron Lett.* **1972**, *13*, 3769-3772.
- [64] G. J. Roth, B. Liepold, S. G. Müller, H. J. Bestmann, *Synthesis* **2004**, *2004*, 59-62.
- [65] Y.-S. Feng, Z.-Q. Xu, L. Mao, F.-F. Zhang, H.-J. Xu, *Org. Lett.* **2013**, *15*, 1472-1475.
- [66] P.-Y. Yao, Y. Zhang, R. P. Hsung, K. Zhao, *Org. Lett.* **2008**, *10*, 4275-4278.
- [67] K. A. DeKorver, M. C. Walton, T. D. North, R. P. Hsung, *Org. Lett.* **2011**, *13*, 4862-4865.
- [68] A. H. Sato, K. Ohashi, K. Ito, T. Iwasawa, *Tetrahedron Lett.* **2013**, *54*, 2878-2881.
- [69] (a) W. T. Brady, G. A. Scherubel, *J. Am. Chem. Soc.* **1973**, *95*, 7447-7449; (b) R. J. Sundberg, J. P. Laurino, *J. Org. Chem.* **1984**, *49*, 249-254; (c) L. De Luca, G. Giacomelli, *J. Org. Chem.* **2008**, *73*, 3967-3969.
- [70] (a) D. H. Huh, J. S. Jeong, H. B. Lee, H. Ryu, Y. G. Kim, *Tetrahedron* **2002**, *58*, 9925-9932; (b) L. Capelli, O. Crescenzi, P. Manini, A. Pezzella, V. Barone, M. d'Ischia, *J. Org. Chem.* **2011**, *76*, 4457-4466.
- [71] A. S. K. Hashmi, J. P. Weyrauch, M. Rudolph, E. Kurpejović, *Angew. Chem. Int. Ed.* **2004**, *43*, 6545-6547.
- [72] (a) C. Nevado, A. M. Echavarren, *Chem. Eur. J.* **2005**, *11*, 3155-3164; (b) D. Wang, R. Cai, S. Sharma, J. Jirak, S. K. Thummanapelli, N. G. Akhmedov, H. Zhang, X. Liu, J. L. Petersen, X. Shi, *J. Am. Chem. Soc.* **2012**, *134*, 9012-9019.
- [73] A. Homs, I. Escofet, A. M. Echavarren, *Org. Lett.* **2013**, *15*, 5782-5785.
- [74] (a) K. A. DeKorver, R. P. Hsung, A. G. Lohse, Y. Zhang, *Org. Lett.* **2010**, *12*, 1840-1843; (b) Y. Zhang, K. A. DeKorver, A. G. Lohse, Y.-S. Zhang, J. Huang, R. P. Hsung, *Org. Lett.* **2009**, *11*, 899-902.
- [75] P. W. Davies, A. Cremonesi, L. Dumitrescu, *Angew. Chem. Int. Ed.* **2011**, *50*, 8931-8935.
- [76] (a) E. S. Hand, W. W. Paudler, *J. Org. Chem.* **1980**, *45*, 3738-3745; (b) K. Vaughan, R. J. LaFrance, Y. Tang, D. L. Hooper, *J. Heterocycl. Chem.* **1991**, *28*, 1709-1713.
- [77] M. S. Jensen, R. S. Hoerrner, W. Li, D. P. Nelson, G. J. Javadi, P. G. Dormer, D. Cai, R. D. Larsen, *J. Org. Chem.* **2005**, *70*, 6034-6039.
- [78] C. Jaramillo, J. E. de Diego, C. Hamdouchi, E. Collins, H. Keyser, C. Sánchez-Martínez, M. del Prado, B. Norman, H. B. Brooks, S. A. Watkins, C. D. Spencer, J. A. Dempsey, B. D. Anderson, R. M. Campbell, T. Leggett, B. Patel,

- R. M. Schultz, J. Espinosa, M. Vieth, F. Zhang, D. E. Timm, *Bioorg. Med. Chem. Lett.* **2004**, *14*, 6095-6099.
- [79] (a) R. J. Bochis, L. E. Olen, M. H. Fisher, R. A. Reamer, G. Wilks, J. E. Taylor, G. Olson, *J. Med. Chem.* **1981**, *24*, 1483-1487; (b) C. Hamdouchi, B. Zhong, J. Mendoza, E. Collins, C. Jaramillo, J. E. De Diego, D. Robertson, C. D. Spencer, B. D. Anderson, S. A. Watkins, F. Zhang, H. B. Brooks, *Bioorg. Med. Chem. Lett.* **2005**, *15*, 1943-1947; (c) C. Jaramillo, J. C. Carretero, J. E. de Diego, M. del Prado, C. Hamdouchi, J. L. Roldán, C. Sánchez-Martínez, *Tetrahedron Lett.* **2002**, *43*, 9051-9054.
- [80] S. Carballares, M. M. Cifuentes, G. A. Stephenson, *Tetrahedron Lett.* **2007**, *48*, 2041-2045.
- [81] K. Groebke, L. Weber, F. Mehlin, *Synlett* **1998**, *1998*, 661-663.
- [82] (a) A. N. Campbell, K. P. Cole, J. R. Martinelli, S. A. May, D. Mitchell, P. M. Pollock, K. A. Sullivan, *Org. Process Res. Dev.* **2013**, *17*, 273-281; (b) M. Hranjec, M. Kralj, I. Piantanida, M. Sedić, L. Šuman, K. Pavelić, G. Karminski-Zamola, *J. Med. Chem.* **2007**, *50*, 5696-5711.
- [83] (a) A. Gueiffier, M. Lhassani, A. Elhakmaoui, R. Snoeck, G. Andrei, O. Chavignon, J.-C. Teulade, A. Kerbal, E. M. Essassi, J.-C. Debouzy, M. Witvrouw, Y. Blache, J. Balzarini, E. De Clercq, J.-P. Chapat, *J. Med. Chem.* **1996**, *39*, 2856-2859; (b) C. Hamdouchi, J. de Blas, M. del Prado, J. Gruber, B. A. Heinz, L. Vance, *J. Med. Chem.* **1999**, *42*, 50-59.
- [84] Y. Rival, G. Grassy, G. Michel, *Chem. Pharm. Bull.* **1992**, *40*, 1170-1176.
- [85] K. C. Rupert, J. R. Henry, J. H. Dodd, S. A. Wadsworth, D. E. Cavender, G. C. Olini, B. Fahmy, J. J. Siekierka, *Bioorg. Med. Chem. Lett.* **2003**, *13*, 347-350.
- [86] W. R. Tully, C. R. Gardner, R. J. Gillespie, R. Westwood, *J. Med. Chem.* **1991**, *34*, 2060-2067.
- [87] (a) H. Shono, T. Ohkawa, H. Tomoda, T. Mutai, K. Araki, *ACS App. Mater. Interfaces* **2011**, *3*, 654-657; (b) S. Furukawa, H. Shono, T. Mutai, K. Araki, *ACS App. Mater. Interfaces* **2014**, *6*, 16065-16070; (c) For an analogous transition-metal-free reaction: A. J. Stasyuk, M. Banasiewicz, M. K. Cyrański, D. T. Gryko, *J. Org. Chem.* **2012**, *77*, 5552-5558.
- [88] L. Ma, X. Wang, W. Yu, B. Han, *Chem. Commun.* **2011**, *47*, 11333-11335.
- [89] (a) T. Kercher, C. Rao, J. R. Bencsik, J. A. Josey, *J. Comb. Chem.* **2007**, *9*, 1177-1187; (b) E. F. DiMauro, J. M. Kennedy, *J. Org. Chem.* **2007**, *72*, 1013-1016; (c) T. H. Al-Tel, R. A. Al-Qawasmeh, W. Voelter, *Eur. J. Org. Chem.* **2010**, *2010*, 5586-5593; (d) T. Meng, Z. Zhang, D. Hu, L. Lin, J. Ding, X. Wang, J. Shen, *J. Comb. Chem.* **2007**, *9*, 739-741; (e) A. Demjén, M. Gyuris, J. Wölfling, L. G. Puskás, I. Kanizsai, *Beilstein J. Org. Chem.* **2014**, *10*, 2338-2344.

- [90] N. Chernyak, V. Gevorgyan, *Angew. Chem. Int. Ed.* **2010**, *49*, 2743-2746.
- [91] M. Chioua, E. Soriano, L. Infantes, M. L. Jimeno, J. Marco-Contelles, A. Samadi, *Eur. J. Org. Chem.* **2013**, *2013*, 35-39.
- [92] Y. Zhang, Z. Chen, W. Wu, Y. Zhang, W. Su, *J. Org. Chem.* **2013**, *78*, 12494-12504.
- [93] Y. Gao, M. Yin, W. Wu, H. Huang, H. Jiang, *Adv. Synth. Catal.* **2013**, *355*, 2263-2273.
- [94] E. P. A. Talbot, M. Richardson, J. M. McKenna, F. D. Toste, *Adv. Synth. Catal.* **2014**, *356*, 687-691.
- [95] (a) C. Y. Legault, A. B. Charette, *J. Am. Chem. Soc.* **2005**, *127*, 8966-8967; (b) C. Legault, A. B. Charette, *J. Am. Chem. Soc.* **2003**, *125*, 6360-6361.
- [96] A. Kakehi, S. Ito, Y. Hashimoto, *Bull. Chem. Soc. Jpn.* **1996**, *69*, 1769-1776.
- [97] (a) T. Sasaki, K. Kanematsu, A. Kakehi, *J. Org. Chem.* **1971**, *36*, 2978-2986; (b) J. J. Mousseau, A. Fortier, A. B. Charette, *Org. Lett.* **2010**, *12*, 516-519; (c) J. J. Mousseau, J. A. Bull, C. L. Ladd, A. Fortier, D. Sustac Roman, A. B. Charette, *J. Org. Chem.* **2011**, *76*, 8243-8261; (d) S. Ding, Y. Yan, N. Jiao, *Chem. Commun.* **2013**, *49*, 4250-4252.
- [98] (a) R. Carceller, J. L. García-Navío, M. L. Izquierdo, J. Alvarez-Builla, *Tetrahedron Lett.* **1993**, *34*, 2019-2020; (b) C. Burgos, F. Delgado, J. Luis García-Navío, M. Luisa Izquierdo, J. Alvarez-Builla, *Tetrahedron* **1995**, *51*, 8649-8654; (c) A. García de Viedma, V. Martínez-Barrasa, C. Burgos, M. L. Izquierdo, J. Alvarez-Builla, *J. Org. Chem.* **1999**, *64*, 1007-1010.
- [99] (a) V. n. Martínez-Barrasa, F. Delgado, C. Burgos, J. Luis García-Navío, M. Luisa Izquierdo, J. Alvarez-Builla, *Tetrahedron* **2000**, *56*, 2481-2490; (b) M. José Reyes, F. Delgado, M. Luisa Izquierdo, J. Alvarez-Builla, *Tetrahedron* **2002**, *58*, 8573-8579.
- [100] R. de la Rosa, V. n. Martínez-Barrasa, C. Burgos, J. Alvarez-Builla, *Tetrahedron Lett.* **2000**, *41*, 5837-5840.
- [101] (a) A. Sánchez, A. Núñez, C. Burgos, J. Alvarez-Builla, *Tetrahedron Lett.* **2006**, *47*, 8343-8346; (b) A. Núñez, A. G. de Viedma, V. Martínez-Barrasa, C. Burgos, J. Alvarez-Builla, *Synlett* **2002**, *2002*, 1093-1096.
- [102] H. Beyer, E. Thieme, *J. Prakt. Chem.* **1966**, *31*, 293-303.
- [103] M. Córdoba, M. L. Izquierdo, J. Alvarez-Builla, *Tetrahedron* **2008**, *64*, 7914-7919.
- [104] R. Castillo, M. J. Reyes, M. L. Izquierdo, J. Alvarez-Builla, *Tetrahedron* **2008**, *64*, 1351-1370.

- [105] A. T. Balaban, D. C. Oniciu, A. R. Katritzky, *Chem. Rev.* **2004**, *104*, 2777-2812.
- [106] C. Enguehard, J.-L. Renou, V. Collot, M. Hervet, S. Rault, A. Gueiffier, *J. Org. Chem.* **2000**, *65*, 6572-6575.
- [107] A. Andreani, M. Rambaldi, A. Leoni, A. Locatelli, A. Ghelli, M. Ratta, B. Benelli, M. D. Esposti, *J. Med. Chem.* **1995**, *38*, 1090-1097.
- [108] M. Palkar, M. Noolvi, R. Sankangoud, V. Maddi, A. Gadad, L. V. G. Nargund, *Arch. Pharm.* **2010**, *343*, 353-359.
- [109] (a) B. H. Yousefi, A. Manook, A. Drzezga, B. v. Reutern, M. Schwaiger, H.-J. Wester, G. Henriksen, *J. Med. Chem.* **2011**, *54*, 949-956; (b) B. H. Yousefi, A. Drzezga, B. von Reutern, A. Manook, M. Schwaiger, H.-J. Wester, G. Henriksen, *ACS Med. Chem. Lett.* **2011**, *2*, 673-677.
- [110] L. Li, B. Zhou, Y.-H. Wang, C. Shu, Y.-F. Pan, X. Lu, L.-W. Ye, *Angew. Chem. Int. Ed.* **2015**, *54*, 8245-8249 vs ref. [47] and M. D. Santos, P.W. Davies, *Chem. Commun.* **2014**, *50*, 6001-6004.
- [111] J. Karolak-Wojciechowska, A. Mrozek, R. Czyrkowski, B. Tekiner-Gulbas, E. Akı-Şener, I. Yalçın, *J. Mol. Struct.* **2007**, *839*, 125-131.
- [112] E. S. Lazer, C. K. Miao, H.-C. Wong, R. Sorcek, D. M. Spero, A. Gilman, K. Pal, M. Behnke, A. G. Graham, *J. Med. Chem.* **1994**, *37*, 913-923.
- [113] (a) A. Costales, M. Mathur, S. Ramurthy, J. Lan, S. Subramanian, R. Jain, G. Atallah, L. Setti, M. Lindvall, B. A. Appleton, E. Ornelas, P. Feucht, B. Warne, L. Doyle, S. E. Basham, I. Aronchik, A. B. Jefferson, C. M. Shafer, *Bioorg. Med. Chem. Lett.* **2014**, *24*, 1592-1596; (b) X. Li, S. R. Srinivasan, J. Connarn, A. Ahmad, Z. T. Young, A. M. Kabza, E. R. P. Zuiderweg, D. Sun, J. E. Gestwicki, *ACS Med. Chem. Lett.* **2013**, *4*, 1042-1047; (c) E. Rolli, M. Incerti, F. Brunoni, P. Vicini, A. Ricci, *Phytochemistry* **2012**, *74*, 159-165; (d) P. C. Fritch, G. McNaughton-Smith, G. S. Amato, J. F. Burns, C. W. Eargle, R. Roeloffs, W. Harrison, L. Jones, A. D. Wickenden, *J. Med. Chem.* **2010**, *53*, 887-896.
- [114] K. Bahrami, M. M. Khodaei, S. Sohrabnezhad, *Tetrahedron Lett.* **2011**, *52*, 6420-6423.
- [115] C. Shu, Y.-H. Wang, C.-H. Shen, P.-P. Ruan, X. Lu, L.-W. Ye, *Org. Lett.* **2016**, *18*, 3254-3257.
- [116] M. N. Soltani Rad, S. Behrouz, A.-R. Nekoei, *Synlett* **2012**, *2012*, 1191-1198.
- [117] M. O. Frederick, J. A. Mulder, M. R. Tracey, R. P. Hsung, J. Huang, K. C. M. Kurtz, L. Shen, C. J. Douglas, *J. Am. Chem. Soc.* **2003**, *125*, 2368-2369.
- [118] R. B. Dateer, B. S. Shaibu, R.-S. Liu, *Angew. Chem. Int. Ed.* **2012**, *51*, 113-117.

- [119] M. Córdoba, M. Galájov, M. L. Izquierdo, J. Alvarez-Builla, *Tetrahedron* **2013**, *69*, 2484-2493.
- [120] S. A. Gawade, D. B. Huple, R.-S. Liu, *J. Am. Chem. Soc.* **2014**, *136*, 2978-2981.
- [121] L. Zhu, M. Zhang, M. Dai, *J. Heterocycl. Chem.* **2005**, *42*, 727-730.
- [122] K. Walczyński, O. P. Zuiderveld, H. Timmerman, *Eur. J. Med. Chem.* **2005**, *40*, 15-23.
- [123] R. Lok, R. E. Leone, A. J. Williams, *J. Org. Chem.* **1996**, *61*, 3289-3297.
- [124] Y. M. Yutilov, I. A. Svertilova, *Chem. Heterocycl. Compd.* **1971**, *7*, 402-403.
- [125] Y. Liu, W. Zhang, L. M. Sayre, *J. Heterocycl. Chem.* **2010**, *47*, 683-686.
- [126] I. Popov, H.-Q. Do, O. Daugulis, *J. Org. Chem.* **2009**, *74*, 8309-8313.